Integral Roles for the Tight Junction Protein Claudin-6 in Regulating Epidermal Homeostasis

Nathalie Larivière

This thesis is submitted as a partial fulfillment of the Ph.D. program in Cellular and Molecular Medicine

Department of Cellular and Molecular Medicine
Faculty of Medicine
University of Ottawa

AUTHORIZATIONS

NATURE PUBLISHING GROUP LICENSE
TERMS AND CONDITIONS

Nov 09, 2013

This is a License Agreement between Nathalie MK Lariviere ("You") and Nature Publishing Group ("Nature Publishing Group") provided by Copyright Clearance Center ("CCC"). The license consists of your order details, the terms and conditions provided by Nature Publishing Group, and the payment terms and conditions.

All payments must be made in full to CCC. For payment instructions, please see information listed at the bottom of this form.

License Number	3265150174230
License date	Nov 09, 2013
Licensed content publisher	Nature Publishing Group
Licensed content publication	Journal of Investigative Dermatology
Licensed content title	Resident and [ldquo]Inflammatory[rdquo] Dendritic Cells in Human Skin
Licensed content author	Lisa C Zaba, James G Krueger and Michelle A Lowes
Licensed content date	Aug 14, 2008
Volume number	129
Issue number	2
Type of Use	reuse in a dissertation / thesis
Requestor type	academic/educational
Format	print and electronic
Portion	figures/tables/illustrations
Number of figures/tables/illustrations	1
High-res required	no
Figures	Figure 2
Author of this NPG article	no
Your reference number	
Title of your thesis / dissertation	Integral roles for the tight junction protein Claudin-6 in regulating epidermal homeostasis
Expected completion date	Jan 2014
Estimated size (number of pages)	200

Total 0.00 USD

Terms and Conditions

Terms and Conditions for Permissions

Nature Publishing Group hereby grants you a non-exclusive license to reproduce this material for this purpose, and for no other use,subject to the conditions below:

1. NPG warrants that it has, to the best of its knowledge, the rights to license reuse of this material. However, you should ensure that the material you are requesting is original to Nature Publishing Group and does not carry the copyright of another entity (as credited in the published version). If the credit line on any part of the material you have requested indicates that it was reprinted or adapted by NPG with permission from another source, then you should also seek permission from that source to reuse the material.

2. Permission granted free of charge for material in print is also usually granted for any electronic version of that work, provided that the material is incidental to the work as a whole and that the electronic version is essentially equivalent to, or substitutes for, the print version.Where print permission has been granted for a fee, separate permission must be obtained for any additional, electronic re-use (unless, as in the case of a full paper, this has already been accounted for during your initial request in the calculation of a print run).NB: In all cases, web-based use of full-text articles must be authorized separately through the 'Use on a Web Site' option when requesting permission.

3. Permission granted for a first edition does not apply to second and subsequent editions and for editions in other languages (except for signatories to the STM Permissions Guidelines, or where the first edition permission was granted for free).

4. Nature Publishing Group's permission must be acknowledged next to the figure, table or abstract in print. In electronic form, this acknowledgement must be visible at the same time as the figure/table/abstract, and must be hyperlinked to the journal's homepage.

5. The credit line should read:
   Reprinted by permission from Macmillan Publishers Ltd: [JOURNAL NAME] (reference citation), copyright (year of publication)
   For AOP papers, the credit line should read:
   Reprinted by permission from Macmillan Publishers Ltd: [JOURNAL NAME], advance online publication, day month year (doi: 10.1038/sj.[JOURNAL ACRONYM].XXXXX)

   Note: For republication from the *British Journal of Cancer*, the following credit lines apply.
   Reprinted by permission from Macmillan Publishers Ltd on behalf of Cancer Research UK: [JOURNAL NAME] (reference citation), copyright (year of publication)For AOP

papers, the credit line should read:
Reprinted by permission from Macmillan Publishers Ltd on behalf of Cancer Research UK: [JOURNAL NAME], advance online publication, day month year (doi: 10.1038/sj.[JOURNAL ACRONYM].XXXXX)

6. Adaptations of single figures do not require NPG approval. However, the adaptation should be credited as follows:

   Adapted by permission from Macmillan Publishers Ltd: [JOURNAL NAME] (reference citation), copyright (year of publication)

   Note: For adaptation from the *British Journal of Cancer*, the following credit line applies.
   Adapted by permission from Macmillan Publishers Ltd on behalf of Cancer Research UK: [JOURNAL NAME] (reference citation), copyright (year of publication)

7. Translations of 401 words up to a whole article require NPG approval. Please visit http://www.macmillanmedicalcommunications.com for more information.Translations of up to a 400 words do not require NPG approval. The translation should be credited as follows:

   Translated by permission from Macmillan Publishers Ltd: [JOURNAL NAME] (reference citation), copyright (year of publication).

   Note: For translation from the *British Journal of Cancer*, the following credit line applies.
   Translated by permission from Macmillan Publishers Ltd on behalf of Cancer Research UK: [JOURNAL NAME] (reference citation), copyright (year of publication)

We are certain that all parties will benefit from this agreement and wish you the best in the use of this material. Thank you.

Special Terms:

v1.1

JOHN WILEY AND SONS LICENSE
TERMS AND CONDITIONS

Oct 27, 2013

This is a License Agreement between Nathalie MK Lariviere ("You") and John Wiley and Sons ("John Wiley and Sons") provided by Copyright Clearance Center ("CCC"). The license consists of your order details, the terms and conditions provided by John Wiley and Sons, and the payment terms and conditions.

All payments must be made in full to CCC. For payment instructions, please see information listed at the bottom of this form.

License Number	3257200213037
License date	Oct 27, 2013
Licensed content publisher	John Wiley and Sons
Licensed content publication	Journal of Anatomy
Licensed content title	Covering the limb – formation of the integument
Licensed copyright line	Copyright © 2003, John Wiley and Sons
Licensed content author	Carolyn Byrne,Matthew Hardman,Kerry Nield
Licensed content date	Jan 24, 2003
Start page	113
End page	123
Type of use	Dissertation/Thesis
Requestor type	University/Academic
Format	Print and electronic
Portion	Figure/table
Number of figures/tables	1
Original Wiley figure/table number(s)	Figure 3
Will you be translating?	No
Total	0.00 USD
Terms and Conditions	

TERMS AND CONDITIONS

This copyrighted material is owned by or exclusively licensed to John Wiley & Sons, Inc. or one of its group companies (each a "Wiley Company") or a society for whom a Wiley Company has exclusive publishing rights in relation to a particular journal (collectively "WILEY"). By clicking "accept" in connection with completing this licensing transaction,

ACCURACY OF ANY INFORMATION CONTAINED IN THE MATERIALS, INCLUDING, WITHOUT LIMITATION, ANY IMPLIED WARRANTY OF MERCHANTABILITY, ACCURACY, SATISFACTORY QUALITY, FITNESS FOR A PARTICULAR PURPOSE, USABILITY, INTEGRATION OR NON-INFRINGEMENT AND ALL SUCH WARRANTIES ARE HEREBY EXCLUDED BY WILEY AND ITS LICENSORS AND WAIVED BY YOU.

6. WILEY shall have the right to terminate this Agreement immediately upon breach of this Agreement by you.

7. You shall indemnify, defend and hold harmless WILEY, its Licensors and their respective directors, officers, agents and employees, from and against any actual or threatened claims, demands, causes of action or proceedings arising from any breach of this Agreement by you.

8. IN NO EVENT SHALL WILEY OR ITS LICENSORS BE LIABLE TO YOU OR ANY OTHER PARTY OR ANY OTHER PERSON OR ENTITY FOR ANY SPECIAL, CONSEQUENTIAL, INCIDENTAL, INDIRECT, EXEMPLARY OR PUNITIVE DAMAGES, HOWEVER CAUSED, ARISING OUT OF OR IN CONNECTION WITH THE DOWNLOADING, PROVISIONING, VIEWING OR USE OF THE MATERIALS REGARDLESS OF THE FORM OF ACTION, WHETHER FOR BREACH OF CONTRACT, BREACH OF WARRANTY, TORT, NEGLIGENCE, INFRINGEMENT OR OTHERWISE (INCLUDING, WITHOUT LIMITATION, DAMAGES BASED ON LOSS OF PROFITS, DATA, FILES, USE, BUSINESS OPPORTUNITY OR CLAIMS OF THIRD PARTIES), AND WHETHER OR NOT THE PARTY HAS BEEN ADVISED OF THE POSSIBILITY OF SUCH DAMAGES. THIS LIMITATION SHALL APPLY NOTWITHSTANDING ANY FAILURE OF ESSENTIAL PURPOSE OF ANY LIMITED REMEDY PROVIDED HEREIN.

9. Should any provision of this Agreement be held by a court of competent jurisdiction to be illegal, invalid, or unenforceable, that provision shall be deemed amended to achieve as nearly as possible the same economic effect as the original provision, and the legality, validity and enforceability of the remaining provisions of this Agreement shall not be affected or impaired thereby.

10. The failure of either party to enforce any term or condition of this Agreement shall not constitute a waiver of either party's right to enforce each and every term and condition of this Agreement. No breach under this agreement shall be deemed waived or excused by either party unless such waiver or consent is in writing signed by the party granting such waiver or consent. The waiver by or consent of a party to a breach of any provision of this Agreement shall not operate or be construed as a waiver of or consent to any other or subsequent breach by such other party.

11. This Agreement may not be assigned (including by operation of law or otherwise) by you without WILEY's prior written consent.

12. Any fee required for this permission shall be non-refundable after thirty (30) days from receipt

---

13. These terms and conditions together with CCC's Billing and Payment terms and conditions (which are incorporated herein) form the entire agreement between you and WILEY concerning this licensing transaction and (in the absence of fraud) supersedes all prior agreements and representations of the parties, oral or written. This Agreement may not be amended except in writing signed by both parties. This Agreement shall be binding upon and inure to the benefit of the parties' successors, legal representatives, and authorized assigns.

14. In the event of any conflict between your obligations established by these terms and conditions and those established by CCC's Billing and Payment terms and conditions, these terms and conditions shall prevail.

15. WILEY expressly reserves all rights not specifically granted in the combination of (i) the license details provided by you and accepted in the course of this licensing transaction, (ii) these terms and conditions and (iii) CCC's Billing and Payment terms and conditions.

16. This Agreement will be void if the Type of Use, Format, Circulation, or Requestor Type was misrepresented during the licensing process.

17. This Agreement shall be governed by and construed in accordance with the laws of the State of New York, USA, without regards to such state's conflict of law rules. Any legal action, suit or proceeding arising out of or relating to these Terms and Conditions or the breach thereof shall be instituted in a court of competent jurisdiction in New York County in the State of New York in the United States of America and each party hereby consents and submits to the personal jurisdiction of such court, waives any objection to venue in such court and consents to service of process by registered or certified mail, return receipt requested, at the last known address of such party.

Wiley Open Access Terms and Conditions

Wiley publishes Open Access articles in both its Wiley Open Access Journals program [http://www.wileyopenaccess.com/view/index.html] and as Online Open articles in its subscription journals. The majority of Wiley Open Access Journals have adopted the Creative Commons Attribution License (CC BY) which permits the unrestricted use, distribution, reproduction, adaptation and commercial exploitation of the article in any medium. No permission is required to use the article in this way provided that the article is properly cited and other license terms are observed. A small number of Wiley Open Access journals have retained the Creative Commons Attribution Non Commercial License (CC BY-NC), which permits use, distribution and reproduction in any medium, provided the original work is properly cited and is not used for commercial purposes.

Online Open articles - Authors selecting Online Open are, unless particular exceptions apply, offered a choice of Creative Commons licenses. They may therefore select from the CC BY, the CC BY-NC and the Attribution-NoDerivatives (CC BY-NC-ND). The CC BY-NC-ND is more restrictive than the CC BY-NC as it does not permit adaptations or modifications without rights holder consent.

Wiley Open Access articles are protected by copyright and are posted to repositories and

- Copying or downloading of articles, or linking to such articles for further redistribution, sale or licensing;
- Copying, downloading or posting by a site or service that incorporates advertising with such content;
- The inclusion or incorporation of article content in other works or services (other than normal quotations with an appropriate citation) that is then available for sale or licensing, for a fee (for example, a compilation produced for marketing purposes, inclusion in a sales pack)
- Use of article content (other than normal quotations with appropriate citation) by for-profit organizations for promotional purposes
- Linking to article content in e-mails redistributed for promotional, marketing or educational purposes;
- Use for the purposes of monetary reward by means of sale, resale, license, loan, transfer or other form of commercial exploitation such as marketing products
- Print reprints of Wiley Open Access articles can be purchased from: corporatesales@wiley.com

The modification or adaptation for any purpose of an article referencing the CC BY-NC-ND License requires consent which can be requested from RightsLink@wiley.com .

Other Terms and Conditions:

BY CLICKING ON THE "I AGREE..." BOX, YOU ACKNOWLEDGE THAT YOU HAVE READ AND FULLY UNDERSTAND EACH OF THE SECTIONS OF AND PROVISIONS SET FORTH IN THIS AGREEMENT AND THAT YOU ARE IN AGREEMENT WITH AND ARE WILLING TO ACCEPT ALL OF YOUR OBLIGATIONS AS SET FORTH IN THIS AGREEMENT.

v1.8

NATURE PUBLISHING GROUP LICENSE
TERMS AND CONDITIONS

Nov 07, 2013

This is a License Agreement between Nathalie MK Lariviere ("You") and Nature Publishing Group ("Nature Publishing Group") provided by Copyright Clearance Center ("CCC"). The license consists of your order details, the terms and conditions provided by Nature Publishing Group, and the payment terms and conditions.

All payments must be made in full to CCC. For payment instructions, please see information listed at the bottom of this form.

License Number	3263800482757
License date	Nov 07, 2013
Licensed content publisher	Nature Publishing Group
Licensed content publication	Nature Reviews Genetics
Licensed content title	Getting under the skin of epidermal morphogenesis
Licensed content author	Elaine FuchsandSrikala Raghavan
Licensed content date	Mar 1, 2002
Volume number	3
Issue number	3
Type of Use	reuse in a thesis/dissertation
Requestor type	academic/educational
Format	print and electronic
Portion	figures/tables/illustrations
Number of figures/tables/illustrations	1
High-res required	no
Figures	Figure 1: The skin and its appendages
Author of this NPG article	no
Your reference number	
Title of your thesis / dissertation	Integral roles for the tight junction protein Claudin-6 in regulating epidermal homeostasis
Expected completion date	Jan 2014
Estimated size (number of pages)	200
Total	0.00 USD

Terms and Conditions

Terms and Conditions for Permissions

Nature Publishing Group hereby grants you a non-exclusive license to reproduce this material for this purpose, and for no other use,subject to the conditions below:

1. NPG warrants that it has, to the best of its knowledge, the rights to license reuse of this material. However, you should ensure that the material you are requesting is original to Nature Publishing Group and does not carry the copyright of another entity (as credited in the published version). If the credit line on any part of the material you have requested indicates that it was reprinted or adapted by NPG with permission from another source, then you should also seek permission from that source to reuse the material.

2. Permission granted free of charge for material in print is also usually granted for any electronic version of that work, provided that the material is incidental to the work as a whole and that the electronic version is essentially equivalent to, or substitutes for, the print version.Where print permission has been granted for a fee, separate permission must be obtained for any additional, electronic re-use (unless, as in the case of a full paper, this has already been accounted for during your initial request in the calculation of a print run).NB: In all cases, web-based use of full-text articles must be authorized separately through the 'Use on a Web Site' option when requesting permission.

3. Permission granted for a first edition does not apply to second and subsequent editions and for editions in other languages (except for signatories to the STM Permissions Guidelines, or where the first edition permission was granted for free).

4. Nature Publishing Group's permission must be acknowledged next to the figure, table or abstract in print. In electronic form, this acknowledgement must be visible at the same time as the figure/table/abstract, and must be hyperlinked to the journal's homepage.

5. The credit line should read:
   Reprinted by permission from Macmillan Publishers Ltd: [JOURNAL NAME] (reference citation), copyright (year of publication)
   For AOP papers, the credit line should read:
   Reprinted by permission from Macmillan Publishers Ltd: [JOURNAL NAME], advance online publication, day month year (doi: 10.1038/sj.[JOURNAL ACRONYM].XXXXX)

   Note: For republication from the *British Journal of Cancer*, the following credit lines apply.
   Reprinted by permission from Macmillan Publishers Ltd on behalf of Cancer Research UK: [JOURNAL NAME] (reference citation), copyright (year of publication)For AOP papers, the credit line should read:

Reprinted by permission from Macmillan Publishers Ltd on behalf of Cancer Research UK: [JOURNAL NAME], advance online publication, day month year (doi: 10.1038/sj.[JOURNAL ACRONYM].XXXXX)

6. Adaptations of single figures do not require NPG approval. However, the adaptation should be credited as follows:

   Adapted by permission from Macmillan Publishers Ltd: [JOURNAL NAME] (reference citation), copyright (year of publication)

   Note: For adaptation from the *British Journal of Cancer*, the following credit line applies.
   Adapted by permission from Macmillan Publishers Ltd on behalf of Cancer Research UK: [JOURNAL NAME] (reference citation), copyright (year of publication)

7. Translations of 401 words up to a whole article require NPG approval. Please visit http://www.macmillanmedicalcommunications.com for more information.Translations of up to a 400 words do not require NPG approval. The translation should be credited as follows:

   Translated by permission from Macmillan Publishers Ltd: [JOURNAL NAME] (reference citation), copyright (year of publication).

   Note: For translation from the *British Journal of Cancer*, the following credit line applies.
   Translated by permission from Macmillan Publishers Ltd on behalf of Cancer Research UK: [JOURNAL NAME] (reference citation), copyright (year of publication)

We are certain that all parties will benefit from this agreement and wish you the best in the use of this material. Thank you.

NATURE PUBLISHING GROUP LICENSE
TERMS AND CONDITIONS

Nov 09, 2013

This is a License Agreement between Nathalie MK Lariviere ("You") and Nature Publishing Group ("Nature Publishing Group") provided by Copyright Clearance Center ("CCC"). The license consists of your order details, the terms and conditions provided by Nature Publishing Group, and the payment terms and conditions.

All payments must be made in full to CCC. For payment instructions, please see information listed at the bottom of this form.

License Number	3264800110253
License date	Nov 09, 2013
Licensed content publisher	Nature Publishing Group
Licensed content publication	Nature Reviews Molecular Cell Biology
Licensed content title	[alpha]-catenin: at the junction of intercellular adhesion and actin dynamics
Licensed content author	Agnieszka Kobielak and Elaine Fuchs
Licensed content date	Aug 1, 2004
Volume number	5
Issue number	8
Type of Use	reuse in a dissertation / thesis
Requestor type	academic/educational
Format	print and electronic
Portion	figures/tables/illustrations
Number of figures/tables/illustrations	1
High-res required	no
Figures	Figure 1 Intercellular Junctions in Skin
Author of this NPG article	no
Your reference number	
Title of your thesis / dissertation	Integral roles for the tight junction protein Claudin-6 in regulating epidermal homeostasis
Expected completion date	Jan 2014
Estimated size (number of pages)	200

Total 0.00 USD

Terms and Conditions

Terms and Conditions for Permissions

Nature Publishing Group hereby grants you a non-exclusive license to reproduce this material for this purpose, and for no other use,subject to the conditions below:

1. NPG warrants that it has, to the best of its knowledge, the rights to license reuse of this material. However, you should ensure that the material you are requesting is original to Nature Publishing Group and does not carry the copyright of another entity (as credited in the published version). If the credit line on any part of the material you have requested indicates that it was reprinted or adapted by NPG with permission from another source, then you should also seek permission from that source to reuse the material.

2. Permission granted free of charge for material in print is also usually granted for any electronic version of that work, provided that the material is incidental to the work as a whole and that the electronic version is essentially equivalent to, or substitutes for, the print version.Where print permission has been granted for a fee, separate permission must be obtained for any additional, electronic re-use (unless, as in the case of a full paper, this has already been accounted for during your initial request in the calculation of a print run).NB: In all cases, web-based use of full-text articles must be authorized separately through the 'Use on a Web Site' option when requesting permission.

3. Permission granted for a first edition does not apply to second and subsequent editions and for editions in other languages (except for signatories to the STM Permissions Guidelines, or where the first edition permission was granted for free).

4. Nature Publishing Group's permission must be acknowledged next to the figure, table or abstract in print. In electronic form, this acknowledgement must be visible at the same time as the figure/table/abstract, and must be hyperlinked to the journal's homepage.

5. The credit line should read:
   Reprinted by permission from Macmillan Publishers Ltd: [JOURNAL NAME] (reference citation), copyright (year of publication)
   For AOP papers, the credit line should read:
   Reprinted by permission from Macmillan Publishers Ltd: [JOURNAL NAME], advance online publication, day month year (doi: 10.1038/sj.[JOURNAL ACRONYM].XXXXX)

   Note: For republication from the *British Journal of Cancer*, the following credit lines apply.
   Reprinted by permission from Macmillan Publishers Ltd on behalf of Cancer Research UK: [JOURNAL NAME] (reference citation), copyright (year of publication)For AOP

papers, the credit line should read:
Reprinted by permission from Macmillan Publishers Ltd on behalf of Cancer Research UK: [JOURNAL NAME], advance online publication, day month year (doi: 10.1038/sj.[JOURNAL ACRONYM].XXXXX)

6. Adaptations of single figures do not require NPG approval. However, the adaptation should be credited as follows:

   Adapted by permission from Macmillan Publishers Ltd: [JOURNAL NAME] (reference citation), copyright (year of publication)

   Note: For adaptation from the *British Journal of Cancer*, the following credit line applies.
   Adapted by permission from Macmillan Publishers Ltd on behalf of Cancer Research UK: [JOURNAL NAME] (reference citation), copyright (year of publication)

7. Translations of 401 words up to a whole article require NPG approval. Please visit http://www.macmillanmedicalcommunications.com for more information.Translations of up to a 400 words do not require NPG approval. The translation should be credited as follows:

   Translated by permission from Macmillan Publishers Ltd: [JOURNAL NAME] (reference citation), copyright (year of publication).

   Note: For translation from the *British Journal of Cancer*, the following credit line applies.
   Translated by permission from Macmillan Publishers Ltd on behalf of Cancer Research UK: [JOURNAL NAME] (reference citation), copyright (year of publication)

We are certain that all parties will benefit from this agreement and wish you the best in the use of this material. Thank you.

NATURE PUBLISHING GROUP LICENSE
TERMS AND CONDITIONS

Nov 19, 2013

This is a License Agreement between Nathalie MK Lariviere ("You") and Nature Publishing Group ("Nature Publishing Group") provided by Copyright Clearance Center ("CCC"). The license consists of your order details, the terms and conditions provided by Nature Publishing Group, and the payment terms and conditions.

All payments must be made in full to CCC. For payment instructions, please see information listed at the bottom of this form.

License Number	3272510373613
License date	Nov 19, 2013
Licensed content publisher	Nature Publishing Group
Licensed content publication	Journal of Investigative Dermatology
Licensed content title	Proliferation, Cell Cycle Exit, and Onset of Terminal Differentiation in Cultured Keratinocytes: Pre-Programmed Pathways in Control of C-Myc and Notch1 Prevail Over Extracellular Calcium Signals
Licensed content author	Carine Kolly,Maja M SuterandEliane J Müller
Licensed content date	May 1, 2005
Volume number	124
Issue number	5
Type of Use	reuse in a dissertation / thesis
Requestor type	academic/educational
Format	print and electronic
Portion	figures/tables/illustrations
Number of figures/tables/illustrations	1
High-res required	no
Figures	Figure 10
Author of this NPG article	no
Your reference number	
Title of your thesis / dissertation	Integral roles for the tight junction protein Claudin-6 in regulating epidermal homeostasis
Expected completion date	Jan 2014
Estimated size (number of pages)	200

Total 0.00 USD

Terms and Conditions

Terms and Conditions for Permissions

Nature Publishing Group hereby grants you a non-exclusive license to reproduce this material for this purpose, and for no other use,subject to the conditions below:

1. NPG warrants that it has, to the best of its knowledge, the rights to license reuse of this material. However, you should ensure that the material you are requesting is original to Nature Publishing Group and does not carry the copyright of another entity (as credited in the published version). If the credit line on any part of the material you have requested indicates that it was reprinted or adapted by NPG with permission from another source, then you should also seek permission from that source to reuse the material.

2. Permission granted free of charge for material in print is also usually granted for any electronic version of that work, provided that the material is incidental to the work as a whole and that the electronic version is essentially equivalent to, or substitutes for, the print version.Where print permission has been granted for a fee, separate permission must be obtained for any additional, electronic re-use (unless, as in the case of a full paper, this has already been accounted for during your initial request in the calculation of a print run).NB: In all cases, web-based use of full-text articles must be authorized separately through the 'Use on a Web Site' option when requesting permission.

3. Permission granted for a first edition does not apply to second and subsequent editions and for editions in other languages (except for signatories to the STM Permissions Guidelines, or where the first edition permission was granted for free).

4. Nature Publishing Group's permission must be acknowledged next to the figure, table or abstract in print. In electronic form, this acknowledgement must be visible at the same time as the figure/table/abstract, and must be hyperlinked to the journal's homepage.

5. The credit line should read:
   Reprinted by permission from Macmillan Publishers Ltd: [JOURNAL NAME] (reference citation), copyright (year of publication)
   For AOP papers, the credit line should read:
   Reprinted by permission from Macmillan Publishers Ltd: [JOURNAL NAME], advance online publication, day month year (doi: 10.1038/sj.[JOURNAL ACRONYM].XXXXX)

Goldweber, Paulette - Hoboken <pgoldweb@wiley.com>

to me

Dear Nathalie:

Thank you for your request to use content from Comprehensive Physiology.

Permission is hereby granted for the use requested subject to the usual acknowledgements (author, title of material, title of book/journal, ourselves as publisher).

Any third party material is expressly excluded from this permission. If any of the material you wish to use appears within our work with credit to another source, authorization from that source must be obtained.

This permission does not include the right to grant others permission to photocopy or otherwise reproduce this material except for accessible versions made by non-profit organizations serving the blind, visually impaired and other persons with print disabilities (VIPs).

Sincerely,

Paulette Goldweber
Associate Manager/Permissions-Global Rights
Professional Development

Wiley
111 River Street, 4-02
Hoboken, NJ 07030-5774
U.S.

ABSTRACT

Forming and maintaining an intact epidermal permeability barrier (EPB) is necessary to mammalian health and dysregulation of this process can result in serious complications. Tight junctions (TJs) and their integral proteins the Claudins (Cldns) have both structural and signaling importance to the skin barrier and the latter is most likely mediated via Cldn tail interaction with cytoplasmic proteins. Given that the family member Cldn6 is known to be important to EPB function, we set out to determine the contribution of its cytoplasmic tail domain to TJ-mediated homoeostasis.

Using transgenic mouse models, we overexpressed epidermal-targeted tail truncation mutants and assessed EPB formation and maintenance. We then used yeast 2-hybrid and quantitative proteomic approaches to identify proteins that interact with this tail region and to assess the downstream effects of overexpressing these proteins in human keratinocytes in culture.

We demonstrate that a 10 amino acid region in the cytoplasmic tail is required for efficient epidermal maturation and injury repair and that our mouse models may be applicable to postnatal epidermal maturation and human skin aging studies. We show that in addition to the known interacting partner ZO1, the C-terminal tail of Cldn6 also binds FIZ1 (Flt3 interacting zinc finger protein-1), which we characterize for the first time as a mitogenic factor for keratinocytes. FIZ1 stimulates autocrine pathways involving secreted heparin-binding factors IGFBP3 and DKK1, sensitization to IGF signaling, MAP/ERK activation and increased G1 progression. Specific transcription

factors, protein kinases and signaling scaffolds that we identified as novel FIZ1-binding partners likely mediate this signaling.

Our studies on the Cldn6 cytoplasmic tail support the importance of this region for epidermal maturation and for maintenance of skin homeostasis throughout life. They also delineate the potential for tail interactors such as ZO1 and FIZ1 to act in concert with Cldns in TJ-based signaling networks to regulate the balance between proliferation and differentiation in keratinocytes. These findings provide new insight into the role of the Cldn6 cytoplasmic tail and will ultimately aid in the development of new diagnostic tools and therapeutic approaches for the treatment of skin conditions rooted in barrier defects.

TABLE OF CONTENTS

LIST OF TABLES

LIST OF FIGURES

LIST OF ABBEVIATIONS

Abbreviation	Meaning
α-SMase	-Acid Sphingomyelinase
(a)PKC	-Protein Kinase C (atypical)
Ago	-Argonaute
AJ	-Adherens Junction
AML	-Acute Myeloid Leukemia
ANOVA	-Analysis of Variance
AP/MS	-Affinity Purification/Mass Spectrometry
AQP	-Aquaporin
AREG	-Amphiregulin
Arg (R)	-Arginine
AUC	-Area under the curve
β-celerase	-β-glucocerebrosidase
BSA	-Bovine Serum Albumin
Ca^{2+}	-Calcium
Cdk	-Cyclin-dependent kinase
CE	-Cornified Envelope
CK	-Casein Kinase
Cl^-	-Chloride Ion
Cldn	-Claudin
Co-IP	-Co-Immunoprecipitation
CO_2	-Carbon Dioxide
CP	-Cytoplasm
CRABP	-Cellular retinoic acid-binding protein
Cys (C)	-Cysteine
DKK1	-Dickkopf WNT Signaling Pathway Inhibitor 1
DMBA	-7,12-dimethylbenz[α]anthracene
DMEM	-Dulbecco's modified Eagle's medium
DNA	-Deoxyribonucleic acid
DPM	-dermal phase meter
E	-Embryonic days post-conception
EDTA	-Ethylenediaminetetraacetic acid
EGF	-Epidermal Growth Factor
EGFR	-Epidermal Growth Factor Receptor
EPB	-Epidermal Permeability Barrier
EphA2	-Ephrin type-A receptor 2
ERK	-Extracellular signal-Regulated Kinase
ES cell	-Embryonic Stem cell
FABP	-Fatty-Acid-Binding Proteins
FBS	-Fetal Bovine Serum
FGF	-Fibroblast Growth Factor
FGFR2/IIIb	-Fibroblast Growth Factor Receptor 2
FHHNC	-Familial hypomagnesemia, hypocalciuria and nephrocalcinosis

FITC	-Fluorescein isothiocyanate
FIZ1	-Flt3 Interacting Zinc finger protein-1
FLT-3	-Fms-like tyrosine kinase 3
FP	-Fluorescent Protein
GAPDH	-Glyceraldehyde 3-Phosphate Dehydrogenase
GFP	-Green Fluorescent Protein
GM-CSF	-Granulocyte-Macrophage Colony-Stimulating Factor
GRK	-G protein-coupled Receptor Kinases
H&E	-Hematoxylin and Eosin
HB-EGF	-Heparin-binding Epidermal Growth Factor
HCl	-Hydrochloric acid
HER	-Human Epidermal growth factor Receptor
hES cells	-Human Embryonic Stem Cells
His (H)	-Histidine
HRP	-Horseradish Peroxidase
IGF	-Insulin-like Growth Factor
IGFR	-Insulin-like Growth Factor Receptor
IGFBP	-Insulin-like growth factor-binding protein
IL	-Interleukin
Inv	-Involucrin
IP	-Immunoprecipitation
IPO	-Importin
JAK	-Janus Kinase
JAM	-Junctional adhesion molecules
JNK	-c-Jun N-terminal kinases
K	-Keratin
KGF	-Keratinocyte Growth Factor
LC-MS/MS	-Liquid chromatography-tandem mass spectrometry
Lys	-Lysine
MAGUK	-Membrane-Associated Guanylate Kinases
MAPK	-Mitogen-Activated Protein Kinase
mCh	-mCherry Fluorescent Protein
MDCK	-Madin Darby Canine Kidney Cells
MEK	-Mitogen-Activated Protein Kinase Kinase
MLCK	-Myosin light-chain kinase
MMP13	-Matrix metallopeptidase
MOB2	-Mps One Binder Kinase Activator 2
mRNA	-messenger Ribonucleic Acid
MUPP1	-Multi-PDZ Domain Protein 1
Na^+	-Sodium Ion
NDR1/STK38	-Nuclear Dbf2-Related Kinase 1/ Serine/Threonine Kinase 38
NDR2/STK38L	-Nuclear Dbf2-Related 2/ Serine/Threonine Kinase 38 Like
NF-κB	-Nuclear Factor Of κ–Light Polypeptide Gene Enhancer In B-cells
NGF	-Nerve Growth Factor
NHE1	-Na^+/H^+ exchanger 1
NICD	-Notch receptor Intracellular Domain

NLS	-Nuclear Localization Signal
NP	-Nucleoplasm
NRG	-Neuregulin
Par	-Partitioning-defective
PATJ	-PALS1- associated TJ protein
PBS	-Phsophate buffered saline
PCR	-Polymerase Chain Reaction
PDGF	-Platelet-Derived Growth Factor
PDK	-Pyruvate Dehydrogenase Kinases
PDZ	-Post synaptic density protein (PSD95), Drosophila disc large tumor suppressor (Dlg1), and Zonula occludens-1 protein (ZO1)
PFA	-Paraformaldehyde
PKA	-Protein Kinase A
PKB (AKT)	-Protein Kinase B
PKG	-Protein Kinase G
PM	-Plasma Membrane
PPAR	-Peroxisome Proliferator-Activated Receptors
qPCR	-Quantitative PCR
RNA	-Ribonucleic Acid
RNAi	-Ribonucleic Acid interference
RT-PCR	-Reverse Transcriptase Polymerase Chain Reaction
S1P	-Sphingosine-1-phosphate
SCC	-Squamous Cell Carcinoma
SCYL2/CVAK104	-SCY1-Like 2 /Coated Vesicle-Associated Kinase Of 104 kDa
SDS	-Sodium Dodecyl Sulfate
SDS-PAGE	-Sodium Dodecyl Sulfate Polyacrylamide Gel Electrophoresis
Ser (S)	-Serine
SILAC	-Stable Isotope Labeling by Amino acids in Culture
SPRRs	-Small Proline-Rich Proteins
STAT	-Signal Transducer And Activator Of Transcription
TACSTD	-Tumor-Associated Calcium Signal Transducer
TAF4	-TAF4 RNA Polymerase II, TATA Box Binding Protein - Associated Factor
TBS	-Tris Buffered Saline
TER	-Trans-Epithelial Resistance
TEWL	-Trans-Epidermal Water Loss
TFIID	-Transcription Factor IID
TG1	-Transglutaminase-1
TGF	-Transforming Growth Factor
Thr (T)	-Threonine
TJ	-Tight Junction
TNF-α	-Tumor Necrosis Factor alpha
TPA	-12-O-tetradecanoyl-phorbol-13-acetate
TRAF4	-TNF Receptor-Associated Factor 4
Tyr	-Tyrosine
UV	-Ultraviolet

VEGF	-Vascular Endothelial Growth Factor
X-gal	-5-bromo-4-chloro-3-indolyl-β-D-galactopyranoside
Y2H	-Yeast two-Hybrid
ZO	-Zonula Occludens
ZONAB	-(ZO1)-associated nucleic acid binding protein

ACKNOWLEDGEMENTS

Many people have contributed to the production of this thesis and I owe countless thanks to each and every one of them.

I would like to express my deepest gratitude to my mentor, Dr. Laura Trinkle-Mulcahy. With her enthusiasm, inspiration, and ability to explain things clearly, Laura helped make research fun for me. She was a constant source of encouragement, sound advice, good teaching, and lots of good ideas. Laura's attentive editing clarified my mangled prose and kept me motivated. She showed me the virtue of skepticism in research and taught me how to be a better scientist. I am eternally grateful to her for adopting me into her lab where my graduate studies suddenly became enjoyable.

A special thanks goes to my advisory committee members, Drs. Ilona Skerjanc, Stephen Gee and David Lohnes whose knowledge and enthusiasm were critical to this effort. I thank all of my committee members for simultaneously encouraging, guiding, and supporting my research ideas and me.

To past and present lab-mates, I consider myself very fortunate to have worked with such bright scientists and great friends. Thank you for everything.

I will forever be thankful for my undergraduate studies supervisor Dr. Andrew Watson. Andy was the reason I decided to go to pursue a career in research. His enthusiasm and love for science is truly contagious.

My family has been a constant source of love, support and strength all these years. They

have helped me stay sane through the difficult times. I greatly value their love and I deeply appreciate their belief in me. I would like to express my heart-felt gratitude to every one of them. Of course, this includes my sweet golden retriever who was the best writing companion. Most importantly, none of this would have been possible without the love and patience of my husband. I cannot overstate how lucky I am to have such a brilliant, handsome and witty chemist in my life.

GENERAL INTRODUCTION

Function of mammalian skin

Skin is one of the largest organs in the body and is essential for mammalian survival (Kanitakis, 2002). Its primary role is protective, via construction of an outer surface barrier between 'inside' and 'outside' environments that resists toxin entry and microbial infection and prevents water and electrolyte loss (desiccation). In healthy individuals, the skin has evolved a robust immune response and ability to repair the barrier when perturbed by aggressions such as lacerations or scrapes (Proksch et al., 2008). Wound contraction and re-epithelialization from the margins of the wound both play important roles in closure, and crosstalk between lower (fibroblasts secreting a growth factor cocktail) and upper (cells that respond to these growth factors) layers of the skin greatly accelerates wound healing (Ghalbzouri et al., 2003). The importance of an intact barrier is apparent in conditions such as premature birth, in which barrier formation is not yet finished (Kalia et al., 1998), and severe burns (Proksch et al., 2008), with affected individuals at risk of transepidermal water loss (dehydration) and transcutaneous heat loss. The disrupted barrier also represents an entry point for toxins and infectious microbes.

In addition to its barrier function, skin also mediates regulation of temperature, sensation, excretion and synthesis of vitamin D, and serves as decoration for social and reproductive behavior (Blanpain and Fuchs, 2006; Boulais and Misery, 2007; Feingold, 2007; Holick, 2006; Lumpkin and Caterina, 2007; Shibasaki, 2006). Although mechanisms are in place to maintain skin integrity, extrinsic or intrinsic changes may have pathological consequences. This includes cancers such as basal and squamous cell carcinomas, which originate in cells in the upper and lower levels of the skin, and melanomas that develop

from pigment-producing melanocyte cells. Other skin diseases include the immune response-related psoriasis (overproduction of new skin cells) and dermatitis (inflammatory disease). In psoriasis, the epidermis is thickened and forms projections into the dermis (see Fig. 1) (Bowcock and Krueger, 2005). The skin displays an abnormal retention of partially processed cells that unnaturally stack up into characteristic psoriatic 'plaques', which are regions of low skin integrity and minimal skin barrier function (Roberson and Bowcock, 2010; Valdimarsson et al., 2009). In dermatitis, increased epidermal proliferation is accompanied by disturbed skin structure, including changes in lipid composition that cause impaired barrier function. This defective permeability barrier function enables enhanced penetration of environmental allergens and initiation of immune responses and inflammation (Bieber, 2010; Proksch et al., 2009). Although rarely life threatening, psoriasis and dermatitis have a significant effect on quality of life and their high prevalence places them among the top four chronic disease groups (Stevens and Gillam, 1998).

Embryonic development of the skin

After fertilization, multicellular organisms undergo a series of cleavage divisions whereby the egg cytoplasm is divided into many smaller nucleated cells called blastomeres. Gastrulation movements that take place over the next few days form the three germ layers: i) Definitive endoderm, which develops into the respiratory system and gut tube lining; ii) Mesoderm, which develops into muscles, skeleton, connective tissue, kidneys, gonads, and blood; iii) Ectoderm, which develops into the skin and nervous system. The covering ectoderm cells start to form the putative epidermis at E8.5 in

Figure 1. Sections of skin from psoriasis and dermatitis lesions compared to a non-lesional control. White bars are included to compare the thickness of the epidermis between sections. *Adapted by permission from Macmillan Publishers Ltd: [Journal of Investigative Dermatology] (Zaba et al., 2008), copyright (2008).*

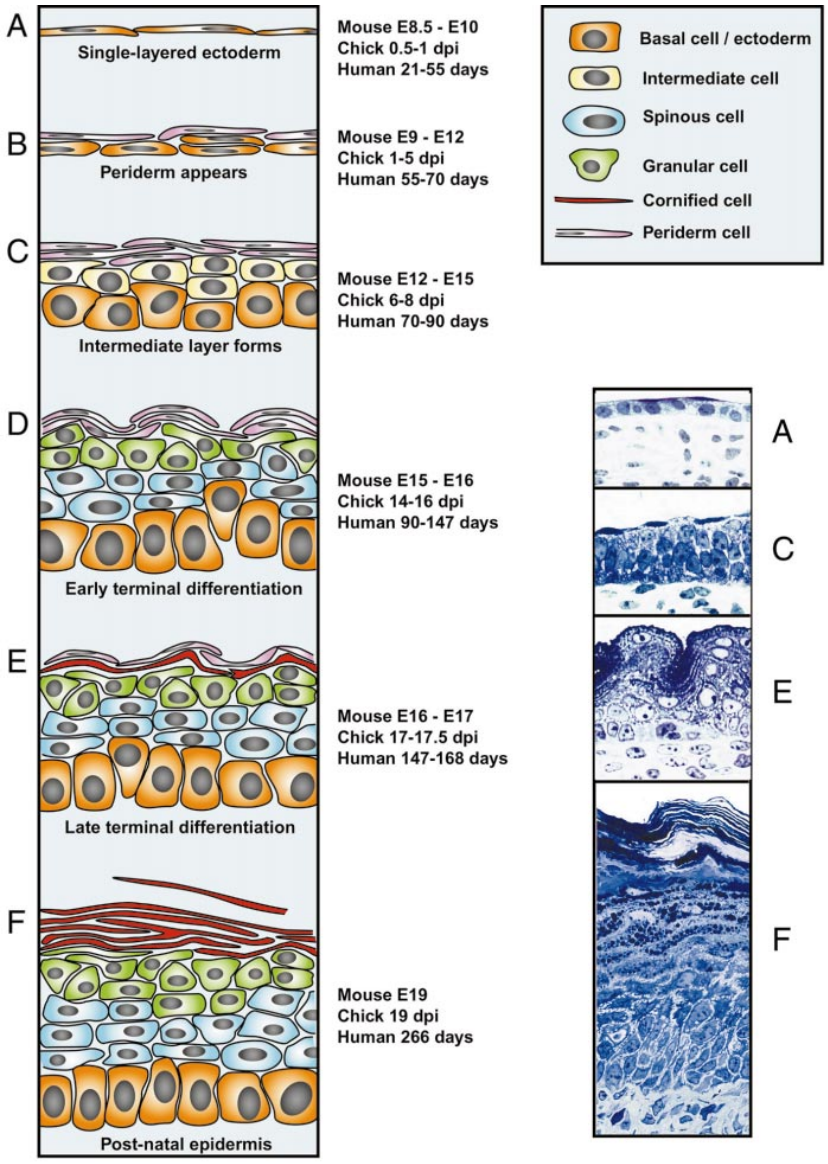

Fig. 2 Epidermal development. Developmental timelines are shown for mouse, chick and human. E, embryonic days post-conception; dpi, embryonic days post-incubation. Histological sections stained with toluidine blue. *Reprinted by permission from (Byrne et al., 2003), copyright (2003).*

mouse and day 21 in human (Fig.2). The periderm, an interface between the embryo and amnionic fluid produced by initial stratification, begins to appear at E9 in mouse and day 55 in human and is shed before birth, often in conjunction with formation of an active skin barrier (Hardman et al., 1999). Further stratification of the ectoderm completes late terminal differentiation of the epidermis by E17-18 in mouse and day 147-168 in human (Byrne et al., 1994; Kopan and Fuchs, 1989; Mack et al., 2005; Weiss and Zelickson, 1975), giving rise to the insoluble cornified envelopes of the stratum corneum (Elias, 2005; Fuchs and Horsley, 2008; Hardman et al., 1998; Kalinin et al., 2002; Troy and Turksen, 2002). The mature epidermis renews itself continuously throughout life, regulated by a finely tuned balance between proliferation and differentiation (Fuchs, 2007; Fuchs and Horsley, 2008; Kaur, 2006; Lavker and T. T. Sun, 2000).

Basic structure of skin

Skin is composed of three layers: the epidermis, dermis and hypodermis. Each layer is distinctive in thickness and function and has layer-specific epithelial-associated structures or appendages such as sweat glands, hair follicles, sebaceous glands and nails (Fig. 3) (Fuchs and Raghavan, 2002). The hypodermis is the deepest layer, separating skin from muscle. Primarily composed of adipocytes, the hypodermis is important for temperature control. Along with the dermis, the hypodermis is vascularized, to maintain nutrient supplies to the skin. The dermis is home to macrophages, neurons, sweat glands and roots of hair follicles, all poised to support the epidermis. Fibroblasts found in this layer produce collagen and elastin, which provide strength and elasticity, respectively (see (Naylor et al., 2011)).

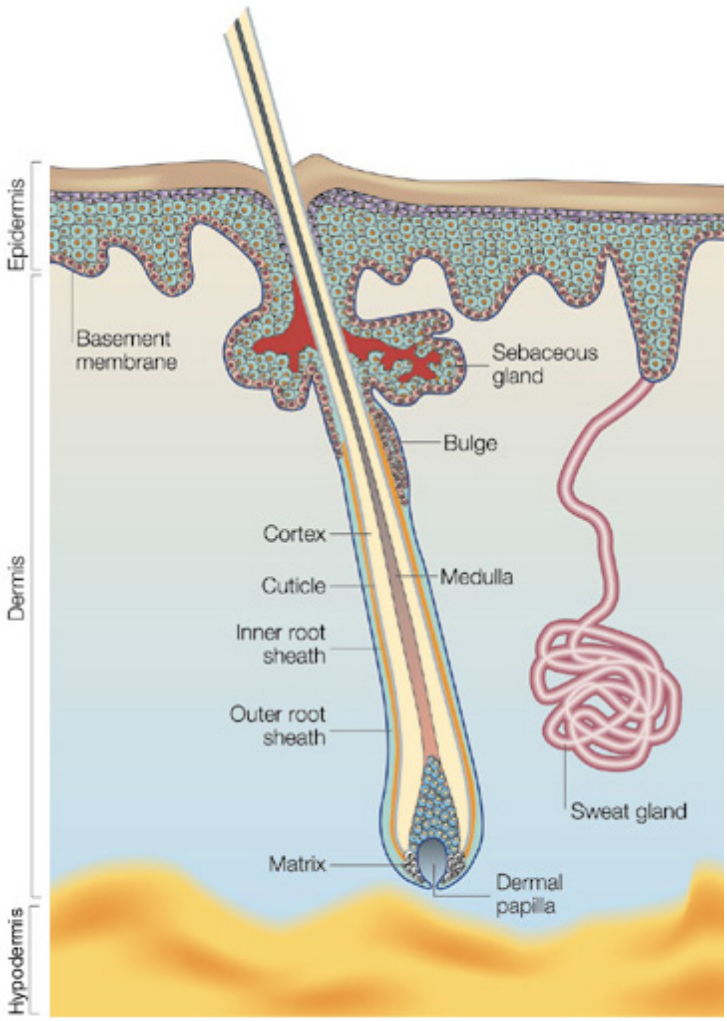

Fig. 3. The skin and its appendages. Mammalian skin consists of the epidermis, dermis and hypodermis. Two examples of epidermal appendages, the hair follicle and sweat gland, are included here. *Adapted by permission from Macmillan Publishers Ltd: [Nature Reviews Genetics] (Fuchs and Raghavan, 2002), copyright (2002).*

The epidermis is the outermost layer of skin. Keratinocytes, which produce the structural keratin proteins, comprise 90% of the cells in this layer, while the remaining 10% is comprised of Langerhans' cells important to immune surveillance, Merkel cells important for sensation and the pigment-producing melanocytes (reviewed in (Geerligs, 2009)). Keratins are the major structural proteins of the skin, providing stability behind the skin barrier (Moll et al., 1982), and the epidermis provides the epidermal permeability barrier (EPB) that is essential to life. The EPB is a dynamic structure whose fidelity depends on proper regulation of the terminal differentiation program of the keratinocytes involved.

Formation of Epidermal layers

The program of terminal differentiation leads to the production of a multilayered, stratified epithelium containing 4 main layers: stratum basale, stratum spinosum, stratum granulosum, and stratum corneum. A fifth layer, the stratum lucidum, can be found at high-stress sites such as the soles of the feet, where a thicker epidermis is required (Fig. 4) [for a comprehensive review of epidermal layers refer to (Kanitakis, 2002; Reichert and Michel, 1993)]. The epidermis begins at the dermal-epidermal junction with the stratum basale, a proliferative layer consisting of columnar cells attached to a basement membrane rich in extracellular matrix and growth factors (Fuchs, 2008). Along with the hair follicle bulge and the base of the sebaceous gland, it is a major niche for epidermal stem cells (Fuchs, 2008). Although it is accepted that epidermal stem cells contribute to skin homeostasis by replacing cells that are shed in the outermost layers of the skin, the mechanism behind the generation of a single proliferative layer and multiple layers of suprabasal cells is still unclear (Cotsarelis, 2006; Jensen et al., 1999; Watt et al., 2006).

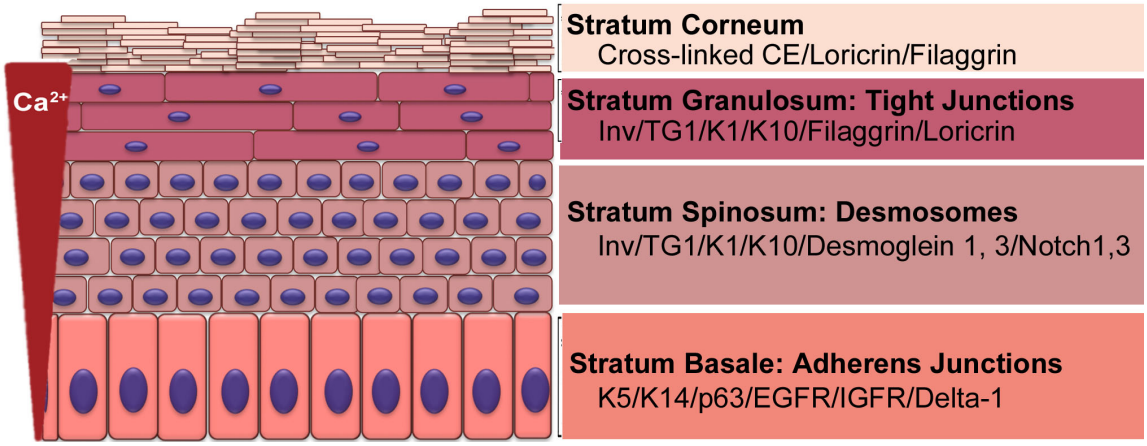

Fig. 4. Layers of the epidermis. Marker proteins and characteristic junctions for each layer are noted.

In both current hypotheses, the basal layer is replenished by symmetrical divisions that produce two stem cells. In the two-step model, a stem cell divides asymmetrically to preferentially provide one daughter cell with proliferation-associated factors and the other with differentiation-inducing components. In the three-step model, an intermediate "transit-amplifying" cell is produced, which divides four to five times before entering into a terminal differentiation program. As committed basal keratinocytes migrate up to the spinous layer they begin to synthesize a different set of structural proteins. Specifically, expression of keratins-5 and -14, the main keratins in proliferating basal cells, is shut down and they are replaced by keratins-1 and -10 (Blanpain and Fuchs, 2006; Turksen and Troy, 1998). Note that throughout development and differentiation, keratinocytes participate in intercellular communication via gap junctions, which allow ions, small molecules, and secondary messengers to pass between cells (Alexander and Goldberg, 2003). Regulation of this intercellular communication system is crucial for maintaining tissue homeostasis (Qiu et al., 2003; Langlois et al., 2007). This and other regulatory mechanisms ensure that skin shedding or "desquamation" is precisely balanced by proliferation in the basal layer (Liu et al., 2009; Steinert, 2000). Progression of keratinocytes into the spinous layer marks the beginning of expression of proteins necessary for the eventual formation of the insoluble hydrophobic outer layer of the stratum corneum (Banks-Schlegel and Green, 1981). In the spinous layer, cells contain lamellar bodies rich in ceramides, cholesterol and free fatty acids in preparation for further processing as they ascend through the epidermal layers. The stratum granulosum, or granular layer, that follows the spinous layer is so named because keratinocytes in this layer contain electron-dense keratohyalin granules rich in filaggrin (Dale et al., 1985), a

protein that facilitates aggregation of keratin filaments. The outermost layer of the epidermis is the stratum corneum, where keratinocytes form the cornified envelope (CE) through the destruction of cellular organelles in combination with the expression, processing and deposition of terminal differentiation proteins (Mack et al., 2005; Schaefer and Redelmeier, 1996). The latter involves covalent crosslinking, by transglutaminase-1 (TG1), of proteins such as involucrin, loricrin, small proline rich proteins (SPRRs), calcium binding S100 proteins and late envelope proteins (Marshall et al., 2001; Schaefer and Redelmeier, 1996; Steinert, 2000). This arrangement of terminally differentiated cells sealed together by a lipid matrix in a "bricks and mortar" fashion helps provide the skin with its permeability barrier. The stratum corneum is a major physical component of the skin barrier and, as expected, diseases or mutations preventing its proper formation manifest in severe phenotypes (Ramos-e-Silva and Jacques, 2012). In fact, it was until recently considered to be an impenetrable wall in healthy mammals. This view was challenged by findings from Tsukita and colleagues in 2002 that provided the first evidence that intrinsic structures mediate the permeability of the epidermal barrier (Furuse et al., 2002).

Junctional complexes in epithelia are key to EPB function

An important characteristic of epithelia is their assembly into barriers selective to ions and size. This function is facilitated by 3 types of junctional complexes, desmosomes, adherens junctions (AJs) and tight junctions (TJs), which connect adjacent cells and enable formation and maintenance of such barriers in epithelia (Fig. 5).

i) Desmosomes

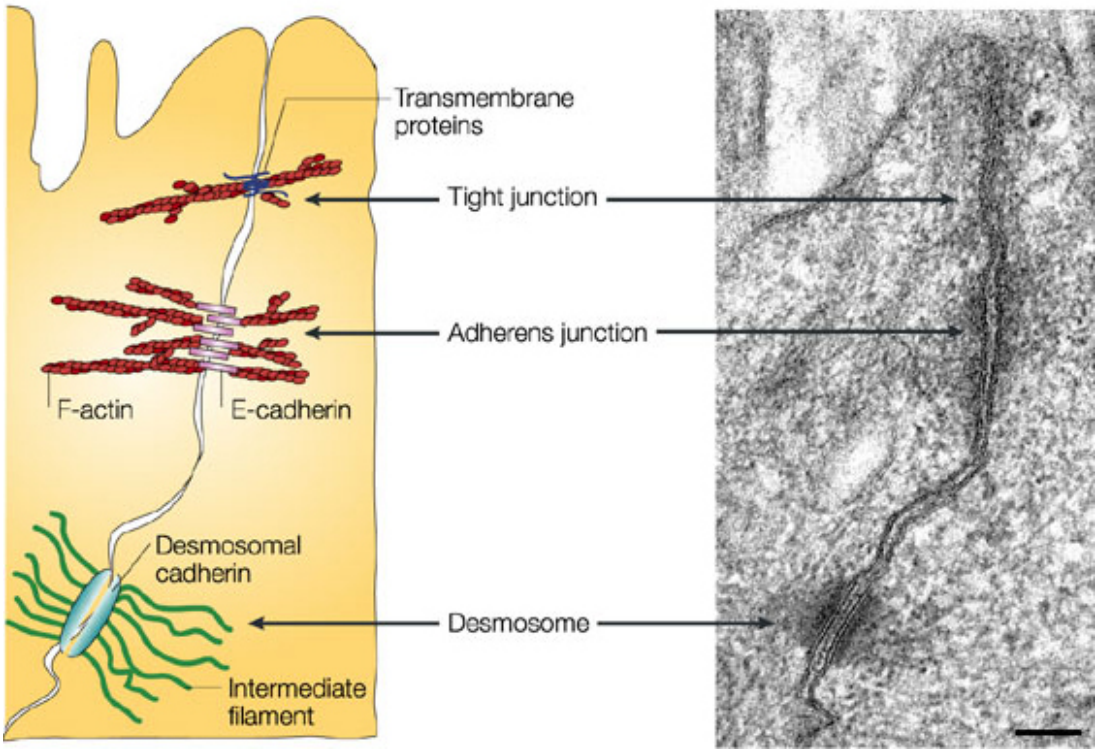

Figure 5. The electron micrograph and corresponding schematic depict the main types of intercellular junction in epithelial cells. Scale bar is 200nm. *Reprinted by permission from Macmillan Publishers Ltd: [Nature Reviews Molecular Cell Biology] (Kobielak and Fuchs, 2004), copyright (2004).*

Desmosomes are adhesive intercellular junctions that anchor the intermediate filament network to the plasma membrane (Kowalczyk et al., 1999). They are composed of the desmosomal cadherins, which, along with the classical cadherins of AJs, are part of the cadherin superfamily. Desmogleins 1-4 and desmocollins 1-3 are found in the human epidermis. Desmosomes play an important role in maintaining tissue integrity, with the intracellular ends of desmosomal cadherins inserted into the molecular network of adaptor proteins that form the desmosomal plaques to which keratin filaments bind (Brandner et al., 2010).

ii) Adherens Junctions

Adherens junctions and tight junctions were first identified at the ultrastructural level in polarized simple epithelia and implicated in barrier function (Farquhar and Palade, 1963). Spatially, AJs are positioned immediately below TJs and are also located outside of these junctional complexes in both epithelial and non-epithelial cells. AJ formation is a prerequisite to the assembly of TJs in a wide variety of tissues. Cadherins such as E-cadherin are the major transmembrane proteins of the AJ, and they initiate intercellular contacts through trans-pairing with cadherins on opposing cells. AJs couple intercellular adhesion to the cytoskeleton, and have also been shown to function as signaling platforms that regulate cytoskeletal dynamics and cell polarity. As such, they regulate a diverse range of cellular processes including cell shape, division, growth, apoptosis and barrier function [reviewed in (Brandner et al., 2010; Hartsock and Nelson, 2008)].

iii) Tight Junctions

Tight junctions are the most apical structure of the junctional complexes. They define

apical and basolateral membrane domains (Cereijido et al., 1998), thereby establishing distinctive environments on either side of polarized cells (Nusrat et al., 2000). There are two fundamental transport pathways across an epithelium, transcellular (across cells) and paracellular (between cells), and epithelial tissue homeostasis relies on the electrochemical gradients established by these routes of transport. While transcellular transport is mediated by energy-dependent transporters and channels distributed on basolateral and apical membranes, TJs are the rate-limiting structure for paracellular transport, spanning the apical intercellular space and forming a regulated, semi-permeable barrier controlling the passive diffusion of ions and small non-charged solutes through the paracellular space. When examined by electron microscopy, the paracellular space at TJ sites is almost eliminated, with adjacent membranes nearly fusing (Fig. 5) (Tsukita et al., 2001) at sites termed 'kissing points' or, more traditionally, *zonulae occluden*s. These 'kissing points' allow specific permeability to small, hydrophilic molecules and ions and are important routes for selective ion transport (Angelow, 2005; Balda and Matter, 1998). Paracellular permeability varies widely among different epithelia, and this appears to be dependent on the protein composition of their TJs (Tsukita et al., 2001; Van Itallie and Anderson, 2006).

Importantly, TJs have also been shown to be much more than simple static barriers. They are dynamic structures that can change their permeability characteristics rapidly in response to physiological needs/stimuli (Tsukita et al., 2001; Van Itallie and Anderson, 2006; Nusrat et al., 2000). Evidence for the rapid remodeling of TJs comes from recent studies examining the distinct and dynamic turnover of specific TJ proteins within these

structures in different cell types (Shen et al., 2008; Yamazaki et al., 2011). Furthermore, TJs have been shown to include several protein complexes that not only regulate cell polarization and junctional assembly but also control signaling molecules that play critical roles in cell differentiation, proliferation and gene expression (Aijaz et al., 2006; Niessen, 2007).

TJ COMPONENTS

Transmembrane Proteins: Occludin

Occludin was the first integral membrane protein to be identified at TJs (Ando-Akatsuka et al., 1996; Furuse et al., 1993). Found in both epithelial and endothelial TJ sheets and selectively concentrated at TJs (Sakakibara et al., 1997), it is an excellent biochemical marker for these complexes. Occludin is a ~65kDa transmembrane protein with a cytoplasmic carboxy-terminal region that binds to cytoplasmic TJ proteins (Furuse et al., 1993). When overexpressed in mouse L-fibroblasts that normally lack TJs and cadherin-mediated cell-cell adhesion, Occludin assembles into cell-cell contacts that can be resolved by microscopy (Furuse et al., 1998b). Overexpression of Occludin in other cell types induces an increase in the strength of TJs, which is measured as trans-epithelial resistance (TER) (McCarthy et al., 1996; Medina et al., 2000). With these observations suggesting an integral role for Occludin in TJ formation, it was surprising to find that it is not essential for this process. Occludin-deficient embryonic stem cells generated by targeted disruption of Occludin alleles have structurally and functionally normal TJs, while Occludin knockout mice, although born with a complex phenotype, have no

morphological or physiological TJ abnormalities (Saitou et al., 1998; 2000). Functional compensation by Occludin-related proteins such as tricellulin (discussed below) may help to explain these unexpected results.

Transmembrane Proteins: Claudins

The existence of TJ strands and barrier function in Occludin knockout mice highlighted the existence of additional components within the complex that contribute to TJ formation and barrier function. Claudins (Cldns), named from the Latin word *claudere*, 'to close', were originally identified as membrane proteins that co-fractionated with Occludin by sucrose density gradient centrifugation of TJ/AJ-enriched membrane fractions (Furuse et al., 1998a). Cldns are members of the much larger pfam00822 or PMP-22/EMP/MP20/Claudin family. Beyond structural similarities, their functions are highly divergent and only a subset appears to play a role in formation of barriers in various tissues, including epidermis (Anderson and Van Itallie, 2009).

The Cldn protein superfamily consists of 27 isoforms with molecular masses in the range of 21-34 kDa that display isoform-specific tissue expression profiles (Angelow et al., 2008; Furuse and Tsukita, 2006; Gunzel and Yu, 2013; Van Itallie and Anderson, 2006). Based on >15 years of Cldn isoform suppression/overexpression studies, these proteins have been shown to play essential roles in barrier function and in the structure and function of TJs (summarized in Table 1 in Appendix 1).

Cldns are integral membrane proteins that have four hydrophobic transmembrane domains and two extracellular loops (Fig. 6). The first loop confers the 'electrostatic selectivity filter' of the TJ as it lines the paracellular pore (Anderson and Van Itallie,

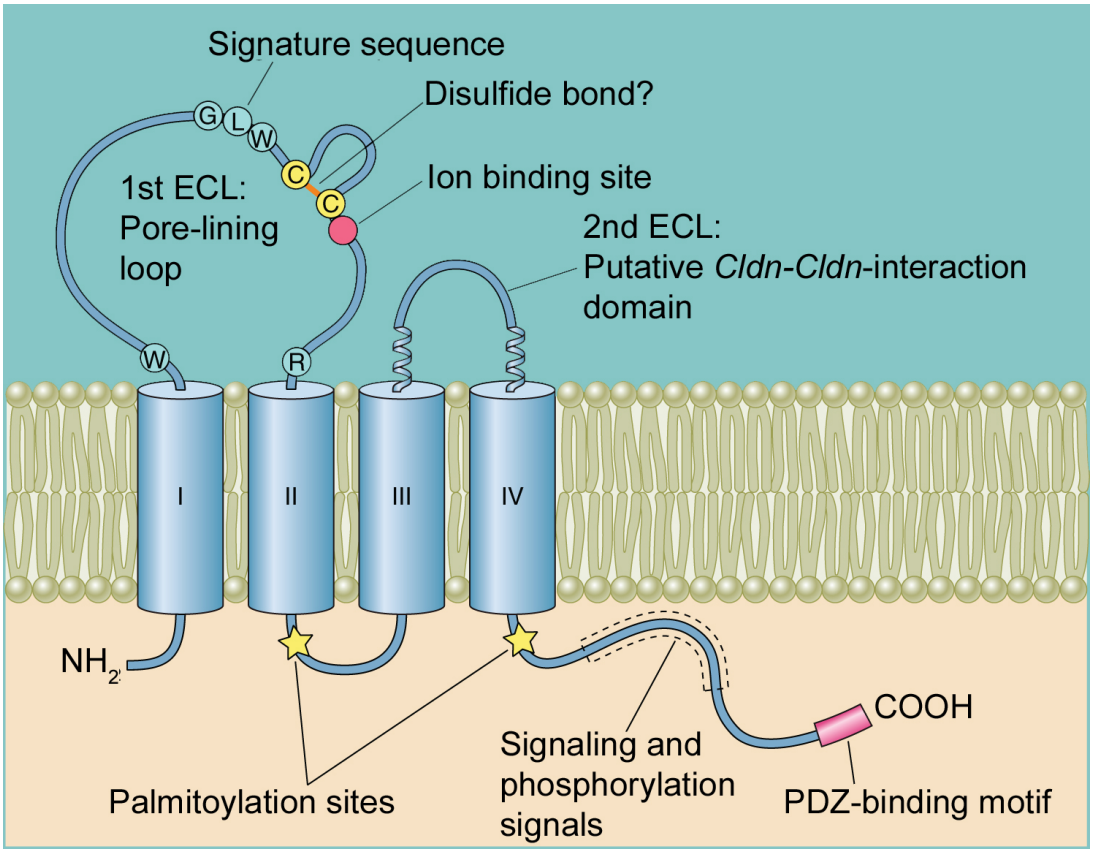

Figure 6. Claudins. Predicted topology, secondary structure and putative functional domains of the Claudin protein family. Roman numerals indicate α-helical transmembrane domains. *Adapted by permission from (Gunzel and Yu, 2013).*

2009), and also contains the highly conserved signature motif (W-x(15,20)-[Gn]-L-W-x(2)-C-x(8,10)-C-x(15,16)-[qR]) (Gunzel and Yu, 2013). The second loop mediates, at least in part, Cldn-Cldn interaction, although the mechanism remains unclear (Piontek et al., 2008). The cytoplasmic tail domain shows sequence divergence among the Cldns and is predicted to be intracellular and largely disordered (Gunzel and Yu, 2013). It has been shown to play a role in trafficking of Cldns to the tight junction as well as in protein degradation (Gunzel and Yu, 2013). The end of the COOH tail contains a PDZ-binding motif in most Cldns (Schneeberger, 2003; Turksen and Troy, 2004), and this motif binds to the PDZ domains of TJ-associated plaque proteins that include the ZO family, MUPP1 and PATJ (Itoh et al., 1999). Notably, although the majority of Cldns have yet to be analyzed, the two regions labeled with stars in Fig 6 contain conserved cysteine residues whose palmitoylation has been suggested to be important for Cldn trafficking to the TJ (Van Itallie, 2005). The cytoplasmic tail domain also appears to be the major site for phosphorylation, which has been implicated in regulation of both Cldn localization and TJ formation (Aono and Hirai, 2008; D'Souza, 2005; Ikari, 2006; Ishizaki et al., 2003; Van Itallie et al., 2012). Please refer to Table 2 in Appendix 1 for an overview of currently mapped and predicted phospho-peptides in Cldn cytoplasmic domains and their physiological importance.

TJ strands are a "mosaic of multiple Cldn types" (Furuse, 2010) forming homotypic and heterotypic interactions between cells, although the generality of heterotypic binding is currently unknown (Anderson and Van Itallie, 2009). Formation of specific multimers has been postulated to affect the function of the resulting TJ, however only a few possible interactions have been investigated to date and results have been inconsistent (Daugherty

et al., 2007; Furuse et al., 1999; Piontek et al., 2011). More detailed Cldn structural information will hopefully resolve this ongoing debate. As noted above, the first extracellular loop of Cldns appears to determine paracellular permeability and thus overall resistance and charge selectivity (Anderson and Van Itallie, 2009). When Cldn2 was introduced into MDCK cells (normally devoid of Cldn2), the trans-epithelial resistance (TER) measurements decreased 20-fold, to measurements characteristic of MDCK II cells (which normally express Cldn2) (Furuse et al., 2001). Furthermore, overexpression of Cldn chimeras containing switched extracellular domains alters TER and permeability to Na^+ relative to Cl^- (Colegio et al., 2003; 2002). The nephron is a naturally occurring physiological example in which Cldn expression profiles determine regional paracellular properties, with Cldns 1, 2, 3, 4, 8, 10, 11 and 16 displaying segment-specific patterns of expression (Kiuchi-Saishin et al., 2002). A total of 18 Cldns have been tested for selectivity, as summarized in Table 3 in Appendix 1. Isoform expression and proportion (mixing ratios) of Cldns therefore creates tissue-specific barrier/channel properties of TJs (Furuse et al., 2001; Van Itallie and Anderson, 2006).

Mutations in Cldns have been causatively coupled to a number of human diseases (Heiskala et al., 2001) (refer to Table 1 of Appendix 1). For example, a mutated Cldn16 is responsible for familial hypomagnesemia with hypercalciuria, an autosomal recessive disease in which the kidney fails to re-absorb calcium and magnesium (Simon et al., 1999) while Cldn11 polymorphisms are associated with loss of TJ fibrils in Sertoli and CNS myelin cells, leading to male sterility and neurological defects (Gow et al., 1999). Although the primary condition of patients with Cldn1 deficiency is liver dysfunction due to neonatal sclerosing cholangitis (bile duct inflammation), they also present with

thickened, scaly skin (ichthyosis) (Hadj-Rabia et al., 2004).

Other TJ proteins

In addition to Occludin and the Cldns, two other TJ structural components have been identified to date, namely junctional adhesion molecule (JAM) and tricellulin. JAM, an IgG superfamily member, has also been shown to be expressed on the surface of circulating leukocytes, erythrocytes and platelets, and has diverse functions including barrier function and stabilization, migration, platelet activation, angiogenesis and retrovirus binding (Bazzoni, 2003; Mandell and Parkos, 2005; Martìn-Padura et al., 1998). Tricellulin was mostly recently identified as a TJ protein, and it is specifically enriched at vertically oriented TJ strands at tricellular contacts (Ikenouchi, 2005; Krug et al., 2009). Like Cldn14, this protein has been linked to recessive, nonsyndromic deafness (Nayak et al., 2013; Riazuddin et al., 2006). Interestingly, knockdown of Occludin in epithelial cells leads to mislocalization of tricellulin to bicellular TJs (Ikenouchi et al., 2008). Despite advancement in understanding its role, the function of tricellulin in TJs currently remains unclear.

TJ-Associated Cytoplasmic Proteins

The cytoplasmic face of the TJ contains aggregated multimolecular protein complexes termed the TJ 'plaque', the structural basis of which is PDZ domain-mediated protein-protein binding. The PDZ domain is a conserved 80–90 residue domain originally identified in Psd-95 (post-synaptic density protein 95), Dlg (Discs-large) and ZO1 (Zonula Occludens 1) (Ponting et al., 1997). There are two major functions of PDZ-domain-containing proteins in the TJ plaque: i) anchorage of integral membrane proteins

through interaction with their cytoplasmic tails and ii) binding to the PDZ domains of other proteins and facilitating the formation of scaffolding networks (Guillemot et al., 2008). Furthermore, several TJ proteins with PDZ-domains contain additional structural domains that have been linked to cellular signaling. TJ plaques also contain proteins that lack PDZ domains. From the literature to date, these proteins appear to regulate signaling at TJs but do not contribute to their structure. Using a proteomic approach, one laboratory analyzed the protein composition of TJs, identifying >912 potential protein components related to signaling, the cytoskeleton, cell adhesion, synapses, vesicular traffic, cell growth, cell migration, transcription and translation (Tang, 2006). Despite an increasing awareness that TJs function as signaling centers in the cell through their plaque proteins and the linking of TJ deregulation to various disease states (Förster, 2008; Kirschner et al., 2009), we are clearly only beginning to understand the complex role(s) these structures play in epithelia.

EPIDERMAL HOMEOSTASIS

Development and maintenance of a functional EPB: Challenges in early and late human life

i) Premature infants:

A variety of maternal and fetal diseases/conditions can lead to premature birth and, for reasons unknown, there have been dramatic increases in premature birth rates around the world over the last decade (Darmstadt et al., 2008; Lang and Iams, 2009; Yeaney et al., 2009). While term infants are born with a well-developed epidermal barrier, that same barrier is poorly developed in immature infants, contributing to neonatal sepsis and

mortality (Rutter, 2000; 1996; Saiman, 2006). Postnatally, the epidermal barrier develops rapidly, with barrier-related problems manifesting within the first week or two of life. For a 600g infant, this represents a critical window of time, and there is a distinct lack of successful approaches/strategies for accelerating the postnatal maturation of the epidermis (McIntire and Leveno, 2008; Shapiro-Mendoza et al., 2008; 2006; Tyson et al., 2008). Topical application of emollients has proven to have some benefit, although it is unclear whether this is providing a temporary pseudo-barrier or inducing signaling pathway responses (Darmstadt et al., 2008). Dissection of the underlying mechanisms, as well as screening for novel therapeutics that may accelerate postnatal barrier function, have been impeded by a lack of suitable models for investigation (Ratajczak et al., 2010).

ii) Intrinsic and extrinsic aging of the human skin

Aging of the skin is a complex biological phenomenon with both intrinsic and extrinsic components. Intrinsic aging is an inevitable set of physical changes due to the passage of time, while extrinsic aging is caused by environmental exposures such as UV, chemicals and pollutants. The latter is more commonly referred to as "photoaging", given that UV-irradiation is the most fundamental type of exposure and can damage skin to such an extent that it appears prematurely aged. While extrinsic factors affect mainly the dermis, intrinsic factors affect the epidermis and are manifested as biochemical changes that include hyperplasia and reduced capacity to repair. These can result in skin conditions such as dermatitis, eczema and ulceration (Davies, 2008; Elias and Ghadially, 2002; Ghadially, 1998; Kligman, 1989; Makrantonaki and Zouboulis, 2007; Ward, 2005). Barrier function was only recently assessed for the first time in aging skin (Barland et al., 2004), with observation of a decreased stratum corneum integrity and a reduced capacity

for barrier homeostasis/repair (Ghadially, 1998). No analysis of Cldn expression in aging skin has yet been reported. There is also a lack of mouse models to study aging skin, as mouse skin does not normally undergo comparable aging-related changes. Knockout mice for a variety of dermal factors that are naturally down-regulated with age have been helpful in understanding the aging dermis (Danielson et al., 1997; Kyriakides et al., 1998; Svensson, 1999), however, as have mouse models used to study photoaging.

Epidermal renewal: Regulation of Proliferation and Differentiation

A tight balance between proliferation and differentiation forms the basis of epidermal renewal, with homeostasis maintained throughout life in response to discrete signals whereby epidermal cells in the proliferative basal compartment become irreversibly committed to terminal differentiation and move upwards away from the basal layer (Byrne, 1997; Fuchs and Horsley, 2008; Ivanova et al., 2005; Turksen and Troy, 1998). A number of key players have been identified to date, and their dysfunction linked to proliferative skin diseases and cancer.

i) MAPK cascade

The mitogen-activated protein kinase (MAPK) cascade plays a key role in regulation of the proliferation/differentiation axis. This cascade is conserved in mammals and is controlled by a variety of upstream signaling inputs (Roux and Blenis, 2004). Activation of the MAPK pathway during normal epidermal homeostasis is mediated by receptor tyrosine kinases including epidermal growth factor receptor (EGFR) (Janes and Watt, 2006) and insulin growth factor receptor 1 (IGFR1) (Boulton et al., 1991), and is negatively regulated by Integrin-related adhesion molecules (Aplin et al., 1999). Briefly,

in non-stimulated conditions, extracellular signal-regulated kinases (ERKs) are anchored in the cytoplasm by association with MAPK kinases (MEKs) (Fukuda et al., 1997) and the microtubule network (Reszka et al., 1995). Upstream stimuli activate the MAPK cascade, resulting in ERK1/2 phosphorylation (Tyr204/187) and rapid and transient activation of kinase activity (peaks at 5-10 minutes). This is followed by a second phosphorylation event (Thr202/185) and lower but maintained activity that continues throughout the G1 phase of the cell cycle (Meloche et al., 1992; Schmidt, 2000). Following the initial phosphorylation event, ERK1/2 dissociates from MEK1/2 and is free to translocate to the nucleus. Nuclear localization is maintained during the entire G1 phase but is dependent on persistence of the mitogenic stimulus. ERK1/2 activation and nuclear translocation have been shown to be necessary but not sufficient for S-phase entry (Cheng et al., 1998; Treinies et al., 1999; Yamamoto et al., 2006), and ERK1/2 is rapidly dephosphorylated and inactivated following the G1/S transition.

Knockout of MEK1/2 in mouse epidermis results in hypoplasia, dehydration and perinatal death due to compromised barrier function (Scholl et al., 2007), while RNAi-mediated knockdown of MEK1/2 in human keratinocytes also yields hypoplasia that can be rescued by overexpression of active ERK2 (Scholl et al., 2007). In contrast, inducible MEK1 overexpression in mouse adult epidermis phenocopies the effects of inducible activation of Ras or Raf in mouse epidermis, namely hyperproliferation, epidermal hyperplasia and downregulation of differentiation markers (Scholl et al., 2004; Tarutani et al., 2003). These studies point to an essential role for the MAPK pathway in epidermal development. Moreover, most squamous cell carcinomas (SCCs) are characterized by Ras activation and downstream up-regulation of MAPK activity (Khavari and Rinn

2007). Mechanistic studies have revealed that the pro-proliferative phenotype of MAPK pathway activation is mediated, at least in part, by transcriptional activation of the growth-promoting Myc oncogene (Atanasova et al., 2007; Gramling and Eischen, 2012).

ii) Myc

Myc, along with Notch1 (discussed below), is a key regulator of the switch from proliferation to differentiation in keratinocytes ((Kolly et al., 2005); Fig. 7). The Myc transcription factor family has been strongly implicated in the control of cell proliferation, differentiation, apoptosis and cancer development (Boxer and Dang, 2001; Grandori et al., 2000; Nilsson et al., 2007), and overexpression of Myc genes has been found in 70% of all rapidly dividing tumors (Boxer and Dang, 2001). Mechanistically, induced Myc expression in mouse fibroblasts is sufficient to drive quiescent (Go) cells into G1 phase and accelerate the proliferation rate (Cavalieri and Goldfarb, 1987). This occurs, at least in part, via its ability to down-regulate levels of $p27^{Kip1}$, both at the protein level (Keller et al., 2007; Yang et al., 2001) and by $p27^{Kip1}$ sequestration (Muller et al., 1997; Perez-Roger et al., 1999; Vlach et al., 1996). Nuclear clearance of c-Myc is therefore required for exit from the cell cycle and commitment to differentiation (Kolly et al., 2005; Waikel et al., 1999).

iii) Notch signaling

Activation of the canonical Notch pathway, triggered by cell-cell contact in culture (Kolly et al., 2005) and by layer-specific expression of ligand and receptors in whole tissues (Blanpain et al., 2006; Moriyama et al., 2008; Vooijs et al., 2006; Watt et al., 2008), is a direct determinant of keratinocyte entry into differentiation (Rangarajan et al., 2001). The best-characterized pathway leading to Notch activation in the epidermis

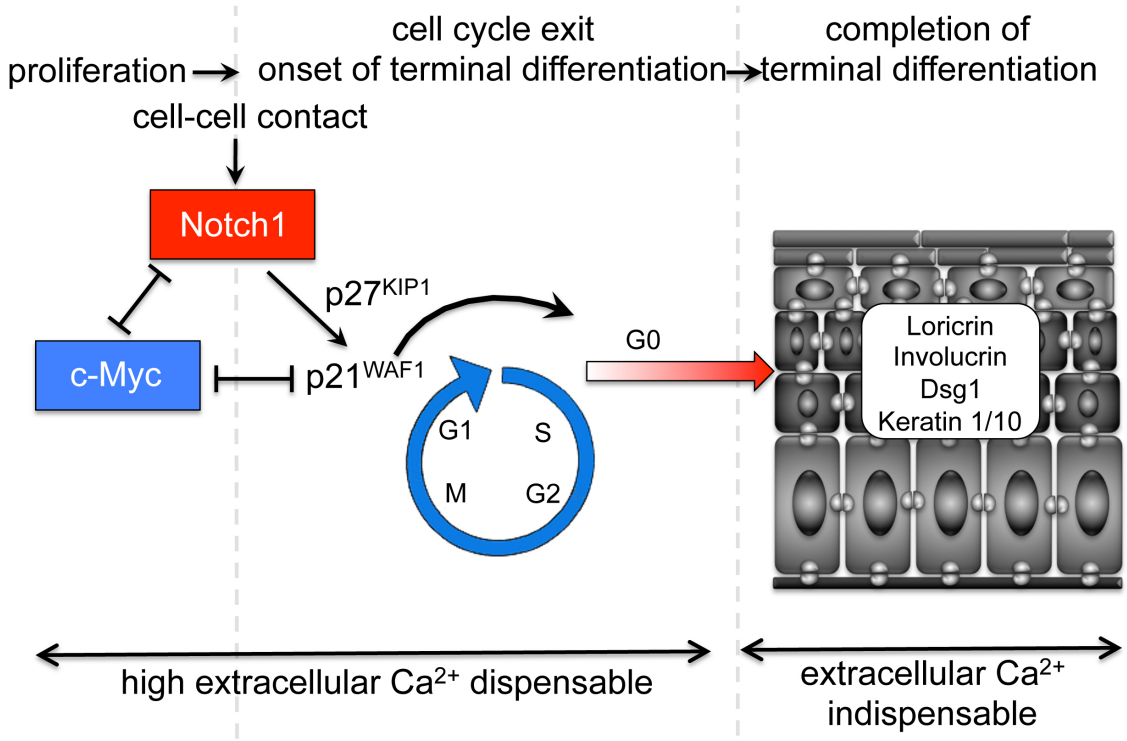

Figure 7. Roles of c-Myc and Notch1 in proliferation, cell cycle exit, and terminal differentiation in keratinocytes. Exit from the cell cycle is triggered at confluency when Notch1 is activated and c-Myc inhibited. These two factors are key determinants in this process and in control of $p21^{WAF1}$ and $p27^{KIP1}$. *Adapted by permission from Macmillan Publisher Ltd: [Journal of Investigative Dermatology] (Kolly et al., 2005), copyright (2005).*

involves the binding of Delta1 or Jagged ligands on neighboring cells, followed by Notch receptor cleavage by a γ-secretase complex. This produces a free intracellular domain of Notch (NICD) that translocates to the nucleus to activate transcription of target genes (Baron, 2003; Mumm and Kopan, 2000). Targeted inactivation of the Notch pathway in mice by knockout of any Notch pathway receptor, enzyme or relaying transcription factor leads to abrogated differentiation and loss of the skin barrier (Blanpain et al., 2006; Moriyama et al., 2008). Conversely, overexpression of NICD in the epidermis leads to expansion of differentiated layers (Blanpain and Fuchs, 2006; Uyttendaele et al., 2004). Collectively, these studies indicate that Notch activation regulates differentiation onset in the epidermis.

iv) Ca^{2+} gradient

The regulation of growth and differentiation by calcium (Ca^{2+}) is fundamental to cell physiology (Breitwieser, 2008), with the epidermis serving as a canonical model for such Ca^{2+}-mediated processes (Watt et al., 1991). Ion-capture cytochemistry and proton-induced X-ray emission analyses have determined that a distinct Ca^{2+} gradient exists in the mammalian epidermis (Fig. 4), increasing from the basal layer and reaching a maximum at the outer granular layer and then decreasing again in the stratum corneum (Kömüves et al., 2002; Menon et al., 1985). While factors responsible for formation and maintenance of the Ca^{2+} gradient remain unclear, its initial setup coincides with barrier formation in development (Elias et al., 1998) and it is indispensible for proper epidermal differentiation (Bikle and Pillai, 1993; Elias and Feingold, 2001). The 'confluency switch' from proliferation to differentiation, which includes nuclear clearance of myc and activation of Notch, is dominant and will occur irrespective of Ca^{2+} conditions, however

extracellular Ca^{2+} is required after the switch to terminal differentiation to sustain upregulation of key proteins and intracellular adhesion molecules (Fig. 4). A common characteristic of skin diseases with abnormal barrier function, such as psoriasis, is loss of the calcium gradient (Menon and Elias, 1991).

v) Autocrine/paracrine signaling

Signaling via autocrine (self-secreted) and paracrine (secreted by neighbouring cells) factors play key roles in maintenance of the proliferation/differentiation axis in the epidermis. Paracrine signaling occurs between epidermal keratinocytes and dermal fibroblasts. Interleukin-1α (IL1α) is a secreted factor expressed in basal keratinocytes important for regulating epidermal proliferation by inducing the expression of fibroblast-derived growth factors such as KGF and FGF10 (Maas-Szabowski and Fusenig, 1996; Maas-Szabowski et al., 1999). These factors then complete the paracrine loop by inducing proliferation of epidermal keratinocytes (Marchese et al., 1990). In culture, keratinocytes can be co-cultured with fibroblasts to promote growth, or with engineered gel matrices containing soluble bioactive growth factors (Bader and Kao, 2009), with the latter holding therapeutic implications for wound healing. Keratinocytes also have the ability to proliferate in an autocrine manner in culture, through the secretion of mitogenic factors such as IGF-1 and EGF and downstream activation of MAPK pathways (Cook et al., 1991; Piepkorn et al., 1994; Pittelkow et al., 1993; Pozzi et al., 2004; Shipley et al., 1989). They can also secrete growth inhibitors, including transforming growth factor β (TGF-β), IGFBP-6 and heparin sulfate (Kato et al., 1995; Shipley et al., 1989).

vi) Growth factors

The insulin-like growth factors (IGF-1 and IGF-2) and epidermal growth factor (EGF) are potent regulators of migration and proliferation (Cook et al., 1991; Duan and Xu, 2005). IGFs are found throughout the body almost entirely in association with six specific, high affinity binding proteins (IGFBP-1-6) that determine IGF availability and activity. The IGFs signal through the type 1 IGF receptor (IGF1R), a heterotetramer with tyrosine kinase activity. The importance of the IGF system to normal epidermal development and differentiation is well established (Liu et al., 1993; Sadagurski et al., 2006). Furthermore, increasing levels of IGFs or IGF1R in human samples are associated with increases in cell proliferation, skin hyperplasia and tumorigenesis (Kanter-Lewensohn et al., 2000).

EGF induces cell proliferation in a variety of cell types by binding to a tyrosine kinase receptor (EGFR) (Yarden and Ullrich, 1988). Ligation of this receptor by EGF activates the MAPK pathway, through Ras-dependent or –independent signaling (Gao et al., 2005; Kato et al., 1998). These pathways downstream of the EGFR are often found to be aberrantly activated in cancer, and are thus promising targets for therapeutic intervention (Roberts and Der, 2007).

Keratinocyte growth factor (KGF)/fibroblast growth factor-7 (FGF-7) is an epithelium-specific paracrine growth factor. It acts through the FGF-7 receptor (FGFR2/IIIb) exclusively, and plays an essential role in the growth of keratinocytes. It is frequently overexpressed in cancers, switching paracrine stimulation of KGF/FGF-7 to an autocrine loop (Niu et al., 2006). It has been demonstrated that KGF has an important role in wound healing, as it stimulates proliferation and migration of these cells (Werner, 1998; Werner et al., 1994). For a list of additional growth factors that have been shown to act

on keratinocytes, please refer to Table 4 in Appendix 1.

vii) TJ-based signaling

TJs can influence gene expression and cell proliferation by a number of mechanisms, including cytoplasmic sequestration of transcription factors. ZO1, for example, accumulates at TJs but also shuttles to the nucleus. It has been demonstrated to directly interact with and sequester the transcription factor ZONAB (ZO1-associated nucleic-acid binding) at TJs. Localization (nuclear in proliferating cells or TJ-associated in differentiating cells) and thus transcriptional activity of ZONAB is regulated by cytoplasmic sequestration (Balda, 2003; Balda and Matter, 2000; Frankel et al., 2005; Kavanagh et al., 2006; Sourisseau et al., 2006). In theory, a similar regulatory mechanism could be proposed for all TJ plaque proteins that localize at both TJs and the nucleus, including ZO1, ZO2, and the Partitioning-defective (Par) proteins Par3 and Par6 (Cline and Nelson, 2007; Fang et al., 2007). TJ proteins can also affect transcription factors indirectly via regulation of small GTPases. Cingulin acts in this manner, having been shown to control Cldn2 expression and cell proliferation by regulation of RhoA activity (Citi et al., 2009; Guillemot et al., 2012). Although this is not an exhaustive list of possible mechanisms, it represents evidence pointing to TJs playing signaling roles in epithelial cells.

The roles of Cldns in epidermal development and maintenance

Cldn6 was one of the first Cldns identified, and is found in both endodermal and epidermal tissues (Turksen and Troy, 2001). While the functional effects of conditional knockout of Cldn6 in endodermal tissue have been studied (Anderson et al., 2008), a

model of epidermal Cldn6 knockout has yet to be reported. To determine its role in epidermal development and homeostasis, transgenic mice overexpressing full-length Cldn6 in suprabasal epidermal tissue (driven by the Involucrin promoter) were generated. Founder *Inv-Cldn6* transgenic animals died within 2 days of birth, with dehydration assays and trans-epidermal water-loss measurements revealing severe EPB dysfunction. This study provided the first insight into the importance of Cldn6 to EPB integrity. Interestingly, the overexpression phenotype showed an expression-level dependence, as analysis of the heterozygous transgenic counterparts revealed a less severe defect in barrier function. In these mice, delayed formation of the barrier is resolved by postnatal completion after 12 days (Troy et al., 2005a). Overexpression of a Cldn6 mutant lacking the entire C-terminal tail domain did not fold properly and was not efficiently recruited to the plasma membrane, thus limiting the applicability of this model for studying TJ-related signaling roles (Arabzadeh et al., 2006). Table 5 in Appendix 1 presents an overview of all epidermal-targeted Cldn6 overexpressing mouse models.

Given that Cldns contain distinct C-terminal cytoplasmic tail regions that are subject to post-translational modifications and can interact with intercellular factors such as the ZO family of proteins, **we hypothesized that the C-terminal tail of Cldn6 mediates TJ-related signaling.** We addressed this hypothesis through two specific aims:

AIM 1. Assess the importance of the C-terminal tail for Cldn6 function by generating transgenic mice overexpressing more minimal truncation mutants in epidermal tissues.

AIM 2. Identify and functionally characterize intracellular proteins that interact with the C-terminal Cldn6 tail.

CHAPTER 1:

Dermatitis and Aging-Related Barrier Dysfunction in Transgenic Mice Overexpressing an Epidermal-Targeted Claudin 6 Tail Deletion Mutant

Tammy-Claire Troy[1], Azadeh Arabzadeh[1,2], Nathalie M.K. Larivière[1,2], Adebola Enikanolaiye[1,2], Kursad Turksen[1,2,3,4*]

[1] Sprott Centre for Stem Cell Research at the Ottawa Hospital Research Institute, Ottawa, Ontario, Canada

[2] Department of Cellular and Molecular Medicine, University of Ottawa, Ottawa, Ontario, Canada

[3] Divisions of Dermatology and Endocrinology, Department of Medicine, University of Ottawa, Ottawa, Ontario, Canada

[4] Division of Reproductive Endocrinology, Department of Obstetrics, Gynaecology, Faculty of Medicine, University of Ottawa, Ottawa, Ontario, Canada

CONTRIBUTIONS

This manuscript was published in PLoS ONE in December of 2009.

Troy, T.-C., Arabzadeh, A., **Lariviere, N. M. K.,** Enikanolaiye, A. and Turksen, K. (2009). Dermatitis and aging-related barrier dysfunction in transgenic mice overexpressing an epidermal-targeted claudin 6 tail deletion mutant. *PLoS ONE* **4**, e7814.

For the immunohistochemistry in this manuscript, replicates were performed by myself (NL), Adebola Enikanolaiye (AE) or Azadeh Arabzadeh (AA). In addition I had a major role in tissue collection, fixation and processing with assistance from Tammy-Claire Troy (TCT) and AA. AE and I were co-responsible for all experiments for revisions. I contributed to written changes for revisions and manuscript editing. TCT assisted with experimentation and wrote the manuscript for first submission. Experiments were conceived and designed by Kursad Turksen who was responsible for final editing and approval of the manuscript.

The lab manager TCT is the first author as she contributed a number of previously established protocols toward these studies and optimized protocols for this particular mouse model. She also wrote the initial manuscript for submission. My colleague AA made some of the initial observations regarding the dermatitis in these mice and for this she earned the second authorship position. I played a major role in all aspects of this paper and appear third in line in the authorships.

ABSTRACT

The barrier function of the skin protects the mammalian body against infection, dehydration, UV irradiation and temperature fluctuation. Barrier function is reduced with the skin's intrinsic aging process, however the molecular mechanisms involved are unknown. We previously demonstrated that Claudin (Cldn)-containing tight junctions (TJs) are essential in the development of the epidermis and that transgenic mice overexpressing Cldn6 in the suprabasal layers of the epidermis undergo a perturbed terminal differentiation program characterized in part by reduced barrier function. To dissect further the mechanisms by which Cldn6 acts during epidermal differentiation, we overexpressed a Cldn6 cytoplasmic tail deletion mutant in the suprabasal compartment of the transgenic mouse epidermis. Although there were no gross phenotypic abnormalities at birth, subtle epidermal anomalies were present that disappeared by one month of age, indicative of a robust injury response. However, with aging, epidermal changes with eventual chronic dermatitis appeared with a concomitant barrier dysfunction manifested in increased trans-epidermal water loss. Immunohistochemical analysis revealed aberrant suprabasal Cldn localization with marked down-regulation of Cldn1. Both the proliferative and terminal differentiation compartments were perturbed as evidenced by mislocalization of multiple epidermal markers. These results suggest that the normally robust injury response mechanism of the epidermis is lost in the aging Involucrin-Cldn6-CΔ196 transgenic epidermis, and provide a model for evaluation of aging-related skin changes.

INTRODUCTION

Formed during development by a series of cell commitment, mesenchymal-epithelial cell interactions, and terminal differentiation, the mammalian epidermis undergoes continuous self-renewal in a tightly regulated process of epidermal cell proliferation and differentiation (Fuchs, 2007; Fuchs and Raghavan, 2002; Turksen and Troy, 1998). As the end result of terminal differentiation, the robust barrier function of the skin protects against microorganism invasion and UV irradiation, inhibits water loss, regulates body temperature and is an important part of the host defense system (Pouillot et al., 2008). These important functions decline in efficiency with aging, leading to an inefficient epidermal injury response and dermatitis (Elias and Ghadially, 2002; Elias et al., 2008; Ghadially, 1998), for reasons that are not yet understood.

Tight junctions (TJs) are essential not only for dividing epidermal cells into apical and basolateral compartments to create cell polarity (Farquhar and Palade, 1963), but also for the existence of skin barrier function by regulating the selective permeability of the paracellular pathway (Chiba et al., 2008; Krause et al., 2008; Paris et al., 2008). The selectivity function of TJs is imparted by Claudins (Cldns), a family of 23 highly conserved tetraspan membrane proteins whose heterogeneity stems in large part from distinctly charged amino acid sequences in the first external loop (Chiba et al., 2008; Katoh, 2003; Turksen and Troy, 2004). Cldn type and mixing ratio thus provide for the specific permeability requirements of different epithelia (Turksen and Troy, 2004). The importance of Cldns in epidermal differentiation and barrier function has been confirmed by experiments in which Cldn expression has been perturbed in epidermal cells; for

example, Cldn1 knockout mice die shortly after birth due to skin barrier dysfunction (Furuse et al., 2002). Involucrin-Cldn6 (Inv-Cldn6) transgenic mice also suffer skin barrier dysfunction, the severity/lethality of which is dependent upon the level of Cldn6 overexpression (Troy et al., 2005a; Turksen and Troy, 2002). Further, Inv-Cldn6-CΔ187 transgenic mice overexpressing a cytoplasmic tail-ablated Cldn6 display epidermal hyperproliferation, apparently due to an inefficiency of Cldn protein membrane targeting, as a result of the unfolded protein response pathway (Arabzadeh et al., 2006).

The latter data suggest the importance of the cytoplasmic tail portion of Cldn molecules in cell signaling during epidermal differentiation. The cytoplasmic tail of different Cldns, while relatively constant in length, is divergent in sequence, but a number of putative functional protein domains are present in many family members (Gonzalez-Mariscal et al., 2003; Turksen and Troy, 2004). To address the activities of the functional domains in more detail, we again used the Involucrin promoter (Inv) this time to target a shorter deletion in the cytoplasmic tail (Cldn6-CΔ196) to the differentiative compartment of the epidermis. The Inv-Cldn6-CΔ196 transgenic mice possess subtle epidermal differentiation abnormalities at birth that by 1-month of age are completely normalized. However, with aging, Inv-Cldn6-CΔ196 mice suffered dermatitis, often manifested as patent wounds in repetitive grooming areas. Normal hydration levels were not maintained in the aging skin, and immunohistochemistry revealed perturbations in the expression and localization of multiple Cldns, as well as various classical markers of epidermal differentiation. These results suggest that the normally robust injury response mechanism of the epidermis is lost in the aging Inv-Cldn6-CΔ196 transgenic epidermis and provides a model for evaluation of chronic dermatitis and aging-related skin changes.

METHODS

Generation of Inv-Cldn6-CΔ196 transgenic mice

The Inv-Cldn6-CΔ196 construct (Troy and Turksen, 2007) was injected into ova collected from superovulated CD1 mice to generate viable lines at the Ottawa Hospital Research Institute (OHRI) Transgenic Mouse Facility as previously described (Troy et al., 2007b). Genotyping was performed by PCR using genomic DNA and primers specific for Cldn6 (5'-ATG GCC TCT ACT GGT CTG CA-3') and the FLAG® tag (5'-TCA CTT GTC ATC GTC GTC CTT G-3'). Age-matched wild type and Inv-Cldn6-CΔ196 transgenic mice were photographed using a Nikon COOL-PIX950 digital camera (Nikon) for image processing with Adobe Photoshop version 7.0 (Adobe Systems). All research complied with the principles and guidelines of the Canadian Council on Animal Care and was approved by the Ottawa Hospital Research Institute Animal Care Committee. Once the dermatitis phenotype became unmanageable, Inv-Cldn6-CΔ196 transgenic mice were euthanized according to institutional and legislative policies.

Sample preparation, histology and immunohistochemistry

a) Sample collection. Freshly dissected skin samples (~1 cm^2) were collected at various postnatal time points (birth, 1 week, 2 weeks, 3 weeks, 1 month, 2 months, 3 months, 5 months, 6 months) from either the mid-dorsal region or areas of frequent grooming (e.g. the neck and behind the ears) of Inv-Cldn6-CΔ196 transgenic mice and their age-matched CD1 counterparts.

b) Frozen sections. Frozen sections were required for immunolocalization with FLAG®

antibodies, whereas histology and all other immunostaining procedures were performed using paraffin-embedded sections. For frozen sections, skin samples were embedded in HistoPrep (Fisher Scientific), solidified using dry ice-chilled isopentane and 5 μm sections were mounted onto Superfrost®/Plus slides (Fisher Scientific) as described (Arabzadeh et al., 2006). Samples were fixed for 10 minutes in methanol (-20°C) and washed with PBS before immunohistochemistry (see below).

c) Paraffin sections and histology. For paraffin sections, skin samples were fixed overnight in Bouin's solution (75% saturated picric acid, 20% formaldehyde, 5% glacial acetic acid) and dehydrated via a graded series of ethanol washes (from 30% to 100%) before paraffin embedding and sectioning (5 μm). Sections mounted onto Superfrost®/Plus slides (Fisher Scientific) were dewaxed using toluene and rehydrated in a reverse graded series of ethanol washes to water. Following antigen unmasking and washing in PBS, sections were either stained with hematoxylin and eosin (H&E) as described (Troy et al., 2005a) or further processed for immunohistochemistry (see below).

d) Immunohistochemistry. After blocking for non-specific antibody binding (10% goat serum, 0.8% BSA, 1% gelatin in PBS), skin samples were incubated for 1 hour in antibodies appropriately diluted in incubation buffer (1% goat serum, 0.8% BSA, 1% gelatin in PBS) (Troy et al., 2005a). Antibodies recognizing the following proteins were used: FLAG® (M2 monoclonal) (1:440; Sigma), K15 (1:100; rabbit #UC55), K5 (1:100; rabbit #5054), K14 (1:100; rabbit #199), K1 (1:100; rabbit #UC81), K6 (1:200; BabCO), K17 (1:500; a gift from Dr. Pierre Coulombe, Johns Hopkins), involucrin (1:100;

BabCO), filaggrin (1:100; BabCO), loricrin (1:100; rabbit #UC84), Cldn1 (6:100; Zymed Laboratories), Cldn2 (1:200; Zymed Laboratories), Cldn3 (1:50; Zymed Laboratories), Cldn5 (1:100; Zymed Laboratories), Cldn6 (1:100; hen #3677), Cldn11 (1:100; hen #3680), Cldn12 (1:100; hen #5186) and Cldn18 (1:100; rabbit #A9953). Following washes (0.8% BSA, 1% gelatin in PBS), skin samples were incubated for 1 hour at room temperature with FITC-conjugated secondary antibodies against mouse, rabbit and chicken (1:50; Jackson ImmunoResearch) diluted in incubation buffer. After washes in wash buffer and PBS, sections were mounted with Moviol 4–88 (Calbiochem) containing 2.5% 1,4 diazobicyclo-[2,2,2]-octane (DABCO; Sigma) for observation on a Zeiss Axioplan 2 fluorescence microscope equipped with an AxioCam camera and Axio Vision 2.05 software (Carl Zeiss); digital images were processed using Adobe Photoshop version 7.0 (Adobe Systems).

Protein isolation and immunoblotting

Skin samples (0.4 g) were dissected from either the mid-dorsal region or areas of frequent grooming (e.g. the neck and behind the ears) of Inv-Cldn6-CΔ196 transgenic mice and their age-matched CD1 counterparts and whole cell protein extracts were prepared by homogenizing in SDS extraction buffer (62.5 mM Tris pH 6.8, 25% glycerol, 2% SDS and 2% β-mercaptoethanol with pepstatin A and a complete mini protease inhibitor cocktail tablet [Roche]) followed by centrifugation. Following a 30-minute incubation in sample reducing buffer (62.5 mM Tris pH 6.8, 25% glycerol, 2% SDS, 0.1% bromophenol blue and 2% β-mercaptoethanol), boiling and centrifugation, 10 μg of soluble proteins were separated on 12% SDS-polyacrylamide gels and transferred to

nitrocellulose (Arabzadeh et al., 2006). After blocking for non-specific antibody binding (5% skim milk, TBS/0.1% tween-20 [TBS-T]), blots were incubated at 4°C overnight with diluted (5% skim milk, TBS-T) antibodies against FLAG® (polyclonal) (1:500; Sigma) and GAPDH (1:20,000; Abcam). After several washes in TBS-T, blots were incubated in diluted (5% skim milk, TBS-T) HRP-conjugated antibodies against mouse and rabbit IgG (1:20,000; Amersham) for 1 hour at room temperature and washed with TBS-T before incubation with chemiluminescent HRP substrate (Millipore) and visualization on BioMax XAR autoradiography film (Kodak). Films were scanned and digital images were prepared using Adobe Photoshop version 7.0 (Adobe Systems).

Barrier integrity assay

Trans-epidermal water loss (e.g. impedence) of both Inv-Cldn6-CΔ196 transgenic and wild type mouse skin was measured using a dermal phase meter (DPM) (Nova Technology Corporation) as described (Turksen and Troy, 2002). Diminished barrier integrity is reflected in higher DPM values over time as depicted digitally with EDWINA software (Nova Technology Corporation) and converted into graphical form with Excel software (Microsoft).

Cornified envelope extracts

Using dorsal skin samples of CD1 and Inv-Cldn6-CΔ196 transgenic mice, purified cornified envelope extracts were prepared as described (Hohl et al., 1991; Troy and Turksen, 2005; Turksen and Troy, 2002). Briefly, skin samples were immersed in hot extraction buffer (0.1 M Tris-HCl pH 8.5, 2% SDS, 20 mM dithiothreitol, 5 mM EDTA),

followed by 15-minute incubation at 95°C and gentle centrifugation before observation using an Olympus CK2 inverted microscope (Olympus) equipped with a Nikon COOLPIX 4500 digital camera (Nikon). Images were produced with Adobe Photoshop version 7.0 (Adobe Systems).

RESULTS

Generation and expression analysis of Inv-Cldn6-CΔ196 transgenic mice

We previously reported that overexpression of a Cldn6 lacking the C-terminal half of the cytoplasmic tail domain (e.g. truncation after amino acid 196; Cldn6-CΔ196) (Figure 1A-C) in the suprabasal compartment of the mouse epidermis results in marked hyperproliferative squamous invaginations/cysts replacing hair follicles and lethal epidermal barrier dysfunction (Troy and Turksen, 2007). The rationale for generating the Δ196 mutation was based on two main factors. First, we already knew that tailless Cldn6 was not targeting to the membrane appropriately. Second, we wanted to delete the PDZ domain that is at the tip of the cytoplasmic tail as well as putative phosphorylation sites, which could be accomplished by deletion from amino acid 196. The choice of 196 rather than 195 or 197, both of which would also have accomplished removal of the PDZ and putative phosphorylation sites, was one of convenience for the steps required to make our mutant insert. Because we have demonstrated previously that the level of Cldn6 overexpression correlates to the severity of the phenotype (Troy et al., 2005a; Turksen and Troy, 2002), we re-derived F0s with lower Cldn6-CΔ196 expression to avoid lethality and explore the function of the Cldn6 tail in postnatal animals; levels of

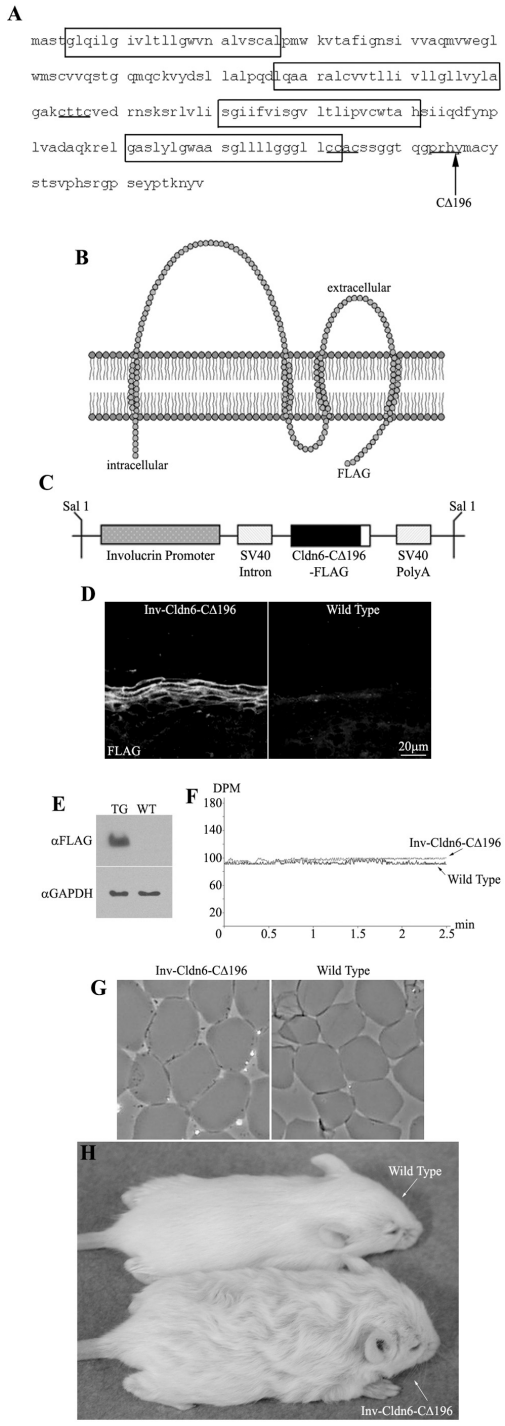

Figure 1. Inv-Cldn6-CΔ196 transgenic mice. The Cldn6 protein sequence is shown; transmembrane-spanning regions are encased within boxes, the CXXC motifs are underlined, and the truncation site is indicated with an arrow (A). The Inv-Cldn6-CΔ196 mutant was created by deleting the C-terminal half of the cytoplasmic tail domain of Cldn6 after amino acid 196 (B). The Inv promoter was use to drive transgene expression to the suprabasal compartment of the transgenic mouse epidermis, where TJs are localized (C). Transgene expression was confirmed to be restricted to the upper spinous and granular layers of the epidermis as visualized by immunohistochemistry using anti-FLAG antibodies (D) and immunoblotting confirmed a ~19.5kDa band corresponding to the transgene product in skin samples from transgenic (TG) but not wild type (WT) skin samples using anti-GAPDH as a loading control (E). Trans-epidermal water loss measurements confirmed no skin barrier dysfunction in the Inv-Cldn6-CΔ196 transgenic mice at birth (F). This was further supported by evaluation of cornified envelopes; which were characterized by a rigid shape and uniform size comparable to that of the wild type (G). Inv-Cldn6-CΔ196 mice were easily identifiable by their frizzed and lackluster coat appearance as compared to the wild type, a phenotype that persisted throughout life (H).

expression of the mutant Cldn6 is half of that observed in our previously generated mice. Nine Inv-Cldn6-CΔ196 positive F0 transgenic mice (five females and four males) were generated and three viable lines exhibiting indistinguishable phenotypes were successfully established. Cldn6-CΔ196 expression was confirmed to be confined to the upper spinous and granular layers of the epidermis and localized to cell membranes, mimicking endogenous Cldn6 expression (Figure 1D). Immunoblotting confirmed a ~19.5kDa band corresponding to the transgene product in skin samples from Inv-Cldn6-CΔ196 but not wild type littermates (Figure 1E).

Inv-Cldn6-CΔ196 neonates displayed no gross phenotypic anomalies compared to their wild type counterparts; trans-epidermal water loss (TEWL) measurements (DPM in the range of 98–105).

Epidermal maturation is delayed in Inv-Cldn6-CΔ196 mice

Although in the epidermis there were no gross phenotypic abnormalities or barrier dysfunction apparent at birth, histological examination revealed that the newborn (Figure 2A) and 1 week- old (not shown) transgenic epidermis was moderately thicker than that of the wild type, with a thicker stratum corneum, a less- compacted granular layer and an overall expanded suprabasal compartment. By 2-weeks of age, the Inv-Cldn6-CΔ196 epidermis displayed a more compact and organized granular layer, but it remained less mature and thicker than that in the wild type animals (Figure 2B). Typical epidermal thinning had commenced in the transgenic epidermis by 3-weeks of age (~1 week later than wild type; not shown) and by 1-month of age the Inv-Cldn6-CΔ196 transgenic

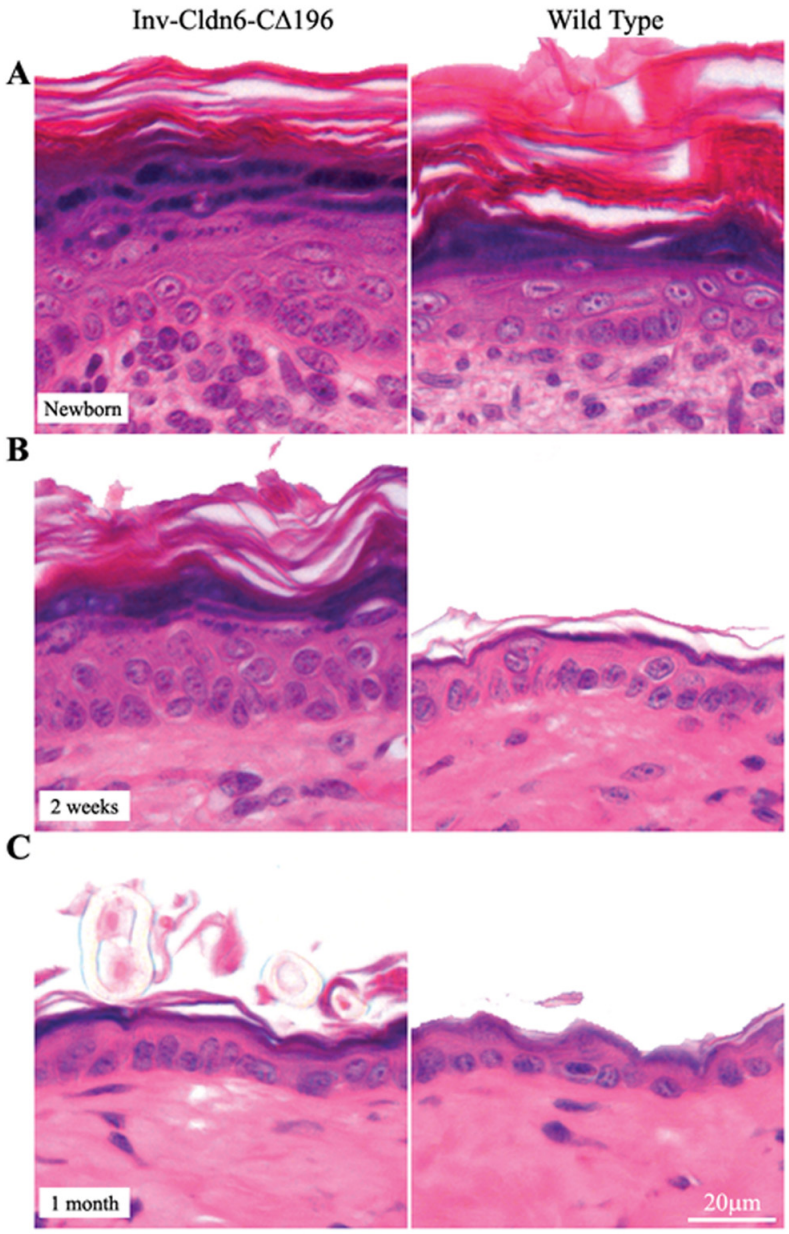

Figure 2. Histological abnormalities in the Inv-Cldn6-CΔ196 transgenic epidermis. Histological analysis of newborn (A) Inv- Cldn6-CΔ196 transgenic mice as compared to the wild type revealed a moderately thicker epidermis in transgenic samples, with a thicker stratum corneum, a less-compacted granular layer and an overall expanded suprabasal compartment. At 2-weeks of age (B), the Inv- Cldn6-CΔ196 epidermis remained somewhat less mature and thicker than that of the wild type; however by 1-month of age (C) the transgenic and wild type samples were histologically indistinguishable.

epidermis was epidermis was histologically indistinguishable from that of the wild type (Figure 2C).

Consistent with the histological results, abnormalities in the expression of epidermal differentiation markers were present in neonatal Inv-Cldn6-CΔ196 mice but these also normalized by 1-month of age (Figure 3; the transgenic and wild type epidermis after 2 weeks and 1 month are shown). For example, K5 and K15 were restricted to basal cells at all time points in both the wild type and Inv-Cldn6-CΔ196 epidermis (not shown), but K14, another basal compartment marker, occupied an expanded zone extending into the suprabasal compartment at birth and until epidermal thinning was achieved in the Inv-Cldn6-CΔ196 epidermis (Figure 3A). The suprabasal layers of the epidermis normally express K1 (Fuchs and Byrne, 1994), and when in a state of hyperproliferation, K6 and K17 (Leigh et al., 1995; McGowan and Coulombe, 1998a; 1998b). While neither K6 nor K17 was expressed throughout the time analyzed (not shown), a broadened compartment of K1-positive cells, consistent with the increased number of suprabasal cell layers observed histologically, was seen early but normalized by 1-month of age in the Inv-Cldn6-CΔ196 transgenic epidermis (Figure 3B). Similarly the expression compartments of various structural proteins in the stratum corneum, including involucrin (Figure 3C), filaggrin and loricrin (not shown), were also expanded in the juvenile Inv-Cldn6-CΔ196 epidermis, and a tightly compacted stratum corneum was not observed in the transgenic epidermis until thinning comparable to that in the wild type was achieved. In parallel with changes in epidermal markers, the thickened newborn and 1-week-old Inv-Cldn6-CΔ196 epidermal basal layer was devoid of Cldn1, which was clearly present in the

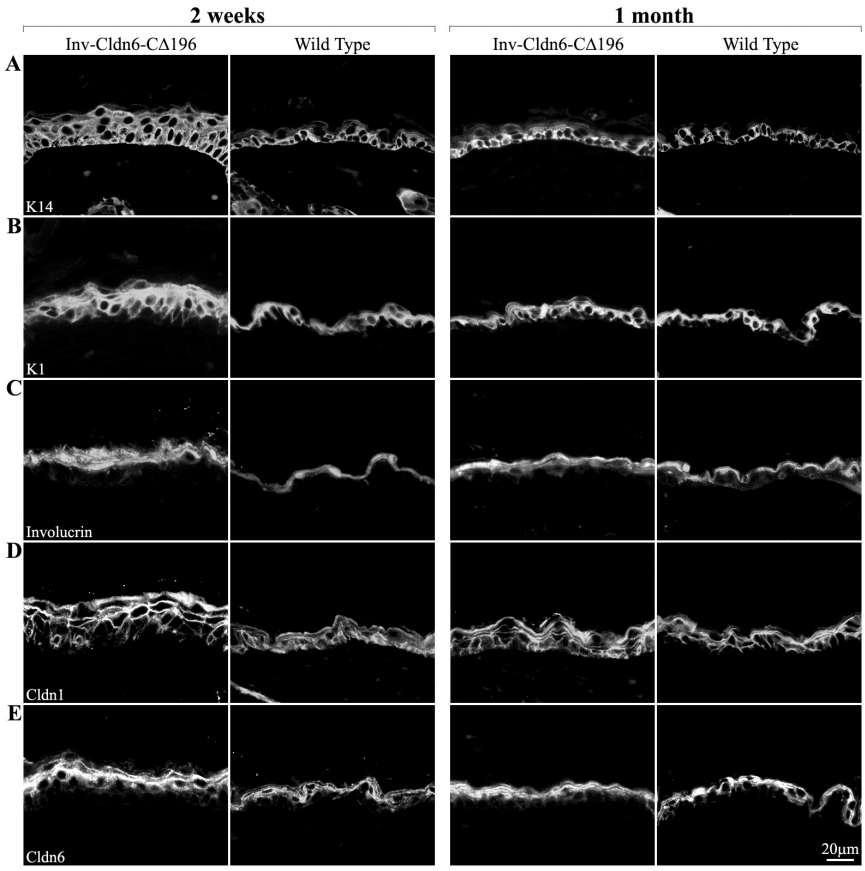

Figure 3. Perturbation of markers of epidermal differentiation. Immunofluorescence was used to evaluate various markers of epidermal differentiation including K14 (A), K1 (B), involucrin (C), Cldn1 (D) and Cldn6 (E) in Inv-Cldn6-CΔ196 mice as compared to their age-matched wild type counterparts. In each case abnormalities were present in samples from 2-week old (left panel) transgenic mice that were normalized by 1-month of age (right panel). For example, the K14 expression zone was extended into the suprabasal compartment the Inv-Cldn6-CΔ196 epidermis until epidermal thinning was achieved. In addition, broadened K1 and involucrin expression compartments was seen early but normalized by 1-month of age. Sporadic Cldn1-positive basal cells were evident in the 2-week old transgenic epidermis; by 1-month of age Cldn1-positive cells occupied both the basal and suprabasal compartments reminiscent of the wild type. Cldn6, a suprabasal-specific Cldn, was observed in an expanded zone early on, and was normalized by 1-month of age.

wild type epidermis (not shown). However, after 2 weeks, sporadic Cldn1-positive basal cells were evident, and the frequency increased as thinning progressed until 1-month of age when Cldn1-positive cells completely occupied the basal and suprabasal compartments in both the transgenic and wild type mice (Figure 3D). The suprabasal-specific Cldns, Cldn6 (Figure 3E), Cldn11, Cldn12 and Cldn18 (not shown) were seen in the expanded suprabasal region of the Inv-Cldn6-CΔ196 epidermis; each Cldn evaluated maintained a strictly membranous localization and normalized by 1-month to a zone comparable to wild type. Cldns that are not normally expressed in the epidermis (e.g. Cldn2, Cldn3 and Cldn5) (Turksen and Troy, 2002) were not observed in either the wild type or Inv-Cldn6-CΔ196 epidermis at any time evaluated (not shown). The data suggest that Inv-Cldn6-CΔ196 transgenic mice are born with differentiation abnormalities leading to slower epidermal maturation, but these are too mild to manifest in skin barrier defects or death, and are repaired between birth and 1-month of age.

Inv-Cldn6-CΔ196 mice experience age-related perturbations in epidermal differentiation and injury repair resulting in chronic dermatitis

Although by 1-month of age the Inv-Cldn6-CΔ196 epidermis was morphologically and biochemically indistinguishable from the wild type (Figure 2 and Figure 3), as early as 2-months (not shown) of age, the transgenic epidermis showed histological evidence of thickening that persisted, and was somewhat exacerbated, at 3 (Figure 4A) and 6 (Figure 4B) months. At the latter ages, an expanded stratum corneum, increased number of suprabasal/spinous cell layers and a less compacted granular layer were clearly present,

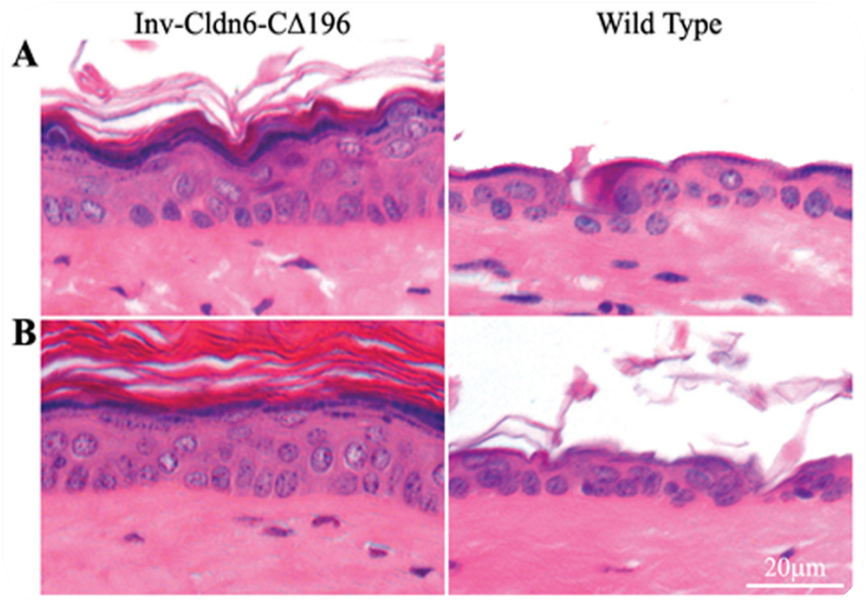

Figure 4. Histological evidence of epidermal abnormalities in the aging Inv-Cldn6-CΔ196 transgenic epidermis. Histological evidence of epidermal abnormalities emerged in aging Inv-Cldn6- CΔ196 transgenic mice after 3 (A) and 6 (B) months as compared to the wild type. These included an expanded stratum corneum, as well as an expanded suprabasal zone and a less compacted granular layer suggesting an intrinsic propensity for injury and inefficient repair that increases with aging in the Inv-Cldn6-CΔ196 epidermis.

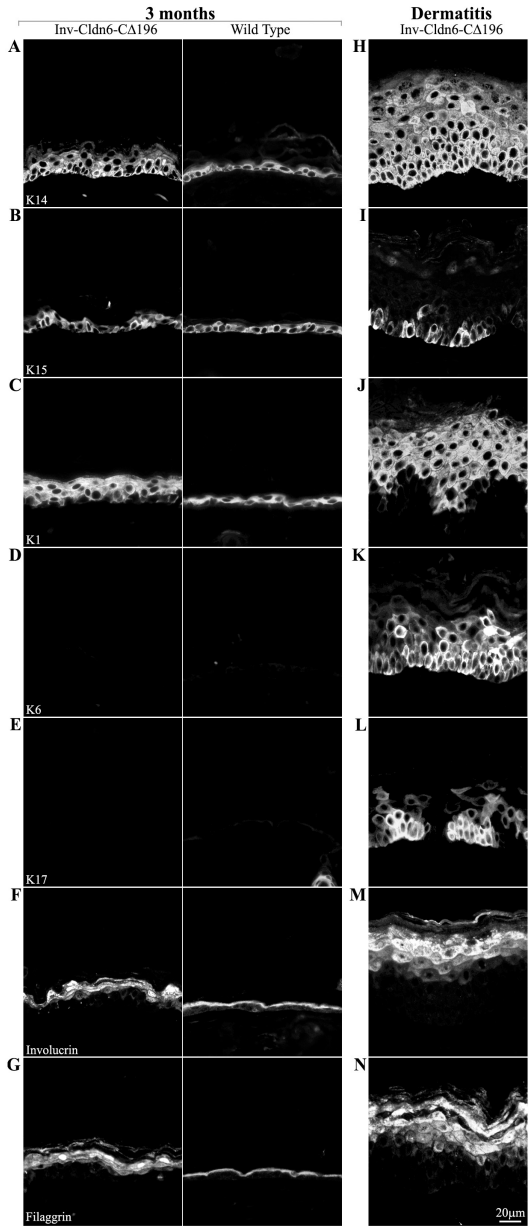

Figure 5. Aberrance in markers of epidermal differentiation during aging. Changes in the epidermal differentiation program of the aging Inv-Cldn6-CΔ196 transgenic epidermis were evaluated by immunofluorescence and compared to their age-matched wild type counterparts (samples from 3-month-old mice are shown – left panel); their expression/localization in dermatitis-affected areas is also indicated (right panel). K14 was expressed throughout the basal and suprabasal compartments in the aging Inv-Cldn6-CΔ196 epidermis (A), while K15 remained restricted to basal cells (B). The zone of K1 expression was expanded in the 3-month-old transgenic epidermis (C); however, neither K6- (D) nor K17-positive (E) cells were observed. An expanded zone of expression, and improper packing, of involucrin (F) and filaggrin (G) suggested perturbations in terminal differentiation program of the aged Inv-Cldn6-CΔ196 epidermis. In the dermatitis- affected areas, K14 (H) expression was expanded far into the suprabasal compartment, while K15 was only sporadically observed (I). A punctate K1 localization was evident throughout the thickened suprabasal zone of the dermatitis-affected Inv-Cldn6-CΔ196 epidermis (J), and K6- (K) and K17-positive (L) basal and suprabasal cells were observed. In addition, involucrin (M) and filaggrin (N) expression compartments were also expanded, with obvious packing defects evident.

and reminiscent of the 2-week-old Inv-Cldn6-CΔ196 epidermis (see above). The histological results suggested that intrinsic changes occurred in the transgenic epidermis, a possibility supported by the perturbed expression of differentiation markers; because results were similar from 2- to 6-months of age, we report results from 3-month-old Inv-Cldn6-CΔ196 transgenic mice only (Figure 5). K14 was expressed throughout the basal and suprabasal compartments in the aging Inv-Cldn6-CΔ196 epidermis (Figure 5A), while K5 (not shown) and K15 (Figure 5B) remained restricted to basal cells as in the wild type epidermis. K1 (Figure 5C) was seen throughout an expanded suprabasal zone in the transgenic epidermis corresponding to the increased number of spinous cell layers; however, neither K6- (Figure 5D) nor K17- positive (Figure 5E) interfollicular epidermal cells were observed nor was there any up-regulation in the expression of Ki67 or CD3 (not shown), suggesting no detectable hyperproliferation or immune cell infiltration. The localization of involucrin (Figure 5F), loricrin (not shown) and filaggrin (Figure 5G) suggested that there were also perturbations in terminal differentiation in the aged Inv-Cldn6-CΔ196 epidermis, with each marker occupying an expanded zone of expression consistent with the abnormal morphological appearance of the stratum corneum described above.

Cldn expression was also modified with striking anomalies consistent with those we reported earlier in an acute irritant (12-O-tetradecanoylphorbol-13-acetate (TPA))-induced epidermal injury response (Arabzadeh et al., 2007a). The number of Cldn1-positive basal and suprabasal cells was reduced (Figure 6A) and an expanded suprabasal zone of Cldn6- (Figure 6B), Cldn11- (Figure 6C), Cldn12- (Figure 6D) and Cldn18-positive cells (Figure 6E) was seen in the transgenic epidermis; concomitantly, a shift

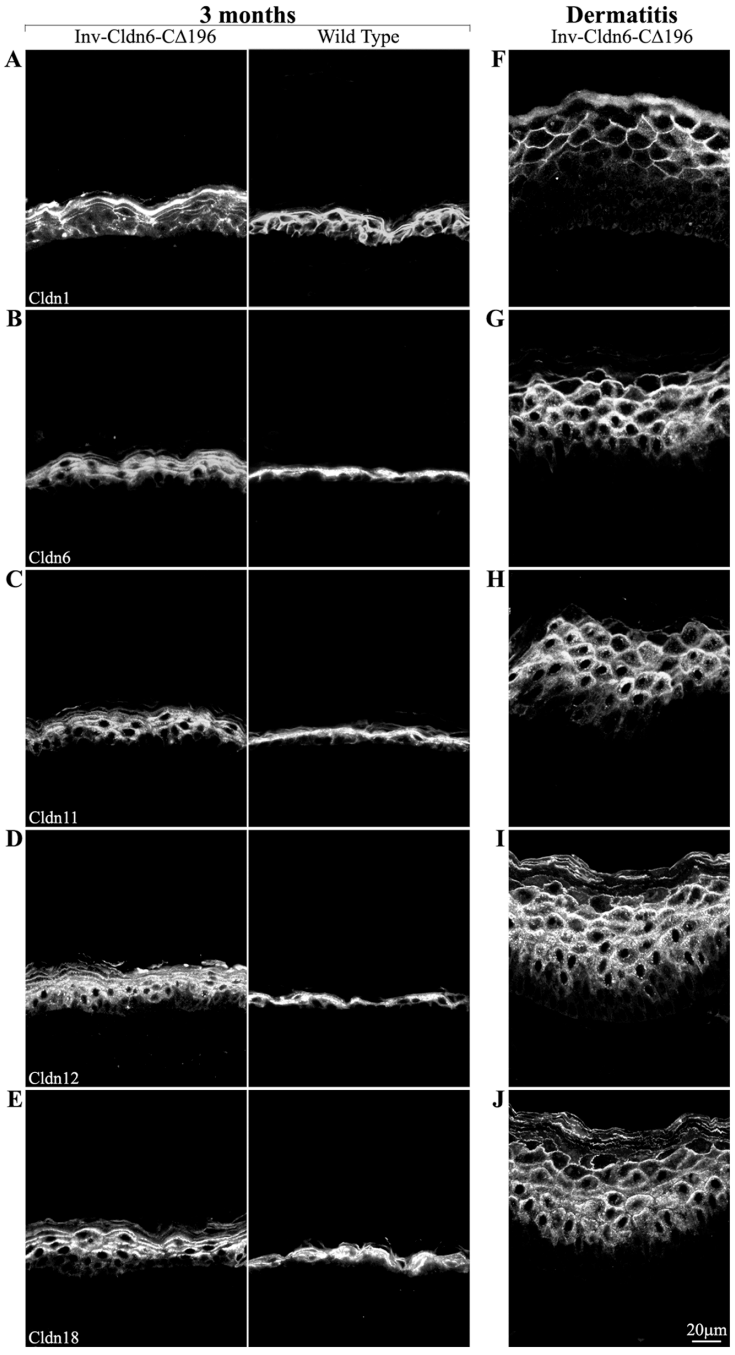

Figure 6. Evaluation of Cldns in the aging Inv-Cldn6-CΔ196 transgenic epidermis. The expression/localization of Cldns was also perturbed in the aging Inv-Cldn6-CΔ196 transgenic epidermis (samples are from 3-month-old mice – left panel); the dermatitis-affected zones are also shown (right panel). Cldn1-positive basal and suprabasal cells were reduced in the aging Inv-Cldn6-CΔ196 epidermis (A). In addition, a shift away from a strictly membrane localization and an expanded zone of suprabasal Cldns was evident - Cldn6 (B), Cldn11 (C), Cldn12 (D) and Cldn18 (E). These abnormalities in were strikingly exacerbated in the dermatitis-affected epidermis. For instance, the basal and lower suprabasal layers were void of Cldn1 localization (F). In addition, Cldn6 (G), Cldn11 (H), Cldn12 (I) and Cldn18 (J) localization was observed throughout the expanded suprabasal zone with membranous localization less evident in the lower suprabasal layers.

away from a strictly membrane localization was evident. Cldn2, Cldn3 and Cldn5 were not expressed in either wild type or transgenic animals (not shown). Taken together, the data suggest an intrinsic propensity for injury and inefficient repair that increases with aging in the Inv-Cldn6-CΔ196 epidermis. This is further supported by two lines of evidence. First, histological and biochemical changes resulting from TPA treatment were seen earlier (4 hours versus 12 hours) and repaired more slowly (no repair versus normalization by 96 hours) in Inv-Cldn6-CΔ196 versus wild type epidermis when mice were tested at 1 month of age (data not shown). Second, obvious signs of dermatitis, especially in areas subjected to repetitive mechanical stress during grooming (e.g. the neck and behind the ears), were seen in the aging Inv Cldn6-CΔ196 epidermis (Figure 7A). Histological evaluation of skin samples from these regions revealed a significantly thickened epidermis with an increased number of spinous/suprabasal cell layers and cellular disorganization; the upper differentiation layers were also abnormal, with parakeratosis, the prevalent appearance of nuclei, an improperly packed granular layer and a thicker stratum corneum (Figure 7B). In the dermatitis-affected areas, K14 (Figure 5H) and K5 (not shown) were expressed in an expanded zone far into the suprabasal compartment, and K15 expression was only sporadically expressed (Figure 5I). K1 was localized throughout the thickened suprabasal zone of the dermatitis-affected Inv-Cldn6-CΔ196 epidermis, and staining appeared punctate, suggesting a keratin filament bundling defect (Figure 5J). K6 was seen consistently throughout the basal and suprabasal layers of the dermatitis-affected epidermis (Figure 5K); K17-positive basal and suprabasal cells were somewhat more sporadically seen (Figure 5L). Expression compartments for involucrin (Figure 5M), loricrin (not shown) and filaggrin (Figure 5N) were also

expanded, with an obvious packing defect reminiscent of the observed histological abnormalities of the stratum corneum. Abnormalities in Cldn1, Cldn6, Cldn11, Cldn12 and Cldn18 localization observed in the aged Inv- Cldn6-CΔ196 transgenic epidermis (see above) were strikingly exacerbated in the dermatitis-affected epidermis. Cldn1 was completely absent in the basal and lower suprabasal layers, but a strictly membranous localization was preserved in the Cldn1-positive upper suprabasal zone (Figure 6F). While the distribution of Cldn6 (Figure 6G), Cldn11 (Figure 6H), Cldn12 (Figure 6I) and Cldn18 (Figure 6J) corresponded to the expanded suprabasal compartment of the dermatitis-affected Inv-Cldn6-CΔ196 epidermis, immunostaining was less intense and membranous localization less evident in lower suprabasal layers.

The morphological and biochemical abnormalities described predict altered permeability barrier properties and potentially barrier dysfunction in areas of repeated insult of the aged Inv-Cldn6-CΔ196 transgenic epidermis. In keeping with this hypothesis, TEWL measurements across the dermatitis-affected transgenic skin increased ~8-fold (DPM in the range of 790–830 versus 95–100 of normal adult skin) (Figure 7C).

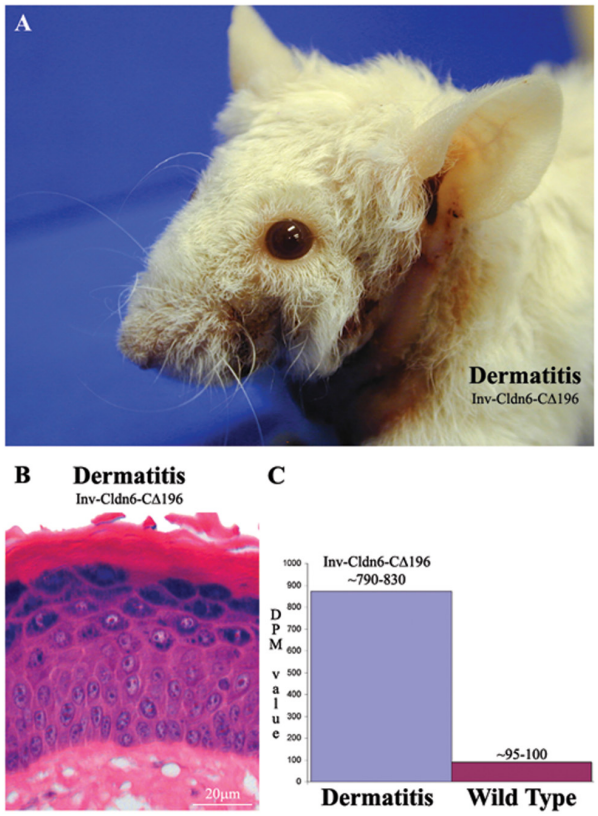

Figure 7. Aging-associated barrier dysfunction. Upon gross observation, obvious signs of dermatitis were evident in aging Inv- Cldn6-CΔ196 transgenic mice, especially in areas subjected to repetitive mechanical stress such as the neck and behind the ears (A). Histological evaluation revealed a significantly thickened epidermis with an increased number of spinous/suprabasal cell layers and cellular disorganization; the upper differentiation layers were also abnormal, with parakeratosis, the prevalent appearance of nuclei, an improperly packed granular layer and a thicker stratum corneum (B). TEWL measurements across the dermatitis-affected transgenic skin confirmed an approximately 8-fold increase in water loss and a barrier deficient phenotype (C).

DISCUSSION

In this study, we used transgenic mouse technology to expand on our structure-function approach to elucidating the role of the cytoplasmic tail of Cldn6 in epidermal development and the formation and maintenance of skin barrier integrity. We demonstrate that Inv-Cldn6-CΔ196 mice display epidermal differentiation abnormalities at birth that result in slower epidermal maturation but are apparently normalized by 1-month of age. However, with aging, intrinsic properties of the Inv-Cldn6-CΔ196 epidermis are manifested by a propensity for injury and inefficient repair, eventually resulting in chronic dermatitis especially in areas subjected to frequent insult via grooming. Changes in Cldn expression and localization suggest marked changes in the presence and function of TJs, as also evidenced by skin barrier dysfunction. Taken together, our data suggest that the overexpression of a Cldn tail truncation mutant in the suprabasal compartment of the mouse epidermis results in its delayed maturation, a propensity for injury, diminished repair and skin barrier deficiency reminiscent of the intrinsic aging process of human skin.

It is well established that the formation of the epidermal permeability barrier (EPB) is developmentally regulated (Byrne and Hardman, 2005; Hardman et al., 1998; 1999; Turksen and Troy, 2002) and that disruption or delay in its formation before birth has a critical role in the survival of the organism (Cartlidge, 2000; Elias, 2005; Mack et al., 2005; Williams et al., 1998). Previously we reported that a perturbation of Cldn6 expression levels at its endogenous site of expression - the suprabasal layer of the epidermis - alters epidermal development and the formation of the EPB (Troy et al.,

2005a; Turksen and Troy, 2002). However, depending on whether normal or mutant forms of Cldn6 are expressed and at what levels, the severity of phenotypic anomalies varies markedly (Arabzadeh et al., 2006; Troy et al., 2005a; Troy and Turksen, 2007; Turksen and Troy, 2002). For example, perinatal lethality resulting from a severely compromised epidermal differentiation program and dysfunctional EPB results when native Cldn6 is expressed at high levels (Turksen and Troy, 2002); while with lower levels of expression, less severe defects occur with the capacity for normalization of EPB function (Troy et al., 2005a). In contrast, apparently normal prenatal epidermal development and formation of a functioning EPB, but an abnormal postnatal lifelong keratinocyte hyperproliferation leading to progressive thickening of the epidermis - but no dermatitis, results when a mutant form of Cldn6 lacking its entire tail domain (Inv-Cldn6-CΔ187) is expressed (Arabzadeh et al., 2006). On the other hand, high overexpression of a different mutant lacking only the C-terminal half of the tail domain of Cldn6 (Inv-Cldn6-CΔ196) results in a lethal barrier dysfunction with marked hyperproliferative squamous invaginations/cysts replacing hair follicles (Troy and Turksen, 2007). We now show that in Inv-Cldn6-CΔ196 mice with lower levels of transgene expression the abnormalities are much more subtle, and manifested by a slower than usual (i.e., 1 month versus 2 week) but otherwise apparently normal maturation of the epidermis from the multilayered structure seen at birth to the thinner 2–3 cell layer mature structure (Troy et al., 2005a). These early postnatal changes in maturation are not accompanied by abnormalities in the formation of a functional skin barrier. It is interesting to note that K6- and K17-positive suprabasal cells, which are normally not present in the mature epidermis except in situations of abnormal cell proliferation and

differentiation (Leigh et al., 1995; McGowan and Coulombe, 1998b; 1998a), are not detectable in the interfollicular epidermis of either the juvenile or aged Inv-Cldn6-CΔ196 transgenic samples, until patent dermatitis is evident (see below).

Phenotypic differences observed in the different transgenic mice appear to reflect different mechanistic consequences of expression of native or mutant Cldn6. Structure-function details of different Cldns are only beginning to emerge, but the COOH-terminal tail varies considerably in length and is the region with the most sequence heterogeneity among Cldn isoforms, and in most cases contains a PDZ-binding motif that enables Cldns to directly interact with the TJ-associated MAGUKs (ZO1, ZO2, and ZO3) as well as with MUPP1 and PATJ (Assémat et al., 2008; Heiskala et al., 2001; Koval, 2006; Roh and Margolis, 2003). For at least some Cldns (e.g., 1 and 5), the cytoplasmic tail upstream of the PDZ-binding motif is thought to be required for targeting to the TJ complex (Rüffer and Gerke, 2004) and contributes to protein stability (Arabzadeh et al., 2006; Van Itallie, 2005). Post-translational modifications within the tail domain, including phosphorylation and palmitoylation, are also thought to regulate Cldn activities, including their targeting to the membrane and insertion into TJs (Simard et al., 2006), but to date most Cldns have not been subjected to exhaustive analysis. Thus, the similarities and differences between Inv-Cldn6-CΔ187 and Inv-Cldn6-CΔ196 mice are of interest. Our data suggest that the phenotype observed in the Inv-Cldn6-CΔ187 epidermis reflects protein instability and an unfolding protein response. On the other hand, the delayed maturation and age-related deficit in wound healing and repair in the Inv-Cldn6-CΔ196 epidermis most likely involves an aberrant interaction with the cytoskeleton. Although to date no direct interaction between the cytoplasmic tail of Cldns and cytoskeletal

molecules has been shown, the possibility of such direct interactions is not unlikely considering the known role of the actin cytoskeleton, for example, in cell shape and cell polarity (Ivanov, 2008; Ivanov et al., 2004; Miyoshi et al., 2008).

Despite the importance of the skin barrier to the survival of the mammalian species, the molecular mechanisms governing its formation and maintenance are not well-understood, nor are the changes that occur during the intrinsic aging process of the skin. In humans, aging-related changes in the skin are widespread and result from both intrinsic (gene mutations, hormonal changes, cellular metabolism) and extrinsic (UV exposure, chemicals, pollutants) factors. While extrinsic factors affect mainly the dermis, the epidermis is the main target of intrinsic skin aging processes where, especially in sun-exposed skin, changes occur often with initial generalized epidermal thickening, indicative of epidermal hyperplasia and reduced capacity to repair, such that the epidermis becomes prone to a number of skin conditions including dermatitis, eczema and ulceration (Davies, 2008; Elias and Ghadially, 2002; Ghadially, 1998; Kligman, 1989; Makrantonaki and Zouboulis, 2007; Ward, 2005). Only recently has it been appreciated that abnormal skin barrier function might underlie these skin conditions (Barland et al., 2004), although no analysis of Cldn expression has been reported. The murine epidermis, however, does not normally undergo comparable aging-related changes; in fact, once the mouse epidermis is matured it maintains a homeostatic balance and undergoes morphological and biochemical changes only in response to injury or disease. Thus, it was extremely interesting to note that in spite of the fact that Inv-Cldn6-CΔ196 mice achieve a normal-appearing epidermis by one-month of age (by morphology and biochemical markers), with aging they have a high propensity for

epidermal injury and a diminished ability to repair lesions, leading eventually to severe dermatitis with associated changes in skin barrier function. It should be noted that this sensitivity to injury and inefficient repair were seen also in young mice subjected to acute injury by application of the irritant TPA (data not shown). As already indicated, the precise mechanisms by which expression of low levels of Cldn6-CΔ196 in the suprabasal layers of the epidermis leads to age-related changes appearing to mimic those seen in humans are currently not known, but our observations suggest that changes in Cldn homeostasis leading to changes in the epidermal differentiation program play important roles. In this regard, not only changes elicited directly by changes in Cldn6 signaling but also changes imparted by alterations in the expression of other Cldns, notably Cldn1, must be considered. In the developing epidermis, Cldn1 is first restricted to the stratifying layers and matures to occupy the basal layer upon the completion of barrier formation at E17.5 (Troy and Turksen, 2007). However, in response to TPA-induced injury and loss of cell polarity seen in tumorigenesis, Cldn1 expression is downregulated in both the basal layer and immediate suprabasal layers of the epidermis (Arabzadeh et al., 2007a; 2007b), alterations seen also with aging of the Inv-Cldn6-CΔ196 epidermis. The drastic changes in TEWL that we observed in severely affected areas of the Inv-Cldn6-CΔ196 epidermis also appear to mimic those seen in the aging human epidermis subjected to stress or injury (Ghadially et al., 1995). Thus the data reported here suggest that the changes in Cldn expression and localization in mice with low expression of Cldn6-CΔ196 in the epidermis lead to relatively subtle changes in the epidermal differentiation program and permeability in the young animal, but render them prone to injury and diminished repair that are exacerbated especially in areas subjected to repeated

mechanical trauma, leading to chronic and increasingly severe dermatitis.

In summary, our data add to the evidence that Cldn6, and in particular the C-terminal half of the Cldn6 tail, contribute to the regulation of epidermal differentiation and skin barrier function throughout life. They also support the utility of the Inv-Cldn6-CΔ196 mouse model for studies aimed at understanding intrinsic changes in the aging epidermis and point towards a need to investigate Cldn expression profiles in the aging human epidermis.

ACKNOWLEDGEMENTS

This study is dedicated to Dr. G. E. Palade for the discovery of tight junctions, together with Dr. M.G. Farquhar. We remain eternally grateful to our dear friend and colleague, Dr. Jane E. Aubin (University of Toronto), for many invaluable discussions and comments on our manuscript. We would like the thank Dr. Pierre Coulombe (Johns Hopkins) for his gift of anti-K17 antibodies as well as Mrs. Adriana Gambarotta and Mr. Pierre Bradley of the animal care facility of the OHRI. Zaida J. Ticas (MLT) (University of Ottawa) prepared paraffin- embedded samples and histological sections for evaluation. KT would like to acknowledge Vittorio Paltrinieri for I Found My Love in Portofino, Giorgio Armani for the pleasure of unstructured tailored lines and Isabella Rossellini for Blue Velvet.

To determine the contribution of the Cldn6 tail to its function, we initially overexpressed a mutant Cldn6 containing a deletion of the 23 extreme C-terminal amino acids (CΔ196) and demonstrated an epidermal defect. Epidermal maturation was delayed in the transgenic mice and they were unable to undergo proper epidermal repair in response to simple stresses such as grooming, with resulting chronic dermatitis.

In order to more minimally map the tail region required for proper Cldn6 function, we deleted 10 fewer amino acids (CΔ206). This retained region contains 3 putative phospho-residues, which have since been mapped in human embryonic stem cell studies (Rigbolt et al., 2011). There is increasing evidence for a role for Cldn phosphorylation both in TJ formation and in Cldn targeting to the TJ (refer to Table 2 in Appendix 1). Furthermore, although the entire Cldn6 tail domain is 83% identical between mouse and human, the final 13 residues are 100% identical, suggesting an evolutionarily conserved role for this region (see alignment in Appendix 1, Fig. 1).

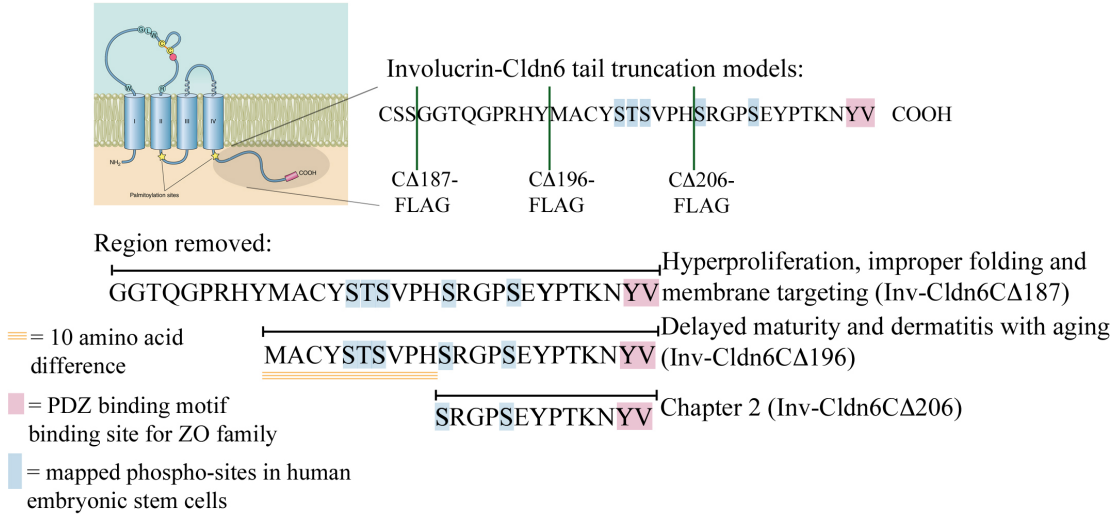

Figure 8: Schematic comparing deleted regions of the C-terminal tail in Cldn6 overexpression models. *Adapted by permission from (Gunzel et al., 2013).*

CHAPTER 2:

Involucrin–claudin-6 tail deletion mutant (CΔ206) transgenic mice: a model of delayed epidermal permeability barrier formation and repair

Adebola Enikanolaiye[1,2,*], Nathalie Larivière[1,2,*], Tammy-Claire Troy[1], Azadeh Arabzadeh[1,2], Elif Atasoy[1,2] and Kursad Turksen[1,2,3,4,‡]

[1] Sprott Centre for Stem Cell Research at the Ottawa Hospital Research Institute, Ottawa, Ontario K1Y 8L6, Canada

[2] Department of Cellular and Molecular Medicine

[3] Department of Medicine, Divisions of Dermatology and Endocrinology, Faculty of Medicine, University of Ottawa, Ottawa, Ontario K1H 8M5, Canada

[4] Regenerative Medicine Program, Sprott Centre for Stem Cell Research at the Ottawa Hospital Research Institute, 501 Smyth Road-CCW5226, Ottawa, Ontario K1Y 8L6, Canada

*These authors contributed equally to this work

CONTRIBUTIONS

This manuscript was published in Disease Models and Mechanisms (Enikanolaiye et al., 2010) **in January 2010.**

Enikanolaiye, A.*, **Lariviere, N.M.K.***, Troy, T.-C., Arabzadeh, A., Atasoy, E., Turksen, K., 2010. Involucrin-claudin-6 tail deletion mutant (CΔ206) transgenic mice: a model of delayed epidermal permeability barrier formation and repair. *Disease Models and Mechanisms* 3, 167–180.

All contributions were shared equally between myself and Adebola Enikanolaiye (AE), as **co-first authors**. We were responsible for performing experiments including tissue/sample collection and processing for immunofluorescence, microscopy and image/figure presentation as well as PCRs and Western blots (2 of 3 independent replicates for immunohistochemistry, all replicates for all other data presented). First replicates for immunohistochemistry were carried out by Elif Atasoy and/or Azadeh Arabzadeh. AE and I were responsible for all revisions requested by reviewers including a manuscript re-write to include a disease focus and translational impact. Tammy-Claire Troy was responsible for the writing of the manuscript prior to revisions, provided reagents and assisted with image acquisition and protocol optimization for all experiments. Kursad Turksen conceived experiments, contributed to data analysis and provided final approval of the manuscript.

SUMMARY

Preterm birth is a major global health problem that results in a large number of infant deaths, many of which are attributable to the complications of an immature epidermal permeability barrier (EPB), for which there is currently no effective therapeutic option. The mammalian EPB is formed during development and is essential for survival as it maintains thermoregulation and hydration, and provides a defense against infection. Using transgenic mouse technology, we have demonstrated the importance of claudin (Cldn)-containing tight junctions (TJs) in epidermal differentiation and, in particular, that epidermal suprabasal overexpression of Cldn6 results in an EPB-deficient phenotype that phenocopies the dysfunctional EPB of premature human infants. In this study, we used the same approach to target a Cldn6 tail deletion mutant to the epidermis of mice [Involucrin (Inv)-Cldn6-CΔ206 transgenic mice]. The Inv-Cldn6-CΔ206 transgenic mice displayed a developmental delay in EPB formation, as shown by the expression of keratins and Cldns, and by X-Gal penetration assays. Trans-epidermal water loss measurements and immunolocalization studies indicated that the epidermal differentiation program was also perturbed in postnatal Inv-Cldn6-CΔ206 transgenic mice resulting in a delayed maturation. Notably, however, expression/localization of epidermal differentiation and maturation markers, including Cldns, indicated that the transgenic epidermis matured and normalized by postnatal day 10, which is 3 days after the wild-type epidermis. Our results suggest that activation of the extracellular signal-regulated kinase 1/2 (Erk1/2) pathway and Cldn1 phosphorylation are associated with the repair and maturation of the skin barrier processes. These studies provide additional support for the crucial role of Cldns in epidermal differentiation, maturation and the

formation of the EPB, and describe a novel animal model for evaluating postnatal epidermal maturation and therapies that may accelerate the process.

INTRODUCTION

The prevalence of preterm birth is widespread with very little understanding of its causes and no unambiguous epidemiological data for predicting its occurrence. Formed in weeks 30 to 33 of pregnancy (D. R. Wilson and Maibach, 1980), the protective epidermal permeability barrier (EPB) of the skin is essential for survival as it provides the first line of defense against infection, environmental insult, and the loss of heat and solutes (Baharestani, 2007; Gibson et al., 2006; Shwayder and Akland, 2005; Soll, 2008). In infants born before 32 weeks of pregnancy, severe EPB dysfunction may result in death or long-term complications (Pilling et al., 2008).

The EPB is formed in the later stages of epidermal terminal differentiation, and consists of tight junction (TJ) strands of adjacent cells that associate laterally (Brandner, 2009; Brandner et al., 2002; Langbein et al., 2002; 2003; Schlüter et al., 2007; Turksen and Troy, 2002) and function in sealing intracellular spaces for paracellular diffusion control (Farquhar and Palade, 1963). The selective permeability of the EPB is provided by a family of 23 highly conserved integral membrane proteins known as claudins (Cldns), a relatively recently identified component of TJs (Angelow et al., 2008; Chiba et al., 2008; Findley and Koval, 2009; Krause et al., 2008; Turksen and Troy, 2004; Van Itallie and Anderson, 2006). Heterogeneity within the Cldn family results from distinctly charged amino acid sequences within the first external loop; thus, the specific permeability properties of different epithelia are attributed to their different Cldn compositions

(Daugherty et al., 2007; Katoh, 2003; Krause et al., 2008; Turksen and Troy, 2004). Recent studies have clearly demonstrated that Cldn-containing TJs are intricately involved in epidermal differentiation programs, and that TJ function, and thus barrier integrity, is modified in response to Cldn modulation (Arabzadeh et al., 2006; Furuse et al., 2002; Troy et al., 2005a; 2007a; Turksen and Troy, 2002). For instance, Cldn1 knockout mice die shortly after birth owing to EPB dysfunction (Furuse et al., 2002). Inv-Cldn6 transgenic mice, in which the involucrin (Inv) promoter targets Cldn6 to the suprabasal layers of the epidermis, also suffer EPB abnormalities with a phenotype mimicking that seen in premature human babies, the severity/lethality of which is dependent upon the level of Cldn6 overexpression (Troy et al., 2005a; Turksen and Troy, 2002). Inefficient membrane targeting of Cldn proteins and a highly proliferative epidermal phenotype – apparently as a result of the unfolded protein response pathway – were observed upon overexpression of a cytoplasmic tail-ablated Cldn6 (Inv-Cldn6-CΔ187) in mice (Arabzadeh et al., 2006). Furthermore, dependent on the level of overexpression, Inv-Cldn6-CΔ196 mice (with half the cytoplasmic tail ablated) (Troy and Turksen, 2007) displayed EPB dysfunction and an aging-related skin barrier defect resulting in an intrinsic propensity for injury, inefficient repair and chronic dermatitis.

These data provide support for the importance of the cytoplasmic tail portion of Cldn molecules in epidermal differentiation and EPB function. Although relatively constant in length, sequences within the Cldn cytoplasmic tail are divergent but include a number of putative functional domains that are present in many family members. To continue to address functional domain activities, we again used the Inv promoter to target a Cldn6 cytoplasmic tail deletion mutant (Cldn6-CΔ206), to the suprabasal compartment of the

epidermis; this deletion encompasses the PDZ-binding domain and a putative protein kinase A (PKA) phosphorylation site. Inv-Cldn6-CΔ206 transgenic mice have a developmental delay in EPB formation, suffer trans-epidermal water loss (TEWL) at birth, and exhibit a perturbed epidermal maturation program manifested by a 3-day lag in the initiation of the normal epidermal thinning process (which occurs at day 10 in the Inv-Cldn6-CΔ206 transgenic mice versus day 7 in the wild-type epidermis). Our data suggest that this process stems from the remodeling of Cldn1 expression in the repairing Inv-Cldn6-CΔ206 transgenic epidermis, and that the first phase of repair requires shedding of phospoCldn1-expressing cells from the differentiated epidermal compartment where extracellular signal-regulated kinase 1/2 (Erk1/2) is activated. These results suggest that although Inv-Cldn6-CΔ206 transgenic mice suffer developmental delays in epidermogenesis, the epidermis undergoes epidermal maturation and repair after birth, normalizing by postnatal day 10, thus providing a model to elucidate the molecular mechanisms by which Cldns regulate the postnatal maturation of the epidermis. This model may also be useful to screen for agents that accelerate formation of a functional barrier, which could provide useful therapeutic options for improvement of the EPB in premature infants.

RESULTS

Generation and phenotype of Inv-Cldn6-CΔ206 transgenic mice

We truncated the C-terminal cytoplasmic tail domain of Cldn6 after amino acid 206 (Cldn6-CΔ206), removing 14 amino acids to encompass a region including the PDZ-binding domain (YV) and a putative PKA phosphorylation site (Fig. 1A,B). Cldn6-

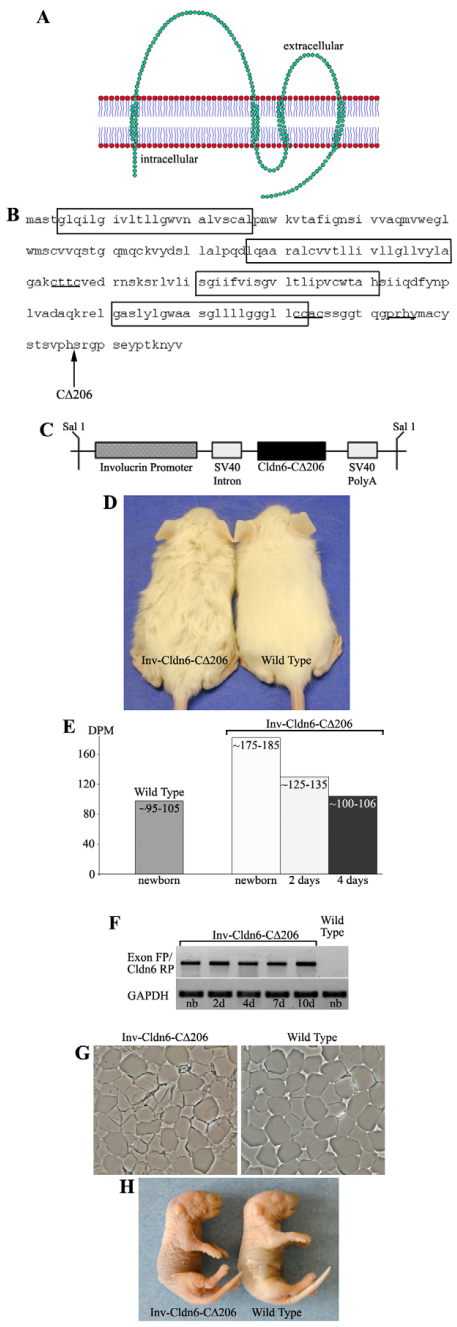

Fig. 1. Inv-Cldn6-CΔ206 transgenic mice. (A) The Inv-Cldn6-CΔ206 mutant was created by truncating the C-terminal cytoplasmic tail domain of Cldn6 after amino acid 206 (Cldn6-CΔ206). (B) The Cldn6 protein sequence is shown; transmembrane-spanning regions are encased within boxes, the CXXC motifs are underlined, and the deletion site is indicated with an arrow. (C) Inv-Cldn6-CΔ206 cDNA was expressed in the suprabasal cells of the transgenic mouse epidermis, where TJs are localized, under the control of the 3.7 kb 5'-flanking element of the human involucrin gene. (D) Inv-Cldn6-CΔ206 mice were easily identifiable by their wiry and lackluster coat, a phenotype that was maintained throughout life. (E) TEWL measurements demonstrated an approximately twofold increase in water loss for transgenic neonates, and daily measurements revealed a robust epidermal repair mechanism where normal hydration levels were achieved by 4 days after birth. (F) RT-PCR using primers spanning the Inv exon and Cldn6 confirmed that transgene expression was consistent and could therefore not be used to explain the changes in TEWL; GAPDH controls are shown. (G,H) Evaluation of cornified envelopes, which were characterized by a rigid shape and uniform size, comparable to that of the wild type (G), and the absence of X-Gal penetration (H) confirmed the presence of sufficient neonatal barrier function in Inv-Cldn6-CΔ206 mice.

CΔ206 cDNA was expressed in the suprabasal cells of the transgenic mouse epidermis, where TJs are localized, under the control of the 3.7 kb 5'-flanking element of the human Inv gene (IVL) (Fig. 1C). Founder Inv-Cldn6-CΔ206 transgenic mice (five females) were identified by PCR, and two lines were established with identical phenotypes. Newborn Inv-Cldn6-CΔ206 transgenic mice appeared grossly phenotypically comparable to the wild type. However, as was observed in our Inv-Cldn6, Inv-Cldn6-CΔ187 and Inv-Cldn6-CΔ196 mouse models, with time the Inv-Cldn6-CΔ206 transgenic mice were easily distinguishable from the wild type by coat appearance: smooth and shiny in the wild-type mice versus wiry and lackluster in the transgenic mice, a phenotype that was maintained throughout the life of the mouse (Fig. 1D). Since it does not appear to have any direct relevance to the delayed epidermal maturation and postnatal EPB formation reported here, coat characteristics have not been investigated further. Although no gross phenotypic abnormalities were apparent at birth, daily dermal phase meter (DPM) measurements (Fig. 1E) demonstrated significant, albeit non-lethal, TEWL in neonatal Inv-Cldn6-CΔ206 transgenic mice. Compared with the wild-type mice (DPM in the range of 95-105), Inv-Cldn6-CΔ206 transgenic neonates expressed DPM values in the range of 175-185. However, DPM levels were already reduced in the transgenic mice at 2 days after birth (~125-135), and by 4 days after birth, DPM values reached wild-type levels (in the range of 100-106). Reverse transcriptase (RT)-PCR with primers spanning the junction of the Inv exon and the Cldn6 sequences in the transgene confirmed that the observed changes in TEWL leading to reversion to a normal or wild-type phenotype are not simply the result of decreased expression of the transgene (Fig. 1F, a GAPDH control is shown). Despite the higher TEWL in transgenic epidermis, the presence of substantial

neonatal barrier function was confirmed not only by mouse viability but also by analysis of cornified envelope extracts from Inv-Cldn6-CΔ206 skin, which appeared relatively normal with a uniform size and rigid shape (Fig. 1G), and the absence of X-Gal (5-bromo-4-chloro-3-indolyl-β-D-galactopyranoside) penetration (Fig. 1H).

Barrier formation and epidermal differentiation is delayed in the Inv-Cldn6-CΔ206 transgenic epidermis during development

Although non-lethal, the significantly higher TEWL observed in neonatal Inv-Cldn6-CΔ206 transgenic mice suggested aberrations in the epidermal differentiation program during development. X-Gal penetration assays confirmed that, at E15.5 (15.5 days post coitum), Inv-Cldn6-CΔ206 transgenic embryos were delayed in barrier formation as compared with their wild-type counterparts (Fig. 2A), a delay that was sustained at E17.5, when EPB function is normally achieved (Fig. 2B) (Hardman et al., 1998; Troy et al., 2007b), and at E18.5 (Fig. 2C, marked with arrows).

To complement these studies, we evaluated transverse histological sections of E15.5 and E17.5 embryo torsos in which the epidermal initiation sites, as well as the dorsal and ventral midlines, were included; because the data were consistent, we report results from E15.5 Inv-Cldn6-CΔ206 transgenic and wild-type mice only. At each site, a somewhat delayed/immature epidermal differentiation program was evident in the transgenic epidermis. For instance, in contrast to the well-established 3–4- cell layered stratum intermedium of the wild-type epidermis (Fig. 3A), the initiation site of the Inv-Cldn6-CΔ206 transgenic epidermis possessed only 2-3 intermediate cell layers. Although the dorsal midline (Fig. 3B) of the developing wild-type epidermis was characterized by a 2–

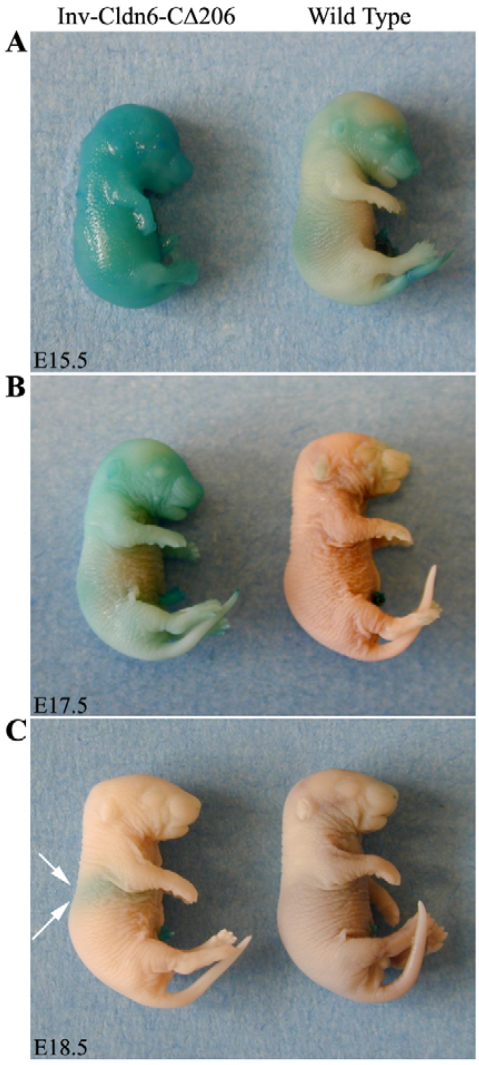

Fig.2. X-Gal assays demonstrate a developmental delay in EPB formation for Inv-Cldn6-CΔ206 transgenic mice. (A-C) Using age-matched wild-type embryos as a control, X-gal penetration assays at E15.5 (A), E17.5(B) and E18.5 (C) confirmed a developmental delay in EPB formation for Inv-Cldn6-CΔ206 transgenic mice. Even at E18.5 there was some evidence that barrier formation had not yet been completed in Inv-Cldn6-CΔ206 transgenic embyos (indicated with arrows).

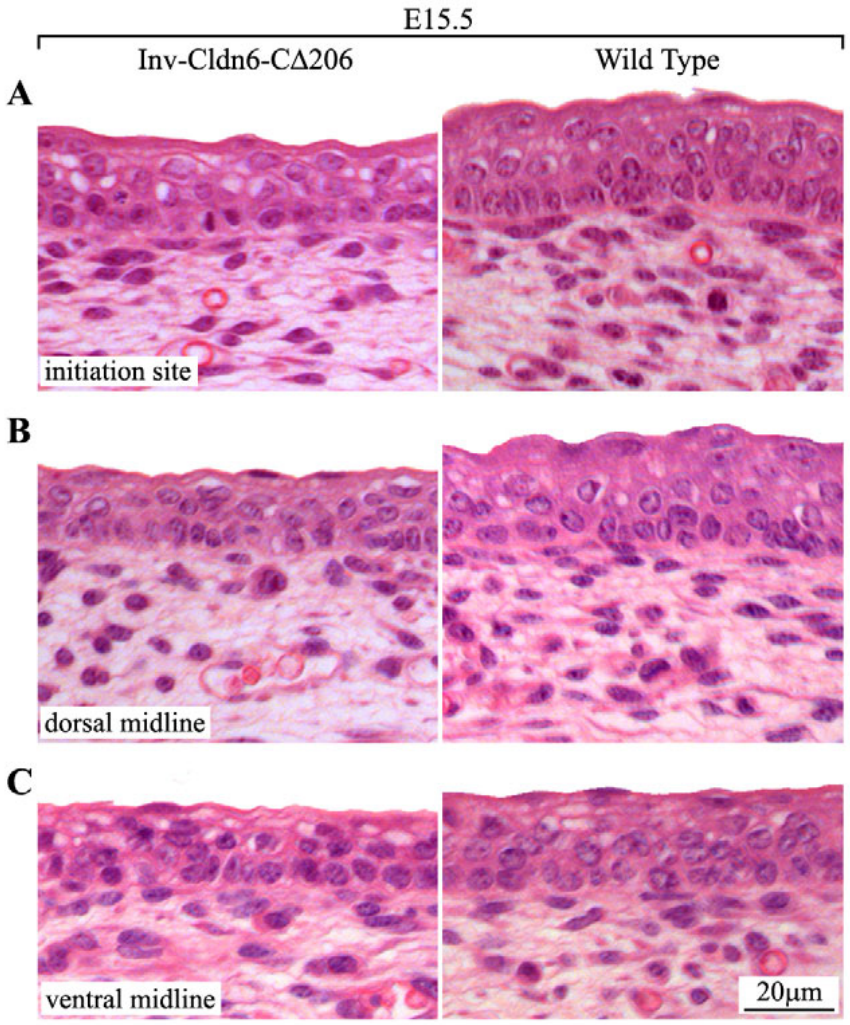

Fig. 3. Histological evidence confirms EPB formation delays in transgenic mice. Evaluation of transverse histological sections at E15.5 confirmed a somewhat delayed epidermal differentiation in Inv-Cldn6-CΔ206 transgenic mice during development. (A) Transgenic epidermal initiation sites were characterized by 2-3 intermediate cell layers in contrast to the more mature 3–4-cell layered stratum intermedium of the wild type. (B,C) There were only 1-2 layers of intermediate cells at the dorsal midline (B) of the Inv-Cldn6-CΔ206 epidermis, whereas that of the wild type possessed 2-3 cell layers, and the transgenic ventral midline (C) was thinner than that of the wild type, with only one defined intermediate cell layer together with some infiltrating intermediate cells. Bar, 20μm.

3-cell layer intermediate zone, that of the transgenic epidermis was thinner with only 1-2 layers of intermediate cells evident between the basal and periderm layers. Furthermore, the ventral midline (Fig. 3C) of the wild-type epidermis was characterized by two layers of intermediate cells, whereas that of the transgenic mice was thinner with only one defined intermediate cell layer together with some nascent infiltrating intermediate cells.

Consistent with the histological results, abnormalities in the expression of epidermal differentiation markers and Cldns were present in the developing Inv-Cldn6-CΔ206 embryo (Fig. 4, E15.5 epidermal initiation sites are shown). Although there was no apparent difference in the transgenic and wild-type epidermal basal compartments, as shown by the localization of K14 (Fig. 4A), K5 and K15 (not shown), K1 (Fig. 4B), which is associated with stratifying suprabasal cells (Fuchs and Byrne, 1994), occupied a moderately thinner compartment in the transgenic epidermis corresponding with the thinner intermediate layer that was observed histologically. Cldn1 (Fig. 4C), Cldn6 (Fig. 4D), Cldn11 (Fig. 4E), Cldn12 (Fig. 4F) and Cldn18 (Fig. 4G), which at this developmental time point are all strictly localized to the epidermal suprabasal compartment (Troy et al., 2007b), also occupied a comparatively thinner zone of expression in the developing Inv-Cldn6-CΔ206 transgenic epidermis. Similarly, the expression compartment of various structural proteins in the stratum corneum, including involucrin (Fig. 4H), filaggrin (Fig. 4I) and loricrin (Fig. 4J) was reduced in the E15.5 Inv-Cldn6-CΔ206 transgenic epidermis.

The epidermis matures postnatally in the Inv-Cldn6-CΔ206 transgenic mice

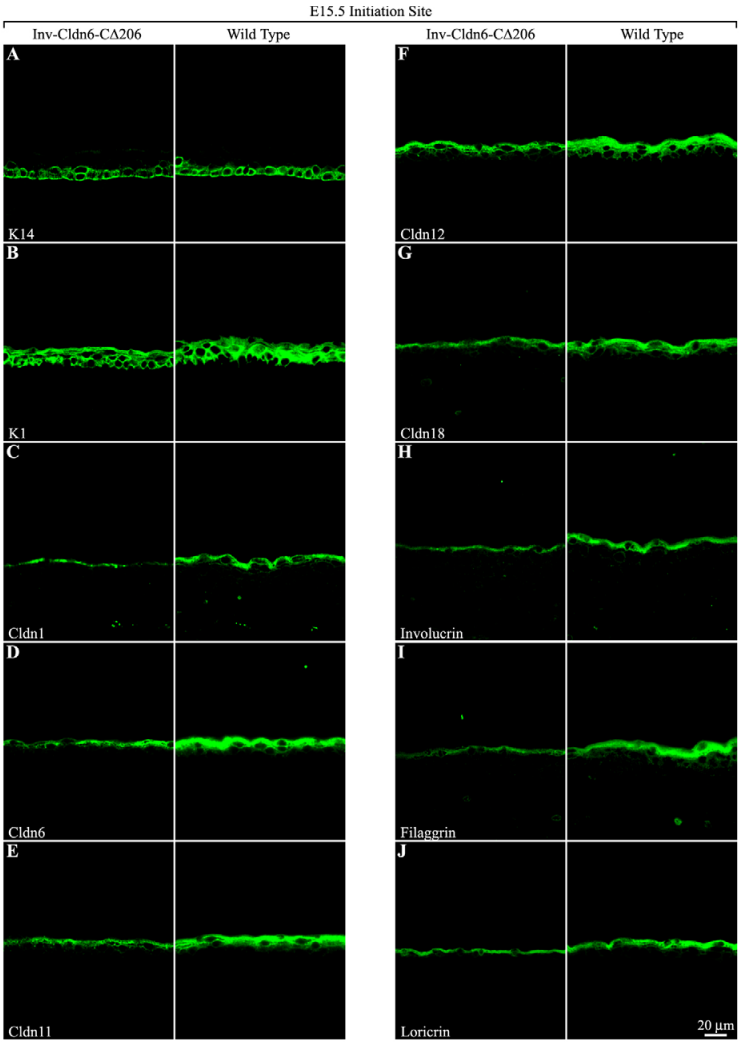

Fig. 4. The localization of epidermal differentiation markers and Cldns is altered in the delayed EPB of the Inv-Cldn6-CΔ206 transgenic epidermis. Immunofluorescence was used to evaluate various markers of epidermal differentiation and Cldns during development in Inv-Cldn6-CΔ206 epidermal initiation sites compared with wild type sites (E15.5 is shown). Although there was no difference in K14 (A) expression (e.g. the basal compartment), markers of the epidermal suprabasal zone occupied a moderately thinner expression compartment in the developing Inv-Cldn6-CΔ206 transgenic epidermis as shown by the expression of K1 (B), Cldn1 (C), Cldn6 (D), Cldn11 (E), Cldn12 (F) and Cldn18 (G). In addition, involucrin (H), filaggrin (I) and loricrin (J) expression compartments were also reduced in the developing Inv-Cldn6-C**Δ**206 transgenic epidermis. Bar, 20μm.

In parallel with the delayed program of epidermal differentiation and EPB formation observed in the developing Inv-Cldn6-CΔ206 transgenic epidermis, postnatal TEWL measurements suggested that the Inv-Cldn6- CΔ206 transgenic epidermis underwent a robust epidermal maturation process after birth. Histological analyses of newborn (Fig. 5A), 2-day-old and 4-day-old skin samples (not shown) revealed that the Inv-Cldn6-CΔ206 transgenic epidermis was comparable to the wild type. However, although by 1 week of age the wild-type epidermis had commenced the normal thinning pattern associated with epidermal maturation, the transgenic epidermis maintained an immature phenotype with many suprabasal cell layers, the prevalent appearance of nuclei in the upper differentiation layers, and a much less compacted granular layer (Fig. 5B). However, by 10 days after birth (Fig. 5C), the Inv-Cldn6-CΔ206 transgenic epidermis had thinned to be morphologically comparable to the wild-type epidermis. Samples from 1-month-old (Fig. 5D) and 3-month-old (not shown) transgenic mice were indistinguishable from wild-type samples.

The histological results suggested that changes occurred in the transgenic epidermis reflecting approximately a 3-day lag in the normal epidermal maturation process, a possibility supported by the expression of epidermal differentiation markers and Cldns. Because results were similar from newborn to 7 days of age, normalized after 10 days, and were maintained throughout life, we report results only from 7- and 10-day-old Inv-Cldn6-CΔ206 transgenic mice compared with 7-day-old wild-type mice. K5 and K15 were restricted to basal cells at all time points in both the wild- type and Inv-Cldn6-Δ206 epidermis (not shown), but K14 occupied an expanded zone extending into the suprabasal compartment until epidermal maturation was achieved in the 10-day-old Inv-Cldn6-

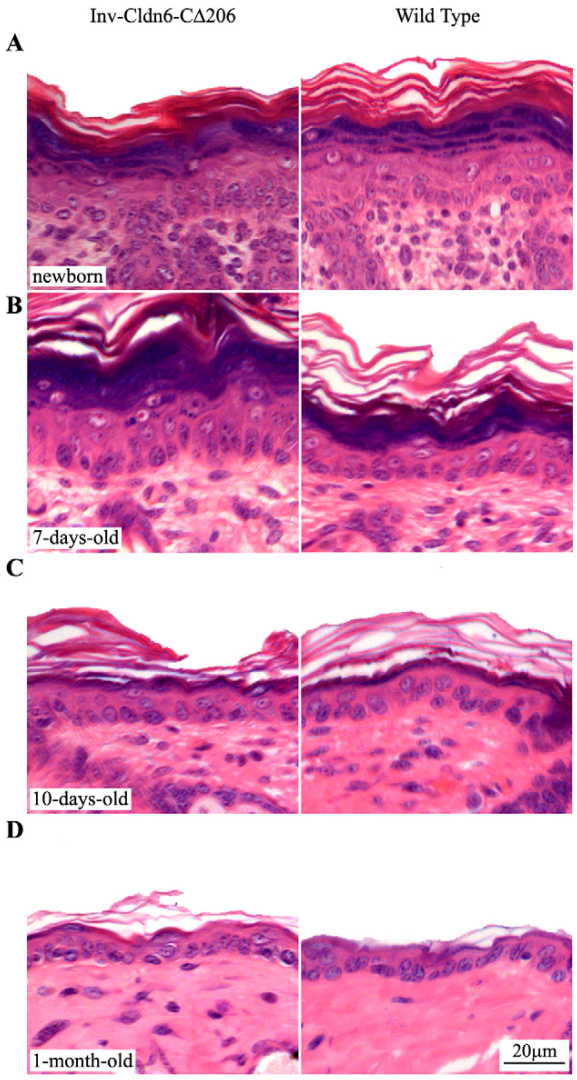

Fig. 5. Histological abnormalities in the Inv-Cldn6-CΔ206 transgenic epidermis after birth. (A) Histological analyses of skin samples revealed that, at newborn stages, the Inv-Cldn6-CΔ206 epidermis was comparable to the wild type. (B) However, it was evident that, after 7 days, the transgenic epidermis did not undergo the normal process of maturation/thinning that was observed in the wild-type epidermis and was characterized by an increased number of suprabasal cell layers, the prevalent appearance of nuclei in the upper differentiation layers, and a much less compacted granular layer. However, representing a 3-day lag behind the wild type, the transgenic epidermis thinned to be morphologically comparable to the wild type by 10 days after birth (C), a phenotype that was maintained after 1 month (D) and throughout life. Bar, 20μm.

CΔ206 transgenic epidermis (Fig. 6A). K6 and K17, which are keratins associated with a hyperproliferative epidermis (Leigh et al., 1995; McGowan and Coulombe, 1998b; 1998a), were not expressed throughout the time analyzed (not shown); however, a broadened K1 (Fig. 6B) expression compartment was seen in the transgenic epidermis early after birth, but normalized by 10 days of age. Similarly, the expression compartments for involucrin (Fig. 6C), filaggrin (Fig. 6D) and loricrin (Fig. 6E) were also expanded, with an obvious packing defect reminiscent of the observed histological abnormalities of the stratum corneum, in the immature Inv-Cldn6-CΔ206 transgenic epidermis until thinning that was comparable to the wild-type epidermis was achieved.

In parallel with changes in epidermal markers, the suprabasal-specific Cldns, Cldn6 (Fig. 7A), Cldn11 (Fig. 7B), Cldn12 (Fig. 7C) and Cldn18 (Fig. 7D) were observed in the expanded suprabasal region of the immature Inv-Cldn6-CΔ206 transgenic epidermis, and immunostaining demonstrated a loss in membranous localization. Each of these Cldns was normalized, with a strictly membranous localization, upon epidermal maturation to a phenotype that was comparable to the wild type. Cldns not normally expressed in the epidermis (e.g. Cldn2, Cldn3 and Cldn5) (Turksen and Troy, 2002) were not observed in either the wild-type or Inv-Cldn6-CΔ206 transgenic epidermis at any time evaluated (not shown). We also compared the expression of markers previously reported to be modulated during the epidermal maturation process in the newborn, 4-, 7- and 10-day-old transgenic mice compared with the wild-type epidermis. Changes in the overall surface pH of the epidermis contribute to the activation of enzymes involved in lipid processing

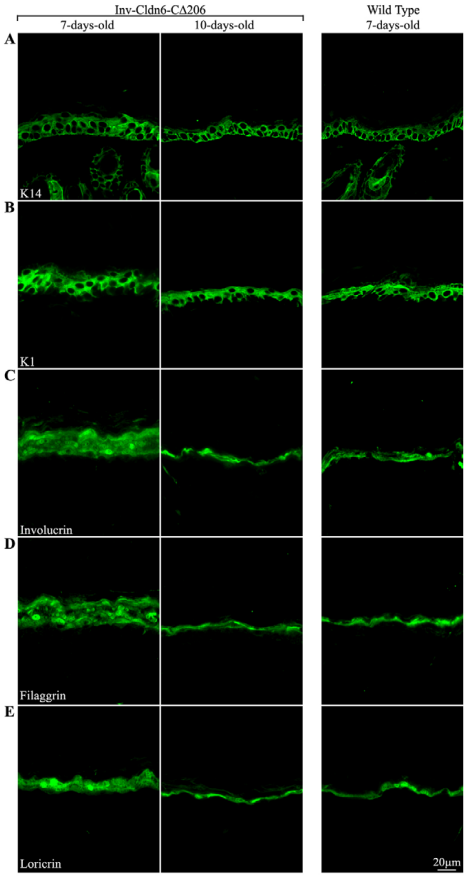

Fig. 6. Perturbation of markers of epidermal differentiation are normalized by postnatal day 10 in the Inv-Cldn6-CΔ206 transgenic epidermis. Changes in the epidermal differentiation program of the Inv-Cldn6-CΔ206 transgenic epidermis were evaluated by immunofluorescence and compared with their age-matched wild-type counterparts (samples from 7 and 10-day-old transgenic mice are shown and compared with the mature wild-type epidermis at 7 days). (A) In the transgenic epidermis, K14 occupied an expanded zone extending into the suprabasal compartment until epidermal maturation was achieved. (B) K1 was first observed in an expanded zone of expression, but normalized by 10 days of age in the Inv-Cldn6-CΔ206 transgenic epidermis. (C-E) Similarly, broadened expression compartments and obvious packing defects for involucrin (C), filaggrin (D) and loricrin (E) characterized the immature Inv-Cldn6-CΔ206 transgenic epidermis until thinning comparable to the wild type was achieved. Bar, 20μm.

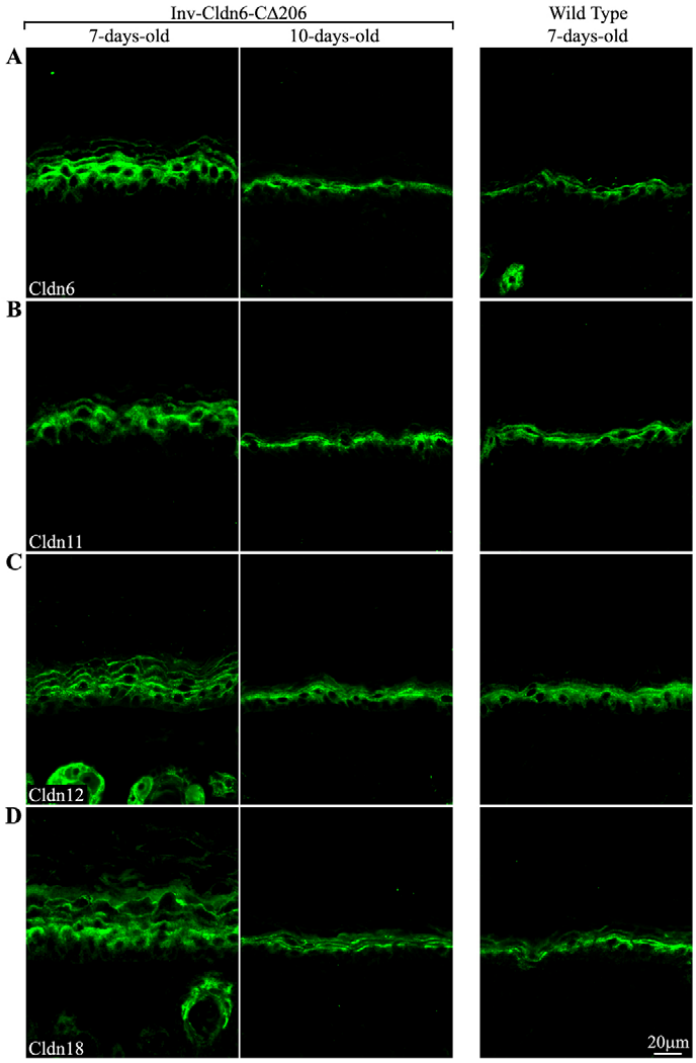

Fig. 7. Evaluation of Cldns in the delayed EPB of Inv-Cldn6-CΔ206 transgenic mice. The expression / localization of Cldns was also perturbed in the immature Inv-Cldn6-CΔ206 epidermis (7- and 10-day-old transgenic samples are shown and compared with the mature wild type samples at 7 days). (A-D) Cldn6 (A), Cldn11 (B), Cldn12 (C) and Cldn18 (D) were observed in an expanded zone early on, demonstrating a loss in membranous localization, and were normalized by 10 days after birth. Bar, 20μm.

for EPB function, and the plasma membrane Na+/H+ exchanger 1 (NHE1) has been implicated in this process (Behne et al., 2003; Fluhr et al., 2004a; 2004b; Hachem et al., 2005). Consistent with earlier reports (Behne et al., 2003), we found that NHE1 was localized in a 'punctate' pattern at the cell membrane of the basal and suprabasal compartments of the newborn wild- type epidermis, and as epidermal maturation progressed, NHE1 was gradually downregulated with localization restricted to the basal compartment by 7 days after birth (Fig. 8A-D, right column). By contrast, NHE1 was persistently upregulated and associated with bot the basal and suprabasal cell compartments of the Inv-Cldn6-CΔ206 transgenic epidermis from birth to 7 days of age; downregulation and strict basal cell association was not observed until postnatal day 10 (Fig. 8A-D, left column). Immunoblot (Fig. 8E) and RT- PCR (Fig. 8F) analyses supported these findings. Similarly, aquaporins (AQPs), which are small integral membrane proteins that selectively transport water across cell membranes, and key lipid processing enzymes [β-glucocerebrosidase (β-celerase) and acid sphingomyelinase (α-SMase)] that are important in EPB homeostasis (Behne et al., 2003; Hara-Chikuma and Verkman, 2008) were also modulated in the Inv-Cldn6-CΔ206 transgenic epidermis versus the wild-type epidermis, as shown by immunoblot (Fig. 8E) and RT-PCR (Fig. 8F) analyses.

Changes in Cldn1, phosphoCldn1 and Erk1/2 expression profiles delineate repair and maturation processes in the Inv-Cldn6-CΔ206 transgenic epidermis

The relatively rapid postnatal normalization of TEWL in Inv-Cldn6-CΔ206 transgenic mice, together with the morphological and marker expression changes observed,

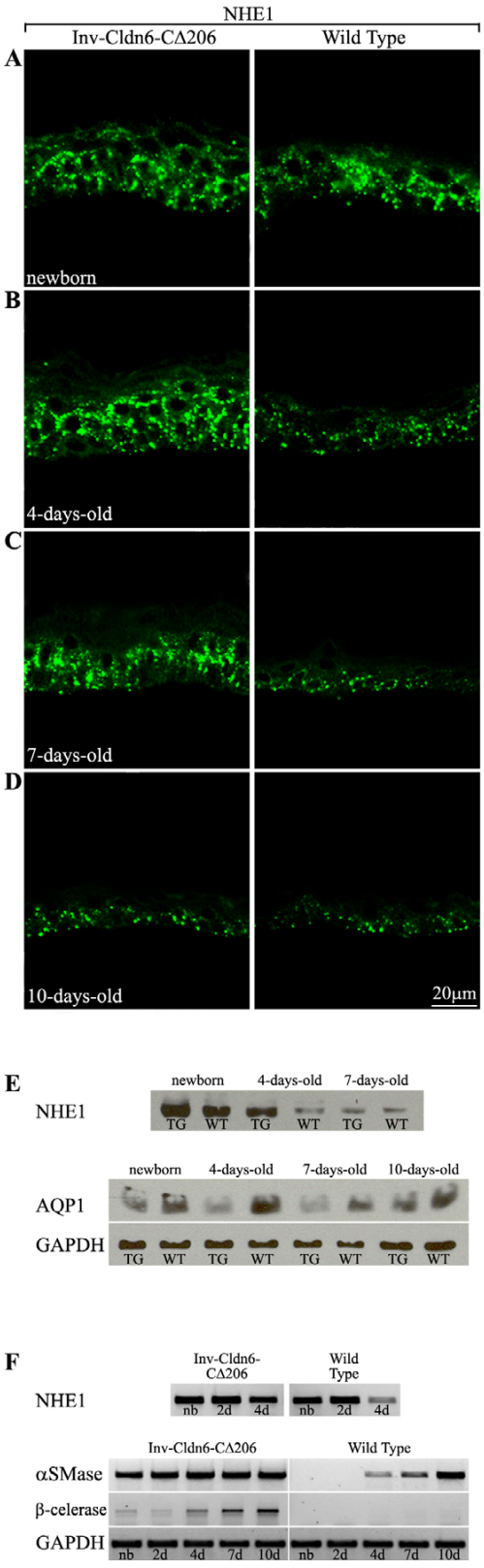

Fig. 8. Modulation in NHE1 expression/ localization. (A-D) Localization of NHE1 was evaluated in skin samples from newborn (A), 4-day-old (B), 7-day- old (C) and 10-day-old (D) Inv-Cldn6-CΔ206 transgenic mice (left column) compared with wild-type mice (right column). In the Inv-Cldn6-CΔ206 transgenic epidermis, NHE1 was upregulated and associated with both the basal and suprabasal cell compartments from newborn to 7 days after birth; downregulation and strict basal cell association was not observed until postnatal day 10. Bar, 20μm. These data were supported by immunoblot (E) and RT-PCR (F) analyses. Modulations in mRNA or protein levels of AQP1, β-celerase and αSMase are also shown relative to GAPDH controls.

suggested a robust maturational or repair process. Previous studies, including our own (see above), have demonstrated the importance of Cldn1 in epidermal morphogenesis, differentiation, and EPB formation and repair. In particular, the expression of Cldn1 is unique compared with other Cldns and undergoes a maturation switch, from a strictly suprabasal association to being localized to cell-cell borders in all the living layers of the epidermis, coinciding with the acquisition of barrier function during epidermogenesis (Troy et al., 2007b). This normal expression profile is maintained throughout life except in response to acute injury and in tumorigenesis, where basal layer association is lost, and Cldn1-null epithelial cells are progressively more frequent in the lower suprabasal compartment (Arabzadeh et al., 2007a; 2007b). In comparison to the wild-type basal to suprabasal localization of Cldn1 (Fig. 9A-D, right column), Cldn1-null epidermal cells were observed in the basal and lower suprabasal layers of the Inv-Cldn6-CΔ206 transgenic epidermis from 4-7 days after birth; as anticipated based on normalization of TEWL and morphology, Cldn1 localization was normalized in samples from 10-day-old mice (Fig. 9A-D, left column). Although no differences were detected in mRNA levels (Fig. 9F), immunoblotting confirmed decreased Cldn1 protein levels (Fig. 9E) in samples of 2-day-old Inv-Cldn6-CΔ206 transgenic epidermis. Given the evidence suggesting that the phosphorylation of different Cldns is involved in either the strengthening or weakening of TJs, and in parallel barrier function (D'Souza et al., 2007; Findley and Koval, 2009; Ikari et al., 2007), we next asked whether expression of the phosphorylated form of Cldn1 (phosphoCldn1) was altered in transgenic versus wild-type epidermis. PhosphoCldn1 was not observed in the wild-type epidermis at any of the time points assayed (data not shown). However, phosphoCldn1 was localized to cell-cell

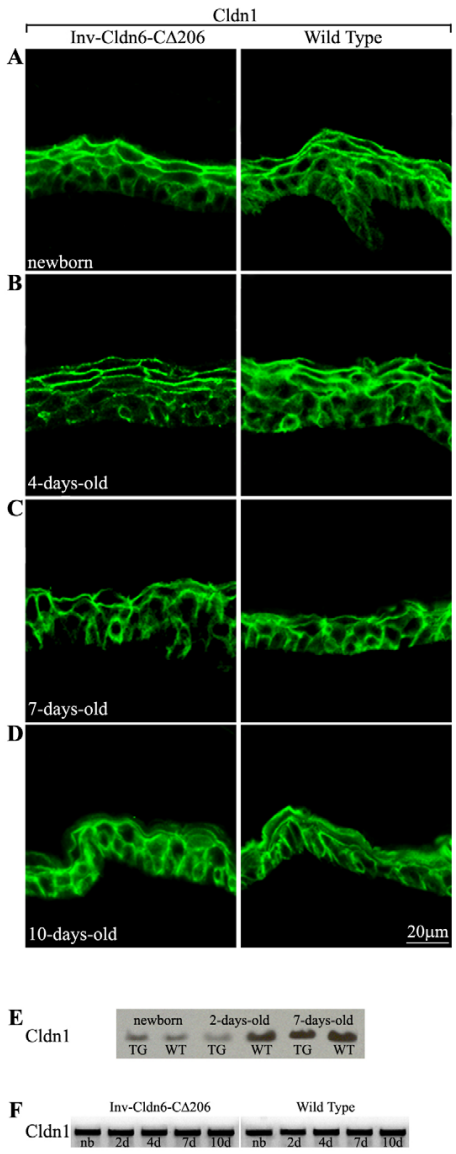

Fig. 9. Changes in Cldn1 expression and localization in the Inv-Cldn6-CΔ206 transgenic epidermis. Unlike the normal wild type (right column) basal to suprabasal localization of Cldn1, the Inv-Cldn6-CΔ206 transgenic epidermis (left column) showed abnormalities. (A-C) Although localization was normal at newborn stages (A), Cldn1-null epidermal cells were observed in the basal and lower suprabasal layers from 4 days (B) to 7 days (C) after birth, and were normalized by 10 days after birth (D). Bar, 20μm. (E-F) Immunoblotting confirmed the changes in Cldn1 protein level (E); whereas RT-PCR indicated that there were no differences at the mRNA level (F).

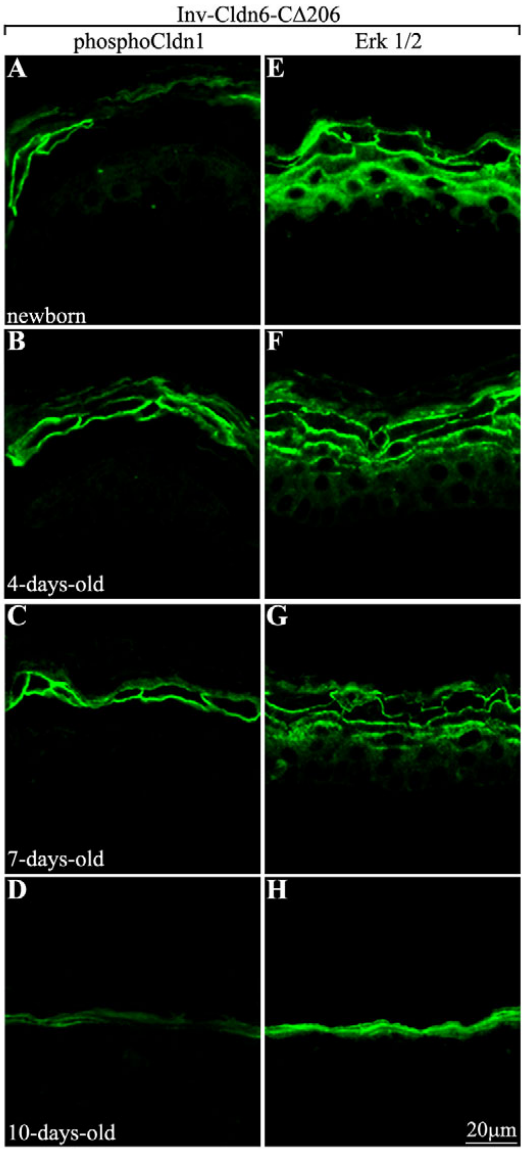

Fig. 10. The localization of phosphoCldn1 and Erk1/2 in the epidermis of Inv-Cldn6-CΔ206 transgenic mice. (A-H) Skin samples from newborn (A,E), 4- day-old (B,F), 7-day-old (C,G) and 10 day-old (D,H) Inv-Cldn6-CΔ206 transgenic mice were used to evaluate the localization of phosphoCldn1 (left column) and Erk1/2 (right column). From newborn to 7 days of age, phosphoCldn1 was localized to cell-cell borders in the upper suprabasal zone of the Inv-Cldn6-CΔ206 transgenic epidermis. Correspondingly, Erk1/2 localization followed the same pattern with a considerable distribution at the cell membrane of differentiating cells. Bar 20μm.

borders in the upper suprabasal zone of the newborn Inv-Cldn6-CΔ206 transgenic epidermis until epidermal repair was achieved at postnatal day 10 (Fig. 10A-D). Concomitantly, expression of Erk1/2 followed the same distribution pattern of phosphoCldn1 (Fig. 10E-H) with a considerable amount of Erk1/2 localized to the cell membrane of differentiating cells in the newborn, 4-, 7- and 10-day-old Inv-Cldn6-CΔ206 transgenic epidermis.

DISCUSSION

In this study, we describe the generation of a novel animal model for evaluating developmental delays in EPB formation and the postnatal epidermal maturation processes that are analogous to those observed in the dysfunctional barrier phenotype of human premature babies. Using skin penetration assays and immunohistochemistry to evaluate the expression and localization of classical markers of epidermal differentiation and maturation, as well as the Cldns and signaling molecules that are involved in EPB formation, we demonstrated that Inv-Cldn6-CΔ206 transgenic mice suffered a developmental delay in epidermal differentiation and EPB formation leading to significant TEWL at birth, despite sufficient neonatal barrier formation (the presence of a cornified envelope) and function (the absence of X-Gal penetration) for survival. Postnatal TEWL measurements, along with changes observed in the expression and localization of keratins and Cldns, suggested that the Inv-Cldn6-CΔ206 transgenic epidermis underwent a robust epidermal maturation process after birth to become indistinguishable from the wild type. Although the molecular mechanisms underlying the delayed maturation and repair of the epidermis and EPB in these transgenic mice have

not yet been delineated, our data indicate that the Inv-Cldn6-CΔ206 mice constitute an attractive model from a therapeutics point of view, i.e. for the identification of lead compounds for accelerated repair of the often life-threatening permeability barrier defects in premature human infants.

Many studies have described the developmental formation of the EPB (Byrne and Hardman, 2005; Hardman et al., 1999; 1998; Turksen and Troy, 2002) and it is well recognized that a disruption or delay in its formation before birth may have severe consequences to the survival of the organism (Cartlidge, 2000; Elias, 2005; Mack et al., 2005; Williams et al., 1998). We described previously that perturbations of Cldn6 expression levels in the suprabasal compartment of the epidermis – its endogenous site – result in epidermal differentiation abnormalities and EPB dysfunction (Troy et al., 2005a; Turksen and Troy, 2002). However, depending on the level of expression, and whether normal or mutant forms of Cldn6 are expressed, the severity of the phenotype varies (Arabzadeh et al., 2006; Troy et al., 2005a; Troy and Turksen, 2007; Turksen and Troy, 2002). For example, severe EPB dysfunction manifested in extreme TEWL and neonatal lethality occurs when native Cldn6 is expressed at high levels (Turksen and Troy, 2002), whereas lower levels of expression result in less severe EPB dysfunction and postnatal normalization (Troy et al., 2005a). Overexpression of a mutant form of Cldn6 lacking its entire tail domain (Inv-Cldn6-CΔ187 mice) does not appear to manifest in any prenatal epidermal developmental defects, but an abnormal, postnatal, lifelong epidermal hyperproliferation is observed (Arabzadeh et al., 2006). High overexpression of a different mutant lacking only the C-terminal half of the tail domain of Cldn6 (Inv-Cldn6-CΔ196 mice) (Troy and Turksen, 2007) results in a lethal barrier dysfunction with

marked hyperproliferative squamous invaginations/cysts replacing hair follicles, while lower-level expression manifests in an aging-related skin barrier defect resulting in an intrinsic propensity for injury, inefficient repair and chronic dermatitis. We now show that transgenic mice expressing a mutant Cldn6 with a shorter tail deletion (removing the PDZ domain and a putative PKA phosphorylation site) possess a distinct developmental defect in epidermal differentiation resulting in EPB formation delays and that a robust repair response occurs for postnatal epidermal maturation. It is notable that formation of a skin barrier with functional TEWL characteristics that are indistinguishable from the wild type occurred more rapidly than, or prior to, complete morphological maturation of the epidermis in the postnatal Cldn6-CΔ206 mice, indicating an ability to disconnect aspects of the two processes, an observation that is interesting from a developmental standpoint but that may also be therapeutically important (see below).

The mechanisms by which the expression of Cldn6-CΔ206 results in a developmental delay in EPB formation and postnatal epidermal maturation and repair are not yet known, but our observations support the need for Cldn homeostasis in a bona fide epidermal differentiation program and in epidermal repair. We have previously demonstrated that there is a defined Cldn expression profile in the epidermis and that changes in epidermal differentiation elicit concomitant modifications in the Cldn expression profile and vice versa (Troy et al., 2005a; Turksen and Troy, 2004; 2002). Upon injury, or in response to differentiation abnormalities, the spatial expression of the suprabasal Cldns (Cldn6, Cldn11, Cldn12 and Cldn18) generally expands or shrinks to encompass all the cells of the perturbed suprabasal zone, with some concomitant loss in cell membrane association (Arabzadeh et al., 2007a; 2006; Troy et al., 2005a; Turksen and Troy, 2002). This was

also true in the immature Inv-Cldn6-CΔ206 epidermis: as the epidermis matured, by postnatal day 10, the localization and expression of the Cldns normalized to a strictly membranous association in a suprabasal zone that was comparable in thickness to that of the wild type. However, Cldn1 undergoes more dramatic alterations in response to epidermal homeostasis dysregulation. In the developing epidermis, Cldn1 is first restricted to the stratifying layers and matures to occupy the basal layer upon the completion of barrier formation at E17.5 (Troy and Turksen, 2007). However, in response to TPA (12-O-tetradecanoyl-phorbol-13-acetate)-induced injury and the loss of cell polarity that is seen in tumorigenesis, Cldn1 expression is downregulated in both the basal layer and immediate suprabasal layers of the epidermis (Arabzadeh et al., 2007a). These changes are also observed in the intrinsic aging process of the Inv-Cldn6-CΔ196 transgenic epidermis and in the delayed epidermal maturation that we now report in Inv-Cldn6-CΔ206 transgenic mice. Notably, Cldn1 expression normalized with the normalization of epidermal differentiation markers and epidermal maturation (see below).

Although Cldns demonstrate amino acid similarity among family members, the cytoplasmic tails of Cldns are divergent in sequence and possess a number of sites that provide clues about their structure-function relationships in epidermal differentiation, including a PDZ binding sequence (YV) and potential phosphorylation sites (Fujibe et al., 2004; Simard et al., 2006). Proteins with a PDZ domain such as the membrane-associated guanylate kinase (MAGUK) family proteins [zonula occludens (ZO)1, ZO2 and ZO3] (Itoh et al., 1999), as well as the recently identified multi-PDZ domain scaffolding proteins PATJ (protein associated to tight junctions) (Lemmers et al., 2002) and multi-PDZ domain protein 1 (MUPP-1) (Hamazaki, 2001), selectively recognize and

bind to this sequence (for a review see (Gonzalez-Mariscal et al., 2003)). However, it seems likely that as yet unidentified novel molecules interact with Cldns in regulating gene expression and epidermal differentiation. Post-translational modifications within the tail domain, including phosphorylation and palmitoylation, are also thought to regulate Cldn activities, including their targeting to the membrane and their insertion into TJs to regulate paracellular permeability (Simard et al., 2006). Phosphorylation of a number of Cldns has been demonstrated to be required for their assembly into TJs [e.g. for Cldn1 and Cldn4 (Banan, 2005), and for Cldn16 (Ikari et al., 2007)] but, to date, most Cldns have not been subjected to exhaustive analysis. Our observation of the association of phosphoCldn1 with the differentiated layers of the immature Inv-Cldn6-CΔ206 transgenic epidermis points towards the potential role of Cldn1 phosphorylation in the process of epidermal maturation and EPB repair.

Although the precise sequence of events in the maturation of the skin barrier is not well understood, the notion that exposure to air after birth functions to initiate and accelerate the maturation and repair of the skin barrier has been suggested (Hanley et al., 1997; Williams et al., 1998). The fetal and neonatal anomalies with spontaneous and apparently complete epidermal maturation and barrier repair that we observe in postnatal Inv-Cldn6-CΔ206 transgenic mice support the view that exposure to air induces an intrinsic repair and maturation pathway. Other support for this hypothesis comes from a number of studies; for example, exposing embryonic immature epidermis to air (Williams et al., 1998), lifting skin-equivalent cultures to the air-liquid interface (Fartasch and Ponec, 1994; Kömüves et al., 1999), and inducing injury to the EPB by tape stripping (Ahn et al., 1999; 2001) each result in a robust EPB repair and epidermal maturation

response. Although collectively these studies do not provide a mechanism for the observed intrinsic repair/maturation process in the epidermis, our studies suggest that the first phase of repair is the shedding of defective differentiation layers, which we identified as phospoCldn1-expressing cells with co-expression of high levels of Erk1/2. Considering the important role of Erk1/2 in epithelial differentiation (Hobbs et al., 2004; Taupin and Podolsky, 1999; Yu et al., 2007), as well as in the regulation of Cldn expression (Lipschutz, 2004), our data support a role for Erk1/2 in the initiation or progression of the epidermal repair and maturation that was observed in Inv-Cldn6-CΔ206 transgenic mice. Concomitantly, initiation probably also involves the well-known phenomena of cross-talk between the differentiating and the basal compartments of the epidermis, which has been demonstrated to tightly regulate the epidermal differentiation program and is responsible for the normal maintenance program of the epidermis (Prowse et al., 1999; Troy et al., 2005a); evidence for this comes from our reported observations regarding the remodeling of Cldn1 expression in the repairing Inv-Cldn6-CΔ206 transgenic epidermis. Further analyses are required to understand how 'air exposure' activates the Erk1/2 pathway and the observed Cldn1 phosphorylation process.

Although a variety of maternal and fetal diseases and conditions can lead to premature birth, the reasons underlying the quite dramatic increases in premature birth, in not only underdeveloped but also developed countries, over the last decade are unknown (Darmstadt et al., 2008; Lang and Iams, 2009; Yeaney et al., 2009). Complications owing to compromised skin barrier function (e.g. poor temperature regulation and dehydration) in premature babies are among the primary causes of neonatal sepsis and mortality (Rutter, 2000; 1996; Saiman, 2006). Given the importance of skin barrier

function in the health of premature babies and the fact that intrinsic risk factors of sepsis include compromised portals of entry for pathogens (Saiman, 2006), there is a surprisingly significant lack of successful approaches/strategies that have been designed specifically to accelerate the postnatal maturation of the epidermis (McIntire and Leveno, 2008; Shapiro-Mendoza et al., 2008; 2006; Tyson et al., 2008). Strategies for reducing the rate of sepsis are currently focused on limiting the spread of infection through aseptic clinical techniques and the use of antibiotics, which are increasingly becoming ineffective (Saiman, 2006). In addition, the topical application of relatively low-cost emollients, especially in underdeveloped countries, has proven to have some benefit, although whether this is from provision of a mechanical barrier or from induction of biological responses to some of the ingredients, or both, is not clear (Darmstadt et al., 2008). Understanding these mechanisms, as well as screening for potential novel therapeutics to accelerate postnatal epidermal maturation, have been hampered by the lack of suitable in vivo models. The capacity of the Inv-Cldn6-CΔ206 transgenic epidermis to undergo a postnatal repair response and acquire a mature epidermis by 10 days after birth makes this transgenic model an excellent tool for investigating not only the molecular changes taking place during this maturation period, but also for screening for novel therapeutics to accelerate this process and improve the health of human premature infants.

METHODS

Generation of Inv-Cldn6-CΔ206 transgenic mice

Inv-Cldn6-CΔ206 mice were generated by truncating the cytoplasmic tail domain of Cldn6 after amino acid 206 (Cldn6-CΔ206) and then subcloning Cldn6-CΔ206 into the

NotI site of the Inv cassette (H3700-pL2) by our previously utilized strategy (Arabzadeh et al., 2006; Troy and Turksen, 2007; Turksen and Troy, 2002). Purified DNA was injected into ova collected from superovulated CD1 mice at the Transgenic Mouse Facility of the Ottawa Hospital Research Institute (OHRI), as described previously (Arabzadeh et al., 2006; Troy and Turksen, 2007; Turksen and Troy, 2002). The presence of the transgene was confirmed by PCR using genomic DNA and specific primers. Photography of age-matched wild-type and Inv-Cldn6-CΔ206 transgenic mice was performed using a Nikon Coolpix 950 digital camera (Nikon) and image processing was performed with Adobe Photoshop version 7.0 (Adobe Systems). All research was carried out in accordance with the principles and guidelines of the Canadian Council on Animal Care, and the policies of the OHRI Animal Care Committee.

RNA isolation and RT-PCR

Skin samples dissected from the mid-dorsal region of transgenic and wild-type mice were frozen in liquid nitrogen, and then homogenized in Trizol (Invitrogen) reagent for total RNA isolation according to the instructions of the manufacturer. After DNase (Invitrogen) treatment, first-strand cDNA was synthesized using random hexamers (Applied Biosystems) and 1 μg of RNA. PCR analysis was then performed, as described previously (Troy et al., 2005a) using the following specific primers: Inv exon-Cldn6 [~350 bp; FP: 5'-CTGCCTCAGCCTTACTGTGAG-3' (KT323), RP: 5'-CCAACAGTGAGTCATACAC-3' (KT1526)], GAPDH [167 bp; FP: 5'-CAGTATGACTCCACTCACGG-3' (KT841), RP: 5'-GTGAAGACACCAGTAGACTCC-3' (KT842)], NHE1 [498 bp; FP: 5'-

GAGATCCACACACAGTTC-3' (KT1515), RP: 5'- TACTGTCAGGTAGTTGGTG-3' (KT1516)], α-SMase [567 bp; FP: 5'-AGACTGGAGAGGTCCTTA-3' (KT1537), RP: 5'-GTCCCAGTGTAGATCAGTAA-3' (KT1538)], β-celerase [512 bp; FP: 5'-TACTTTAGGAGAGACACACC-3'(KT1539),RP:5'- GGTAAGTGTGAATGGAGTAG -3' (KT1540)] and Cldn1 [644 bp; FP: 5'-AAAGAGCCATGGCCAACGC -3' (KT1315), RP: 5'- TCACACATAGTCTTTCCCACTAG -3' (KT1316)]. RT-PCR products, relative to a housekeeping control (GAPDH), were separated on ethidium bromide-containing agarose gels, visualized by ultraviolet light, and images were acquired using AlphaEaseFC software version 4.0 (Alpha Innotech Corporation).

Skin permeability assays

X-gal penetration assay

Freshly dissected Inv-Cldn6-CΔ206 transgenic embryos (E15.5, E17.5 and E18.5; the embryonic age was estimated based on the appearance of the vaginal plug at E0.5) and euthanized neonates, along with their age-matched wild-type counterparts, were rinsed in PBS and immersed in X-Gal reaction mix at pH 4.5 [100 mM $NaPO_4$, 1.3 mM $MgCl_2$, 3 mM $K_3Fe(CN)_6$, 3 mM $K_4Fe(CN)_6$ and 1 mg/ml X-Gal], as described previously (Hardman et al., 1998; Turksen and Troy, 2003; 2002). Following an overnight room temperature incubation, specimens were fixed with formalin and images were acquired using a Nikon Coolpix 950 digital camera followed by processing with Adobe Photoshop version 7.0.

Trans-epidermal water loss (TEWL) measurements

A dermal phase meter (DPM) (Nova Technology Corporation) was used to measure the dorsal and ventral impedance/TEWL of Inv-Cldn6-CΔ206 transgenic and wild-type mice, as described previously (Troy et al., 2005a; Turksen and Troy, 2002), at various postnatal time points from birth to the emergence of coat hairs, at which time measurements are no longer feasible owing to improper contact between the meter probe and the skin. Higher DPM values measured over time translate to reduced barrier integrity, illustrated digitally by EDWINA (Nova Technology Corporation) and Excel (Microsoft) software programs.

Cornified envelope extracts

Purified cornified envelope extracts were prepared from CD1 and Inv-Cldn6-CΔ206 transgenic mice by immersion of dorsal skin samples into hot extraction buffer (0.1M Tris-HCl, pH 8.5, 2% SDS, 20 mM dithiothreitol, 5 mM EDTA), followed by a 15-minute incubation at 95°C and gentle centrifugation, as described previously (Hohl et al., 1991; Troy et al., 2005a; Turksen and Troy, 2002).

Sample collection, histology and immunolocalization

Sample preparation

Freshly dissected skin samples (~1 cm) and whole embryos were collected from wild-type and Inv-Cldn6-CΔ206 transgenic mice at various embryonic and postnatal time points (E15.5, E17.5, E18.5, newborn, and 2 days, 4 days, 6 days, 7 days, 8 days, 10 days, 12 days, 2 weeks, 3 weeks, 1 month and 3 months of age).

Paraffin sections and histology

Following an overnight fixation in Bouin's solution (75% saturated picric acid, 20% formaldehyde, 5% glacial acetic acid), skin samples were dehydrated by a graded series of ethanol washes (from 30% to 100%) and embedded in paraffin. Sections (5 μm) were mounted onto Superfrost/Plus slides (Fisher Scientific), and were dewaxed using toluene and rehydrated in a reverse series of ethanol washes to water. Following antigen unmasking and washes in PBS, sections were either stained with hematoxylin and eosin (H&E), as described previously (Troy et al., 2005b), or used for immunohistochemistry (see below).

Immunohistochemistry

Non-specific antibody binding (10% goat serum, 0.8% BSA, 1% gelatin in PBS) was blocked, followed by incubation for 1 hour in antibodies that were diluted appropriately with incubation buffer (1% goat serum, 0.8% BSA, 1% gelatin in PBS) (Troy et al., 2005b). Antibodies against the following antigens were evaluated: K15 (1:100; rabbit #UC55), K5 (1:100; rabbit #5054), K14 (1:100; rabbit #199), K1 (1:100; rabbit #UC81), K6 (1:200; BabCO), K17 (1:500; a gift from Dr Pierre Coulombe, Johns Hopkins University School of Medicine, Baltimore, MD), involucrin (1:100; BabCO), filaggrin (1:100; BabCO), loricrin (1:100; rabbit #UC84), Cldn1 (6:100; Zymed Laboratories), Cldn2 (1:200; Zymed Laboratories), Cldn3 (1:50; Zymed Laboratories), Cldn5 (1:100; Zymed Laboratories), Cldn6 (1:100; chicken #3677), Cldn11 (1:100; chicken #3680), Cldn12 (1:100; chicken #5186), Cldn18 (1:100; rabbit #A9953), NHE1 [3:100; Chemicon-AB3031 (incubation was overnight at 4°C)], phosphoCldn1 [1:100; a custom antibody generated from rabbit #2827 against the tail domain of the mouse phosphoCldn1

sequence (Ac-C-Ahx-PYPKP[pT]PSSGKDY-amide), 21st Century Biochemicals] and Erk1/2 (1:100; StressMarq Biosciences Inc.). After incubations in wash buffer (0.8% BSA, 1% gelatin in PBS), FITC-conjugated secondary antibodies against mouse, rabbit and chicken (1:50; Jackson ImmunoResearch) were diluted in incubation buffer and used for 1-hour incubations at room temperature. Following the final washes, skin samples were mounted with Mowiol 4-88 (Calbiochem), containing 2.5% 1,4 diazobicyclo-[2,2,2]-octane (DABCO; Sigma), for observation with a Zeiss Axioplan 2 fluorescence microscope equipped with an AxioCam camera and Axio Vision 2.05 software (Carl Zeiss). Digital photography was presented with Adobe Photoshop version 7.0.

Protein Isolation and Immunoblotting

Freshly dissected back skin samples (0.4 grams) were homogenized in SDS extraction buffer [62.5 mM Tris, pH 6.8, 25% glycerol, 2% SDS and 2% β–mercaptoethanol, with pepstatin A and a complete mini protease inhibitor cocktail (Roche Diagnostics) tablet] followed by high-speed centrifugation. The supernatant containing the proteins was collected and assayed for protein concentration. Proteins were incubated at room temperature for 30 minutes in sample reducing buffer (62.5 mM Tris, pH 6.8, 6 M urea, 25% glycerol, 2% SDS, 0.1% Bromophenol Blue and 2% β-mercaptoethanol), boiled for 5 minutes (samples were not boiled for analysis of NHE1), and centrifuged at high speed for 10 minutes before 5-50 μg samples were separated on 7.5-12% SDS-PAGE gels, transferred to nitrocellulose and incubated in blocking buffer [5% skimmed milk in TBS/0.1% Tween-20 (TBS-T)] for 1 hour at room temperature. Appropriately diluted (5% skimmed milk in TBS-T) antibodies were used for overnight incubations at 4°C.

The following antibodies were used: NHE1 (91 kDa, 1:1000; Chemicon), AQP1 (28 kDa, 1:1000; Alpha Diagnostic), Cldn1 (23 kDa, 1:1000; Zymed Laboratories) and GAPDH (36 kDa, 1:10,000; Abcam). After washing in TBS-T, blots were incubated for 1 hour at room temperature in HRP-conjugated secondary antibodies against rabbit or mouse (1:20,000; Amersham Biosciences), then diluted in 5% skimmed milk/TBS-T. Following washes in TBS-T, the Immobilon Western blotting detection system (Millipore) was used for detection, and expression levels were normalized to a housekeeping control (GAPDH) and visualized on Kodak BioMaxXAR film (Kodak). Films were digitally scanned and images were processed with Adobe Photoshop version 7.0.

TRANSLATIONAL IMPACT

Clinical issue: An estimated 28% of the 4 million annual neonatal deaths are because of preterm birth. It is likely that many of these deaths result from an immature permeability barrier, leading to dehydration and infection with associated septic shock. The statistics published by the March of Dimes indicate a 36% increase in premature births in America in the last 25 years, and the cause is not understood. This is an alarming, and emotionally and ethically complex, situation that adds significant pressure to pediatric medicine. The absence of appropriate disease models in which to delineate the basis of barrier dysfunction and test new therapies limits progress in the field.

Results: Here, the authors characterize a mouse model that mimics a debilitating, non-fatal form of a dysfunctional epidermal permeability barrier, similar to that seen in human premature babies. The tight junction-associated proteins, claudins, play a crucial role in establishing the epidermal permeability barrier. One theory is that claudin-containing

tight junctions act as command centers in which the claudin extracellular loops influence selective permeability, while their cytoplasmic tail domains send signals to other receptors to coordinate downstream effectors, such as the cytoskeleton. The transgenic mouse reported here contains a short claudin-6 tail truncation. This mutation results in a delayed and defective epidermal permeability barrier that, surprisingly, is repaired within 2-4 days after birth. The repair process was associated with remodeling of the claudin-1 expression domains that eliminated the defective differentiated epidermal cells and replaced them with apparently 'normal' and terminally differentiated epidermal cells. The trigger for repair appears to be exposure to air. The potential signaling pathways involved include the sphingosine-1-phosphate (S1P) pathway and preliminary observations implicate Erk1/2 downstream of the S1P-receptor 2. The relevance of this model for understanding human disease is confirmed by the authors' observations of similar features in specimens from premature babies, including dramatic delays in barrier formation and dysregulation of claudin expression, notably claudin-1.

Implications and future directions: Clinical outcomes for premature babies have been improved by using incubators that carefully control heat and humidity, but currently there are no therapeutic approaches for accelerating repair of the premature epidermal permeability barrier. The observation that activation of S1P and S1P-receptor 2 induce permeability repair processes suggests the therapeutic potential of selective receptor agonists. A few agonists have been described and this model is a viable model to test them. In summary, we think it is important to have made a model that mimics a repairable human epidermal permeability barrier, to have documented important cellular mechanisms of that repair, and to have begun delineation of the underlying molecular

mechanisms, which are also pointing towards potential new therapies.

ACKNOWLEDGEMENTS

This work is dedicated to Dr George E. Palade for his discovery of tight junctions with Marilyn G. Farquhar in 1963. We are indebted to Dr Jane E. Aubin (University of Toronto) for her tireless efforts and vigorous dedication to every aspect of our studies. We would also like to thank Dr Pierre Coulombe (Johns Hopkins) for his gift of the anti-K17 antibodies, and StressMarq Biosciences Inc. for their gift of the Erk1/2 antibodies. We acknowledge Mrs Adriana Gambarotta and Mr Pierre Bradley of the animal care facility of the OHRI for their great efforts, and Zaida J. Ticas (MLT) (University of Ottawa) who prepared our histological and paraffin-embedded sections. We also acknowledge Dr. Vivian Siegel for her editorial insights. K.T. would like to acknowledge Paul Newman for Cool Hand Luke, eggs and 'What we got here is...failure to communicate'. This work was sponsored by a research grant from the Canadian Institutes of Health Research (# MOP 84464).

Identification and Validation of a Cldn6 C-terminal Interacting Partner

To identify cytoplasmic factors interacting with this extreme C-terminal region, a yeast 2-hybrid (Y2H) screen was conducted on an early epidermal differentiation (embryonic day E15.5) mouse library using the entire Cldn6 cytoplasmic tail (35 amino acids) as bait. The screen identified the known interactor ZO1, along with the novel hits Filamin and the putative transcription factor FIZ1 (Flt3 interacting zinc finger protein-1).

FIZ1 is expressed in various epithelia (Wolf and Rohrschneider, 1999), although it has been primarily studied in retinal cells (Mali et al., 2008; 2007; Mitton et al., 2003). Our studies are the first to assess FIZ1 in the epidermis. While there are currently no published reports examining Fiz1 protein modulation in mouse models, preliminary analysis of a Fiz1 knockout mouse indicated that the newborn epidermis is moderately thicker than the wild type counterpart, with keratinocytes displaying nuclear retention in the suprabasal layers (parakeratosis). This could be indicative of a less mature phenotype or a hyperproliferative phenotype, but at least suggests a defect in signaling (A2 Fig.1A).

The Y2H-predicted interaction was validated by reciprocal co-immunoprecipitation of Cldn6 and Fiz1 in mouse newborn skin lysates (A2 Fig. 2A-B). Due to reagent limitations, functional characterization of FIZ1 was carried out in the HaCaT human keratinocyte cell line, which is a widely-used model system for the analysis of epidermal homeostasis (Boukamp et al., 1988). FIZ1 expression and binding to CLDN6 were confirmed in HaCaT cells (A2 Fig.2C-E). In keratinocytes, FIZ1 is predominantly nuclear under both proliferating and differentiating conditions, although it is also detected in soluble cytoplasmic fractions by Western blot analysis. No detectable FIZ1 was found at the plasma membrane (A2 Fig. 3A-D). In contrast, CLDN6 is only detected in

differentiating keratinocytes and accumulates predominantly at the plasma membrane, with a smaller percentage detected in the cytoplasm (A2 Fig. 3A-D). We validated an interaction between FIZ1 and CLDN6 specifically in the soluble cytoplasmic fraction of HaCaT cells (A2 Fig. 3C). Our data suggest the potential for these proteins to interact with and influence each other's function, perhaps serving as a means for TJ signaling propagation to the nucleus.

We mapped a minimal region (12aa) of the CLDN6 C-terminal tail necessary and sufficient to mediate FIZ1 binding in keratinocytes (A2 Fig. 3E), and investigated the contribution of the CLDN6 PDZ binding motif to FIZ1 binding. Although FIZ1 does not contain a predicted PDZ domain, it does show binding specificity for CLDNs that contain a C-terminal "YV" PDZ binding motif (Cldns1, 6 and 18) and does not interact with CLDN12, which lacks this domain (A2 Fig. 4A-B). Deleting the C-terminal Valine in the PDZ binding motif of CLDN6 disrupted interaction with ZO1, as expected (Schneeberger, 2004), but had no effect on FIZ1 interaction (A2 Fig.3E), confirming that binding is mediated by a region upstream of this motif. Interestingly, the Tyrosine residue in the "YV" motif was recently mapped as a phospho-residue (Rigbolt et al., 2011) and is conserved in CLDNs 1,6 and 18 (A2 Fig. 4B). Given that we have narrowed down the FIZ1 interaction domain to 12 amino acids, future studies could remove these remaining residues sequentially, starting with this conserved Tyrosine, to determine their contribution to the binding event. Furthermore, although we have not demonstrated here whether binding is direct or indirect, the fact that the interaction was originally identified in a Y2H screen suggests that it is direct.

CHAPTER 3:

FIZ1 promotes proliferation of human keratinocytes via autocrine signaling pathways

Nathalie Larivière[1,2], Jennifer Law[1] and *Laura Trinkle-Mulcahy[1]

[1]Department of Cellular & Molecular Medicine and Ottawa Institute of Systems Biology, University of Ottawa, Ottawa, Ontario, Canada

[2]The Ottawa Hospital Research Institute, Ottawa, Ontario, Canada

*corresponding author

CONTRIBUTIONS

This manuscript was submitted to Biochemical Journal January 17, 2014.

FIZ1 promotes proliferation of human keratinocytes via autocrine signaling pathways

Nathalie Larivière[1,2], Jennifer Law[1] and *Laura Trinkle-Mulcahy[1]

The work presented here was carried out in collaboration between all authors. LTM and I designed experiments, analyzed the data, interpreted the results and wrote the paper including all data presentation. I carried out laboratory experiments. JL contributed reagents and conducted cloning for the interactome validation. All authors contributed to and approved the manuscript.

Summary Statement

FIZ1 is a signal transducer/transcription factor that we show here can be harnessed to promote proliferation of keratinocytes via increased autocrine mitogenic signaling, with the underlying protein- protein interactions and downstream signaling events comprehensively mapped using a multi-faceted quantitative proteomic approach.

Abstract

Epidermal homeostasis is a balancing act governed by a multitude of underlying regulatory events. Several growth factors and signaling pathways have been implicated in regulation of the balance between proliferation and differentiation in keratinocytes, and we show here that the transcription factor/signal transducer FIZ1 (Flt3 interacting zinc finger protein-1) is a previously unknown player in this key regulatory axis. FIZ1 promotes proliferation via autocrine signaling through the MAP/ERK kinase pathway, with increased proliferation driven by a more rapid G1/S progression. Quantitative SILAC-based secretome analysis identified the insulin growth factor binding protein IGFBP3 as a key mediating factor, with elevated FIZ1 levels promoting increased IGFBP3 expression/secretion and a concurrent increase in sensitivity to IGF1 signaling. Mapping the interactome of FIZ1 in both proliferating and differentiating cells identified 8 novel binding partners, including the MOB2/NDR1/NDR2 kinase complex and TAF4 transcription factor, that may act in concert with FIZ1 to contribute to regulation of epidermal homeostasis.

Introduction

The mammalian epidermis is a stratified squamous epithelium that forms the selective epidermal permeability barrier essential for mammalian survival. Tight regulation of the processes that underlie self-renewal of the mature epidermis and wound healing are critical, with dysfunctions in the homeostatic balance between epidermal proliferation and differentiation leading to diseases such as atopic dermatitis, psoriasis and cancer (Ratushny et al., 2012).

Development begins with commitment of a single layer of multipotent ectodermal cells to an epidermal cell fate and lineage. Keratinocytes in the proliferative basal compartment receive signals to differentiate and exit this layer, becoming irreversibly committed to terminal differentiation (for review, see (Fuchs, 2007)). The cells exit the cell cycle and initiate expression of differentiation markers, moving suprabasally as they become part of the upper stratified layers. The end result is a barrier separating the external and internal environments of the organism, with selective permeability to solutes regulated by tight junction complexes (Furuse, 2010). Although the contributions of several known signaling pathways have been evaluated, a comprehensive list of the key players and how all of the underlying events are coordinated remains elusive.

FIZ1 (Flt3 interacting zinc finger protein-1) is a putative transcription factor that was originally identified as a novel interactor for the pro-proliferative hematopoietic progenitor cell receptor tyrosine kinase FLT3 (Wolf and Rohrschneider, 1999) and has been shown to play a role in transducing FLT3 signals in B lymphoblastic lymphomas (Tsuruyama et al., 2010). Although FIZ1 is more widely expressed than FLT3, its

potential contribution as a downstream factor in mitogenic signaling pathways has, to date, only been assessed in hematopoietic cells, while studies in retinal cells have identified it as part of a regulatory protein complex present on active photoreceptor-specific gene promoters (Mali et al., 2008; 2007; Mitton et al., 2003). Given its potential to transduce extracellular signals both via interaction with upstream receptors and downstream transcription factors, we set out to functionally assess the role of FIZ1 in keratinocytes, demonstrating a previously unknown regulatory role in epidermal homeostasis. Elevated FIZ1 levels promote proliferation in these cells, and our multi-faceted quantitative secretome/proteome/interactome approach highlighted both the signaling pathways that are altered under these conditions and the underlying protein-protein binding events that may mediate them.

Materials & Methods

Plasmids and cell culture

The pCMV6-XL5-FIZ1-Myc-DDK construct encodes full-length human FIZ1 fused to C-terminal Myc and FLAG® tags. Coding sequences for FIZ1 interactors were amplified from donor constructs (Table S1) using specific oligonucleotide primers and and inserted into the mammalian expression vector pEGFP-C1 (Clontech). Constructs were confirmed by DNA sequencing (performed by Nanuq sequencing service, McGill University and Génome Québec Innovation Center).

HaCaT spontaneously immortalized human keratinocytes (ATCC) were maintained at 37°C/5% CO_2 in Dulbecco's modified Eagle's medium (DMEM) supplemented with 10%

FBS and 100 U/ml penicillin/streptomycin. HaCaT^{FIZ1} cell lines were established by stable incorporation of transiently transfected plasmids and clonal selection in G418-containing media. All cell counts were performed in triplicate using the Countess cell counter (Life Technologies), with Day 0 counts carried out 2 hours after seeding to confirm the number of adhered cells. For FGF7/KGF stimulation, cells were plated at a lower density and the media changed at Day 2 to include 10 ng/mL FGF7/KGF. Cell cycle progression was monitored by FACS as previously described (Prévost et al., 2013). For RNAi experiments, cells were transfected 18 hrs after plating with 1 μg of either FIZ1-targeted siRNA duplexes or control scrambled duplexes (see Table S2 for sequences), using DharmaFECT (Dharmacon) according to the manufacturer's recommended protocol.

Western blotting, affinity purification and PCR

Whole cell extracts were prepared by sonication (6 × 10 s at 75% power) in ice-cold RIPA buffer (50 mM Tris pH 7.5, 150 mM NaCl, 1% NP-40, 0.5% deoxycholate, protease inhibitors) then cleared by centrifuging at 2800 g (3500 rpm, GH3.8 rotor; Beckman Coulter GS-6) for 10 min at 4°C to isolate the soluble fraction. Total protein concentrations were measured using Pierce® BCA Protein Assay Kit (Thermo Scientific, Rockford, IL). For affinity purification of FLAG®- and GFP-tagged proteins, extracts (3-10cm plates per IP) were first pre-cleared with either FLAG®-M2 agarose (Sigma-Aldrich) or GFP-Trap_A™ (Chromotek) for 30 mins. Extracts were then incubated with either FLAG®-M2 agarose (Sigma-Aldrich) for 2 hrs or GFP-Trap_A™ (Chromotek) for 1 hr. For endogenous FIZ1 pulldowns, ⟨αFIZ1 (Abcam) or purified rabbit IgG (control))

were covalently conjugated to protein G Sepharose beads (GE Healthcare) at 1 mg/ml.

Briefly, for covalent conjugation, beads were incubated with antibody for 1 h at 4°C and then washed twice with 10 volumes of 0.1 M sodium borate, pH 9. Next, the beads were incubated with 10 volumes of borate buffer containing 20 mM dimethylpimelimidate (DMP; Sigma-Aldrich) for 30 min at room temperature. The beads were pelleted and resuspended with 10 volumes of freshly prepared 20 mM DMP in borate buffer for an additional 30-min incubation. The beads were washed twice with 10 volumes of ice-cold 50 mM glycine (pH 2.5) to remove unbound antibody and then washed several times with PBS or RIPA buffer for use and/or storage at 4°C.

After IP, lysates were separated from beads and beads washed with RIPA buffer 5 times. HRP-conjugated secondary antibodies were from obtained from Thermo Scientific prepared in 5% skim milk prepared in PBS-Tween. Quantification was conducted with Multigauge software (GE Healthcare) including background subtraction with areas compared of the same size and in comparison to internal controls (tubulin or GAPDH), measured and calculated as intensity/area. Western blots were imaged/quantified using an LAS4000 chemiluminescence system (GE Healthcare). See Table S1 for a detailed list of primary antibodies and dilutions used.

Total cellular RNA was isolated with RNeasy Mini Kit (Qiagen, Valencia, CA) according to the manufacturer's instructions and quantified using a Nanodrop 2000 (ThermoScientific, Rockford, IL). RNA was reverse transcribed (AMV Reverse Transcription Kit, Promega). For qPCR, 4 µl of each cDNA reaction was analyzed in duplicate using iTaq Universal SYBR Green Supermix (BioRad) and a Rotor-Gene Q

PCR Machine (Qiagen). The comparative CT method (Schmittgen and Livak, 2008) was used to compare relative levels of mRNA in HaCaT^{FIZ1} vs. parental HaCaT cells, using GAPDH as an internal standard. See Table S2 for a full list of PCR primers.

Fluorescence Microscopy

Fluorescence imaging was performed using a wide-field fluorescence microscope (DeltaVision CORE; GE Healthcare) equipped with a three-dimensional motorized stage and CoolSNAP coupled-charge device (CCD) camera (Roper Scientific). Cells growing on coverslips were fixed with 3.7% paraformaldehyde (PFA) in CSK buffer for 5 minutes and permeabilized with Triton X-100, stained with either anti-Occludin (Life Technologies) or anti-FIZ1 (Abcam) primary antibodies detected with Dy488-anti–rabbit secondary antibodies (Jackson Laboratories) and the DNA dye Hoechst No 33342 (Sigma-Aldrich), and mounted in FluorSave mounting media (Calbiochem). Cells were imaged using a 60x NA 1.4 Plan-Apochromat objective (Olympus) and the appropriate filter sets (Chroma Technology Corp.), with 20 optical sections of 0.5 μM each acquired. SoftWorX software (GE Healthcare) was used for both acquisition and deconvolution. All images are single, deconvolved optical sections. For fluorescence imaging of GFP-tagged interactors, HaCaT cells were grown on coverslips and transfected using Effectene (Qiagen), followed by PFA fixation and mounting 18 hrs later. For nuclear retention assays, proliferating (Day 2) and differentiating (Day 10) cells grown on coverslips were incubated for 5 min with 0.1% Triton X- 100 in ASE buffer (20 mM Tris pH 7.5, 5mM MgCl2, 0.5mM EGTA) at 37°C prior to PFA-fixation, Triton X-100 permeabilization and staining as described above. For nuclease digestion, benzonase was added at

125U/coverslip. Mock permeabilized samples were incubated for 5 min in ASE buffer with no Triton X-100.

Mass Spectrometry

Quantitative SILAC-based affinity purification experiments were carried out as previously described (Trinkle-Mulcahy et al., 2008). Cells were grown in custom-made DMEM (minus arginine and lysine; Invitrogen) supplemented with 10% dialyzed fetal calf serum (Invitrogen) and penicillin/streptomycin (Invitrogen). For double encoding experiments, L-arginine (84 μg/ml; Sigma-Aldrich) and L-lysine (146 μg/ml lysine; Sigma-Aldrich) were added to the "light" media, while L-arginine ^{13C} and L-lysine ^{13C} (Cambridge Isotope Laboratory) were added to the "heavy" media at the same concentrations. For triple encoding experiments, L-arginine and L-lysine were added to the "light", L-arginine ^{13C} and L-lysine 4,4,5,5-D4 (Cambridge Isotope Laboratory) to the "medium", and L-arginine $^{13C/15N}$ and L-lysine $^{13C/15N}$ (Cambridge Isotope Laboratory) to the " heavy" media. The amino acid concentrations are based on the formula for normal DMEM (Invitrogen). Once pre- pared, the SILAC media was mixed well, filtered through a 0.22-μm filter (Millipore) using a suction pump, and stored at 4°C.

Protein purifications were carried out separately, the extracts removed and beads washed once with ice-cold RIPA buffer, and then beads washed with ice-cold RIPA buffer. To ensure efficient elution of bound proteins, a bead-equivalent volume of 1% SDS was added, the matrix boiled for 10 min and then a 4x volume of dH_2O added. The matrix was vortexed and the solution removed and reduced to the original bead-equivalent

volume (and 1% SDS concentration) using a speedvac. Proteins were reduced and alkylated in this solution, first by the addition of 10 mM DTT (boil for 2 min), and then the addition of 50 mM iodoacetamide (incubate at room temperature in the dark for 30 min). A small aliquot of Laemmli sample buffer was added and proteins were separated by running halfway down NuPAGE 12% Bis-Tris gels. Gels were Coomassie stained and de-stained overnight before excision of slices. An aliquot of each tryptic digest (prepared in 5% acetonitrile/0.1% trifluoro-acetic acid in water) was analyzed by LC-MS/MS (liquid chromatography – tandem mass spectrometry) on an UltiMate 3000 RSLC nano HPLC (Dionex) and an LTQ Orbitrap XL hybrid mass spectrometer with nanospray ionization source (Thermo Scientific) at the OHRI Proteomics Core Facility (Ottawa, Canada). The system was controlled by Xcalibur software version 2.0.7 (Thermo Scientific). Peptides were loaded onto a C18 CapTrap column (Michrom) for 5 minutes at a flow rate of 15 microlitres per minute and then eluted over a 60 minute gradient of 3% - 45% acetonitrile with 0.1% formic acid at a flow rate of 0.3 microlitres per minute onto a 10-cm long column with integrated emitter tip (Picofrit PF360-75-15-N-5, New Objective packed with Zorbax SB-C18, 5 micron, Agilent), and nanosprayed into the mass spectrometer. MS scans were acquired in FTMS mode at a resolution setting of 60000. MS^2 scans were acquired in ion trap CID mode using data-dependent acquisition of the top 5 ions from each MS scan.

For secretome mapping, 4 x 15 cm dishes per cell line were labeled and 60 mls of conditioned media collected, cleared (1000 rpm x 4 min) and incubated with 250 ml of heparin-agarose for 1 hr at 4°C. After media was removed for secretome mapping, labeled cells were harvested for proteome mapping and equal protein amounts of whole

cell extract combined for analysis. For interactome mapping by quantitative AP/MS, 10 x 15 cm dishes of cells were encoded in SILAC media for 14 days, passaging at days 2, 6, 9 and 12 to maintain in a proliferative state ("light" HaCaT and "medium" HaCaT^{FIZ1}) or only at days 2 and 4 to allow them to reach confluence and differentiate ("heavy" HaCaT^{FIZ1}). Equal protein amounts of whole cell extract were incubated with 100µl of FLAG®-M2 agarose for 2 hrs at 4℃, the beads combined and proteins eluted for subsequent analysis.

Statistical analysis

Three independent experiments were carried out for all growth assays and quantified Western blots. AUCs were calculated and statistical analyses (ANOVA and Student's t-tests: 2 tailed unpaired or paired tests) performed using GraphPad Prism 5.0 (GraphPad Software). Data reported as mean ± SE for 3 biological replicates each having 3 technical replicates. All western blots were conducted and quantified in triplicate. Statistical significance indicated for a threshold $p < 0.01$ except where indicated.

Results and Discussion

Elevated FIZ1 levels promote keratinocyte proliferation

HaCaT cells expressing FIZ1 at levels ~2.5-fold higher than parental cells (Fig. S1A) reach confluence more rapidly in both standard and reduced serum media and show increased persistence of proliferation in serum-free media (Fig. 1A-B). Despite an

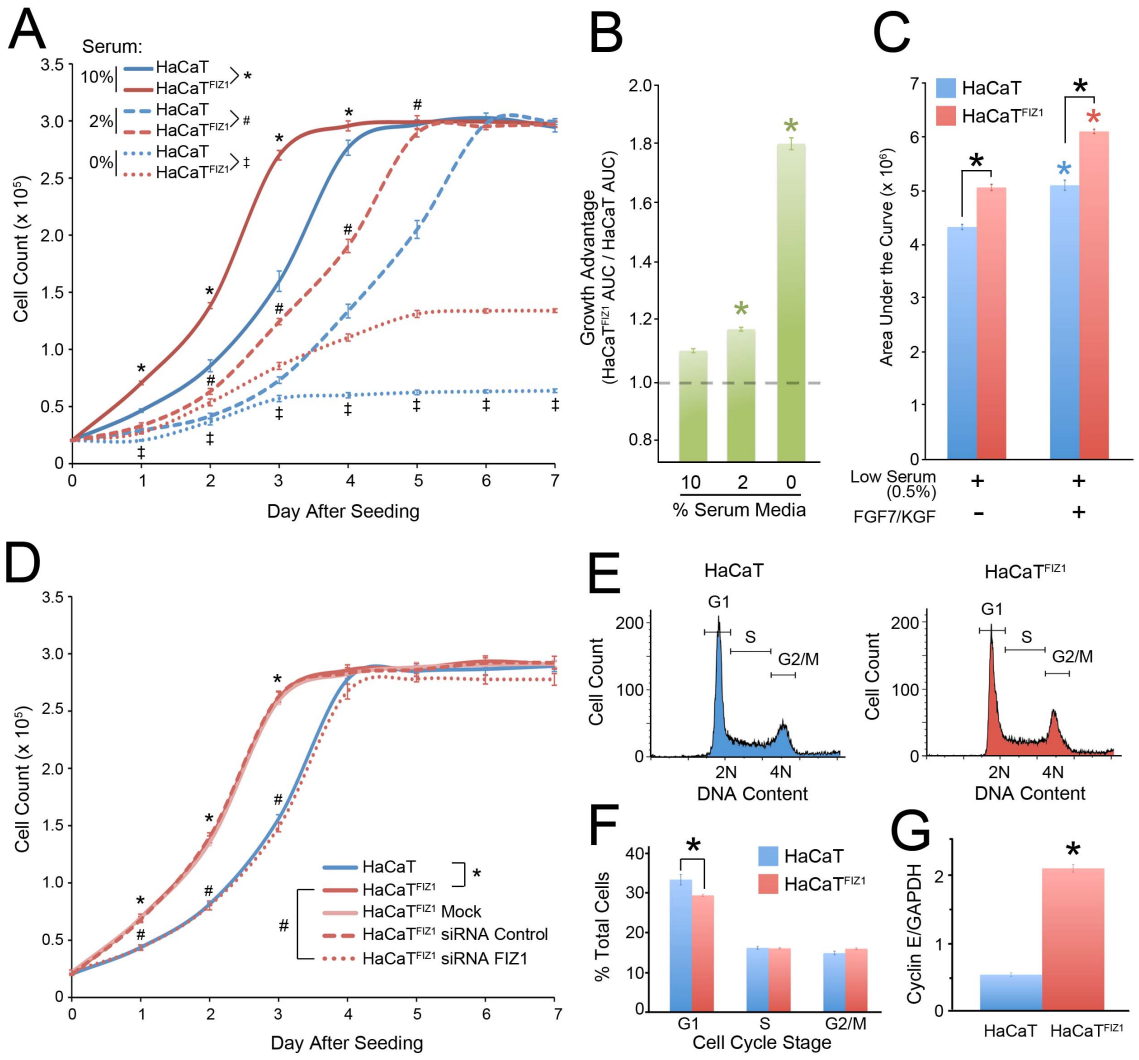

Figure 1. Elevated FIZ1 levels stimulate HaCaT proliferation. A. Growth curves in standard (10%) and reduced (2%, 0%) serum conditions. B. Areas Under the Curve (AUCs) calculated for (A) and expressed as a ratio of HaCaT^{FIZ1} / HaCaT. C. AUCs plotted for growth curves in low serum (0.5%) media ± exogenous FGF7/KGF (10 ng/mL). D. Growth curves for HaCaT^{FIZ1} cells ± siRNA-mediated reduction of FIZ1 to near parental levels. E. Representative FACS analyses of proliferating cell populations. F. Summary of FACS analyses, showing distribution of cells between cell cycle stages. G. Western blot analysis of Cyclin E levels (normalized to GAPDH) in proliferating cell lysates. Data plotted as mean ± SE for 3 biological replicates. Symbols (*, #, ‡) indicate statistically significant differences for a threshold $p < 0.01$.

increased basal proliferation rate, they remain responsive to exogenous growth factors (Fig. 1C; Fig. S1B-C; Fig. 3G), indicating that mitogenic signaling is not saturated. RNAi-mediated reduction of FIZ1 to near endogenous levels (Fig. S1E-F) leads to a concomitant drop in the proliferation rate (Fig. 1D), confirming that it is excess FIZ1 that drives the enhanced proliferation. Analysis of HaCaT^{FIZ1} cell cycle distribution revealed a small but significant decrease in the percentage in G1 (Fig. 1E-F), indicating faster progression through this stage. Consistent with this, HaCaT^{FIZ1} cells have higher levels of cyclin E (Fig. 1G; Fig. S1D) which, together with the cyclin-dependent kinase Cdk2, promotes progression to S phase (Siu et al., 2012). Although HaCaT^{FIZ1} cells show more rapid closure in scratch wound assays, ablation by treatment with the mitotic inhibitor mitomycin C (Fig. S1H) indicates that it is driven solely by enhanced proliferation. Interestingly, knockdown of endogenous FIZ1 levels by 80% in HaCaT cells did not affect proliferation rate at early time points in a growth curve, however cells exited the cell cycle prematurely (Fig. S1G), suggesting that FIZ1 may be required for prevention of premature differentiation.

Excess FIZ1 does not impede contact-induced differentiation

Similar to parental cells, proliferative markers disappear and early differentiation markers appear in HaCaT^{FIZ1} cells shortly after reaching confluence (Fig. 2A). Occludin, which accumulates at tight junctions, is observed at the periphery of both HaCaT and HaCaT^{FIZ1} cells in late differentiation (Fig. 2B), confirming that excess FIZ1 does not inhibit formation of these structures.

HaCaT^{FIZ1} cells are, however, resistant to the differentiation program induced in HaCaT

Figure 2

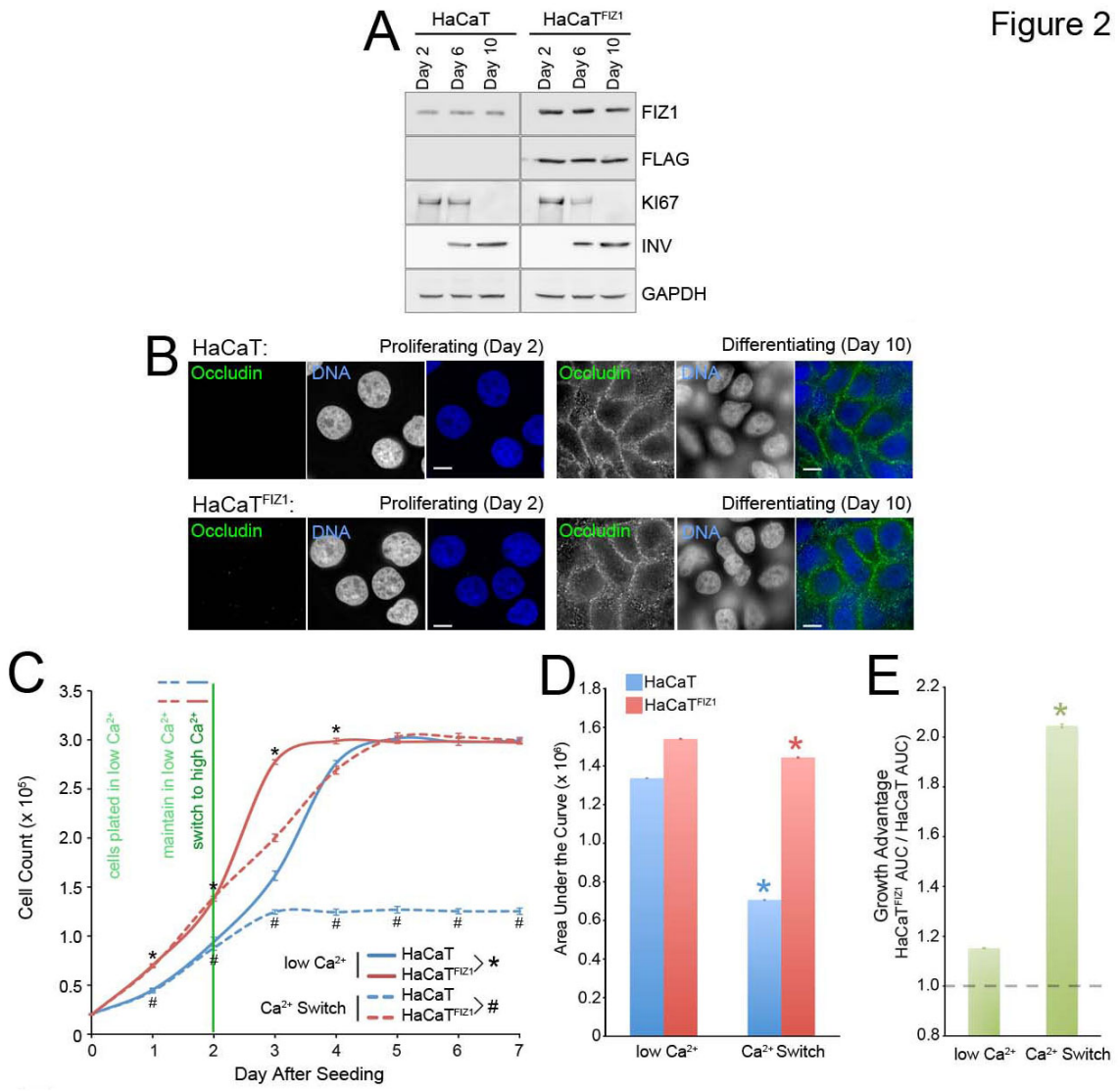

Figure 2A-E. FIZ1 overexpression overrides Ca2+- but not contact-induced differentiation.

A. Western blot analysis of cell lysates collected on Day 2 (proliferating), Day 6 (confluent/early differentiation) and Day 10 (late differentiation) post-seeding. B. Immunostaining of Occludin at Days 2 and 10. Images are single optical sections and scale bars are 5 μm. C. Growth curves for cells plated in low Ca^{2+} (0.03 mM) media and at Day 2 either maintained in this (solid lines) or switched to high (2.8 mM) Ca^{2+} media (dashed lines). D. AUCs calculated for (C). E. AUCs in (D) expressed as a ratio of $HaCaT^{FIZ1}$ / HaCaT. Data plotted as mean ± SE for 3 biological replicates. Symbols (*, #) indicate statistically significant differences for a threshold $p < 0.01$.

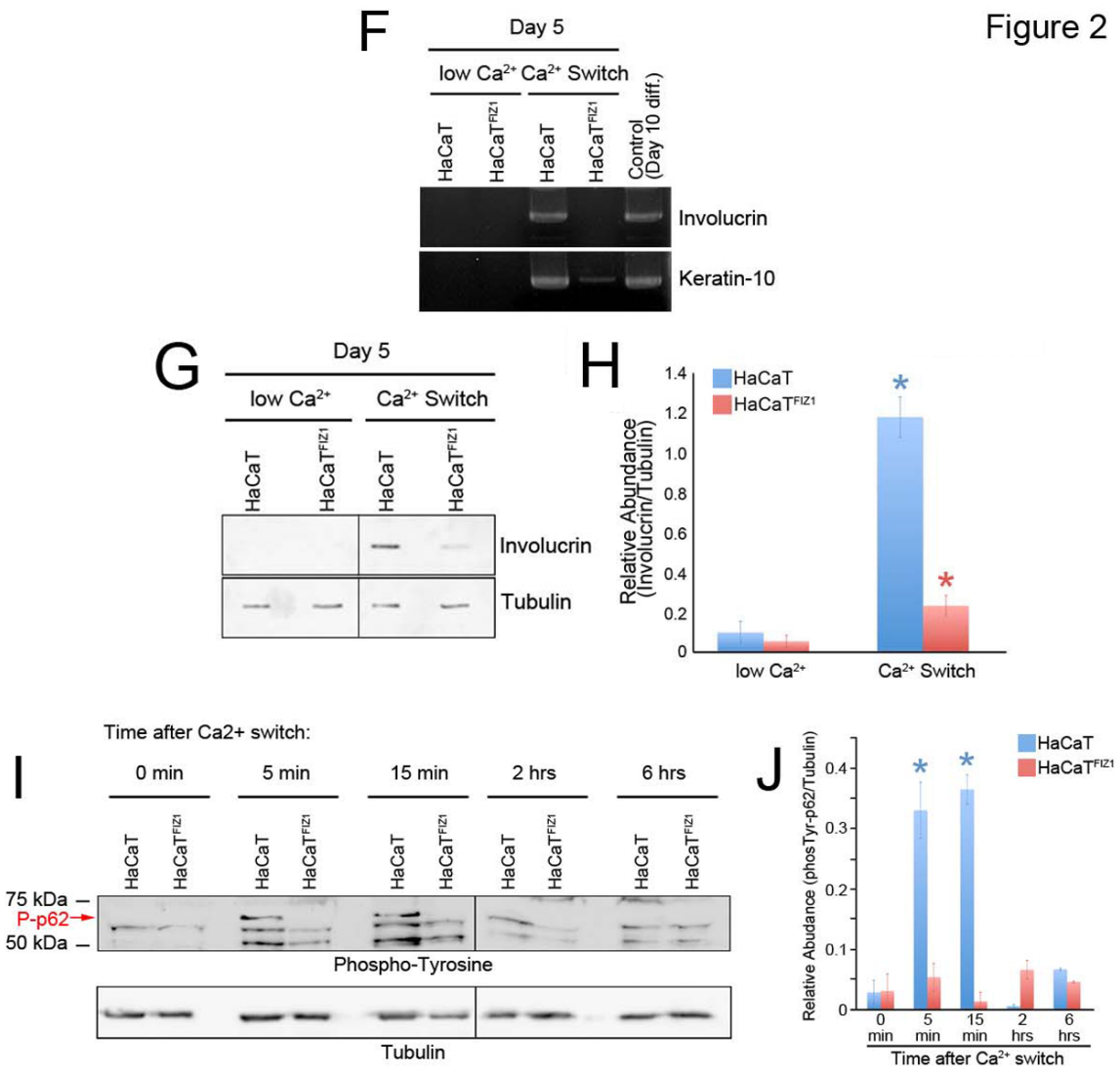

Figure 2F-J. FIZ1 overexpression overrides Ca2+- but not contact-induced differentiation. F. RT-PCR detection of differentiation marker transcripts. G. Detection of Involucrin protein levels by immunoblotting. H. Quantitation of Involucrin protein levels at Day 5 relative to Tubulin. I. Western blot assessing global tyrosine phosphorylation. Red arrow indicates the phospho-p62 band. J. Quantitation of phosTyr-p62 levels relative to Tubulin. Data plotted as mean ± SE for 3 biological replicates. Symbols (*, #) indicate statistically significant differences for a threshold $p < 0.01$.

cells by a switch from low to high Ca^{2+} (Deyrieux and Wilson, 2007). While parental cells exited the cell cycle and showed upregulation of transcript and protein levels for early differentiation markers following the Ca^{2+} switch, $HaCaT^{FIZ1}$ cells continued to proliferate, albeit with a lag that delayed reaching confluency (Fig. 2C-H). A hallmark of this pathway is the rapid and transient tyrosine phosphorylation of the ras-GTPase activating protein (ras-GAP)-associated protein p62/SAM68 (Filvaroff et al., 1990). This phospho-band was observed in HaCaT, but not $HaCaT^{FIZ1}$ cells, 5 min after the Ca^{2+} switch (Fig. 2I-J), indicating that FIZ1 overexpression abrogates activation of the relevant signaling pathway. A similar resistance to Ca^{2+}- but not contact-induced differentiation was observed for the murine squamous cell carcinoma (SCC) cell line PAM212 (Filvaroff et al., 1990). Given that $HaCaT^{FIZ1}$ and primary cutaneous SCC cells also show some overlap of upregulated factors (IGFBP3, MMP13, MATN2; (Toriseva et al., 2012)), it is possible that they may share some common signaling events.

Increased $HaCaT^{FIZ1}$ proliferation involves autocrine signaling

Parental HaCaT cells show increased proliferation when grown in $HaCaT^{FIZ1}$ cell-conditioned media (Fig. 3A), indicating that the mitogenic signaling is mediated, at least in part, by secreted factors. Pre-treatment with heparan sulfate or depletion of heparin-binding factors removed the stimulatory effect of the conditioned media, and addition of heparan sulfate to $HaCaT^{FIZ1}$ cells removed their growth advantage (Fig. 3B). This suggests involvement of one or more heparin-binding growth factors. To identify this factor(s), we utilized the quantitative mass spectrometry technique SILAC (Stable Isotope Labeling by Amino acids in Culture; (Ong et al., 2002)). Parental HaCaT cells

Figure 3

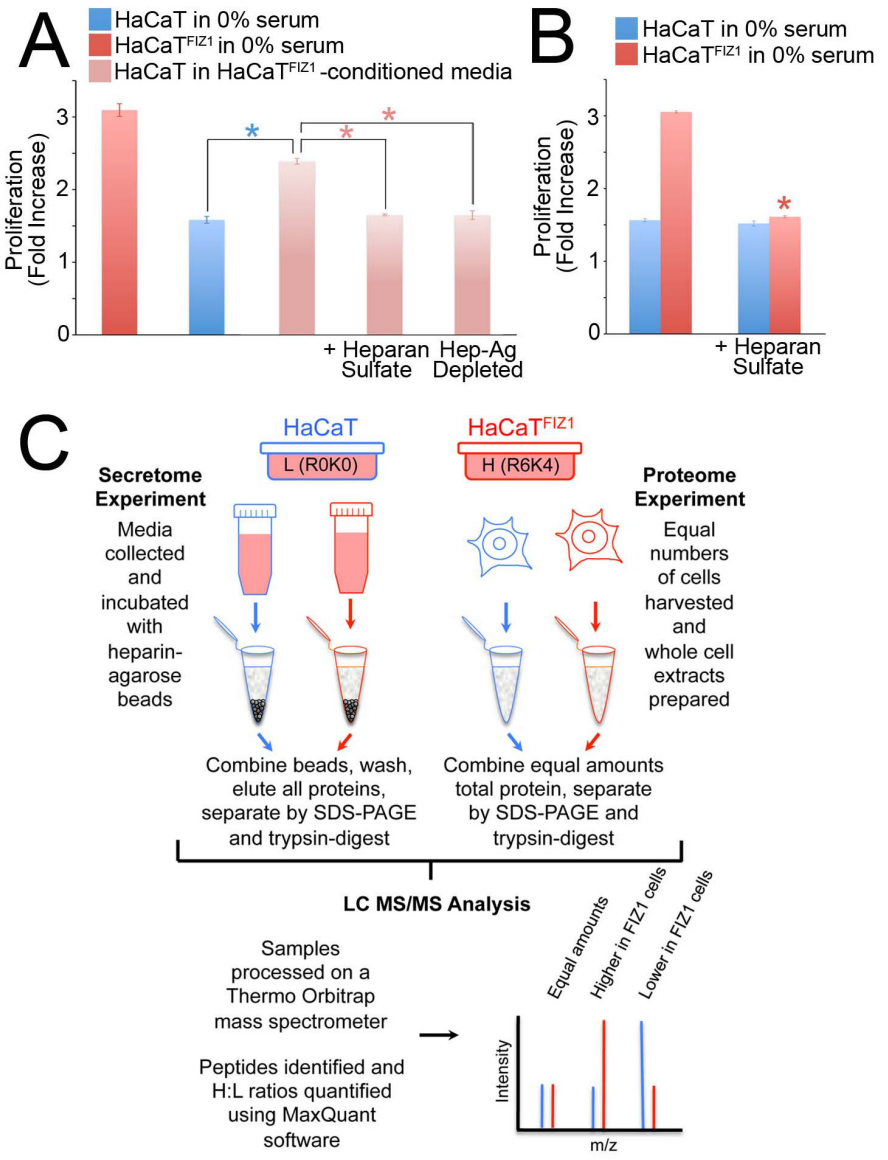

Figure 3A-C. Autocrine signaling mediates FIZ1-induced proliferation. A. Two-day growth assays showing significant (blue asterisk) increase in HaCaT proliferation in HaCaT^{FIZ1}-conditioned media and its ablation (pink asterisks) by addition of heparan sulfate (20 μg/ml) or depletion of heparin-binding factors using heparin-agarose. B. Two-day growth assays in serum-free media ± heparan sulfate C. Design of quantitative secretome/proteome experiment. Data plotted as mean ± SE for 3 biological replicates. Asterisks indicate statistically significant differences for a threshold $p < 0.01$.

Figure 3

D

Gene Name	Protein Name	UniProt	# Peptides Total/Unique	Ratio H:L	Normalized Intensity
IGFBP3	Insulin-like growth factor-binding protein 3	P17936	16/16	12.82	649.3
DKK1	Dickkopf-related protein 1	O94907	3/3	5.15	17.09
MYO1B	Unconventional myosin-1b	O43795	2/2	4.11	3.45
CCDC80	Coiled-coil domain-containing protein 80	Q76M96	35/35	2.79	182.92
KAL1	Anosmin-1	P23352	2/2	2.21	3.27
MMP13	Collagenase 3	G5E971	18/18	1.69	265.33

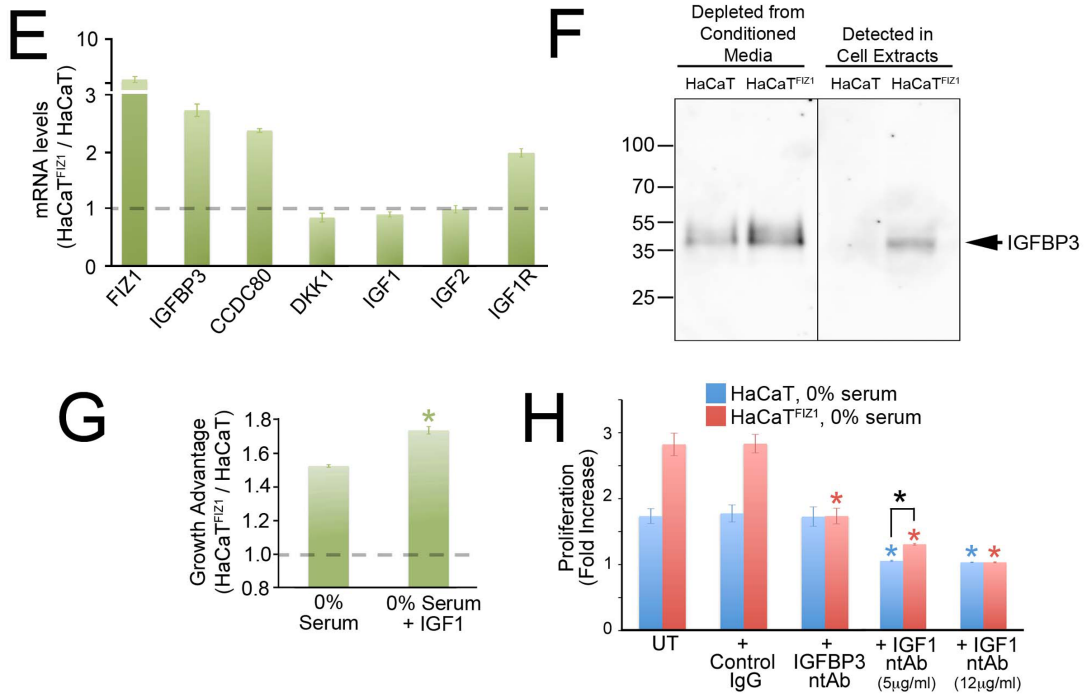

Figure 3D-H. Autocrine signaling mediates FIZ1-induced proliferation. D. Top hits in HaCaT^{FIZ1} cell secretome. E. qPCR results for selected secretome hits. F. Western blot showing increased levels of IGFBP3 captured on heparin-agarose beads from HaCaT^{FIZ1} cell-conditioned media and present in cell extracts. G. Two-day growth assays in serum-free media comparing the relative response of HaCaT and HaCaT^{FIZ1} cells to exogenous IGF1. H. Two-day growth assays in serum-free media testing the effect of IGFBP3 and IGF1 neutralizing antibodies (ntAb). Data plotted as mean ± SE for 3 biological replicates. Asterisks indicate statistically significant differences for a threshold $p < 0.01$.

were labeled by growth in "light" media containing environmental isotopes of arginine and lysine while HaCaT^{FIZ1} cells were labeled by growth in "heavy" media containing ^{13}C-arginine and D4-lysine (Fig. 3C). The isotopes shift the mass of Arg- and Lys-containing peptides, with relative levels of heavy and light peptides reflecting the amount of protein in each condition. Cells were passaged in 10% serum SILAC media for 7 days and then transferred to serum-free SILAC media for 3 days. The conditioned media was collected, incubated with heparin-agarose, the beads washed and combined, and bound proteins eluted for gel separation and MS analysis. We identified/quantified 353 proteins, most of which were found in equal amounts. Known heparin-binding growth factors such as FGF7/KGF, HB-EGF and AREG were not detected, although HB-EGF transcript levels are upregulated in HaCaT^{FIZ1} cells (Fig. S2B). Of the subset of heparin-binding factors enriched in HaCaT^{FIZ1}-conditioned media, the top hit was IGFBP3, an insulin growth-factor binding protein (Fig. 3D). Both qPCR (Fig. 3E) and Western blot analysis (Fig. 3F) confirmed higher levels of IGFBP3 expression/secretion.

Increased FIZ1 expression sensitizes cells to IGF signaling

The role of IGFBP3 is controversial, given that its high affinity binding to IGFs has been shown in various cell lines to either prevent the growth factors' pro-proliferative signaling or to prolong the lifespan of active IGF molecules (for review, see (Yamada and Lee, 2009)). IGFBP3 is also known to have IGF- independent roles (Ingermann et al., 2010; Oh et al., 1993; Rajah, 1997). We found that addition of IGFBP3 neutralizing antibodies abolished the HaCaT^{FIZ1} growth advantage in serum-free media (Fig. 3G) and significantly reduced it in the more complicated background of 10% serum media (Fig.

S2F). To compare IGF signaling between HaCaT and HaCaT^{FIZ1} cells, we stimulated them with exogenous IGF1 in serum-free media. The more robust response of HaCaT^{FIZ1} cells to IGF1 (Fig. 3G) is consistent with sensitization to this growth factor. Furthermore, HaCaT^{FIZ1} cells are more resistant than parental cells to the downregulation of autocrine IGF signaling by the addition of IGF1 neutralizing antibodies (Fig. 3H). Levels of IGF1/IGF2 transcripts in HaCaT^{FIZ1} cells are similar to those in parental cells, however there is an upregulation of transcript levels for the IGF1R receptor, through which both can signal (Fig. 3E). Thus, although we cannot rule out an IGF-independent role for IGFBP3 in FIZ1-mediated signaling, our data suggest that increased IGFBP3, likely in combination with increased IGF1R levels, mediates hypersensitivity of HaCaT^{FIZ1} cells to IGF signaling. IGF1R expression has already been linked to regulation of the proliferation/differentiation axis in keratinocytes, as it is necessary for proliferation but has also been shown to actively suppress differentiation (Sadagurski et al., 2006).

Other factors implicated in FIZ1-mediated signaling

While IGFBP3 was the most highly enriched protein in the HaCaT^{FIZ1} cell secretome, other heparin- binding signaling factors were also detected at elevated levels (Fig. 3D). These include CCDC80 and DKK1 which, like IGFBP3, have been reported to have conflicting and system-dependent effects on proliferation (Menezes et al., 2011; Tremblay et al., 2009; Yamaguchi et al., 2007). DKK1 is of particular interest, in that Wnt signaling has been shown to inhibit growth and promote terminal differentiation in keratinocytes (Slavik et al., 2007). Consistent with this, DKK1 has been shown to promote proliferation of keratinocytes and regulate skin thickness (Yamaguchi et al.,

2009). While not upregulated at the mRNA level (Fig. 3E), quantitative Western blot analysis confirmed moderately higher DKK1 secretion from HaCaT^{FIZ1} cells (Fig. S2D). Addition of DKK1 neutralizing antibodies to HaCaT^{FIZ1} cells reduced their growth advantage in serum-free media (Fig. S2E), although they remained more proliferative than parental cells, suggesting that DKK1 is contributing player in the signaling pathways activated by elevated FIZ1 activity.

MAP/ERK kinase activation is involved in FIZ1-induced proliferation

Whole proteome comparison also identified a subset of signaling factors selectively upregulated in HaCaT^{FIZ1} cells (Fig. S2A,C). They include CRABP2 and FABP4/5, which have been linked to retinoic acid and PPAR-mediated signaling (Schug et al., 2007; Tan et al., 2002), and the cell surface receptor TACSTD2/TROP2, which has been linked to activation of mitogenic signaling via NF-κB and MAP/ERK kinase and implicated in tumour development (Guerra et al., 2012). We tested the contribution of these downstream signaling pathways to the growth advantage of HaCaT^{FIZ1} cells in serum-free media, and found that proliferation of parental HaCaT cells was equally sensitive to or more sensitive than that of HaCaT^{FIZ1} cells to inhibition by most signaling pathway inhibitors tested (Fig. 4A). Only PD98059, which blocks phosphorylation/activation of the MAP/ERK kinases ERK1/2, had a selective effect on HaCaT^{FIZ1} cells. At higher concentrations PD98059 inhibited proliferation of both cell lines, but at 1 μM it selectively reduced the growth advantage of HaCaT^{FIZ1} cells in both serum-free and 10% serum media (Fig. 4B). Measurement of active ERK1/2 levels confirmed increased signaling through this pathway (Fig. 4C-D), with PD98059

Figure 4

A

Drug	Target	Concentration	Serum-Free Media % Max Growth HaCaT	Serum-Free Media % Max Growth HaCaT^{FIZ1}
PD98059	MAP/ERK kinase (MEK) inhibitor	1 μM	99	65
GSK0660	PPAR β/δ antagonist	1 μM	89	89
FH535	Tcf/β-catenin and PPAR γ and δ inhibitor	1 μM	70	81
RAR	Retinoic Acid Receptor Antagonist	10 μM	99	100

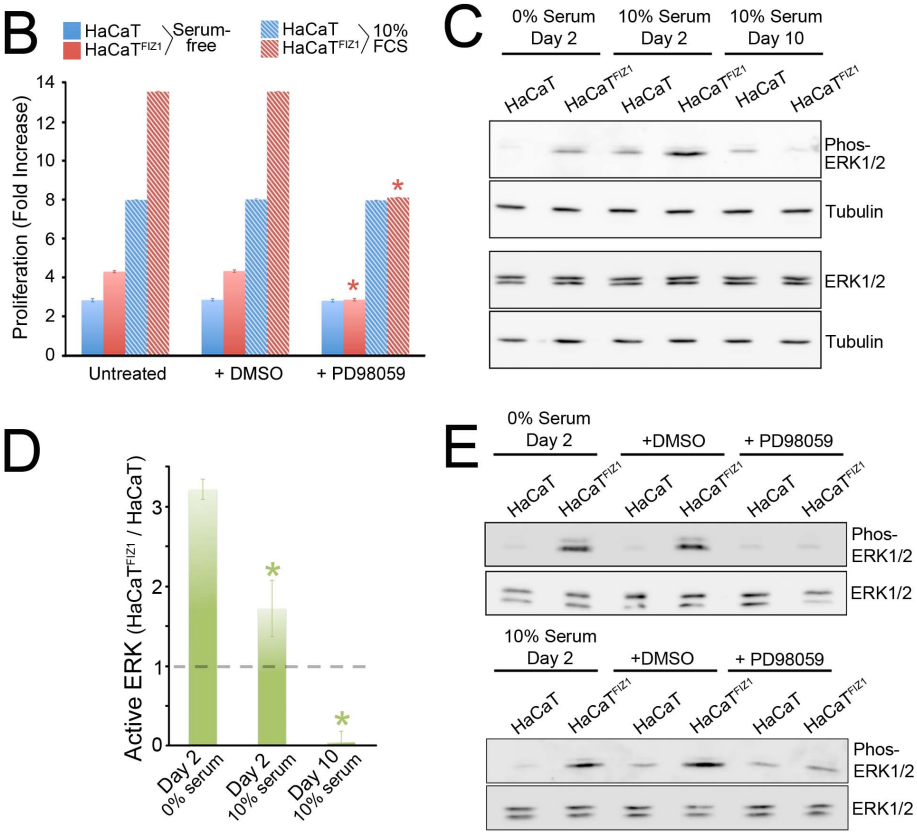

Figure 4. ERK1/2 activation is involved in FIZ1-induced proliferation. A. Summary of effects of signaling pathway inhibitors on HaCaT and HaCaT^{FIZ1} cell growth in serum-free media. B. Two-day growth assays in serum-free or 10% serum media in the presence or absence of 1 μM PD98059 (or DMSO carrier alone) C. Western blot analysis of cell lysates, with Phos-ERK1/2 levels normalized to total ERK1/2 levels and tubulin shown as a loading control. D. Relative levels of phospho/activated ERK1/2 in HaCaT^{FIZ1} vs. parental HaCaT cells. E. Western blot analysis of cell lysates collected at Day 2 of serum-free or 10% serum growth curves, showing that treatment with 1 μM PD98059 reduces the level of phosphoERK1/2 in HaCaT^{FIZ1} cells to that of parental HaCaT cells. Data plotted as mean ± SE for 3 biological replicates. Asterisks indicate statistically significant differences for a threshold $p < 0.01$.

treatment reducing levels to those in parental cells (Fig. 4E). Therefore, while multiple pathways contribute to basal HaCaT proliferation, only inhibition of MAP/ERK signaling removes the selective growth advantage conferred by excess FIZ1. Given that IGFs can signal through this pathway, we propose that the predominant pro-proliferative mechanism activated by excess FIZ1 in HaCaT cells is sensitization to IGF with increased downstream signaling via ERK1/2.

FIZ1 interacts with signaling and transcription factors

In order to identify protein-protein interactions that may mediate the role of FIZ1, we mapped its interactome under both proliferating and differentiating conditions. Quantitative affinity purification/mass spectrometry (AP/MS) identified several proteins that co-purify with FIZ1 (Fig. 5A- B). The top hits (Fig. 5C; Fig. S3A) were validated by co-IP/Western blot analysis with both tagged (Fig. 5D) and endogenous (Fig. S3B) FIZ1, and by reciprocal co-IP (Fig. S3C-D).

The 8 novel FIZ1 interactors reported here range from signaling molecules and import factors to proteins involved in receptor recycling and gene transcription. Half are protein kinases: the NDR1 and 2 kinases (and their associated regulatory protein MOB2), JAK1 and SCYL2/CVAK104. Interactions between FIZ1 and the signaling scaffold TRAF4, the transcription factor TAF4 and the importin IPO8 were also demonstrated. Only IPO8 showed selective association with FIZ1 under the conditions tested, with the complex detected predominantly in proliferating cells (Fig. 5C-D). While IPO8 may mediate nuclear import of FIZ1, which contains a predicted monopartite NLS, FIZ1 is predominantly nuclear even in differentiating cells (Fig. 5E). A stable and proliferation-

Figure 5

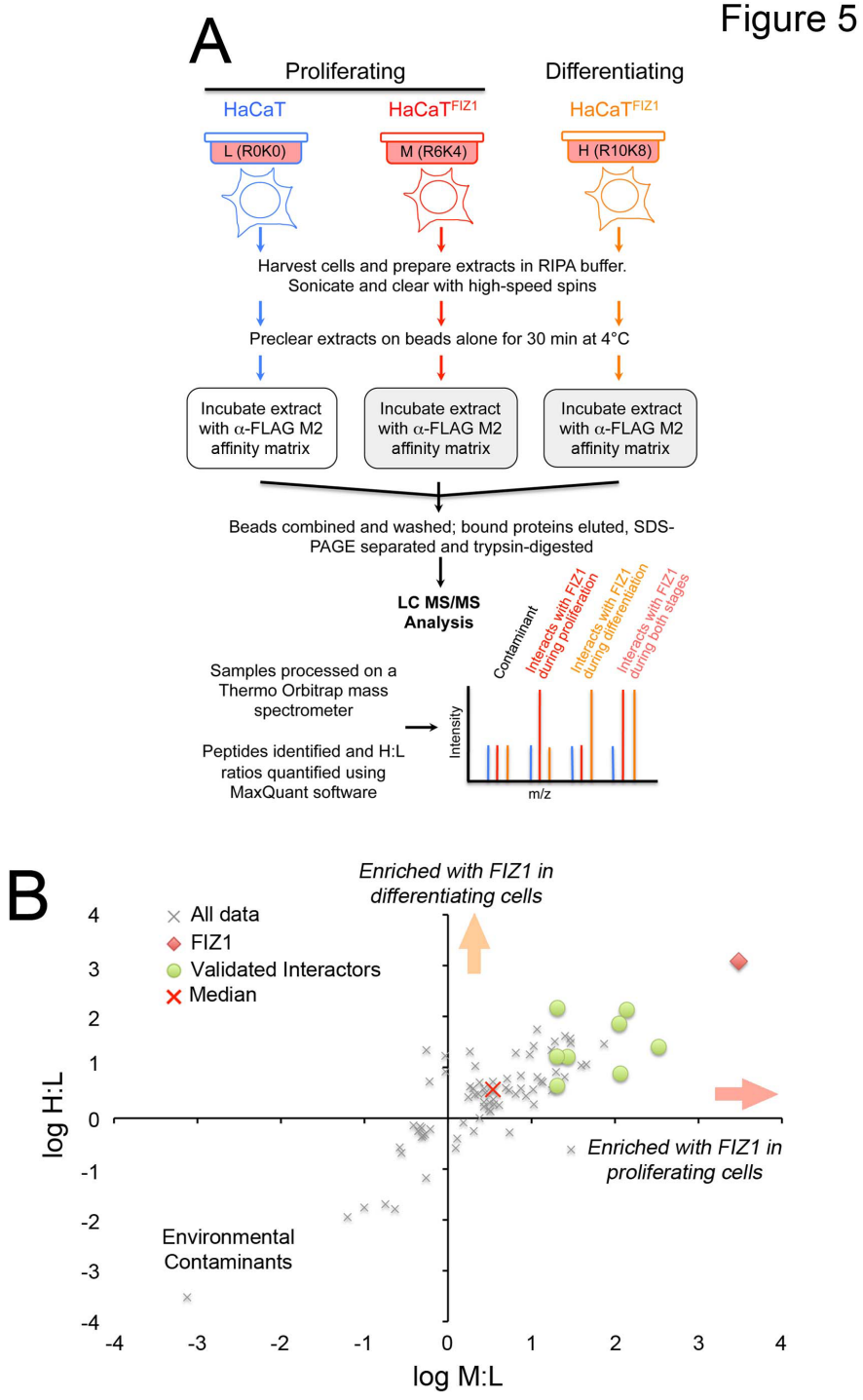

Figure 5A-B. FIZ1 interacts with signaling and transcription-related proteins. A. Design of quantitative AP/MS experiment. B. Data plotted as log ratio H:L vs. log ratio M:L. FIZ1-FLAG (red diamond) and the 8 validated interactors (green circles) are enriched above median (red X).

Figure 5

C

				Prolif	Diff	Diff:Prolif
Pathway	**Gene**	**Protein**	**# peptides**	**M:L**	**H:L**	**H:M**
	FIZ1	**Flt3-interacting zinc finger protein 1**	**5**	**11.17**	**8.49**	**0.91**
MOB/NDR complexes	MOB2	MOB kinase activator 2	3	4.41	4.38	1.13
	NDR1/STK38	Serine/threonine-protein kinase 38	21	2.48	1.56	0.69
	NDR2/STK38L	Serine/threonine-protein kinase 38-like	13	4.14	3.63	1.00
Nuclear import	IPO8	Importin-8	26	5.75	2.64	0.54
Transcription	TRAF4	TNF receptor-associated factor 4	2	4.18	1.84	0.94
	TAF4	Transcription initiation factor TFIID subunit 4	11	2.48	4.50	1.92
JAK/STAT signaling	JAK1	Tyrosine-protein kinase JAK1	4	2.47	2.32	1.00
	STAT3	Signal transducer/activator of transcription 3	2	3.15	2.08	0.71
Receptor recycling	SCYL2	SCY1-like protein 2	34	2.70	2.31	0.92

D

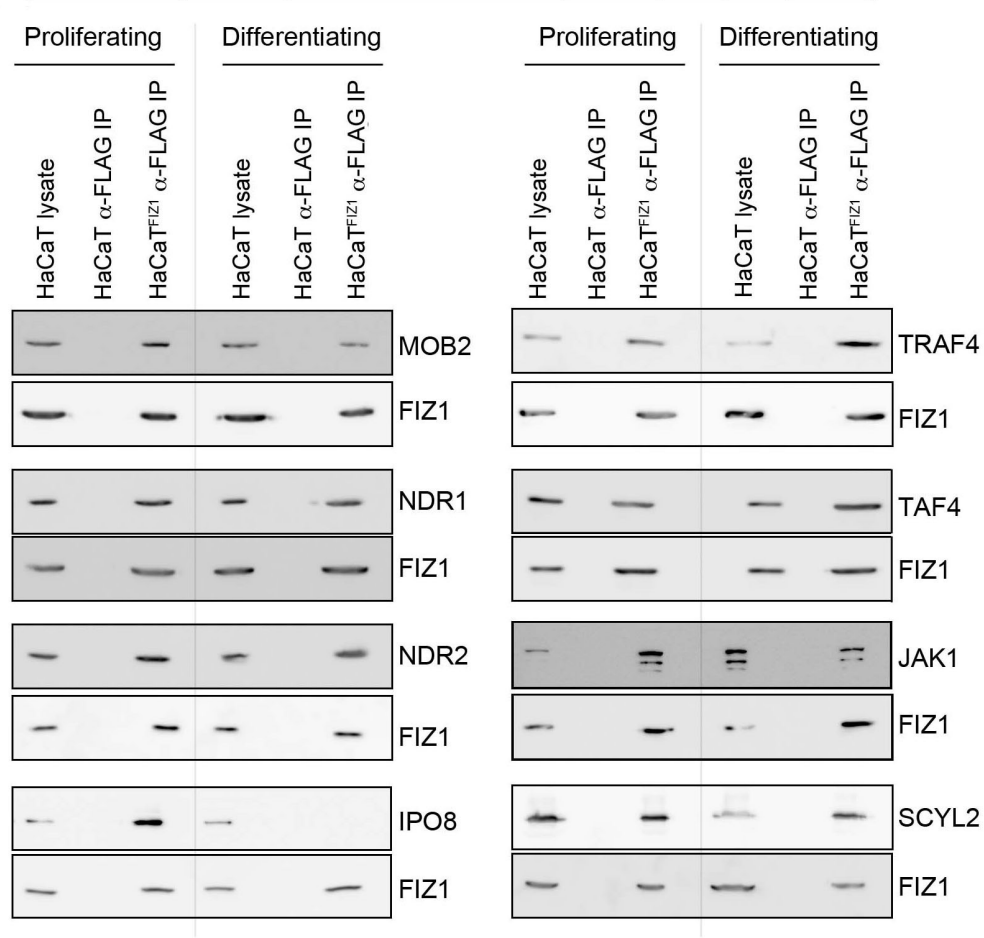

Figure 5C-D. FIZ1 interacts with signaling and transcription-related proteins. C. Top hits in the interactome. Ratio H:M compares association with FIZ1 in differentiating (H) vs. proliferating (M) cells. D. Co-IP/Western blot validation, with endogenous interactors detected in FIZ1-FLAG pulldowns.

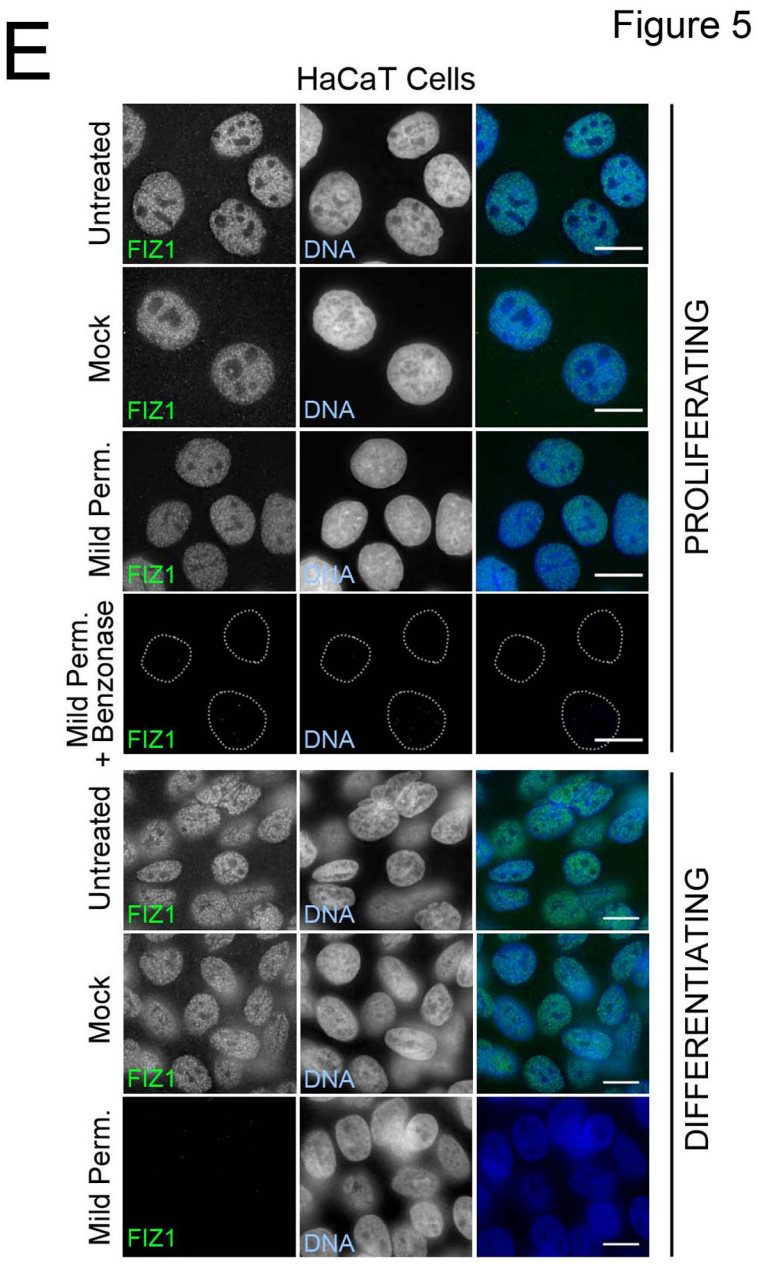

Figure 5E. FIZ1 interacts with signaling and transcription-related proteins. E. Nuclear retention assay with endogenous FIZ1 (green) and DNA (Hoechst 33342; blue) stained in cells following mild permeabilization (0.1% Triton X-100). Where indicated, benzonase was added at 125 U/coverslip (nuclei outlined). Scale bars are 5 μM.

specific complex with IPO8 suggests an alternate or parallel function. IPO8 mediates nuclear import of Smad4 (Yao et al., 2008), which is involved in TGFβ-induced cell cycle arrest in HaCaT cells (Levy and Hill, 2005). It is also a gene silencing factor that targets Argonaute (Ago) proteins to specific mRNAs (Weinmann et al., 2009). Interestingly, although FIZ1 did not enrich Ago proteins, we did find overlap with Ago3/4 interactomes (IPO8, NDR1, JAK1, spindlin).

The kinases NDR1/2 and their associated regulatory protein MOB2 have been linked to regulation of G1/S progression (Cornils et al., 2011), and NDR1 opposes the cell cycle inhibition mediated by TGFβ signaling in HaCaT and other cell lines (Pot et al., 2013). Their association with FIZ1 may therefore be related to the increased G1/S progression in $HaCaT^{FIZ1}$ cells. JAK1 tyrosine kinase is involved in numerous signaling pathways, coupling binding of cytokine ligands (including IGF1) to phosphorylation of signaling proteins and activation of STAT transcription factors. Although we could not reliably validate a FIZ1/STAT3 interaction by co-IP/Western blot, that may be due to it being indirect/transient. The JAK1 signaling via STAT1 and STAT3 has been shown to promote myoblast proliferation while preventing premature differentiation (Sun et al., 2007).

SCYL2/CVAK104 kinase is involved in receptor internalization and regulates the Wnt/β-catenin pathway (Terabayashi et al., 2009), while TRAF4 is a signaling scaffold that links receptors to kinases and their regulators in signaling cascades (Wajant et al., 2001). Interestingly, TRAF4 has been shown to associate with tight junctions in a dynamic fashion, and to potentiate ERK1/2 phosphorylation/activation in proliferating but not quiescent cells (Kédinger et al., 2008). Given the novel association that we have

identified between TRAF4 and FIZ1, it is tempting to speculate that these proteins may work together to transduce extracellular signals from tight junctions that affect downstream regulation of the balance of keratinocyte proliferation/differentiation.

TAF4 is a subunit of the core TFIID RNA Polymerase II complex that mediates promoter responses to various activators/repressors. It has been linked to autocrine signaling pathways and negative regulation of proliferation (Davidson et al., 2005), and inactivation of Taf4 in mouse embryonic fibroblasts induced serum-independent autocrine growth accompanied by deregulation of >1000 genes (Mengus et al., 2005). Furthermore, conditional Taf4 inactivation in mouse basal keratinocytes promotes epidermal hyperplasia, affects EPB development and provokes enhanced formation of chemically-induced tumours (Fadloun et al., 2007). It is likely that more than one signaling pathway feeds into TAF4 regulation in keratinocytes, and we suggest that its interaction with FIZ1, a known transcriptional repressor that we have shown here to promote keratinocyte proliferation and to be stably associated with chromatin in proliferating but not differentiating cells (Fig. 5E), raises the possibility that FIZ1 is a negative regulator of TAF4 in this system. This will be assessed in future studies, which will include a more comprehensive analysis of the global impact of altered FIZ1 levels on transcription and ChIP-seq experiments to identify docking sites on chromatin.

Concluding Remarks

In summary, we show here that the transcription factor/signal transducer FIZ1 is expressed in human keratinocytes as a predominantly nuclear protein that can associate with chromatin, and that elevated FIZ1 levels drive increased proliferation. We have

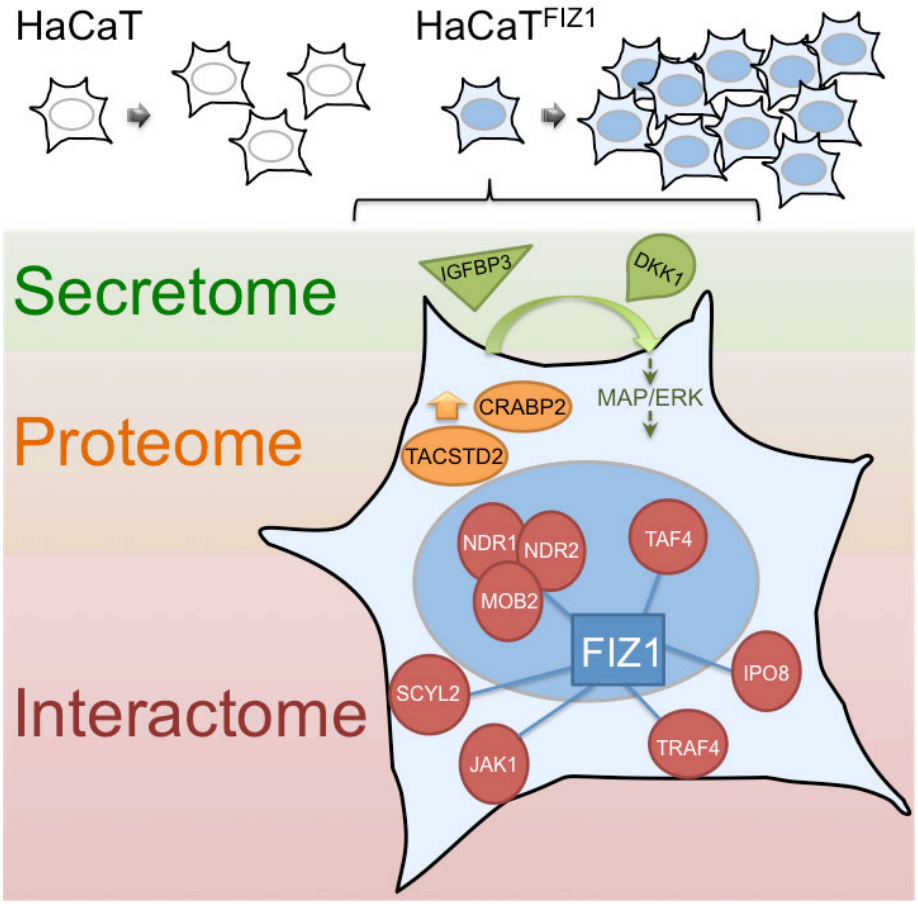

Figure 6. Diagram summarizing key findings from the multi-faceted quantitative proteomic assessment of HaCaT^{FIZ1} cells. As indicated, elevated FIZ1 levels promote increased proliferation in HaCaT cells, driven by increased secretion of growth factors and activation of MAP/ERK signaling. Within the cells, FIZ1 is found to associate with factors linked to both signal transduction and transcriptional regulation.

shown, via non-biased quantitative proteomics and in vivo assays, that this pro-proliferative signaling involves increased secretion of the heparin-binding factor IGFBP3 and sensitization to IGF signaling, and is mediated via activation of MAP/ERK kinases (Fig. 6). Reducing FIZ1 levels leads to early exit from the cell cycle, indicating that it may be required to prevent premature differentiation. Despite their enhanced proliferation rate, however, cells expressing excess FIZ1 remain subject to contact-induced terminal differentiation. Taken together, our results provide valuable functional clues to the role(s) of FIZ1 in epidermal homeostasis and open up new avenues of research into its therapeutic potential, both in promoting wound healing and in treating disorders in which epidermal homeostasis is dysregulated.

ACKNOWLEDGEMENTS

We thank Delphine Chamousset for assistance with FACS analysis and colleagues in the Trinkle lab for helpful discussions and suggestions. We also thank Drs. Kursad Turksen, Brian Hemmings, Harald Wajant and Nadine Wiper-Bergeron for advice and reagents, and Lawrence Puente at the Ottawa Hospital Research Institute Proteomics Core Facility for technical support. This work was supported by the Terry Fox Research Institute (Ref: 20148) and NSERC (Ref: 372370). N. Larivière holds a CIHR Banting & Best Scholarship and LTM holds a CIHR New Investigator Award.

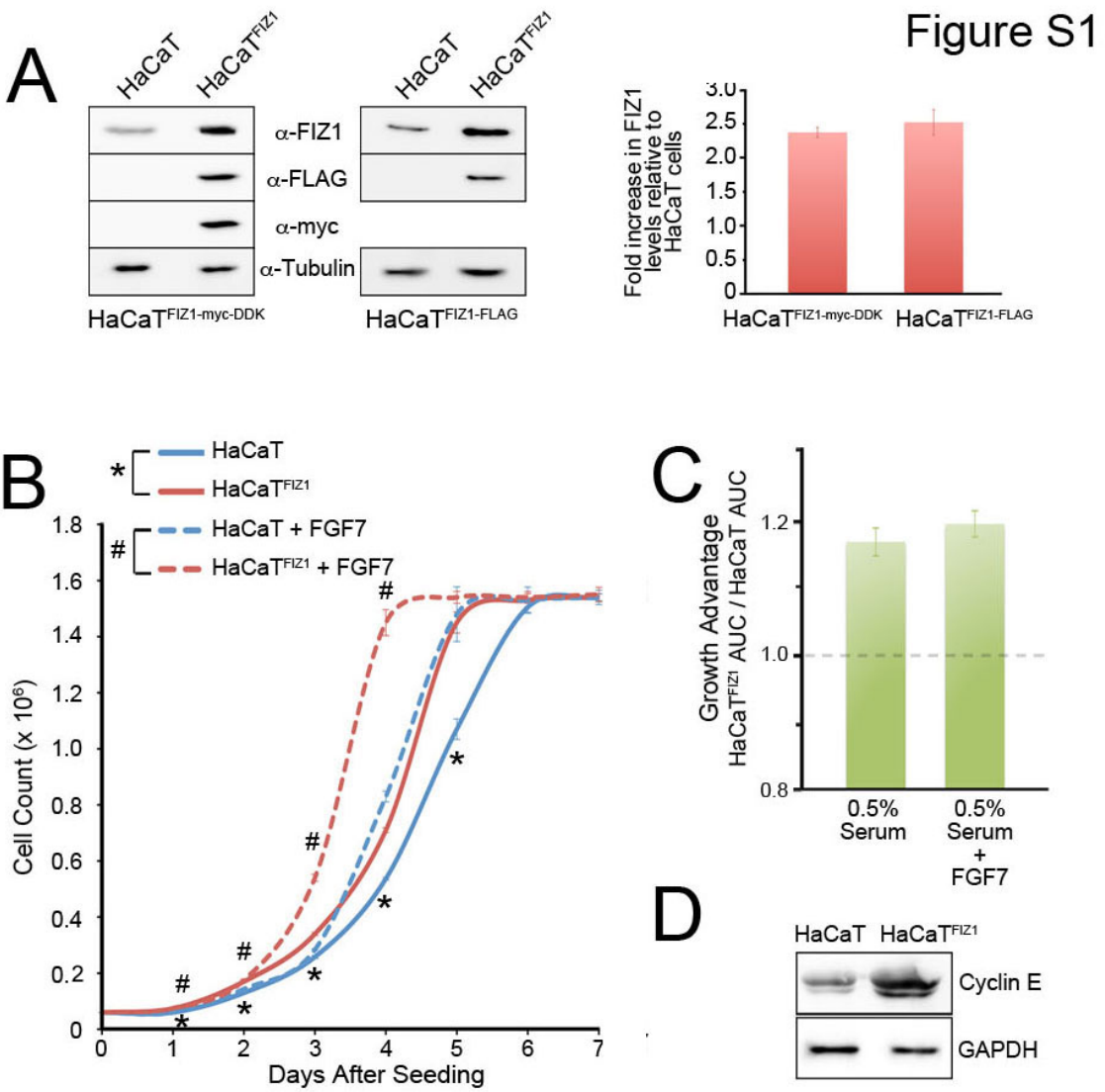

Figure S1A-D. A. Western blot analysis of clonal cell lines isolated after stable incorporation of FIZ1 plasmids. Tagged FIZ1 co-migrates with endogenous FIZ1, and the fold-increase in total FIZ1 (normalized to tubulin) is plotted as mean ± SE for 6 independent cell lines. B. Growth curves in 0.5% serum media ± exogenous FGF7/KGF (10 ng/ml). C. AUCs calculated for (B) and expressed as a ratio of HaCaT^{FIZ1} / HaCaT. D. Representative Western blot demonstrating increased Cyclin E levels (normalized to GAPDH) in proliferating HaCaT^{FIZ1} cells. Data plotted as mean ± SE. Symbols (*, #) indicate statistically significant differences for a threshold $p < 0.01$.

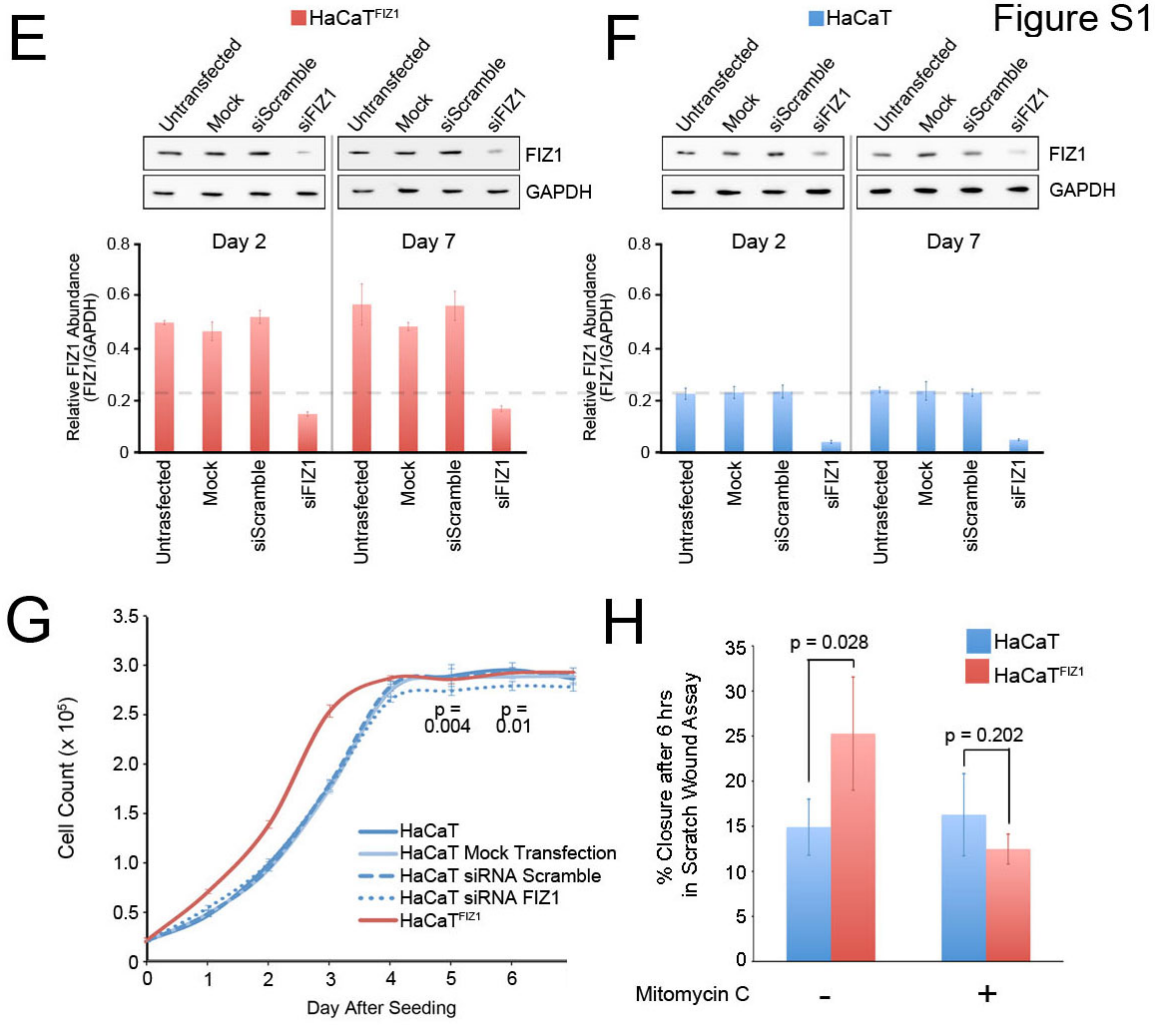

Figure S1E-H. E. FIZ1 levels (normalized to GAPDH) in HaCaT^{FIZ1} cells monitored by immunoblotting, for the siRNA knockdown experiments. Levels were reduced to just below those in parental HaCaT cells (dashed line) and the knockdown maintained for 7 days. F. FIZ1 levels (normalized to GAPDH) in HaCaT cells show an ~80% reduction with FIZ1-targeted siRNA that is maintained for 7 days. G. Growth curve analysis of FIZ1 knockdown in HaCaT cells. G. Scratch wound assay ± Mitomycin C (15 μM), with p values indicated. Data plotted as mean ± SE. Symbols (*, #) indicate statistically significant differences for a threshold $p < 0.01$.

A

Figure S2

Gene Name	Protein Name	UniProt	# Peptides Total/Unique	Ratio H:L	Normalized Intensity
FABP4	Fatty acid-binding protein, adipocyte	P15090	5/5	8.29	88.68
CRABP2	Cellular retinoic acid-binding protein 2	P29373	2/2	1.83	11.09
MYH14	Myosin-14	G8JLL9	4/2	1.61	0.33
AIMP1	Aminoacyl tRNA synthase complex interactor	Q12904	2/2	1.47	3.02
MYO1C	Unconventional myosin-Ic	O00159	7/7	1.43	7.75
FABP5	Fatty acid-binding protein, epidermal	Q01469	2/2	1.39	8.38
MYO1B	Unconventional myosin-Ib	O43795	9/9	1.39	5.29
TACSTD2	Tumor-associated calcium signal transducer 2	P09758	5/5	1.38	35.07

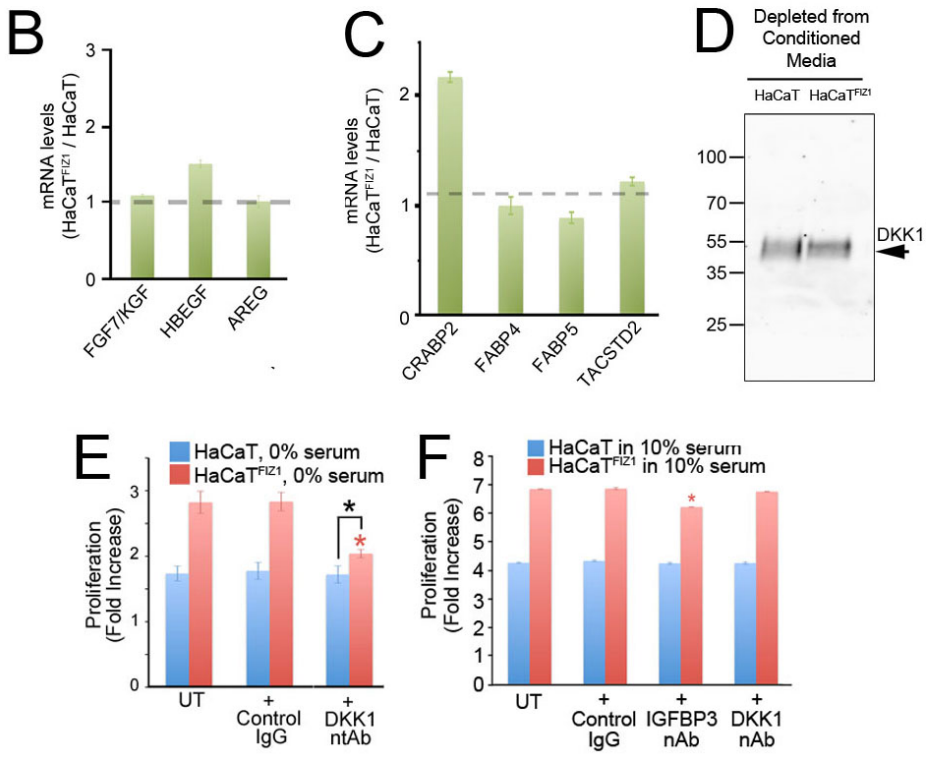

Figure S2. A. Proteins enriched in the HaCaT^{FIZ1} cell proteome. B. qPCR results for known heparin-binding HaCaT growth factors, reported as relative mRNA levels vs. HaCaT cells. C. qPCR results for selected proteome hits, reported as relative mRNA levels in HaCaT^{FIZ1} vs. HaCaT cells. D. Western blot assessing levels of DKK1 captured on heparin-agarose beads. E. Growth assays demonstrating the significant reduction in HaCaT^{FIZ1} cell proliferation in serum-free media following addition of DKK1 neutralizing antibodies. F. Two-day growth assays demonstrating significant reduction in HaCaT^{FIZ1} cell proliferation following addition of IGFBP3 neutralizing antibodies to media containing 10% serum. Data plotted as mean ± SE for 3 biological replicates. Asterisks indicate statistically significant differences for a threshold $p < 0.01$.

Figure S3

A

Interactor	Antibody	Cloned	Detected in FLAG-FIZ1 IP Proliferating/whole cell	Detected in FLAG-FIZ1 IP Differentiating/whole cell	Detected in IP of endogenous FIZ1	Endogenous FIZ1 co-IPs with GFP-tagged protein
MOB2	Yes	Yes	✓	✓	* antibody reactivity lost	✓
NDR1	Yes	Yes	✓	✓	✓	✓
NDR2	Yes	Yes	✓	✓	✓	✓
IPO8	Yes	No	✓		✓	* interactor not cloned
TRAF4	Yes	Yes	✓	✓	✓	✓
TAF4	Yes	No	✓	✓	✓	* interactor not cloned
JAK1	Yes	Yes	✓	✓	✓	✓
SCYL2	Yes	Yes	✓	✓	✓	✓

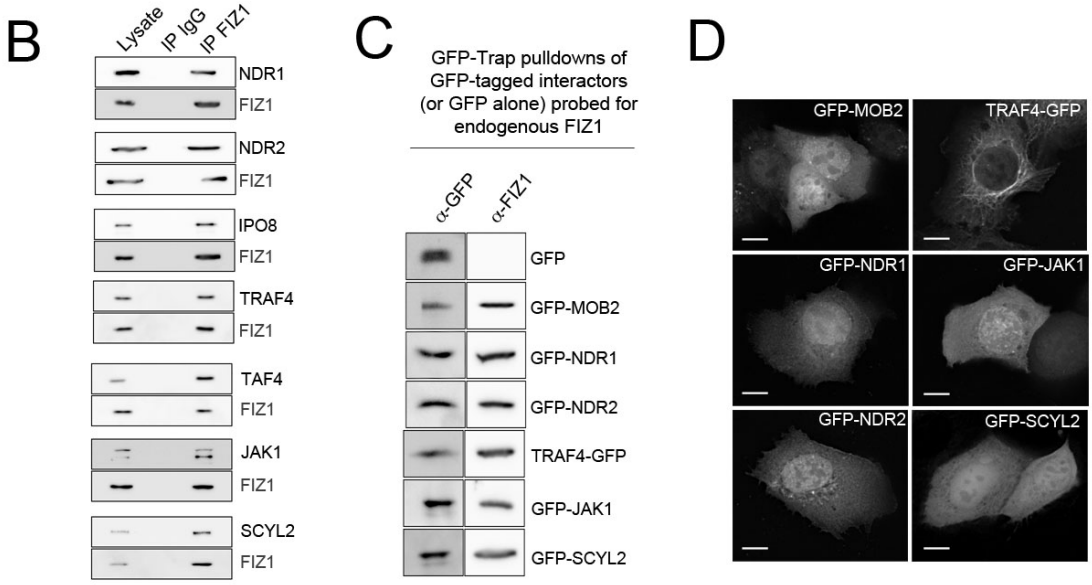

Figure S3. A Table summarizing the FIZ1 interactor validation experiments. B. Co-IP/Western blot, with α-FIZ1 and control IgG pulldowns probed with antibodies to endogenous interactors. C. Co-IP/Western blot validation of endogenous FIZ1 association with tagged interactors. GFP-tagged proteins (or GFP alone) were transiently expressed in HaCaT cells and affinity purified using the GFP-Trap. Co-purified FIZ1 was detected using α-FIZ1. D. Fluorescence imaging of GFP-tagged interactors transiently expressed in HaCaT cells. Scale bars are 5 μM.

Table S1. All plasmids and antibodies used in this study.

Plasmids:	Source:	Type:
pCMV6-XL5-FIZ-MYC-DDK	Origene	Plasmid
pReceiver-M13-FIZ1-FLAG	Dr. Kursad Turksen	Plasmid
TRAF4-GFP	Dr. Harald Wajant	Plasmid
Donor Plasmids or cDNA for Cloning:	Source:	Type:
pDONR223-JAK1	Addgene	Plasmid
pDONR223-SCYL2	Addgene	Plasmid
NDR1 MHS6278-202806050	OpenBiosystems, ThermoScientific	cDNA
NDR2 MHS6278-202807055	OpenBiosystems, ThermoScientific	cDNA
MOB2 MHS6278-202809106	OpenBiosystems, ThermoScientific	cDNA

Antibodies:	Source:	Western Blot Dilutions:
CyclinE	Abcam	4 μg/mL
ERK1/2	StressMarq	1:1000
FIZ1	Abcam	1 μg/mL
FLAG	Sigma-Aldrich	1 μg/mL
GAPDH	Covance	1 μg/mL
IGFBP3	R&D Systems	0.1 μg/mL
Involucrin	Sigma-Aldrich	1 μg/mL
IPO8	ThermoScientific	0.5 μg/mL
JAK1	Abcam	1 μg/mL
KI67	BD Biosciences	1.5 μg/mL
Mob2	Dr. Brian Hemmings	1:500
Myc	ATCC Hybridoma line 9E10	1:25
NDR1	Dr. Brian Hemmings	1:500
NDR2	Dr. Brian Hemmings	1:500
Phospho-ERK (Phospho 44/42 MAPK)	Cell Signaling Technology	1:1000
Phosphotyrosine	Millipore	2 μg/mL
SCYL2	Abcam	1 μg/mL
STAT3	ThermoScientific	0.2 μg/mL
TAF4	Sigma-Aldrich	0.2 μg/mL
TRAF4	Sigma-Aldrich	3 μg/mL
Tubulin	Sigma-Aldrich	0.5 μg/mL

Table S2. Primers for RT-PCR and qPCR, designed using Primer 3 by Steve Rozen and Helen J. Skaletsky (1998; code available at http://www-genome.wi.mit.edu/genome_software/other/primer3.html) and list of sequences for siRNA duplexes (all obtained from Thermo-Scientific).

RT-PCR	Sequence 5' - 3' (Sense):	Sequence 5' - 3' (Anti-sense):
GAPDH	GAGTCAACGGATTTGGTCGT	TTGATTTTGGAGGGATCTCG
INVOLUCRIN	CCCATCAAAGCAAGAGGAAA	GCTGCTGATCCCTTTGTG
K10	CATCCTGCTTCAGATCGACA	TCATTTCCTCCTCGTGGTTC
qPCR	Sequence 5' - 3' (Sense):	Sequence 5' - 3' (Anti-sense):
AREG	TGGATTGGACCTCAATGACA	AGCCAGGTATTTGTGGTTCG
CCDC80	ACAAGTCCCACCAACCAGAG	AAGGCAGTGGTGGTCATAGG
CRABP2	TGCTGAGGAAGATTGCTGTG	GGAGCTTCTGCTCACAGACC
DKK1	TCCGAGGAGAAATTGAGGAA	CCTGAGGCACAGTCTGATGA
FABP4	TCAGTGTGAATGGGGATGTG	TGCACATGTACCAGGACACC
FABP5	AATGGCCAAGCCAGATTGTA	CACTCCTGATGCTGAACCAA
FGF7	TTTGGAAAGAGCGACGACTT	GGCAGGATCCGTGTCAGTAT
FIZ1	GGCAGCAGTAGGGTTTCTCA	CTGCAGTGAATGTGGCAAGA
GAPDH	GAGTCAACGGATTTGGTCGT	TTGATTTTGGAGGGATCTCG
HB-EGF	GGCAGATCTGGACCTTTTGA	CCCATGACACCTCTCTCCAT
IGF-1	GCTCTTCAGTTCGTGTGTGG	CCTGCACTCCCTCTACTTGC
IGF-1R	CCAAAACTGAAGCCGAGAAG	ATCGATGCGGTACAATGTGA
IGF2	CAATGGGGAAGTCGATGCTG	GGAAACAGCACTCCTCAACG
IGFBP3	CCTGCCGTAGAGAAATGGAA	AGGCTGCCCATACTTATCCA
INVOLUCRIN	GATGTCCCAGCAACACACAC	TGCTCACATTCTTGCTCAGG
TACSTD2	CACATCCTCATTGACCTGCG	CCTCTCGAAGTAGTAGGCGG

siRNA FIZ1	Sequence:
ON-TARGETplus SMARTpool siRNA J-015014-21	AGUGCUACCUCAAGCGCCA
ON-TARGETplus SMARTpool siRNA J-015014-20	GCGAGAAGCUGUUCCGCUC
ON-TARGETplus SMARTpool siRNA J-015014-19	GGCACAAGCUGACGCACGA
ON-TARGETplus SMARTpool siRNA J-015014-18	GAAAAUGGAUAUAGCCGAA
siScramble	DY647-CAGUCGCGUUUGCGACUGG

GENERAL DISCUSSION

Epidermal homeostasis is a balancing act governed by a multitude of underlying regulatory events, an example of which is controlled protein expression. Epidermal layer-specific expression of the Cldn family results in a distribution profile where Cldns 6, 11, 12 and 18 are expressed in the suprabasal layers only while Cldn 1 is expressed in all living layers of the epidermis (Kirschner and Brandner, 2012). Perturbation of epidermal homeostasis, such as in psoriasis, results in altered expression and localization of Cldn family members (Watson et al., 2007). Ongoing research, including our own, seeks to gain a better understanding of how homeostasis is coordinated and the key players involved.

An appreciation of the contribution of TJs to barrier function of stratified epithelia (Furuse et al., 2002) led to a reassessment of the TJ complex, and in particular the Cldn family of adhesion molecules intimately associated the barrier. While these initial studies focused on Cldn1, Turksen and colleagues co-identified another family member, Cldn6, which they showed to be one of the earliest factors expressed in embryonic stem cells committed to the epithelial fate (Turksen and Troy, 2001) and whose altered expression had downstream effects on epidermal barrier formation (Troy et al., 2005a; Turksen and Troy, 2002). More recently, conditional Cldn6 expression was shown to induce epithelial differentiation in mouse stem cells (Sugimoto et al., 2013). With the C-terminal tail region representing the site most likely to be involved in Cldn-mediated TJ signaling, the Turksen group set out to assess the effect of targeted overexpression of a tail-deletion mutant on epidermal barrier formation and function. Although providing further confirmation that Cldn6 is important for epidermal homeostasis, improper folding and membrane targeting of the exogenously expressed mutant protein limited the applicability

of this model for studying TJ-related signaling (Arabzadeh et al., 2006; Troy et al., 2005a; Turksen and Troy, 2002). This is likely due to truncation of the protein too close to a conserved Cysteine residue (C184), palmitoylation of which has been shown to promote TJ localization of other Cldns (Van Itallie, 2005).

We adopted a similar structure/function approach to study the effect of targeted overexpression of Cldn6 mutants on epidermal development, albeit utilizing more minimal truncations that show similar localization to endogenous Cldn6. A comparison of all three truncation mutants, which vary by the sequential removal of 10 fewer amino acids, is shown in Discussion Fig. 1, and a summary of the phenotypes of the more minimal tail truncation mutant mouse models is presented in Discussion Table 1. In both cases mice were born with sufficient barrier function for survival but had delayed epidermal thinning. Interestingly, the more minimal (13 amino acid) truncation mutant showed expedited maturation compared to the 23 amino acid truncation (3 day lag vs 2 weeks), suggesting that, within those 10 amino acids, lies an interaction and/or modification that plays a role in epidermal maturation. Bioinformatic analysis identified a cluster of putative phosphorylation sites that may be involved (S201, T202 and S203), with predicted kinases outlined in Table 2 in Appendix 1. Several studies have since mapped phosphorylation of these sites in CLDN6 in human embryonic stem (hES) cells (Phanstiel et al., 2011; Rigbolt et al., 2011; Van Hoof et al., 2009), which increases significantly following induction of differentiation in these cells (Rigbolt et al., 2011; Van Hoof et al., 2009). Phosphorylation of a related site in Cldn1 (T202) has been shown to promote barrier function and to be required for efficient incorporation into TJs (French et al., 2009; Fujibe et al., 2004). Modifications within this region therefore have

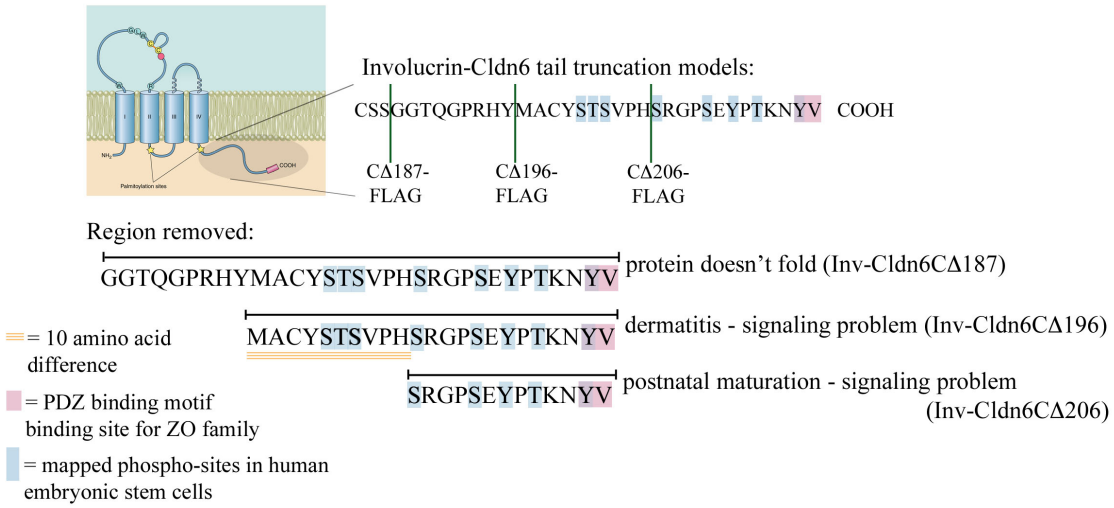

Discussion Fig.1: Summary of more minimal Cldn6 tail truncations. Sequences are listed with mapped phospho-sites and PDZ motif highlighted in blue and pink as indicated. The 10 amino acid difference between truncation mutants is underlined in orange. All transgenes were targeted to the suprabasal layers of the epidermis specifically, driven by the Involucrin promoter.

Mouse model	Overall Phenotype	Barrier Function		Epidermal Structure	
		TEWL	Dye penetration	H&E	CEs
Cldn6 overexpressed with tail deletion at CΔ196 *Removal of 23 amino acids from C-terminal end.* *LOW transgene level*	Normal barrier at birth 2 week lag in epidermal maturation. Epidermis is: 1. thickened with aging (2mo+) 2. Sensitized to injury (all ages) Dermatitis (age 2 months+)	Young: Normal Aged: 8x⇧ water loss in dermatitis lesions.	No dye penetration (normal)	Thickened during 2 week lag in epidermal maturation. Indistinguishable from wild type by 1 month after birth. Thickened epidermis with aging. Dermatitis appears with aging.	Normal: uniform size, rigid structure.
Cldn6 overexpressed with tail deletion at CΔ206 *Removal of 13 amino acids from C-terminal end.*	Sufficient barrier function at birth 3 day lag in epidermal maturation.	Non-lethal barrier defect: 1.8x⇧ water loss at birth, normal by 4 days after birth	Delayed barrier formation in development Normal at birth	Thickened during 3 day lag in epidermal maturation. Indistinguishable from wild type by 10 days after birth	Normal: uniform size, rigid structure.

Discussion Table 1: Comparison of Inv-Cldn6-CΔ196 (Chapter 1) and Inv-Cldn6-CΔ206 (Chapter 2) mouse models. Purple shading indicates observations/phenotype unique to a model. TEWL = transepidermal water loss, H&E = hematoxylin and eosin, CEs = cornified envelopes

the potential to affect TJ structure and signaling, and to impact on the progression of epidermal maturation. Future experiments will be necessary to confirm phosphorylation of these sites in CLDN6 in differentiating keratinocytes. Initial assessment of the structural relevance could be carried in HaCaT cells, to determine both the ability of a phosphomutant (e.g. T202A or T202D) to be targeted to the plasma membrane and TJs and any dominant-negative effects of its overexpression on localization of endogenous Cldn6 and other Cldns. Functional relevance could be addressed both in HaCaT cells (via measurement of transepithelial resistance and proliferation/differentiation balance) and by generation of a mouse model with targeted suprabasal epidermal overexpression of any promising candidates. Depending on its specificity, identification of the relevant kinase may provide the potential for therapeutic application in accelerated postnatal maturation of skin. Considering that current standard practice for premature infant barrier maturation is topical application of emollients (Reviewed in (Telofski et al., 2012)), any new avenue of research in this field would be of particular interest.

Another intriguing difference in the tail truncation model with 23 residues deleted is sensitization to injury, evident even in young mice (1 month of age). As the mice age, aberrant repair is exacerbated to the point where they develop dermatitis lesions in areas of natural mechanical stress (i.e. from grooming). This parallels the reduced ability to repair observed in the aging human epidermis and suggests the applicability of this mouse model to study injury response in the context of aging. Despite the existence of a sizeable body of literature (and a number of mouse models) addressing photo-aging and dermal structural changes associated with aging of human skin (Hwang et al., 2011; Kochevar et al., 1994; Moloney et al., 1992), sensitization to injury is a facet that has not

yet been sufficiently addressed.

The dramatic changes in dermal structure that occur in the aging skin include reduction in the levels of collagen, a marker for diminished functionality of dermal fibroblasts (Zouboulis et al., 2008). Preliminary results using picrosirius red histological stain in our mouse model revealed a less dense dermal collagen matrix. While it is not yet clear how overexpression of truncated Cldn6 could affect fibroblast-related functions, keratinocytes and fibroblasts interact through a variety of soluble factors (Maas-Szabowski et al., 1999; Smola et al., 1993), and this interaction may mediate the phenotype. Fibroblasts play a central role in wound healing and have been demonstrated to enhance re-epithelialization in wounded human skin equivalents (Ghalbzouri et al., 2003). They were recently shown to be involved in the pathogenesis of dermatitis by influencing skin barrier structure, which they do via regulation of Filaggrin expression, a protein important to keratin aggregation in the granular layer in which TJs are also found (Berroth et al., 2013). It is clear that a more detailed examination of the dermis of our mouse model needs to be carried out in order to understand both the delayed wound healing and dermatitis phenotype and to assess the potential role of Cldn6 in fibroblast function. Our findings implicating Cldn6 in the aging epidermis call for a need to examine Cldn expression profiles in aging, which has not yet been reported in the literature.

Given the importance of the Cldn6 cytoplasmic tail region both for epidermal maturation and maintenance of skin homeostasis throughout life, identification and functional characterization of protein-protein interactions mediated by this region will help to shed light on the underlying cellular pathways that are disrupted by overexpression of the

Cldn6 mutant. The Cldn binding partner ZO1, for example, inhibits the transcriptional activity of ZONAB by sequestering this nuclear protein at TJs (Balda and Matter, 2000), with studies in retinal pigment epithelial cells demonstrating that both overexpression of ZONAB and knockdown of ZO1 lead to increased proliferation (Georgiadis et al., 2010). In addition to confirming interaction of ZO1 with CLDN6 in keratinocytes, we identified FIZ1, a Cys2His2-type zinc finger transcription factor, as another tail-specific CLDN6 binding partner. Given that FIZ1 is part of a regulatory protein complex on active photoreceptor-specific gene promoters in retinal cells (Mali et al., 2008; 2007; Mitton et al., 2003), it is likely that its role in keratinocytes also involves transcriptional regulation. Although we mapped binding of both ZO1 and FIZ1 to the minimal 13 amino acid C-terminal tail of CLDN6, FIZ1 does not contain a PDZ binding domain, and thus it is not surprising that binding is not affected by deletion of the terminal Valine residue in the PDZ binding motif "YV" (although ZO1 interaction was lost) (Appendix 2 Fig.3E). This does not, however, rule out the possibility that their binding is mutually exclusive and their effects on CLDN6 antagonistic. In HaCaT cells, we detected interaction of CLDN6 with ZO1 in the plasma membrane fraction, while interaction with FIZ1 was specific to the soluble cytoplasmic fraction (Appendix 2, Fig.3C). An interesting parallel can be found in the adherens junction protein β-catenin that can localize to all three cell compartments: the plasma membrane, the cytoplasm and the nucleus. In ensuring compartment-specific function, both regulation of protein stability and structural organization of β-catenin itself plays a role as most of its protein-interacting motifs overlap so that interaction with one partner can block binding of others all at once (Orsulic et al., 1999). In our system, it is tempting to propose a mechanism by which

CLDN6, cycling between the plasma membrane and cytosol, could be regulated by binding to either ZO1 or FIZ1, which in turn mediates TJ signaling from the plasma membrane to the cell interior. The next step is to determine the specific binding site for FIZ1 on the CLDN6 tail and to assess whether binding of FIZ1 and ZO1 to CLDN6 is indeed mutually exclusive. It will also be important to identify any potential post-translational modifications that may mediate protein-protein binding, such as phosphorylation of the Tyrosine residue in the "YV" PDZ binding domain or the upstream Serine and Threonine residues mapped in differentiating hES cells.

It is important to note the potential generality of the interaction between FIZ1 and CLDNs. Although we initially identified FIZ1 as a CLDN6 interactor, assessment of its specificity for this isoform using a panel of CLDN antibodies revealed that it also binds CLDNs 1 and 18, but not CLDN12. A recent comparison by Günzel and Fromm presents a unified phylogenetic tree that sorts human CLDNs into 8 subgroups, forming 4 major clusters (Discussion Figure 2). CLDN12 is the most distantly related of all CLDNs examined, suggesting that FIZ1 binding is associated with structural evolution of the protein family (Günzel and Fromm, 2012). Interaction with multiple CLDN isoforms implies a more general role for FIZ1 in CLDN turnover at TJs or CLDN-mediated TJ signaling, and it will be important to assess the functional relevance of these interactions in other cell types in which these two proteins are co-expressed.

Although our initial hypothesis was that any Cldn6 tail binding partners that we identified would likely play roles in keratinocyte differentiation/maturation, our studies revealed that FIZ1 is in fact a mitogenic factor for these cells, promoting increased proliferation

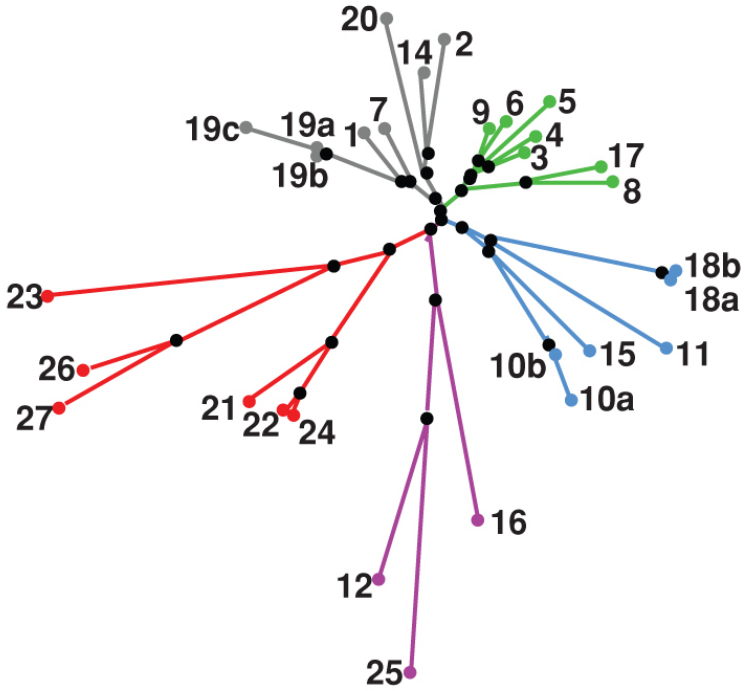

Discussion Figure 2: Phylogenetic tree for classification of CLDNs. *Reproduced by permission from (Günzel et al., 2012), copyright 2012.*

via upregulated expression and secretion of autocrine growth factors and increased transit through the cell cycle. Importantly, FIZ1-induced mitogenic signaling does not override normal cell contact-induced differentiation, which makes this factor a potential candidate for therapeutic promotion of wound healing.

This pro-proliferative phenotype is particularly interesting given that FIZ1 was originally described as an FLT3 (fms-like receptor tyrosine kinase 3) interacting protein (Wolf and Rohrschneider, 1999). Internal tandem duplication mutations in FLT3 have been identified in 30% of acute myeloid leukemia (AML) patients, and this kinase is therefore a key therapeutic target. With a demonstrated role in dendritic cell development, FLT3 has also been linked to autoimmune diseases such as psoriasis (reviewed in (Whartenby et al., 2008)). Sorafenib is the best-known FLT3 inhibitor, although it also blocks RAF, VEGF receptors -2, -3, platelet-derived growth factor receptor-b and KIT. An unexpected side effect noticed in patients treated with Sorafenib was the emergence of skin tumors (both benign and malignant), increased keratinocyte proliferation and increased MAPK pathway activation (Arnault et al., 2011). Although the phenotype is complicated by the multiple receptors inhibited by the drug and by the link between FLT3 and psoriasis, it is tempting to speculate that it may also be linked, at least in part, to disruption of normal FLT3/FIZ1 signaling.

In our analyses of FIZ1 in HaCaT cells, we focused primarily on dissecting the signaling pathways that are activated when it is upregulated and the proteins with which it interacts in multiprotein complexes. To complement this proteomic approach, future studies should include comprehensive mapping of its targets as a putative transcription factor,

utilizing the powerful and non-biased ChIP-SEQ approach (Johnson et al., 2007). Our localization studies suggest that FIZ1 is stably associated with chromatin only in proliferating cells, and the downstream changes observed in the cellular proteome and secretome with increased FIZ1 could therefore reflect a positive role in regulating transcription of specific genes. Conversely, interaction with the transcription factor and TFIID subunit TAF4 is likely repressive, given that this protein has been shown to negatively regulate keratinocyte proliferation and possesses tumour suppressor activity in the mouse epidermis. Conditional inactivation of Taf4 in the basal layer of the epidermis resulted in hyperproliferation and hyperplasia (Fadloun et al., 2007). Furthermore, with Taf4 null skin already in a hyperproliferative state, treatment of these mice with the tumour initiator DMBA (7,12-dimethylbenz(α)anthracene) resulted in a large tumour burden. Based on these correlations, a next obvious step would be to assess the functional implication of the interaction of FIZ1 with TAF4 using *in vivo* reporter gene assays.

Given the pro-proliferative role that we uncovered for FIZ1 and the signaling pathways implicated in this role (MAPK, IGFs and others), it is possible that FIZ1 may act in the full thickness epidermis to promote wound healing in response to injury. An inherent feature of keratinocytes is the ability to respond rapidly to epidermal injury with a surge in cell proliferation and migration to regenerate the damaged region. The efficiency of re-epithelialization depends on the presentation of and signaling by growth factors and cytokines that are secreted by dermal fibroblasts, activated keratinocytes and infiltrated immune cells (Ghalbzouri et al., 2003; Werner and Grose, 2003). Interestingly, several studies have demonstrated a beneficial effect of exogenous IGF1 on wound healing,

particularly in combination with other growth factors. Our studies have demonstrated that HaCaT cells with increased FIZ1 levels have a more robust response to exogenous IGF1 and an increased resistance to IGF1 neutralizing antibodies, in addition to increased transcript levels of IGF1R (Supplemental Fig.S2F,G and D respectively in Chapter 3 manuscript). These data suggest not only sensitization to this factor, but also the possibility that in healthy, full-thickness epidermis, FIZ1 plays a role in keratinocyte re-epithelialization. FIZ1 overexpressing cells exhibit accelerated wound closure in scratch wound assays compared to parental cells, and ablation of this effect following mitotic inhibition suggests that it is due primarily to their increased proliferative rate (Supplementary figure S1G in Chapter 3 manuscript). Although increased FIZ1 did not have an obvious effect on cell migration, this would need to be properly assessed (along with the effect of FIZ1 knockdown in parental cells) in transwell migration assays. The scratch wound experiments could also be extended to test whether knockdown of FIZ1 affects wound healing in parental HaCaT cells, and wounding experiments could be carried out in Fiz1 knockout mice or in primary cell cultures derived from this line. Additionally, a more effective knock down in culture could be revisited using a gene editing tool such as CRISPR (Clustered Regularly Interspaced Short Palindromic Repeats) in which the DNA-cutting enzyme Cas9 finds its target with the help of an RNA guide sequence (Shalem et al., 2014) and can be engineered to target FIZ1.

Although we are primarily interested in its potential to promote wound healing, one concern is that FIZ1 may be oncogenic. The online integrated cancer database canSAR (Halling-Brown et al., 2011) reports upregulated levels of FIZ1 in 5 cancers of epithelial origin and 2 leukemias. In culture, despite its promotion of keratinocyte proliferation, we

would not classify FIZ1 as a potential oncogene, given that the cells remain subject to contact-induced exit from the cell cycle and terminal differentiation. Resistance to Ca^{2+}-induced differentiation *in vitro*, however, is a feature that they have in common with the PAM212 squamous cell carcinoma (SCC) cell line (Filvaroff et al., 1990). Interestingly, SCC cells show upregulation of an overlapping set of genes, namely the matrix metallopeptidase MMP13, the matrix assembly protein MATN2 and the growth factor IGFBP3 (Toriseva et al., 2012), suggesting that hyperproliferative keratinocytes may share some common features.

Certain FIZ1 interacting factors that we identified have also been shown to be upregulated in cancer, such as the cell cycle-promoting complex NDR1/2. NDR1 mRNA is consistently upregulated in ductal carcinoma in situ (Adeyinka et al., 2002), while NDR2 is upregulated in the highly metastatic non-small cell lung cancer cell line NCI-H460 (Ross et al., 2000). The therapeutic potential of FIZ1 for promoting wound healing will thus be dependent on whether or not it has the potential to induce unregulated keratinocyte proliferation. Also, given that dysregulated FIZ1 may contribute to other hyperproliferative skin diseases such as dermatitis, its potential as a therapeutic target for these conditions should be explored.

In summary, our studies on the Cldn6 cytoplasmic tail region and our identification of the novel mitogenic factor FIZ1 have provided the field not only with a mouse model that may be useful for the study of skin maturation and aging, but also with numerous avenues of TJ-mediated signaling research to follow up and a number of novel therapeutic targets that may prove useful once their full potential is assessed.

REFERENCES

Adeyinka, A., Emberley, E., Niu, Y., Snell, L., Murphy, L.C., Sowter, H., Wykoff, C.C., Harris, A.L., Watson, P.H., 2002. Analysis of gene expression in ductal carcinoma in situ of the breast. Clin. Cancer Res. 8, 3788–3795.

Ahn, S.K., Hwang, S.M., Jiang, S.J., Choi, E.H., Lee, S.H., 1999. The changes of epidermal calcium gradient and transitional cells after prolonged occlusion following tape stripping in the murine epidermis. J. Invest. Dermatol. 113, 189–195.

Ahn, S.K., Jiang, S.J., Hwang, S.M., Choi, E.H., Lee, J.S., Lee, S.H., 2001. Functional and structural changes of the epidermal barrier induced by various types of insults in hairless mice. Arch Dermatol Res 293, 308–318.

Aijaz, S., Balda, M.S., Matter, K., 2006. Tight Junctions: Molecular Architecture and Function, in: International Review of Cytology, International Review of Cytology. Elsevier, pp. 261–298.

Anderson, J.M., Van Itallie, C.M., 2009. Physiology and Function of the Tight Junction. Cold Spring Harbor Perspectives in Biology 1, a002584–a002584.

Anderson, W.J., Zhou, Q., Alcalde, V., Kaneko, O.F., Blank, L.J., Sherwood, R.I., Guseh, J.S., Rajagopal, J., Melton, D.A., 2008. Genetic targeting of the endoderm with claudin-6CreER. Dev. Dyn. 237, 504–512.

Ando-Akatsuka, Y., Saitou, M., Hirase, T., Kishi, M., Sakakibara, A., Itoh, M., Yonemura, S., Furuse, M., Tsukita, S., 1996. Interspecies diversity of the occludin sequence: cDNA cloning of human, mouse, dog, and rat-kangaroo homologues. The Journal of Cell Biology 133, 43–47.

Angelow, S., 2005. Claudin-8 modulates paracellular permeability to acidic and basic ions in MDCK II cells. The Journal of Physiology 571, 15–26.

Angelow, S., Ahlstrom, R., Yu, A.S.L., 2008. Biology of claudins. AJP: Renal Physiology 295, F867–F876.

Aono, S., Hirai, Y., 2008. Phosphorylation of claudin-4 is required for tight junction formation in a human keratinocyte cell line. Experimental Cell Research 314, 3326–3339.

Aplin, A.E., Howe, A.K., Juliano, R.L., 1999. Cell adhesion molecules, signal transduction and cell growth. Current Opinion in Cell Biology 11, 737–744.

Arabzadeh, A., Troy, T.-C., Turksen, K., 2006. Role of the Cldn6 cytoplasmic tail domain in membrane targeting and epidermal differentiation in vivo. Molecular and Cellular Biology 26, 5876–5887.

Arabzadeh, A., Troy, T.-C., Turksen, K., 2007a. Claudin Expression Modulations Reflect an Injury Response in the Murine Epidermis. Journal of Investigative Dermatology 128, 237–240.

Arabzadeh, A., Troy, T.-C., Turksen, K., 2007b. Changes in the distribution pattern of Claudin tight junction proteins during the progression of mouse skin tumorigenesis. BMC Cancer 7, 196.

Assémat, E., Bazellières, E., Pallesi-Pocachard, E., Le Bivic, A., Massey-Harroche, D., 2008. Polarity complex proteins. Biochimica et Biophysica Acta (BBA) - Biomembranes 1778, 614–630.

Atanasova, G.N., Isaeva, A.R., Zhelev, N., Poumay, Y., Mitev, V.I., 2007. Effects of the CDK-inhibitor CYC202 on p38 MAPK, ERK1/2 and c-Myc activities in papillomavirus type 16 E6- and E7-transformed human keratinocytes. Oncol. Rep. 18, 999–1005.

Bader, R.A., Kao, W.J., 2009. Modulation of the Keratinocyte–Fibroblast Paracrine Relationship with Gelatin-Based Semi-interpenetrating Networks Containing Bioactive Factors for Wound Repair. Journal of Biomaterials Science, Polymer Edition 20, 1005–1030.

Baharestani, M.M., 2007. An overview of neonatal and pediatric wound care knowledge and considerations. Ostomy Wound Management 53, 34–36–38–40.

Balda, M.S., 2003. The ZO-1-associated Y-box factor ZONAB regulates epithelial cell proliferation and cell density. The Journal of Cell Biology 160, 423–432.

Balda, M.S., Matter, K., 1998. Tight junctions. Journal of Cell Science 111 (Pt 5), 541–547.

Balda, M.S., Matter, K., 2000. The tight junction protein ZO-1 and an interacting transcription factor regulate ErbB-2 expression. EMBO J 19, 2024–2033.

Banan, A., 2005. Isoform of Protein Kinase C Alters Barrier Function in Intestinal Epithelium through Modulation of Distinct Claudin Isotypes: A Novel Mechanism for Regulation of Permeability. Journal of Pharmacology and Experimental Therapeutics 313, 962–982.

Banks-Schlegel, S., Green, H., 1981. Involucrin synthesis and tissue assembly by keratinocytes in natural and cultured human epithelia. The Journal of Cell Biology 90, 732–737.

Barland, C.O., Zettersten, E., Brown, B.S., Ye, J., Elias, P.M., Ghadially, R., 2004. Imiquimod-induced interleukin-1 alpha stimulation improves barrier homeostasis in aged murine epidermis. J. Invest. Dermatol. 122, 330–336.

Baron, M., 2003. An overview of the Notch signalling pathway. Seminars in Cell &

Developmental Biology 14, 113–119.

Bazzoni, G., 2003. The JAM family of junctional adhesion molecules. Current Opinion in Cell Biology 15, 525–530.

Behne, M.J., Barry, N.P., Hanson, K.M., Aronchik, I., Clegg, R.W., Gratton, E., Feingold, K., Holleran, W.M., Elias, P.M., Mauro, T.M., 2003. Neonatal development of the stratum corneum pH gradient: localization and mechanisms leading to emergence of optimal barrier function. J. Invest. Dermatol. 120, 998–1006.

Berroth, A., Kühnl, J., Kurschat, N., Schwarz, A., Stäb, F., Schwarz, T., Wenck, H., Fölster-Holst, R., Neufang, G., 2013. Role of fibroblasts in the pathogenesis of atopic dermatitis. Journal of Allergy and Clinical Immunology 131, 1547–1554.e6.

Bieber, T., 2010. Atopic dermatitis. Ann Dermatol 22, 125–137.

Bikle, D.D., Pillai, S., 1993. Vitamin D, calcium, and epidermal differentiation. Endocr. Rev. 14, 3–19.

Blanpain, C., Fuchs, E., 2006. Epidermal stem cells of the skin. Annu. Rev. Cell Dev. Biol. 22, 339–373.

Blanpain, C., Lowry, W.E., Pasolli, H.A., Fuchs, E., 2006. Canonical notch signaling functions as a commitment switch in the epidermal lineage. Genes & Development 20, 3022–3035.

Boukamp, P., Petrussevska, R.T., Breitkreutz, D., Hornung, J., Markham, A., Fusenig, N.E., 1988. Normal keratinization in a spontaneously immortalized aneuploid human keratinocyte cell line. The Journal of Cell Biology 106, 761–771.

Boulais, N., Misery, L., 2007. Merkel cells. Journal of the American Academy of Dermatology 57, 147–165.

Boulton, T.G., Nye, S.H., Robbins, D.J., Ip, N.Y., Radziejewska, E., Morgenbesser, S.D., DePinho, R.A., Panayotatos, N., Cobb, M.H., Yancopoulos, G.D., 1991. ERKs: a family of protein-serine/threonine kinases that are activated and tyrosine phosphorylated in response to insulin and NGF. Cell 65, 663–675.

Bowcock, A.M., Krueger, J.G., 2005. Getting under the skin: the immunogenetics of psoriasis. Nat Rev Immunol 5, 699–711.

Boxer, L.M., Dang, C.V., 2001. Translocations involving c-myc and c-myc function. Oncogene 20, 5595–5610.

Brandner, J.M., 2009. Tight junctions and tight junction proteins in mammalian epidermis. European Journal of Pharmaceutics and Biopharmaceutics 72, 289–294.

Brandner, J.M., Haftek, M., Niessen, C.M., 2010. Adherens junctions, desmosomes and tight junctions in epidermal barrier function. The Open Dermatology Journal 4, 14–20.

Brandner, J.M., Kief, S., Grund, C., Rendl, M., Houdek, P., Kuhn, C., Tschachler, E., Franke, W.W., Moll, I., 2002. Organization and formation of the tight junction system in human epidermis and cultured keratinocytes. Eur. J. Cell Biol. 81, 253–263.

Breitwieser, G.E., 2008. Extracellular calcium as an integrator of tissue function. The International Journal of Biochemistry & Cell Biology 40, 1467–1480.

Byrne, C., 1997. Regulation of gene expression in developing epidermal epithelia. BioEssays 19, 691–698.

Byrne, C., Hardman, M.J., 2005. Whole-mount assays for gene induction and barrier formation in the developing epidermis. Methods in molecular biology (Clifton, N.J.)

289, 127–136.

Byrne, C., Tainsky, M., Fuchs, E., 1994. Programming gene expression in developing epidermis. Development 120, 2369–2383.

Cartlidge, P., 2000. The epidermal barrier. Seminars in Fetal and Neonatology 5, 273–280.

Cavalieri, F., Goldfarb, M., 1987. Growth factor-deprived BALB/c 3T3 murine fibroblasts can enter the S phase after induction of c-myc gene expression. Molecular and Cellular Biology 7, 3554–3560.

Cereijido, M., Valdés, J., Shoshani, L., Contreras, R.G., 1998. Role of tight junctions in establishing and maintaining cell polarity. Annu. Rev. Physiol. 60, 161–177.

Chamousset, D., De Wever, V., Moorhead, G.B., Chen, Y., Boisvert, F.-M., Lamond, A.I., Trinkle-Mulcahy, L., 2010. RRP1B targets PP1 to mammalian cell nucleoli and is associated with Pre-60S ribosomal subunits. Mol. Biol. Cell 21, 4212–4226.

Chen, Z., Smith, C.W., Kiel, D., Van Waes, C., 1997. Metastatic variants derived following in vivo tumor progression of an in vitro transformed squamous cell carcinoma line acquire a differential growth advantage requiring tumor-host interaction. Clin. Exp. Metastasis 15, 527–537.

Cheng, X., Ma, Y., Moore, M., Hemmings, B.A., Taylor, S.S., 1998. Phosphorylation and activation of cAMP-dependent protein kinase by phosphoinositide-dependent protein kinase. Proc. Natl. Acad. Sci. U.S.A. 95, 9849–9854.

Chiba, H., Osanai, M., Murata, M., Kojima, T., Sawada, N., 2008. Transmembrane proteins of tight junctions. Biochimica et Biophysica Acta (BBA) - Biomembranes 1778, 588–600.

Citi, S., Paschoud, S., Pulimeno, P., Timolati, F., De Robertis, F., Jond, L., Guillemot, L., 2009. The Tight Junction Protein Cingulin Regulates Gene Expression and RhoA Signaling. Annals of the New York Academy of Sciences 1165, 88–98.

Cline, E.G., Nelson, W.J., 2007. Characterization of Mammalian Par 6 as a Dual-Location Protein. Molecular and Cellular Biology 27, 4431–4443.

Colegio, O.R., Van Itallie, C., Rahner, C., Anderson, J.M., 2003. Claudin extracellular domains determine paracellular charge selectivity and resistance but not tight junction fibril architecture. Am. J. Physiol., Cell Physiol. 284, C1346–54.

Colegio, O.R., Van Itallie, C.M., McCrea, H.J., Rahner, C., Anderson, J.M., 2002. Claudins create charge-selective channels in the paracellular pathway between epithelial cells. Am. J. Physiol., Cell Physiol. 283, C142–7.

Cook, P.W., Pittelkow, M.R., Shipley, G.D., 1991. Growth factor-independent proliferation of normal human neonatal keratinocytes: production of autocrine- and paracrine-acting mitogenic factors. J. Cell. Physiol. 146, 277–289.

Cornils, H., Kohler, R.S., Hergovich, A., Hemmings, B.A., 2011. Human NDR kinases control G(1)/S cell cycle transition by directly regulating p21 stability. Molecular and Cellular Biology 31, 1382–1395.

Cotsarelis, G., 2006. Epithelial Stem Cells: A Folliculocentric View. Journal of Investigative Dermatology 126, 1459–1468.

Cox, J., Matic, I., Hilger, M., Nagaraj, N., Selbach, M., Olsen, J.V., Mann, M., 2009. A practical guide to the MaxQuant computational platform for SILAC-based quantitative proteomics. Nat Protoc 4, 698–705.

D'Souza, T., 2005. Phosphorylation of Claudin-3 at Threonine 192 by cAMP-dependent

Protein Kinase Regulates Tight Junction Barrier Function in Ovarian Cancer Cells. Journal of Biological Chemistry 280, 26233–26240.

D'Souza, T., Indig, F.E., Morin, P.J., 2007. Phosphorylation of claudin-4 by PKCε regulates tight junction barrier function in ovarian cancer cells. Experimental Cell Research 313, 3364–3375.

Dale, B.A., Resing, K.A., Lonsdale-Eccles, J.D., 1985. Filaggrin: a keratin filament associated protein. Annals of the New York Academy of Sciences 455, 330–342.

Danielson, K.G., Baribault, H., Holmes, D.F., Graham, H., Kadler, K.E., Iozzo, R.V., 1997. Targeted disruption of decorin leads to abnormal collagen fibril morphology and skin fragility. The Journal of Cell Biology 136, 729–743.

Darmstadt, G.L., Saha, S.K., Ahmed, A., Ahmed, S., Chowdhury, M.A.K.A., Law, P.A., Rosenberg, R.E., Black, R.E., Santosham, M., 2008. Effect of Skin Barrier Therapy on Neonatal Mortality Rates in Preterm Infants in Bangladesh: A Randomized, Controlled, Clinical Trial. Pediatrics. 121, 522–529.

Daugherty, B.L., Ward, C., Smith, T., Ritzenthaler, J.D., Koval, M., 2007. Regulation of heterotypic claudin compatibility. J. Biol. Chem. 282, 30005–30013.

Davidson, I., Kobi, D., Fadloun, A., Mengus, G., 2005. New insights into TAFs as regulators of cell cycle and signaling pathways. Cell Cycle 4, 1486–1490.

Davies, A., 2008. Management of dry skin conditions in older people. British Journal of Community Nursing 13, 254–257.

Deyrieux, A.F., Wilson, V.G., 2007. In vitro culture conditions to study keratinocyte differentiation using the HaCaT cell line. Cytotechnology 54, 77–83.

Duan, C., Xu, Q., 2005. Roles of insulin-like growth factor (IGF) binding proteins in

regulating IGF actions. General and Comparative Endocrinology 142, 44–52.

Elias, P.M., 2005. Stratum corneum defensive functions: an integrated view. J. Invest. Dermatol. 125, 183–200.

Elias, P.M., Feingold, K.R., 2001. Coordinate regulation of epidermal differentiation and barrier homeostasis. Skin Pharmacology and Physiology 14, 128–134.

Elias, P.M., Ghadially, R., 2002. The Aged Epidermal Permeability Barrier: Basis for Functional Abnormalities. Clinics in Geriatric Medicine 18, 103–120.

Elias, P.M., Nau, P., Hanley, K., Cullander, C., Crumrine, D., Bench, G., Sideras-Haddad, E., Mauro, T., Williams, M.L., Feingold, K.R., 1998. Formation of the epidermal calcium gradient coincides with key milestones of barrier ontogenesis in the rodent. J. Invest. Dermatol. 110, 399–404.

Elias, P.M., Williams, M.L., Holleran, W.M., Jiang, Y.J., Schmuth, M., 2008. Thematic review series: Skin Lipids. Pathogenesis of permeability barrier abnormalities in the ichthyoses: inherited disorders of lipid metabolism. The Journal of Lipid Research 49, 697–714.

Enikanolaiye, A., Lariviere, N.M.K., Troy, T.-C., Arabzadeh, A., Atasoy, E., Turksen, K., 2010. Involucrin-claudin-6 tail deletion mutant (CDelta206) transgenic mice: a model of delayed epidermal permeability barrier formation and repair. Disease Models and Mechanisms 3, 167–180.

Fadloun, A., Kobi, D., Pointud, J.C., Indra, A.K., Teletin, M., Bole-Feysot, C., Testoni, B., Mantovani, R., Metzger, D., Mengus, G., Davidson, I., 2007. The TFIID subunit TAF4 regulates keratinocyte proliferation and has cell-autonomous and non-cell-autonomous tumour suppressor activity in mouse epidermis. Development 134,

2947–2958.

Fang, L., Wang, Y., Du, D., Yang, G., Tak Kwok, T., Kai Kong, S., Chen, B., Chen, D.J., Chen, Z., 2007. Cell polarity protein Par3 complexes with DNA-PK via Ku70 and regulates DNA double-strand break repair. Nature Publishing Group 17, 100–116.

Farquhar, M.G., Palade, G.E., 1963. Junctional complexes in various epithelia. The Journal of Cell Biology 17, 375–412.

Fartasch, M., Ponec, M., 1994. Improved barrier structure formation in air-exposed human keratinocyte culture systems. J. Invest. Dermatol. 102, 366–374.

Feingold, K.R., 2007. The Importance of Lipids in Cutaneous Function. The Journal of Lipid Research 48, 2529–2530.

Ferrar, T., Chamousset, D., De Wever, V., Nimick, M., Andersen, J., Trinkle-Mulcahy, L., Moorhead, G.B.G., 2012. Taperin (c9orf75), a mutated gene in nonsyndromic deafness, encodes a vertebrate specific, nuclear localized protein phosphatase one alpha (PP1) docking protein. Biology Open 1, 128–139.

Filvaroff, E., Stern, D.F., Dotto, G.P., 1990. Tyrosine phosphorylation is an early and specific event involved in primary keratinocyte differentiation. Molecular and Cellular Biology 10, 1164–1173.

Findley, M.K., Koval, M., 2009. Regulation and roles for claudin-family tight junction proteins. IUBMB Life 61, 431–437.

Fluhr, J.W., Behne, M.J., Brown, B.E., Moskowitz, D.G., Selden, C., Mao-Qiang, M., Mauro, T.M., Elias, P.M., Feingold, K.R., 2004a. Stratum corneum acidification in neonatal skin: secretory phospholipase A2 and the sodium/hydrogen antiporter-1 acidify neonatal rat stratum corneum. J. Invest. Dermatol. 122, 320–329.

Fluhr, J.W., Mao-Qiang, M., Brown, B.E., Hachem, J.-P., Moskowitz, D.G., Demerjian, M., Haftek, M., Serre, G., Crumrine, D., Mauro, T.M., Elias, P.M., Feingold, K.R., 2004b. Functional consequences of a neutral pH in neonatal rat stratum corneum. J. Invest. Dermatol. 123, 140–151.

Förster, C., 2008. Tight junctions and the modulation of barrier function in disease. Histochem Cell Biol 130, 55–70.

Frankel, P., Aronheim, A., Kavanagh, E., Balda, M.S., Matter, K., Bunney, T.D., Marshall, C.J., 2005. RalA interacts with ZONAB in a cell density-dependent manner and regulates its transcriptional activity. EMBO J 24, 54–62.

French, A.D., Fiori, J.L., Camilli, T.C., Leotlela, P.D., O'Connell, M.P., Frank, B.P., Subaran, S., Indig, F.E., Taub, D.D., Weeraratna, A.T., 2009. PKC and PKA phosphorylation affect the subcellular localization of claudin-1 in melanoma cells. Int J Med Sci 6, 93–101.

Fuchs, E., 2007. Scratching the surface of skin development. Nature 445, 834–842.

Fuchs, E., 2008. Skin stem cells: rising to the surface. The Journal of Cell Biology 180, 273–284.

Fuchs, E., Byrne, C., 1994. The epidermis: rising to the surface. Current Opinion in Genetics & Development 4, 725–736.

Fuchs, E., Horsley, V., 2008. More than one way to skin . . . Genes & Development 22, 976–985.

Fuchs, E., Raghavan, S., 2002. Getting uder the skin of eidermal morphogenesis. Nat. Rev. Genet. 3, 199–209.

Fujibe, M., Chiba, H., Kojima, T., Soma, T., Wada, T., Yamashita, T., Sawada, N., 2004.

Thr203 of claudin-1, a putative phosphorylation site for MAP kinase, is required to promote the barrier function of tight junctions. Experimental Cell Research 295, 36–47.

Fukuda, M., Gotoh, Y., Nishida, E., 1997. Interaction of MAP kinase with MAP kinase kinase: its possible role in the control of nucleocytoplasmic transport of MAP kinase. EMBO J 16, 1901–1908.

Furuse, M., 2010. Molecular Basis of the Core Structure of Tight Junctions. Cold Spring Harbor Perspectives in Biology 2, a002907–a002907.

Furuse, M., Fujita, K., Hiiragi, T., Fujimoto, K., Tsukita, S., 1998a. Claudin-1 and -2: novel integral membrane proteins localizing at tight junctions with no sequence similarity to occludin. The Journal of Cell Biology 141, 1539–1550.

Furuse, M., Furuse, K., Sasaki, H., Tsukita, S., 2001. Conversion of zonulae occludentes from tight to leaky strand type by introducing claudin-2 into Madin-Darby canine kidney I cells. The Journal of Cell Biology 153, 263–272.

Furuse, M., Hata, M., Furuse, K., Yoshida, Y., Haratake, A., Sugitani, Y., Noda, T., Kubo, A., Tsukita, S., 2002. Claudin-based tight junctions are crucial for the mammalian epidermal barrier: a lesson from claudin-1-deficient mice. The Journal of Cell Biology 156, 1099–1111.

Furuse, M., Hirase, T., Itoh, M., Nagafuchi, A., Yonemura, S., Tsukita, S., Tsukita, S., 1993. Occludin: a novel integral membrane protein localizing at tight junctions. The Journal of Cell Biology 123, 1777–1788.

Furuse, M., Sasaki, H., Fujimoto, K., Tsukita, S., 1998b. A single gene product, claudin-1 or -2, reconstitutes tight junction strands and recruits occludin in fibroblasts. The

Journal of Cell Biology 143, 391–401.

Furuse, M., Sasaki, H., Tsukita, S., 1999. Manner of interaction of heterogeneous claudin species within and between tight junction strands. The Journal of Cell Biology 147, 891–903.

Furuse, M., Tsukita, S., 2006. Claudins in occluding junctions of humans and flies. Trends in Cell Biology 16, 181–188.

Gao, J., Li, J., Ma, L., 2005. Regulation of EGF-induced ERK/MAPK Activation and EGFR Internalization by G Protein-coupled Receptor Kinase 2. Acta Biochim Biophys Sinica 37, 525–531.

Geerligs, M., 2009. Skin layer mechanics. Koninklijke Philips.

Georgiadis, A., Tschernutter, M., Bainbridge, J.W.B., Balaggan, K.S., Mowat, F., West, E.L., Munro, P.M.G., Thrasher, A.J., Matter, K., Balda, M.S., Ali, R.R., 2010. The Tight Junction Associated Signalling Proteins ZO-1 and ZONAB Regulate Retinal Pigment Epithelium Homeostasis in Mice. PLoS ONE 5, e15730.

Ghadially, R., 1998. Aging and the epidermal permeability barrier: implications for contact dermatitis. Am. J. Contact Dermatitis 9, 162–169.

Ghadially, R., Brown, B.E., Sequeira-Martin, S.M., Feingold, K.R., Elias, P.M., 1995. The aged epidermal permeability barrier. Structural, functional, and lipid biochemical abnormalities in humans and a senescent murine model. J. Clin. Invest. 95, 2281–2290.

Ghalbzouri, El, A., Hensbergen, P., Gibbs, S., Kempenaar, J., Schors, R.V.D., Ponec, M., 2003. Fibroblasts facilitate re-epithelialization in wounded human skin equivalents. Lab Invest 84, 102–112.

Gibson, A., Carney, S., Wales, J.K., 2006. Growth and the premature baby. Hormone Research 65, 75–81.

Gonzalez-Mariscal, L., Betanzos, A., Nava, P., Jaramillo, B.E., 2003. Tight junction proteins. Prog. Biophys. Mol. Biol. 81, 1–44.

Gow, A., Southwood, C.M., Li, J.S., Pariali, M., Riordan, G.P., Brodie, S.E., Danias, J., Bronstein, J.M., Kachar, B., Lazzarini, R.A., 1999. CNS myelin and sertoli cell tight junction strands are absent in Osp/claudin-11 null mice. Cell 99, 649–659.

Gramling, M.W., Eischen, C.M., 2012. Suppression of Ras/Mapk pathway signaling inhibits Myc-induced lymphomagenesis. Cell Death Differ 19, 1220–1227.

Grandori, C., Cowley, S.M., James, L.P., Eisenman, R.N., 2000. The Myc/Max/Mad network and the transcriptional control of cell behavior. Annu. Rev. Cell Dev. Biol. 16, 653–699.

Guerra, E., Trerotola, M., Aloisi, A.L., Tripaldi, R., Vacca, G., La Sorda, R., Lattanzio, R., Piantelli, M., Alberti, S., 2012. The Trop-2 signalling network in cancer growth. Oncogene 32, 1594–1600.

Guillemot, L., Paschoud, S., Pulimeno, P., Foglia, A., Citi, S., 2008. The cytoplasmic plaque of tight junctions: A scaffolding and signalling center. Biochimica et Biophysica Acta (BBA) - Biomembranes 1778, 601–613.

Guillemot, L., Schneider, Y., Brun, P., Castagliuolo, I., Pizzuti, D., Martines, D., Jond, L., Bongiovanni, M., Citi, S., 2012. Cingulin is dispensable for epithelial barrier function and tight junction structure, and plays a role in the control of claudin-2 expression and response to duodenal mucosa injury. Journal of Cell Science 125, 5005–5014.

Gunzel, D., Yu, A.S.L., 2013. Claudins and the Modulation of Tight Junction Permeability. Physiological Reviews 93, 525–569.

Günzel, D., Fromm, M., 2012. Claudins and Other Tight Junction Proteins. John Wiley & Sons, Inc., Hoboken, NJ, USA.

Hachem, J.-P., Behne, M., Aronchik, I., Demerjian, M., Feingold, K.R., Elias, P.M., Mauro, T.M., 2005. Extracellular pH Controls NHE1 expression in epidermis and keratinocytes: implications for barrier repair. J. Invest. Dermatol. 125, 790–797.

Hadj-Rabia, S., Baala, L., Vabres, P., Hamel-Teillac, D., Jacquemin, E., Fabre, M., Lyonnet, S., De Prost, Y., Munnich, A., Hadchouel, M., Smahi, A., 2004. Claudin-1 gene mutations in neonatal sclerosing cholangitis associated with ichthyosis: a tight junction disease. Gastroenterology 127, 1386–1390.

Halling-Brown, M.D., Bulusu, K.C., Patel, M., Tym, J.E., Al-Lazikani, B., 2011. canSAR: an integrated cancer public translational research and drug discovery resource. Nucleic Acids Res. 40, D947–D956.

Hamazaki, Y., 2001. Multi-PDZ Domain Protein 1 (MUPP1) Is Concentrated at Tight Junctions through Its Possible Interaction with Claudin-1 and Junctional Adhesion Molecule. Journal of Biological Chemistry 277, 455–461.

Hanley, K., Jiang, Y., Elias, P.M., Feingold, K.R., Williams, M.L., 1997. Acceleration of Barrier Ontogenesis *in Vitro* through Air Exposure. Pediatric Research 41, 2930299.

Hara-Chikuma, M., Verkman, A.S., 2008. Roles of Aquaporin-3 in the Epidermis. Journal of Investigative Dermatology 128, 2145–2151.

Hardman, M.J., Moore, L., Ferguson, M.W., Byrne, C., 1999. Barrier formation in the human fetus is patterned. J. Invest. Dermatol. 113, 1106–1113.

Hardman, M.J., Sisi, P., Banbury, D.N., Byrne, C., 1998. Patterned acquisition of skin barrier function during development. Development 125, 1541–1552.

Hartsock, A., Nelson, W.J., 2008. Adherens and tight junctions: Structure, function and connections to the actin cytoskeleton. Biochimica et Biophysica Acta (BBA) - Biomembranes 1778, 660–669.

Heiskala, M., Peterson, P.A., Yang, Y., 2001. The roles of claudin superfamily proteins in paracellular transport. Traffic 2, 93–98.

Hobbs, R.M., Silva-Vargas, V., Groves, R., Watt, F.M., 2004. Expression of activated MEK1 in differentiating epidermal cells is sufficient to generate hyperproliferative and inflammatory skin lesions. J. Invest. Dermatol. 123, 503–515.

Hohl, D., Mehrel, T., Lichti, U., Turner, M.L., Roop, D.R., Steinert, P.M., 1991. Characterization of human loricrin. Structure and function of a new class of epidermal cell envelope proteins. J. Biol. Chem. 266, 6626–6636.

Holick, M.F., 2006. Resurrection of vitamin D deficiency and rickets. J. Clin. Invest. 116, 2062–2072.

Hwang, K.-A., Yi, B.-R., Choi, K.-C., 2011. Molecular Mechanisms and In VivoMouse Models of Skin Aging Associated with Dermal Matrix Alterations. Lab Anim Res 27, 1.

Ikari, A., 2006. Phosphorylation of paracellin-1 at Ser217 by protein kinase A is essential for localization in tight junctions. Journal of Cell Science 119, 1781–1789.

Ikari, A., Ito, M., Okude, C., Sawada, H., Harada, H., Degawa, M., Sakai, H., Takahashi, T., Sugatani, J., Miwa, M., 2007. Claudin-16 is directly phosphorylated by protein kinase a independently of a vasodilator-stimulated phosphoprotein-mediated

pathway. J. Cell. Physiol. 214, 221–229.

Ikenouchi, J., 2005. Tricellulin constitutes a novel barrier at tricellular contacts of epithelial cells. The Journal of Cell Biology 171, 939–945.

Ikenouchi, J., Sasaki, H., Tsukita, S., Furuse, M., Tsukita, S., 2008. Loss of occludin affects tricellular localization of tricellulin. Mol. Biol. Cell 19, 4687–4693.

Ingermann, A.R., Yang, Y.F., Han, J., Mikami, A., Garza, A.E., Mohanraj, L., Fan, L., Idowu, M., Ware, J.L., Kim, H.S., Lee, D.Y., Oh, Y., 2010. Identification of a Novel Cell Death Receptor Mediating IGFBP-3-induced Anti-tumor Effects in Breast and Prostate Cancer. Journal of Biological Chemistry 285, 30233–30246.

Ishizaki, T., Chiba, H., Kojima, T., Fujibe, M., Soma, T., Miyajima, H., Nagasawa, K., Wada, I., Sawada, N., 2003. Cyclic AMP induces phosphorylation of claudin-5 immunoprecipitates and expression of claudin-5 gene in blood–brain-barrier endothelial cells via protein kinase A-dependent and -independent pathways. Experimental Cell Research 290, 275–288.

Itoh, M., Furuse, M., Morita, K., Kubota, K., Saitou, M., Tsukita, S., 1999. Direct binding of three tight junction-associated MAGUKs, ZO-1, ZO-2, and ZO-3, with the COOH termini of claudins. The Journal of Cell Biology 147, 1351–1363.

Ivanov, A., 2008. Actin motors that drive formation and disassembly of epithelial apical junctions. Frontiers in bioscience 13, 6662–6681.

Ivanov, A.I., McCall, I.C., Parkos, C.A., Nusrat, A., 2004. Role for actin filament turnover and a myosin II motor in cytoskeleton-driven disassembly of the epithelial apical junctional complex. Mol. Biol. Cell 15, 2639–2651.

Ivanova, I.A., D'Souza, S.J.A., Dagnino, L., 2005. Signalling in the epidermis: the E2F

cell cycle regulatory pathway in epidermal morphogenesis, regeneration and transformation. Int. J. Biol. Sci. 1, 87–95.

Janes, S.M., Watt, F.M., 2006. New roles for integrins in squamous-cell carcinoma. Nat Rev Cancer 6, 175–183.

Jensen, U.B., Lowell, S., Watt, F.M., 1999. The spatial relationship between stem cells and their progeny in the basal layer of human epidermis: a new view based on whole-mount labelling and lineage analysis. Development 126, 2409–2418.

Kalia, Y.N., Nonato, L.B., Lund, T.B., Guy, R.H., 1998. Development of skin barrier function in premature infants. Journal of Investigative Dermatology 111, 320–326.

Kalinin, A.E., Kajava, A.V., Steinert, P.M., 2002. Epithelial barrier function: assembly and structural features of the cornified cell envelope. BioEssays 24, 789–800.

Kanitakis, J., 2002. Anatomy, histology and immunohistochemistry of normal human skin. European journal of Dermatology : EJD 12, 390–399.

Kanter-Lewensohn, L., Dricu, A., Girnita, L., Wejde, J., Larsson, O., 2000. Expression of insulin-like growth factor-1 receptor (IGF-1R) and p27Kip1 in melanocytic tumors: a potential regulatory role of IGF-1 pathway in distribution of p27Kip1 between different cyclins. Growth Factors 17, 193–202.

Kato, M., Ishizaki, A., Hellman, U., Wernstedt, C., Kyogoku, M., Miyazono, K., Heldin, C.H., Funa, K., 1995. A human keratinocyte cell line produces two autocrine growth inhibitors, transforming growth factor-beta and insulin-like growth factor binding protein-6, in a calcium- and cell density-dependent manner. J. Biol. Chem. 270, 12373–12379.

Kato, Y., Tapping, R.I., Huang, S., Watson, M.H., Ulevitch, R.J., Lee, J.D., 1998.

Bmk1/Erk5 is required for cell proliferation induced by epidermal growth factor. Nature 395, 713–716.

Katoh, M., 2003. CLDN23 gene, frequently down-regulated in intestinal-type gastric cancer, is a novel member of the CLAUDIN gene family. Internal Journal of Molecular Medicine 11, 683–689.

Kaur, P., 2006. Interfollicular epidermal stem cells: identification, challenges, potential. J. Invest. Dermatol. 126, 1450–1458.

Kavanagh, E., Buchert, M., Tsapara, A., Choquet, A., Balda, M.S., Hollande, F., Matter, K., 2006. Functional interaction between the ZO-1-interacting transcription factor ZONAB/DbpA and the RNA processing factor symplekin. Journal of Cell Science 119, 5098–5105.

Keller, U.B., Old, J.B., Dorsey, F.C., Nilsson, J.A., Nilsson, L., MacLean, K.H., Chung, L., Yang, C., Spruck, C., Boyd, K., Reed, S.I., Cleveland, J.L., 2007. Myc targets Cks1 to provoke the suppression of p27Kip1, proliferation and lymphomagenesis. EMBO J 26, 2562–2574.

Kédinger, V., Alpy, F., Baguet, A., Polette, M., Stoll, I., Chenard, M.-P., Tomasetto, C., Rio, M.-C., 2008. Tumor Necrosis Factor Receptor-Associated Factor 4 Is a Dynamic Tight Junction-Related Shuttle Protein Involved in Epithelium Homeostasis. PLoS ONE 3, e3518.

Kirschner, N., Brandner, J.M., 2012. Barriers and more: functions of tight junction proteins in the skin. Annals of the New York Academy of Sciences 1257, 158–166.

Kirschner, N., Poetzl, C., den Driesch, von, P., Wladykowski, E., Moll, I., Behne, M.J., Brandner, J.M., 2009. Alteration of Tight Junction Proteins Is an Early Event in

Psoriasis. The American Journal of Pathology 175, 1095–1106.

Kiuchi-Saishin, Y., Gotoh, S., Furuse, M., Takasuga, A., Tano, Y., Tsukita, S., 2002. Differential expression patterns of claudins, tight junction membrane proteins, in mouse nephron segments. J. Am. Soc. Nephrol. 13, 875–886.

Kligman, L.H., 1989. Photoaging. Manifestations, prevention, and treatment. Clinics in Geriatric Medicine 5, 235–251.

Kochevar, I.E., Moran, M., Granstein, R.D., 1994. Experimental photoaging in C3H/HeN, C3H/HeJ, and Balb/c mice: comparison of changes in extracellular matrix components and mast cell numbers. J. Invest. Dermatol. 103, 797–800.

Kolly, C., Suter, M.M., Müller, E.J., 2005. Proliferation, cell cycle exit, and onset of terminal differentiation in cultured keratinocytes: pre-programmed pathways in control of C-Myc and Notch1 prevail over extracellular calcium signals. J. Invest. Dermatol. 124, 1014–1025.

Kopan, R., Fuchs, E., 1989. A new look into an old problem: keratins as tools to investigate determination, morphogenesis, and differentiation in skin. Genes & Development 3, 1–15.

Koval, M., 2006. Claudins—Key Pieces in the Tight Junction Puzzle. Cell Commun Adhes 13, 127–138.

Kowalczyk, A.P., Bornslaeger, E.A., Norvell, S.M., Palka, H.L., Green, K.J., 1999. Desmosomes: intercellular adhesive junctions specialized for attachment of intermediate filaments. Int. Rev. Cytol. 185, 237–302.

Kömüves, L., Oda, Y., Tu, C.-L., Chang, W.H., Ho-Pao, C.L., Mauro, T., Bikle, D.D., 2002. Epidermal expression of the full-length extracellular calcium-sensing receptor

is required for normal keratinocyte differentiation. J. Cell. Physiol. 192, 45–54.

Kömüves, L.G., Hanley, K., Jiang, Y., Katagiri, C., Elias, P.M., Williams, M.L., Feingold, K.R., 1999. Induction of selected lipid metabolic enzymes and differentiation-linked structural proteins by air exposure in fetal rat skin explants. J. Invest. Dermatol. 112, 303–309.

Krause, G., Winkler, L., Mueller, S.L., Haseloff, R.F., Piontek, J., Blasig, I.E., 2008. Structure and function of claudins. Biochimica et Biophysica Acta (BBA) - Biomembranes 1778, 631–645.

Krug, S.M., Amasheh, S., Richter, J.F., Milatz, S., Günzel, D., Westphal, J.K., Huber, O., Schulzke, J.D., Fromm, M., 2009. Tricellulin forms a barrier to macromolecules in tricellular tight junctions without affecting ion permeability. Mol. Biol. Cell 20, 3713–3724.

Kyriakides, T.R., Zhu, Y.H., Smith, L.T., Bain, S.D., Yang, Z., Lin, M.T., Danielson, K.G., Iozzo, R.V., LaMarca, M., McKinney, C.E., Ginns, E.I., Bornstein, P., 1998. Mice that lack thrombospondin 2 display connective tissue abnormalities that are associated with disordered collagen fibrillogenesis, an increased vascular density, and a bleeding diathesis. The Journal of Cell Biology 140, 419–430.

Lang, C.T., Iams, J.D., 2009. Goals and Strategies for Prevention of Preterm Birth: An Obstetric Perspective. Pediatric Clinics of North America 56, 537–563.

Langbein, L., Grund, C., Kuhn, C., Praetzel, S., Kartenbeck, J., Brandner, J.M., Moll, I., Franke, W.W., 2002. Tight junctions and compositionally related junctional structures in mammalian stratified epithelia and cell cultures derived therefrom. Eur. J. Cell Biol. 81, 419–435.

Langbein, L., Pape, U., Grund, C., Kuhn, C., Praetzel, S., Moll, I., Moll, R., Franke, W.W., 2003. Tight junction-related structures in the absence of a lumen: occludin, claudins and tight junction plaque proteins in densely packed cell formations of stratified epithelia and squamous cell carcinomas. Eur. J. Cell Biol. 82, 385–400.

Lavker, R.M., Sun, T.T., 2000. Epidermal stem cells: properties, markers, and location. Proc. Natl. Acad. Sci. U.S.A. 97, 13473–13475.

Leigh, I., Navsaria, H., Purkis, P., McKay, I., Bowden, P., Riddle, P., 1995. Keratins (K16 and K17) as markers of keratinocyte hyperproliferation in psoriasis in vivo and in vitro. Br J Dermatol 133, 501–511.

Lemmers, C., Médina, E., Delgrossi, M.-H., Michel, D., Arsanto, J.-P., Le Bivic, A., 2002. hINADl/PATJ, a homolog of discs lost, interacts with crumbs and localizes to tight junctions in human epithelial cells. J. Biol. Chem. 277, 25408–25415.

Levy, L., Hill, C.S., 2005. Smad4 Dependency Defines Two Classes of Transforming Growth Factor (TGF) Target Genes and Distinguishes TGF-Induced Epithelial-Mesenchymal Transition from Its Antiproliferative and Migratory Responses. Molecular and Cellular Biology 25, 8108–8125.

Lipschutz, J.H., 2004. Extracellular Signal-regulated Kinases 1/2 Control Claudin-2 Expression in Madin-Darby Canine Kidney Strain I and II Cells. Journal of Biological Chemistry 280, 3780–3788.

Liu, J.P., Baker, J., Perkins, A.S., Robertson, E.J., Efstratiadis, A., 1993. Mice carrying null mutations of the genes encoding insulin-like growth factor I (Igf-1) and type 1 IGF receptor (Igf1r). Cell 75, 59–72.

Liu, Y., Petreaca, M., Yao, M., Martins-Green, M., 2009. Cell and molecular

mechanisms of keratinocyte function stimulated by insulin during wound healing. BMC Cell Biol 10, 1.

Lumpkin, E.A., Caterina, M.J., 2007. Mechanisms of sensory transduction in the skin. Nature 445, 858–865.

Maas-Szabowski, N., Fusenig, N.E., 1996. Interleukin-1-induced growth factor expression in postmitotic and resting fibroblasts. J. Invest. Dermatol. 107, 849–855.

Maas-Szabowski, N., Shimotoyodome, A., Fusenig, N.E., 1999. Keratinocyte growth regulation in fibroblast cocultures via a double paracrine mechanism. Journal of Cell Science 112 (Pt 12), 1843–1853.

Mack, J.A., Anand, S., Maytin, E.V., 2005. Proliferation and cornification during development of the mammalian epidermis. Birth Defect Res C 75, 314–329.

Makrantonaki, E., Zouboulis, C.C., 2007. Molecular Mechanisms of Skin Aging: State of the Art. Annals of the New York Academy of Sciences 1119, 40–50.

Mali, R.S., Peng, G.-H., Zhang, X., Dang, L., Chen, S., Mitton, K.P., 2008. FIZ1 is part of the regulatory protein complex on active photoreceptor-specific gene promoters in vivo. BMC Mol Biol 9, 87.

Mali, R.S., Zhang, X., Hoerauf, W., Doyle, D., Devitt, J., Loffreda-Wren, J., Mitton, K.P., 2007. FIZ1 is expressed during photoreceptor maturation, and synergizes with NRL and CRX at rod-specific promoters in vitro. Exp. Eye Res. 84, 349–360.

Mandell, K., Parkos, C., 2005. The JAM family of proteins. Advanced Drug Delivery Reviews 57, 857–867.

Marchese, C., Rubin, J., Ron, D., Faggioni, A., Torrisi, M.R., Messina, A., Frati, L., Aaronson, S.A., 1990. Human keratinocyte growth factor activity on proliferation

and differentiation of human keratinocytes: differentiation response distinguishes KGF from EGF family. J. Cell. Physiol. 144, 326–332.

Marshall, D., Hardman, M.J., Nield, K.M., Byrne, C., 2001. Differentially expressed late constituents of the epidermal cornified envelope. Proc. Natl. Acad. Sci. U.S.A. 98, 13031–13036.

Martìn-Padura, I., Lostaglio, S., Schneemann, M., Williams, L., Romano, M., Fruscella, P., Panzeri, C., Stoppacciaro, A., Ruco, L., Villa, A., Simmons, D., Dejana, E., 1998. Junctional adhesion molecule, a novel member of the immunoglobulin superfamily that distributes at intercellular junctions and modulates monocyte transmigration. The Journal of Cell Biology 142, 117–127.

McCarthy, K.M., Skare, I.B., Stankewich, M.C., Furuse, M., Tsukita, S., Rogers, R.A., Lynch, R.D., Schneeberger, E.E., 1996. Occludin is a functional component of the tight junction. Journal of Cell Science 109 (Pt 9), 2287–2298.

McGowan, K.M., Coulombe, P.A., 1998a. The wound repair-associated keratins 6,16, and 17. Insights into the role of intermediate filaments in specifying keratinocyte cytoarchitecture. Subcellular Biochemistry 31, 173–204.

McGowan, K.M., Coulombe, P.A., 1998b. Onset of keratin 17 expression coincides with the definition of major epithelial lineages during skin development. The Journal of Cell Biology 143, 469–486.

McIntire, D.D., Leveno, K.J., 2008. Neonatal mortality and morbidity rates in late preterm births compared with births at term. Obstet Gynecol 111, 35–41.

Medina, R., Rahner, C., Mitic, L.L., Anderson, J.M., Van Itallie, C.M., 2000. Occludin Localization at the Tight Junction Requires the Second Extracellular Loop. Journal of

Membrane Biology 178, 235–247.

Meloche, S., Seuwen, K., Pagès, G., Pouysségur, J., 1992. Biphasic and synergistic activation of p44mapk (ERK1) by growth factors: correlation between late phase activation and mitogenicity. Mol. Endocrinol. 6, 845–854.

Menezes, M.E., Devine, D.J., Shevde, L.A., Samant, R.S., 2011. Dickkopf1: A tumor suppressor or metastasis promoter? Int. J. Cancer 130, 1477–1483.

Mengus, G., Fadloun, A., Kobi, D., Thibault, C., Perletti, L., Michel, I., Davidson, I., 2005. TAF4 inactivation in embryonic fibroblasts activates TGF beta signalling and autocrine growth. EMBO J 24, 2753–2767.

Menon, G.K., Elias, P.M., 1991. Ultrastructural localization of calcium in psoriatic and normal human epidermis. Arch Dermatol 127, 57–63.

Menon, G.K., Grayson, S., Elias, P.M., 1985. Ionic calcium reservoirs in mammalian epidermis: ultrastructural localization by ion-capture cytochemistry. Journal of Investigative Dermatology 84, 508–512.

Mitton, K.P., Swain, P.K., Khanna, H., Dowd, M., Apel, I.J., Swaroop, A., 2003. Interaction of retinal bZIP transcription factor NRL with Flt3-interacting zinc-finger protein Fiz1: possible role of Fiz1 as a transcriptional repressor. Human Molecular Genetics 12, 365–373.

Miyoshi, M., Usami, M., Ohata, A., 2008. Short-chain fatty acids and trichostatin A alter tight junction permeability in human umbilical vein endothelial cells. Nutrition 24, 1189–1198.

Moll, R., Franke, W.W., Schiller, D.L., Geiger, B., Krepler, R., 1982. The catalog of human cytokeratins: patterns of expression in normal epithelia, tumors and cultured

cells. Cell 31, 11–24.

Moloney, S.J., Edmonds, S.H., Giddens, L.D., Learn, D.B., 1992. The hairless mouse model of photoaging: evaluation of the relationship between dermal elastin, collagen, skin thickness and wrinkles. Photochem. Photobiol. 56, 505–511.

Moriyama, M., Durham, A.-D., Moriyama, H., Hasegawa, K., Nishikawa, S.-I., Radtke, F., Osawa, M., 2008. Multiple Roles of Notch Signaling in the Regulation of Epidermal Development. Developmental Cell 14, 594–604.

Muller, D., Bouchard, C., Rudolph, B., Steiner, P., Stuckmann, I., Saffrich, R., Ansorge, W., Huttner, W., Eilers, M., 1997. Cdk2-dependent phosphorylation of p27 facilitates its Myc-induced release from cyclin E/cdk2 complexes. Oncogene 15, 2561–2576.

Mumm, J.S., Kopan, R., 2000. Notch Signaling: From the Outside In. Developmental Biology 228, 151–165.

Nayak, G., Lee, S.I., Yousaf, R., Edelmann, S.E., Trincot, C., Van Itallie, C.M., Sinha, G.P., Rafeeq, M., Jones, S.M., Belyantseva, I.A., Anderson, J.M., Forge, A., Frolenkov, G.I., Riazuddin, S., 2013. Tricellulin deficiency affects tight junction architecture and cochlear hair cells. J. Clin. Invest. 123, 4036–4049.

Naylor, E.C., Watson, R.E.B., Sherratt, M.J., 2011. Molecular aspects of skin ageing. Maturitas 69, 249–256.

Niessen, C.M., 2007. Tight Junctions/Adherens Junctions: Basic Structure and Function. Journal of Investigative Dermatology 127, 2525–2532.

Nilsson, H., Dragomir, A., Ahlander, A., Johannesson, M., Roomans, G.M., 2007. Effects of hyperosmotic stress on cultured airway epithelial cells. Cell Tissue Res 330, 257–269.

Niu, J., Chang, Z., Peng, B., Xia, Q., Lu, W., Huang, P., Tsao, M.S., Chiao, P.J., 2006. Keratinocyte Growth Factor/Fibroblast Growth Factor-7-regulated Cell Migration and Invasion through Activation of NF- B Transcription Factors. Journal of Biological Chemistry 282, 6001–6011.

Nusrat, A., Turner, J.R., Madara, J.L., 2000. Molecular physiology and pathophysiology of tight junctions. IV. Regulation of tight junctions by extracellular stimuli: nutrients, cytokines, and immune cells. Am. J. Physiol. Gastrointest. Liver Physiol. 279, G851–7.

Oh, Y., Müller, H.L., Lamson, G., Rosenfeld, R.G., 1993. Insulin-like growth factor (IGF)-independent action of IGF-binding protein-3 in Hs578T human breast cancer cells. Cell surface binding and growth inhibition. J. Biol. Chem. 268, 14964–14971.

Ong, S.-E., Blagoev, B., Kratchmarova, I., Kristensen, D.B., Steen, H., Pandey, A., Mann, M., 2002. Stable isotope labeling by amino acids in cell culture, SILAC, as a simple and accurate approach to expression proteomics. Mol. Cell Proteomics 1, 376–386.

Orsulic, S., Huber, O., Aberle, H., Arnold, S., Kemler, R., 1999. E-cadherin binding prevents beta-catenin nuclear localization and beta-catenin/LEF-1-mediated transactivation. Journal of Cell Science 112 (Pt 8), 1237–1245.

Paris, L., Tonutti, L., Vannini, C., Bazzoni, G., 2008. Structural organization of the tight junctions. Biochimica et Biophysica Acta (BBA) - Biomembranes 1778, 646–659.

Perez-Roger, I., Kim, S.H., Griffiths, B., Sewing, A., Land, H., 1999. Cyclins D1 and D2 mediate myc-induced proliferation via sequestration of p27(Kip1) and p21(Cip1). EMBO J 18, 5310–5320.

Phanstiel, D.H., Brumbaugh, J., Wenger, C.D., Tian, S., Probasco, M.D., Bailey, D.J., Swaney, D.L., Tervo, M.A., Bolin, J.M., Ruotti, V., Stewart, R., Thomson, J.A., Coon, J.J., 2011. Proteomic and phosphoproteomic comparison of human ES and iPS cells. Nat Meth 8, 821–827.

Piepkorn, M., Lo, C., Plowman, G., 1994. Amphiregulin-dependent proliferation of cultured human keratinocytes: autocrine growth, the effects of exogenous recombinant cytokine, and apparent requirement for heparin-like glycosaminoglycans. J. Cell. Physiol. 159, 114–120.

Pilling, E.L., Elder, C.J., Gibson, A.T., 2008. Growth patterns in the growth-retarded premature infant. Best Practice & Research Clinical Endocrinology & Metabolism 22, 447–462.

Piontek, J., Fritzsche, S., Cording, J., Richter, S., Hartwig, J., Walter, M., Yu, D., Turner, J.R., Gehring, C., Rahn, H.-P., Wolburg, H., Blasig, I.E., 2011. Elucidating the principles of the molecular organization of heteropolymeric tight junction strands. Cell. Mol. Life Sci. 68, 3903–3918.

Piontek, J., Winkler, L., Wolburg, H., Müller, S.L., Zuleger, N., Piehl, C., Wiesner, B., Krause, G., Blasig, I.E., 2008. Formation of tight junction: determinants of homophilic interaction between classic claudins. The FASEB Journal 22, 146–158.

Pittelkow, M.R., Cook, P.W., Shipley, G.D., Derynck, R., Coffey, R.J., 1993. Autonomous growth of human keratinocytes requires epidermal growth factor receptor occupancy. Cell Growth Differ. 4, 513–521.

Ponting, C.P., Phillips, C., Davies, K.E., Blake, D.J., 1997. PDZ domains: targeting signalling molecules to sub-membranous sites. BioEssays 19, 469–479.

Pot, I., Patel, S., Deng, L., Chandhoke, A.S., Zhang, C., Bonni, A., Bonni, S., 2013. Identification of a Novel Link between the Protein Kinase NDR1 and TGFβ Signaling in Epithelial Cells. PLoS ONE 8, e67178.

Pouillot, A., Dayan, N., Polla, A.S., Polla, L.L., Polla, B.S., 2008. The stratum corneum: a double paradox. J Cosmet Dermatol 7, 143–148.

Pozzi, G., Guidi, M., Laudicina, F., Marazzi, M., Falcone, L., Betti, R., Crosti, C., Muller, E.E., DiMattia, G.E., Locatelli, V., Torsello, A., 2004. IGF-I stimulates proliferation of spontaneously immortalized human keratinocytes (HACAT) by autocrine/paracrine mechanisms. Journal of Endocrinological investigation 27, 142–149.

Prévost, M., Chamousset, D., Nasa, I., Freele, E., Morrice, N., Moorhead, G., Trinkle-Mulcahy, L., 2013. Quantitative fragmentome mapping reveals novel, domain-specific partners for the modular protein RepoMan (recruits PP1 onto mitotic chromatin at anaphase). Mol. Cell Proteomics 12, 1468–1486.

Proksch, E., Brandner, J.M., Jensen, J.-M., 2008. The skin: an indispensable barrier. Experimental Dermatology 17, 1063–1072.

Proksch, E., Fölster-Holst, R., Bräutigam, M., Sepehrmanesh, M., Pfeiffer, S., Jensen, J.-M., 2009. Role of the epidermal barrier in atopic dermatitis. J Dtsch Dermatol Ges 7, 899–910.

Prowse, D.M., Lee, D., Weiner, L., Jiang, N., Magro, C.M., Baden, H.P., Brissette, J.L., 1999. Ectopic expression of the nude gene induces hyperproliferation and defects in differentiation: implications for the self-renewal of cutaneous epithelia. Developmental Biology 212, 54–67.

Rajah, R., 1997. Insulin-like Growth Factor (IGF)-binding Protein-3 Induces Apoptosis and Mediates the Effects of Transforming Growth Factor-beta 1 on Programmed Cell Death through a p53- and IGF-independent Mechanism. Journal of Biological Chemistry 272, 12181–12188.

Ramos-e-Silva, M., Jacques, C.D.-M.-C., 2012. Epidermal barrier function and systemic diseases. Clinics in Dermatology 30, 277–279.

Rangarajan, A., Talora, C., Okuyama, R., Nicolas, M., Mammucari, C., Oh, H., Aster, J.C., Krishna, S., Metzger, D., Chambon, P., Miele, L., Aguet, M., Radtke, F., Dotto, G.P., 2001. Notch signaling is a direct determinant of keratinocyte growth arrest and entry into differentiation. EMBO J 20, 3427–3436.

Ratajczak, C.K., Fay, J.C., Muglia, L.J., 2010. Preventing preterm birth: the past limitations and new potential of animal models. Disease Models and Mechanisms 3, 407–414.

Reichert, U., Michel, S., 1993. The cornified envelope, in: Darmon, M., Blumberg, M. (Eds.), Molecular Biology of the Skin. Academic Press Inc., pp. 107–150.

Reszka, A.A., Seger, R., Diltz, C.D., Krebs, E.G., Fischer, E.H., 1995. Association of mitogen-activated protein kinase with the microtubule cytoskeleton. Proc. Natl. Acad. Sci. U.S.A. 92, 8881–8885.

Riazuddin, S., Ahmed, Z.M., Fanning, A.S., Lagziel, A., Kitajiri, S.-I., Ramzan, K., Khan, S.N., Chattaraj, P., Friedman, P.L., Anderson, J.M., Belyantseva, I.A., Forge, A., Riazuddin, S., Friedman, T.B., 2006. Tricellulin is a tight-junction protein necessary for hearing. Am. J. Hum. Genet. 79, 1040–1051.

Rigbolt, K.T.G., Prokhorova, T.A., Akimov, V., Henningsen, J., Johansen, P.T.,

Kratchmarova, I., Kassem, M., Mann, M., Olsen, J.V., Blagoev, B., 2011. System-wide temporal characterization of the proteome and phosphoproteome of human embryonic stem cell differentiation. Science Signaling 4, rs3.

Roberson, E.D.O., Bowcock, A.M., 2010. Psoriasis genetics: breaking the barrier. Trends in Genetics 1–9.

Roberts, P.J., Der, C.J., 2007. Targeting the Raf-MEK-ERK mitogen-activated protein kinase cascade for the treatment of cancer. Oncogene 26, 3291–3310.

Roh, M.H., Margolis, B., 2003. Composition and function of PDZ protein complexes during cell polarization. Am. J. Physiol. Renal Physiol. 285, F377–87.

Ross, D.T., Scherf, U., Eisen, M.B., Perou, C.M., Rees, C., Spellman, P., Iyer, V., Jeffrey, S.S., Van de Rijn, M., Waltham, M., Pergamenschikov, A., Lee, J.C., Lashkari, D., Shalon, D., Myers, T.G., Weinstein, J.N., Botstein, D., Brown, P.O., 2000. Systematic variation in gene expression patterns in human cancer cell lines. Nat. Genet. 24, 227–235.

Roux, P.P., Blenis, J., 2004. ERK and p38 MAPK-Activated Protein Kinases: a Family of Protein Kinases with Diverse Biological Functions. Microbiology and Molecular Biology Reviews 68, 320–344.

Rutter, N., 1996. The immature skin. Eur. J. Pediatr. 155 Suppl 2, S18–20.

Rutter, N., 2000. Clinical consequences of an immature barrier. Seminars in Neonatology 5, 281–287.

Rüffer, C., Gerke, V., 2004. The C-terminal cytoplasmic tail of claudins 1 and 5 but not its PDZ-binding motif is required for apical localization at epithelial and endothelial tight junctions. Eur. J. Cell Biol. 83, 135–144.

Sadagurski, M., Yakar, S., Weingarten, G., Holzenberger, M., Rhodes, C.J., Breitkreutz, D., LeRoith, D., Wertheimer, E., 2006. Insulin-Like Growth Factor 1 Receptor Signaling Regulates Skin Development and Inhibits Skin Keratinocyte Differentiation. Molecular and Cellular Biology 26, 2675–2687.

Saiman, L., 2006. Strategies for prevention of nosocomial sepsis in the neonatal intensive care unit. Curr. Opin. Pediatr. 18, 101–106.

Saitou, M., Fujimoto, K., Doi, Y., Itoh, M., Fujimoto, T., Furuse, M., Takano, H., Noda, T., Tsukita, S., 1998. Occludin-deficient embryonic stem cells can differentiate into polarized epithelial cells bearing tight junctions. The Journal of Cell Biology 141, 397–408.

Saitou, M., Furuse, M., Sasaki, H., Schulzke, J.D., Fromm, M., Takano, H., Noda, T., Tsukita, S., 2000. Complex phenotype of mice lacking occludin, a component of tight junction strands. Mol. Biol. Cell 11, 4131–4142.

Sakakibara, A., Furuse, M., Saitou, M., Ando-Akatsuka, Y., Tsukita, S., 1997. Possible involvement of phosphorylation of occludin in tight junction formation. The Journal of Cell Biology 137, 1393–1401.

Schaefer, H., Redelmeier, T.E., 1996. Skin barrier: principles of percutaneous absorption. Karger.

Schlüter, H., Moll, I., Wolburg, H., Franke, W.W., 2007. The different structures containing tight junction proteins in epidermal and other stratified epithelial cells, including squamous cell metaplasia. Eur. J. Cell Biol. 86, 645–655.

Schmidt, M., 2000. Ras-independent Activation of the Raf/MEK/ERK Pathway upon Calcium-induced Differentiation of Keratinocytes. Journal of Biological Chemistry

275, 41011–41017.

Schmittgen, T.D., Livak, K.J., 2008. Analyzing real-time PCR data by the comparative CT method. Nat Protoc 3, 1101–1108.

Schneeberger, E.E., 2003. Claudins form ion-selective channels in the paracellular pathway. Focus on "Claudin extracellular domains determine paracellular charge selectively and resistance but not tight junction fibril architecture". Am. J. Physiol., Cell Physiol. 284, C1331–3.

Schneeberger, E.E., 2004. The tight junction: a multifunctional complex. AJP: Cell Physiology 286, C1213–C1228.

Scholl, F.A., Dumesic, P.A., Barragan, D.I., Harada, K., Bissonauth, V., Charron, J., Khavari, P.A., 2007. Mek1/2 MAPK kinases are essential for Mammalian development, homeostasis, and Raf-induced hyperplasia. Developmental Cell 12, 615–629.

Scholl, F.A., Dumesic, P.A., Khavari, P.A., 2004. Mek1 alters epidermal growth and differentiation. Cancer Research 64, 6035–6040.

Shalem, O., Sanjana, N.E., Hartenian, E., Shi, X., Scott, D.A., Mikkelsen, T.S., Heckl, D., Ebert, B.L., Root, D.E., Doench, J.G., Zhang, F., 2014. Genome-Scale CRISPR-Cas9 Knockout Screening in Human Cells. Science 343, 84–87.

Shapiro-Mendoza, C.K., Tomashek, K.M., Kotelchuck, M., Barfield, W., Nannini, A., Weiss, J., Declercq, E., 2008. Effect of Late-Preterm Birth and Maternal Medical Conditions on Newborn Morbidity Risk. Pediatrics. 121, e223–e232.

Shapiro-Mendoza, C.K., Tomashek, K.M., Kotelchuck, M., Barfield, W., Weiss, J., Evans, S., 2006. Risk Factors for Neonatal Morbidity and Mortality Among

"Healthy," Late Preterm Newborns. Seminars in Perinatology 30, 54–60.

Shen, L., Weber, C.R., Turner, J.R., 2008. The tight junction protein complex undergoes rapid and continuous molecular remodeling at steady state. The Journal of Cell Biology 181, 683–695.

Shibasaki, M., 2006. Neural control and mechanisms of eccrine sweating during heat stress and exercise. Journal of Applied Physiology 100, 1692–1701.

Shipley, G.D., Keeble, W.W., Hendrickson, J.E., Coffey, R.J., Pittelkow, M.R., 1989. Growth of normal human keratinocytes and fibroblasts in serum-free medium is stimulated by acidic and basic fibroblast growth factor. J. Cell. Physiol. 138, 511–518.

Shwayder, T., Akland, T., 2005. Neonatal skin barrier: structure, function, and disorders. Dermatol Ther 18, 87–103.

Simard, A., Pietro, E.D., Young, C.R., Plaza, S., Ryan, A.K., 2006. Alterations in heart looping induced by overexpression of the tight junction protein Claudin-1 are dependent on its C-terminal cytoplasmic tail. Mech. Dev. 123, 210–227.

Simon, D.B., Lu, Y., Choate, K.A., Velazquez, H., Al-Sabban, E., Praga, M., Casari, G., Bettinelli, A., Colussi, G., Rodriguez-Soriano, J., McCredie, D., Milford, D., Sanjad, S., Lifton, R.P., 1999. Paracellin-1, a renal tight junction protein required for paracellular Mg2+ resorption. Science 285, 103–106.

Siu, K.T., Rosner, M.R., Minella, A.C., 2012. An integrated view of cyclin E function and regulation. Cell Cycle 11, 57–64.

Smola, H., Thiekötter, G., Fusenig, N.E., 1993. Mutual induction of growth factor gene expression by epidermal-dermal cell interaction. The Journal of Cell Biology 122,

417–429.

Soll, R.F., 2008. Heat loss prevention in neonates. J Perinatol 28, S57–S59.

Sourisseau, T., Georgiadis, A., Tsapara, A., Ali, R.R., Pestell, R., Matter, K., Balda, M.S., 2006. Regulation of PCNA and cyclin D1 expression and epithelial morphogenesis by the ZO-1-regulated transcription factor ZONAB/DbpA. Molecular and Cellular Biology 26, 2387–2398.

Steinert, P.M., 2000. The complexity and redundancy of epithelial barrier function. The Journal of Cell Biology 151, F5–8.

Stevens, A., Gillam, S., 1998. Needs assessment: from theory to practice. BMJ 316, 1448–1452.

Sugimoto, K., Ichikawa-Tomikawa, N., Satohisa, S., Akashi, Y., Kanai, R., Saito, T., Sawada, N., Chiba, H., 2013. The Tight-Junction Protein Claudin-6 Induces Epithelial Differentiation from Mouse F9 and Embryonic Stem Cells. PLoS ONE 8, e75106.

Sun, L., Ma, K., Wang, H., Xiao, F., Gao, Y., Zhang, W., Wang, K., Gao, X., Ip, N., Wu, Z., 2007. JAK1 STAT1 STAT3, a key pathway promoting proliferation and preventing premature differentiation of myoblasts. The Journal of Cell Biology 179, 129–138.

Svensson, L., 1999. Fibromodulin-null Mice Have Abnormal Collagen Fibrils, Tissue Organization, and Altered Lumican Deposition in Tendon. Journal of Biological Chemistry 274, 9636–9647.

Tang, V.W., 2006. Proteomic and bioinformatic analysis of epithelial tight junction reveals an unexpected cluster of synaptic molecules. Biol Direct 1, 37.

Tarutani, M., Cai, T., Dajee, M., Khavari, P.A., 2003. Inducible activation of Ras and Raf in adult epidermis. Cancer Research 63, 319–323.

Taupin, D., Podolsky, D.K., 1999. Mitogen-activated protein kinase activation regulates intestinal epithelial differentiation. Gastroenterology 116, 1072–1080.

Telofski, L.S., Morello, A.P., Mack Correa, M.C., Stamatas, G.N., 2012. The Infant Skin Barrier: Can We Preserve, Protect, and Enhance the Barrier? Dermatology Research and Practice 2012, 1–18.

Terabayashi, T., Funato, Y., Fukuda, M., Miki, H., 2009. A Coated Vesicle-associated Kinase of 104 kDa (CVAK104) Induces Lysosomal Degradation of Frizzled 5 (Fzd5). Journal of Biological Chemistry 284, 26716–26724.

Toriseva, M., Ala-aho, R., Peltonen, S., Peltonen, J., Grénman, R., Kähäri, V.-M., 2012a. Keratinocyte Growth Factor Induces Gene Expression Signature Associated with Suppression of Malignant Phenotype of Cutaneous Squamous Carcinoma Cells. PLoS ONE 7, e33041.

Treinies, I., Paterson, H.F., Hooper, S., Wilson, R., Marshall, C.J., 1999. Activated MEK stimulates expression of AP-1 components independently of phosphatidylinositol 3-kinase (PI3-kinase) but requires a PI3-kinase signal To stimulate DNA synthesis. Molecular and Cellular Biology 19, 321–329.

Tremblay, F., Revett, T., Huard, C., Zhang, Y., Tobin, J.F., Martinez, R.V., Gimeno, R.E., 2009. Bidirectional Modulation of Adipogenesis by the Secreted Protein Ccdc80/DRO1/URB. Journal of Biological Chemistry 284, 8136–8147.

Troy, T.-C., Arabzadeh, A., Yerlikaya, S., Turksen, K., 2007a. Claudin immunolocalization in neonatal mouse epithelial tissues. Cell Tissue Res 330, 381–

388.

Troy, T.-C., Li, Y., O'Malley, L., Turksen, K., 2007b. The temporal and spatial expression of Claudins in epidermal development and the accelerated program of epidermal differentiation in K14-CaSR transgenic mice. Gene Expression Patterns 7, 423–430.

Troy, T.-C., Rahbar, R., Arabzadeh, A., Cheung, R.M.-K., Turksen, K., 2005a. Delayed epidermal permeability barrier formation and hair follicle aberrations in Inv-Cldn6 mice. Mech. Dev. 122, 805–819.

Troy, T.-C., Rahbar, R., Diker, B., Turksen, K., 2005b. Immunolocalization in the epidermis. Methods in molecular biology (Clifton, N.J.) 289, 113–120.

Troy, T.-C., Turksen, K., 2005. Commitment of embryonic stem cells to an epidermal cell fate and differentiation in vitro. Dev. Dyn. 232, 293–300.

Troy, T.-C., Turksen, K., 2007. The targeted overexpression of a Claudin mutant in the epidermis of transgenic mice elicits striking epidermal and hair follicle abnormalities. Mol Biotechnol 36, 166–174.

Troy, T.C., Turksen, K., 2002. ES cell differentiation into the hair follicle lineage in vitro. Methods in molecular biology (Clifton, N.J.) 185, 255–260.

Tsukita, S., Furuse, M., Itoh, M., 2001. Multifunctional strands in tight junctions. Nat Rev Mol Cell Biol 2, 285–293.

Tsuruyama, T., Imai, Y., Takeuchi, H., Hiratsuka, T., Maruyama, Y., Kanaya, K., Kaszynski, R., Jin, G., Okuno, T., Ozeki, M., Nakamura, T., Takakuwa, T., Manabe, T., Tamaki, K., Hiai, H., 2010. Dual retrovirus integration tagging: identification of new signaling molecules Fiz1 and Hipk2 that are involved in the IL-7 signaling

pathway in B lymphoblastic lymphomas. Journal of Leukocyte Biology 88, 107–116.

Turksen, K., Troy, T.-C., 2001. Claudin-6: A novel tight junction molecule is developmentally regulated in mouse embryonic epithelium. Dev. Dyn. 222, 292–300.

Turksen, K., Troy, T.-C., 2002. Permeability barrier dysfunction in transgenic mice overexpressing claudin 6. Development 129, 1775–1784.

Turksen, K., Troy, T.-C., 2003. Overexpression of the calcium sensing receptor accelerates epidermal differentiation and permeability barrier formation in vivo. Mech. Dev. 120, 733–744.

Turksen, K., Troy, T.-C., 2004. Barriers built on claudins. Journal of Cell Science 117, 2435–2447.

Turksen, K., Troy, T.C., 1998. Epidermal cell lineage. Biochem. Cell Biol. 76, 889–898.

Tyson, J.E., Parikh, N.A., Langer, J., Green, C., Higgins, R.D., National Institute of Child Health and Human Development Neonatal Research Network, 2008. Intensive care for extreme prematurity--moving beyond gestational age. N. Engl. J. Med. 358, 1672–1681.

Uyttendaele, H., Panteleyev, A.A., de Berker, D., Tobin, D.T., Christiano, A.M., 2004. Activation of Notch1 in the hair follicle leads to cell-fate switch and Mohawk alopecia. Differentiation 72, 396–409.

Valdimarsson, H., Thorleifsdottir, R.H., Sigurdardottir, S.L., Gudjonsson, J.E., Johnston, A., 2009. Psoriasis – as an autoimmune disease caused by molecular mimicry. Trends in Immunology 30, 494–501.

Van Hoof, D., Muñoz, J., Braam, S.R., Pinkse, M.W.H., Linding, R., Heck, A.J.R., Mummery, C.L., Krijgsveld, J., 2009. Phosphorylation Dynamics during Early

Differentiation of Human Embryonic Stem Cells. Cell Stem Cell 5, 214–226.

Van Itallie, C.M., 2005. Palmitoylation of claudins is required for efficient tight-junction localization. Journal of Cell Science 118, 1427–1436.

Van Itallie, C.M., Anderson, J.M., 2006. Claudins and epithelial paracellular transport. Annu. Rev. Physiol. 68, 403–429.

Van Itallie, C.M., Tietgens, A.J., LoGrande, K., Aponte, A., Gucek, M., Anderson, J.M., 2012. Phosphorylation of claudin-2 on serine 208 promotes membrane retention and reduces trafficking to lysosomes. Journal of Cell Science 125, 4902–4912.

Vlach, J., Hennecke, S., Alevizopoulos, K., Conti, D., Amati, B., 1996. Growth arrest by the cyclin-dependent kinase inhibitor p27Kip1 is abrogated by c-Myc. EMBO J 15, 6595–6604.

Vooijs, M., Ong, C.T., Hadland, B., Huppert, S., Liu, Z., Korving, J., van den Born, M., Stappenbeck, T., Wu, Y., Clevers, H., Kopan, R., 2006. Mapping the consequence of Notch1 proteolysis in vivo with NIP-CRE. Development 134, 535–544.

Waikel, R.L., Wang, X.J., Roop, D.R., 1999. Targeted expression of c-Myc in the epidermis alters normal proliferation, differentiation and UV-B induced apoptosis. Oncogene 18, 4870–4878.

Wajant, H., Henkler, F., Scheurich, P., 2001. The TNF-receptor-associated factor family: scaffold molecules for cytokine receptors, kinases and their regulators. Cell Signal 13, 389–400.

Ward, S., 2005. Eczema and dry skin in older people: identification and management. British Journal of Community Nursing 10, 453–456.

Watson, R., Poddar, R., Walker, J.M., McGuill, I., Hoare, L.M., Griffiths, C., O'Neill,

C.A., 2007. Altered claudin expression is a feature of chronic plaque psoriasis. J. Pathol. 212, 450–458.

Watt, F.M., Celso, C.L., Silva-Vargas, V., 2006. Epidermal stem cells: an update. Current Opinion in Genetics & Development 16, 518–524.

Watt, F.M., Estrach, S., Ambler, C.A., 2008. Epidermal Notch signalling: differentiation, cancer and adhesion. Current Opinion in Cell Biology 20, 171–179.

Watt, F.M., Hudson, D.L., Lamb, A.G., Bolsover, S.R., Silver, R.A., Aitchison, M.J., Whitaker, M., 1991. Mitogens induce calcium transients in both dividing and terminally differentiating keratinocytes. Journal of Cell Science 99 (Pt 2), 397–405.

Weinmann, L., Höck, J., Ivacevic, T., Ohrt, T., Mütze, J., Schwille, P., Kremmer, E., Benes, V., Urlaub, H., Meister, G., 2009. Importin 8 is a gene silencing factor that targets argonaute proteins to distinct mRNAs. Cell 136, 496–507.

Weiss, L.W., Zelickson, A.S., 1975. Embryology of the epidermis: ultrastructural aspects. III. Maturation and primary appearance of dendritic cells in the mouse with mammalian comparisons. Acta Derm. Venereol. 55, 431–442.

Werner, S., 1998. Keratinocyte growth factor: a unique player in epithelial repair processes. Cytokine Growth Factor Rev. 9, 153–165.

Werner, S., Grose, R., 2003. Regulation of wound healing by growth factors and cytokines. Physiological Reviews 83, 835–870.

Werner, S., Smola, H., Liao, X., Longaker, M.T., Krieg, T., Hofschneider, P.H., Williams, L.T., 1994. The function of KGF in morphogenesis of epithelium and reepithelialization of wounds. Science 266, 819–822.

Whartenby, K.A., Small, D., Calabresi, P.A., 2008. FLT3 inhibitors for the treatment of

autoimmune disease. Expert Opin Investig Drugs 17, 1685–1692.

Williams, M.L., Hanley, K., Elias, P.M., Feingold, K.R., 1998. Ontogeny of the epidermal permeability barrier. J Investig Dermatol Symp Proc 3, 75–79.

Wilson, D.R., Maibach, H.I., 1980. Transepidermal water loss in vivo. Premature and term infants. Biology of the neonate 37, 180–185.

Wolf, I., Rohrschneider, L.R., 1999. Fiz1, a novel zinc finger protein interacting with the receptor tyrosine kinase Flt3. J. Biol. Chem. 274, 21478–21484.

Yamada, P.M., Lee, K.W., 2009. Perspectives in mammalian IGFBP-3 biology: local vs. systemic action. AJP: Cell Physiology 296, C954–C976.

Yamaguchi, Y., Morita, A., Maeda, A., Hearing, V.J., 2009. Regulation of Skin Pigmentation and Thickness by Dickkopf 1 (DKK1). J Investig Dermatol Symp Proc 14, 73–75.

Yamaguchi, Y., Passeron, T., Hoashi, T., Watabe, H., Rouzaud, F., Yasumoto, K.I., Hara, T., Tohyama, C., Katayama, I., Miki, T., Hearing, V.J., 2007. Dickkopf 1 (DKK1) regulates skin pigmentation and thickness by affecting Wnt/ -catenin signaling in keratinocytes. The FASEB Journal 22, 1009–1020.

Yamamoto, T., Ebisuya, M., Ashida, F., Okamoto, K., Yonehara, S., Nishida, E., 2006. Continuous ERK Activation Downregulates Antiproliferative Genes throughout G1 Phase to Allow Cell-Cycle Progression. Current Biology 16, 1171–1182.

Yamazaki, Y., Tokumasu, R., Kimura, H., Tsukita, S., 2011. Role of claudin species-specific dynamics in reconstitution and remodeling of the zonula occludens. Mol. Biol. Cell 22, 1495–1504.

Yang, W., Shen, J., Wu, M., Arsura, M., FitzGerald, M., Suldan, Z., Kim, D.W.,

Hofmann, C.S., Pianetti, S., Romieu-Mourez, R., Freedman, L.P., Sonenshein, G.E., 2001. Repression of transcription of the p27(Kip1) cyclin-dependent kinase inhibitor gene by c-Myc. Oncogene 20, 1688–1702.

Yao, X., Chen, X., Cottonham, C., Xu, L., 2008. Preferential Utilization of Imp7/8 in Nuclear Import of Smads. Journal of Biological Chemistry 283, 22867–22874.

Yarden, Y., Ullrich, A., 1988. Growth factor receptor tyrosine kinases. Annu. Rev. Biochem. 57, 443–478.

Yeaney, N.K., Murdoch, E.M., Lees, C.C., 2009. The extremely premature neonate: anticipating and managing care. BMJ 338, b2325–b2325.

Yu, X.-J., Li, C.-Y., Dai, H.-Y., Cai, D.-X., Wang, K.-Y., Xu, Y.-H., Chen, L.-M., Zhou, C.-L., 2007. Expression and localization of the activated mitogen-activated protein kinase in lesional psoriatic skin. Experimental and Molecular Pathology 83, 413–418.

Zouboulis, C.C., Adjaye, J., Akamatsu, H., Moe-Behrens, G., Niemann, C., 2008. Human skin stem cells and the ageing process. Experimental Gerontology 43, 986–997.

APPENDICES

APPENDIX 1

Claudin	Model	Physiological Impact	Reference
1	Knockout mouse	Barrier dysfunction, dehydration and death	(Furuse et al., 2002)
1	Downregulation in skin	Skin disease: psoriasis and dermatitis	(De Benedetto et al., 2011, Watson et al., 2007)
1	Loss of function mutation	Liver dysfunction and neonatal scaly skin disease (ichthyosis)	(Hadj-Rabia et al., 2004)
2	Knockout mouse	Hypocalciuria	(Muto et al., 2010)
5	Knockout mouse	Death within 10 hours of birth, cause unclear	(Morrow et al., 2010)
6	Inhibition by clostridium perfringens enterotoxin (also inhibits Cldn4)	Inhibits blastocyst formation via trophectoderm barrier breakdown	(Moriwaki et al., 2007)
6	Knockout mouse - Endoderm targeted in development	No effect on mouse development, viability or behaviour at birth	(Anderson et al., 2008)
6	Epidermal specific overexpression	Barrier dysfunction, dehydration and death	(Turksen and Troy, 2002)
7	Knockout mouse	Urinary ion wasting and dehydration resulting in death within 12 days	(Tatum et al., 2009)
9	Missense mutation	Deafness associated with high perilymph potassium levels	(Nakano et al., 2009)
11	Knockout mouse	Sterile, slowed nerve conduction, inner ear deafness	(Gow et al., 1999)
14	Knockout mouse	Deafness due to degeneration of outer hair cells, renal absorption problems	(Gong et al. 2012, Ben-Yosef et al., 2003)
15	Knockout mouse	Enlargement of the small intestine	(Tamura et al., 2008)
16	Mutant	Familial hypomagnesemia, hypocalciuria and nephrocalcinosis (FHHNC)	(Gunzel et al., 2009)
16	Knockout mouse	Renal divalent cation wasting	(Will et al., 2010)
16	Deletion in Japanese Black Cattle	Growth retardation and renal failure	(Ohba et al., 2000)
18	Knockout mouse	Osteporosis due to increased bone resorption by osteoclasts	(Linares et al., 2012)
19	Knockout mouse	Peripheral neuropathy	(Miyamoto et al., 2005)
19	Mutations	Severe FHHNC with ocular defects	(Konrad et al., 2006)

A1 Table 1. Summary of published models/examples of modulated Claudin expression and physiological impact. Please note that Claudin isoform-specific ion selectivity data are not included in this table as they are found in A1 Table 2.

Claudin	Phospho-sites Mapped or Predicted	Associated/Predicted Kinase	Physiological Importance	Reference
1	T203 (mouse only)	MAP kinase	essential for insertion into TJ	(Fujibe et al., 2004)
1	S192, T190, T191, T195	aPKC, PKA	essential for insertion into TJ	(French et al., 2009; Nunbhakdi-Craig et al., 2002)
1	S185,S205,S206	PKG, cdk5, MAPK, PKB and others		
1	Y210			
2	S208	cPKC,nPKC,p38,ERK1/2,JNK	essential for insertion into TJ	(Van Itallie et al., 2012)
3	T192	PKA	TJ breakdown	(D'Souza et al., 2005)
4	S194	PKC or aPKC	essential for TJ formation	(Aono and Hirai, 2008; D'Souza et al., 2005)
4	T208	EphA2	TJ breakdown	(Tanaka et al., 2005)
5	Not determined	PKA/MLCK	TJ breakdown	(Ishizaki et al., 2003; Haorah et al., 2005)
6	S201, S212	PKA and many predicted for S212		(Rigbolt et al., 2011; Phanstiel et al., 2011; Van Hoof et al., 2009)
6	S194,T202,S203,S208,T216	GRK,PKB,CK2,PDK and others		(Rigbolt et al., 2011; Phanstiel et al., 2011; Van Hoof et al., 2009)
6	Y200,Y214,Y219	Y200,Y214: Receptor kinases		(Phanstiel et al., 2011)
12	S204,S216,S221,S228,S231	PKA,PKB,PKG and others		
12	Y211,Y220	Receptor kinases predicted		
16	S217	PKA	essential for insertion into TJ	(Ikari et al., 2006)
18	T204,S210,T247,S256	PKC, PKB		
18	Y206,Y260	Y206:Receptor kinases		

A1 Table 2. Phospho-sites and kinases mapped or predicted for the Claudin family. Gray shading indicates a residue or kinase predicted by online software: NetPhosK1.9 Server, NetPhos 2.0, ELM Tool or PKAps. ES cell = human embryonic stem cells.

Claudin	Ion Selectivity	References
Predominantly Barrier-Forming (Tighter)		
1	↓ permeability to cations	(Inai et al., 1999; McCarthy et al., 2000)
3	↓ permeability to cations	(Milatz et al., 2010)
4	↓ permeability to cations	(Van Itallie et al., 2001; Hou et al., 2009; Hou et al., 2010)
5	↓ permeability to cations	(Wen et al., 2004)
6	↓ permeability to cations	(Sas et al., 2008)
8	↓ permeability to cations	(Angelow, 2005; A. S. L. Yu, 2003)
9	↓ permeability to cations	(Sas et al., 2008)
11	↓ permeability to cations	(Van Itallie et al., 2003)
14	↓ permeability to cations	(Ben-Yosef, 2003)
18	↓ permeability to cations	(Jovov et al., 2007)
7	↓ permeability to anions	(Alexandre et al., 2005; Alexandre et al., 2007)
19	↓ permeability to anions*	(Hou et al., 2008; Angelow and Yu, 2007)
Predominantly Pore-Forming (Leakier)		
2	↑ permeability to cations	(Amasheh et al., 2009; Colegio et al., 2002; Furuse et al., 2001; Yu et al., 2009)
10a	↑ permeability to cations	(Van Itallie and Anderson, 2006)
10b	↑ permeability to cations	(Van Itallie and Anderson, 2006)
15	↑ permeability to cations	(Colegio et al., 2002; Colegio et al., 2003; Van Itallie et al., 2003; Tamura et al., 2011; Inai et al., 2011)
16	↑ permeability to cations*	(Hou, 2005; Ikari et al., 2007; Hou et al., 2008; Kausalya et al., 2006)
17	↑ permeability to anions	(Krug et al., 2012)

A1 Table 3. Selective ion permeability of different Claudin isoforms. The data presented represent the findings from a range of overexpression, knockdown and chimera studies in cultured epithelial cell lines. Asterisk indicates the existence of conflicting data for a particular isoform.

Growth Factor/Cytokines	Receptor
EGF (epidermal growth factor)	EGFR (EGF receptor)
AREG (Amphiregulin)	EGFR
HB-EGF (heparin-binding epidermal growth factor)	EGFR
Epiregulin	EGFR
Betacellulin	EGFR
Epigen	EGFR
NRG-1 to 6 (Neuregulin-1 - Neuregulin- 6)	EGFR
KGF/FGF-7 (keratinocyte growth factor)	FGFR2-IIIb receptor
FGF1 (Fibroblast growth factor-1)	FGF receptor
FGF-2	FGF receptor
FGF-4	FGF receptor
FGF-7	FGF receptor 2IIIb
FGF-10	FGF receptor
IGF1	IGF1R
IGF2	IGF1R
NDF (Neu differentiation factor)	HER2 and HER3 (human epidermal growth factor receptors)
NGF (Nerve growth factor)	Tyrosine kinase receptors TrkA and p75 (NTR)
IL-1 (interleukin-1)	IL-1 receptor
IL-6 (Interleukin-6)	IL-6 receptor
TNF-α (tumor necrosis factor α)	TNF receptor-1
PDGF (platelet-derived growth factor)	PDGF receptors α and β
VEGF family (vascular endothelial growth factor)	Tyrosine kinase receptors Flt-1 (VEGFR1) and KDR (VEGFR2)
TGF-α (transforming growth factor α)	EGFR
TGF-β (transforming growth factor β)	Type I and type II serine-threonine kinase receptors
GM-CSF (Granulocyte Macrophage-colony stimulating factor)	GM-CSF receptor (CD116)

A1 Table 4. Overview of growth factors/cytokines demonstrated to act on keratinocytes. Expression and physiological roles of these factors have been reviewed extensively by (Barrientos et al., 2008; Hänel et al., 2013; Werner and Grose, 2003).

Mouse model	Overall Phenotype	Barrier Function		Epidermal Structure		Reference
		TEWL	Dye penetration	H&E	CEs	
Cldn6 overexpressed (full-length) *homozygous*	Barrier defect, lethal ~24-48hrs after birth due to dehydration. Thickened epidermis Weight ~30% of age-matched wild type mice.	Lethal barrier defect: ~3x⇧ water loss death by 24-48 hours after birth	No evidence of barrier formation at birth. Complete dye penetration	Thinner skin but thicker epidermis due to decreased subcutaneous fats. Disorganized epidermal layers (improper packing).	Rounder, irregular shape vs. wild type	(Turksen and Troy, 2002)
Cldn6 overexpressed (full-length) *heterozygous*	Sufficient barrier function for survival at birth. Thinner skin at birth with epidermal hyperkeratosis and decreased dermal collagen. Altered hair type-distibution and hair cycle altered.	Non-lethal barrier defect: ~2x⇧ water loss at birth, normal by 12 days after birth	Delayed barrier formation Dye penetration until 12 days postnatal	Thinner skin at birth. Thicker epidermis than wild type by day 4 and thickness maintained throughout adult life.	Not examined	(Troy et al., 2005)
Cldn6 overexpressed with tail deletion at CΔ187 *Removal of 32 amino acids from C-terminal end.*	Mutant does not localize to the membrane **cannot dissect signaling roles from structural roles with this model*	Normal: No measurable defect reported	Normal: No measurable defect reported	Indistinguishable from wild type at birth, thickening with age (1 week +) as a result of hyperproliferation.	Normal: uniform size, rigid structure	(Arabzadeh et al., 2006)
Cldn6 overexpressed with tail deletion at CΔ196 *Removal of 23 amino acids from C-terminal end.* *HIGH transgene level*	Barrier defect, lethal ~1month after birth. Nude mice, hair follicles replaced by cysts. Epidermal hyperplasia and hyperkeratosis. Weighed 50% less than wild type.	Lethal barrier defect: ~2.5x⇧ water loss and death by 1 month of age	Not examined	Hyperplasia, hyperkeratosis of the epidermis. Hair follicles absent, replaced by squamous invaginations/cysts	Smaller in size, irregular shape compared to wild type	(Troy and Turksen, 2007)
Cldn6 overexpressed with tail deletion at CΔ196 *Removal of 23 amino acids from C-terminal end.* *LOW transgene level*	Normal barrier at birth 2 week lag in epidermal maturation. Epidermis is: 1. thickened with aging 2. Sensitized to injury (all ages) Dermatitis (age 2 months+)	Young: Normal Aged: 8x⇧ water loss in dermatitis lesions	No dye penetration (normal)	Thickened during 2 week lag in epidermal maturation. Indistinguishable from wild type by 1 month after birth. Thickened epidermis with aging. Dermatitis appears with aging.	Normal: uniform size, rigid structure	(Troy et al., 2009)
Cldn6 overexpressed with tail deletion at CΔ206 *Removal of 13 amino acids from C-terminal end.*	Sufficient barrier function at birth 3 day lag in epidermal maturation.	Non-lethal barrier defect: 1.8x⇧ water loss at birth, normal by 4 days after birth	Delayed barrier formation in development Normal at birth	Thickened during 3 day lag in epidermal maturation. Indistinguishable from wild type by 10 days after birth	Normal: uniform size, rigid structure	(Enikanolaiye, Lariviere et al., 2010)

A1 Table 5. Table summarizing phenotypes of all published transgenic mouse models overexpressing Cldn6 in the epidermis.

A1 Figure 1

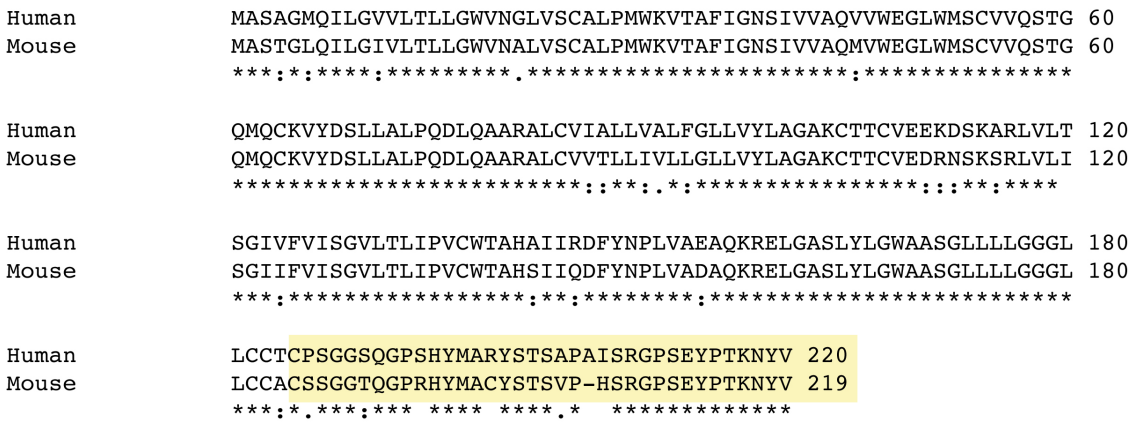

A1 Figure 1. Alignment of mouse and human Cldn6/CLDN6. Sequences were aligned using online software Clustal W2 (http://www.ebi.ac.uk/Tools/msa/clustalw2/). C-terminal tail domains are highlighted in yellow. Asterisks indicate conserved amino acids.

APPENDIX 2

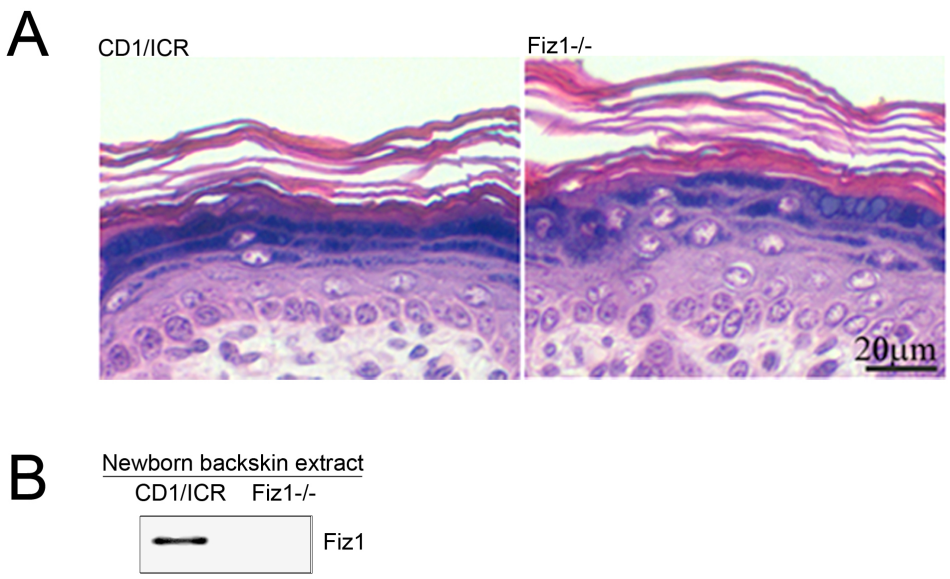

A2 Figure 1. Preliminary data from a Fiz1 Gene Trap Mouse Model

A Fiz1 gene trap clone [#366E4] (http://www.cmhd.ca) was used to initiate the generation of the Fiz-/- mouse model. The chimeras were generated by aggregated embryo transfer into pseudo-pregnant recipients. Chimeras were tested for germ line transmission, and heterozygous founders for the null allele were expanded. A. Hematoxylin and Eosin stained newborn mouse back skin sections. B. Immunoblot of newborn Fiz1 gene trap (Fiz1-/-) and wild type (CD1/ICR) newborn mouse back skin extract demonstrating Fiz1 expression levels using a peptide-specific Fiz1 antibody.

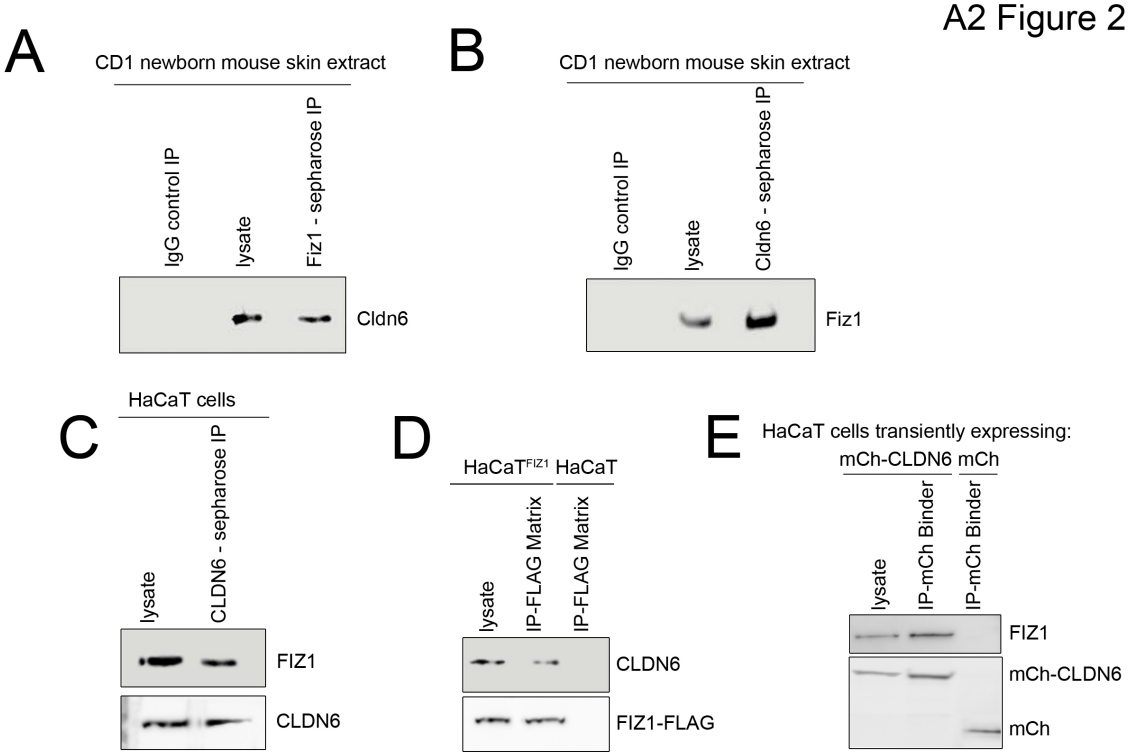

A2 Figure 2. Validation of interaction in mouse skin (Cldn6-Fiz1) and HaCaT cells (CLDN6-FIZ1). A. Co-IP/Western blot, where pulldowns with Fiz1 antibody conjugated to sepharose beads were probed with antibodies for endogenous Cldn6 in protein lysates from newborn mouse back skin. For the reciprocal IP shown in B., pulldowns with Cldn6 antibody conjugated to sepharose beads were probed with antibodies for endogenous Fiz1 in protein lysates from newborn mouse back skin. C. Endogenous IP of FIZ1 with CLDN6 antibody conjugated to sepharose beads in HaCaT cells. D. Co-IP/Western blot, with α-FLAG pulldowns probed with antibodies to endogenous CLDN6 in HaCaT and HaCaT^{FIZ1} cells. E. HaCaT cells transiently expressing either mCherry (mCh) or mCh-tagged CLDN6 (as indicated) were immunoprecipitated with an mCh-specific binder and probed for endogenous FIZ1.

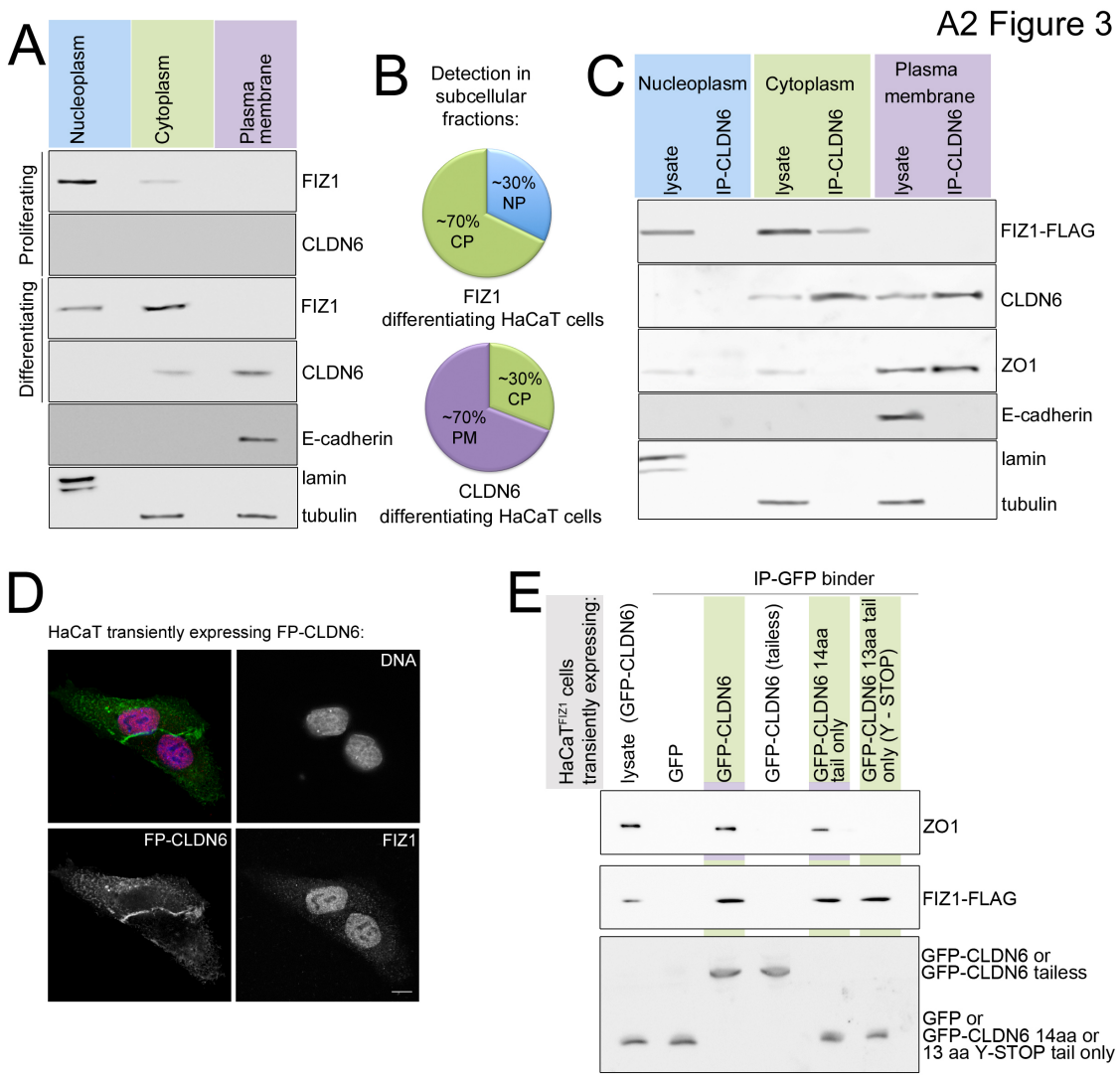

A2 Figure 3. CLDN6 and FIZ1 subcellular localization and CLDN6 cytoplasmic tail-specific interaction with FIZ1. A. FIZ1 and CLDN6 subcellular localization is demonstrated by fractionation in undifferentiated (Day 2) and differentiated (Day 10) cell lysates. B. Pie charts outline the subcellular distribution of FIZ1 and CLDN6 as detected by fractionation and Western blot quantification. C. Co-IP/Western blot, with pulldowns using α-CLDN6 complexed to Dynabeads in each fraction probed for FIZ1-FLAG. ZO1 is included as a positive control for the CLDN6 IP in the insoluble membrane fraction. D. Immunofluorescence of HaCaT cells transiently expressing Fluorescent Protein (FP)-

CLDN6 to examine FIZ1 localization. Bar represents 5μM. E. Co-IP/Western blot, with α-GFP binder pulldowns probed with antibodies for endogenous ZO1 or FIZ1-FLAG. HaCaT^{FIZ} cells transiently expressing GFP-tagged CLDN6 full length and mutants as indicated were used for IPs. ZO1 is included as a control as a known binding partner to the CLDN6 tail at the extreme C-terminal PDZ motif "YV". Green/purple shading behind blots indicates conditions for which GFP-IP pulls down FIZ1-FLAG. For each fractionation (A and C), E-cadherin, lamin and tubulin are included to validate the protocol efficacy. For each immunoprecipitation, a protein pulldown validation blot is included (GFP or CLDN6).

A2 Figure 4

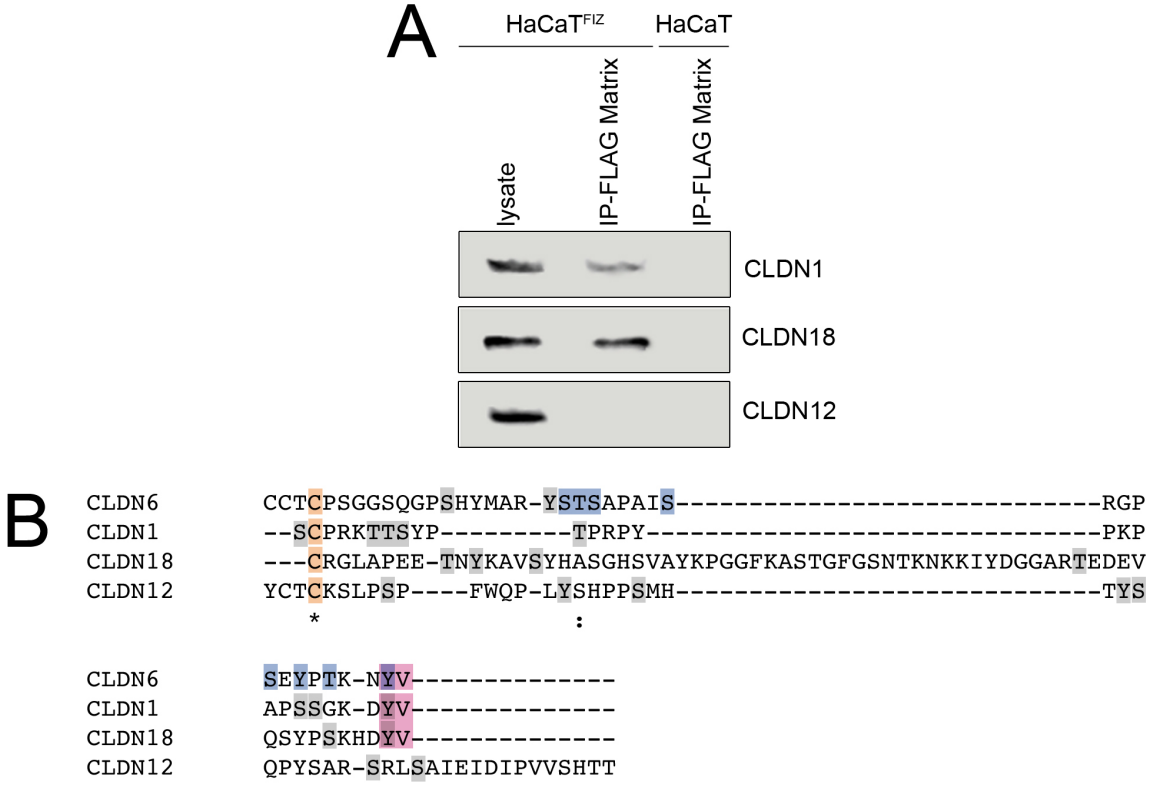

A2 Figure 4. FIZ1 binds other members of the CLDN family.

A. Immunoprecipitation of FIZ1-FLAG with endogenous CLDN family proteins detected in HaCaT cells. Alignment of the C-terminal cytoplasmic domains by Clustal W2 (http://www.ebi.ac.uk/Tools/msa/clustalw2/) is shown in B. PDZ binding motif is highlighted in pink. Mapped phospho-sites highlighted in blue, predicted phospho-residues highlighted in gray. Palmitoylation-related cysteine conserved in all CLDNs included here highlighted in orange. The following online phospho-peptide and kinase prediction tools were used: NetPhosK1.0 Sever, NetPhos 2.0, ELM Tool, PKAps.

APPENDIX 3

A3 Figure 1

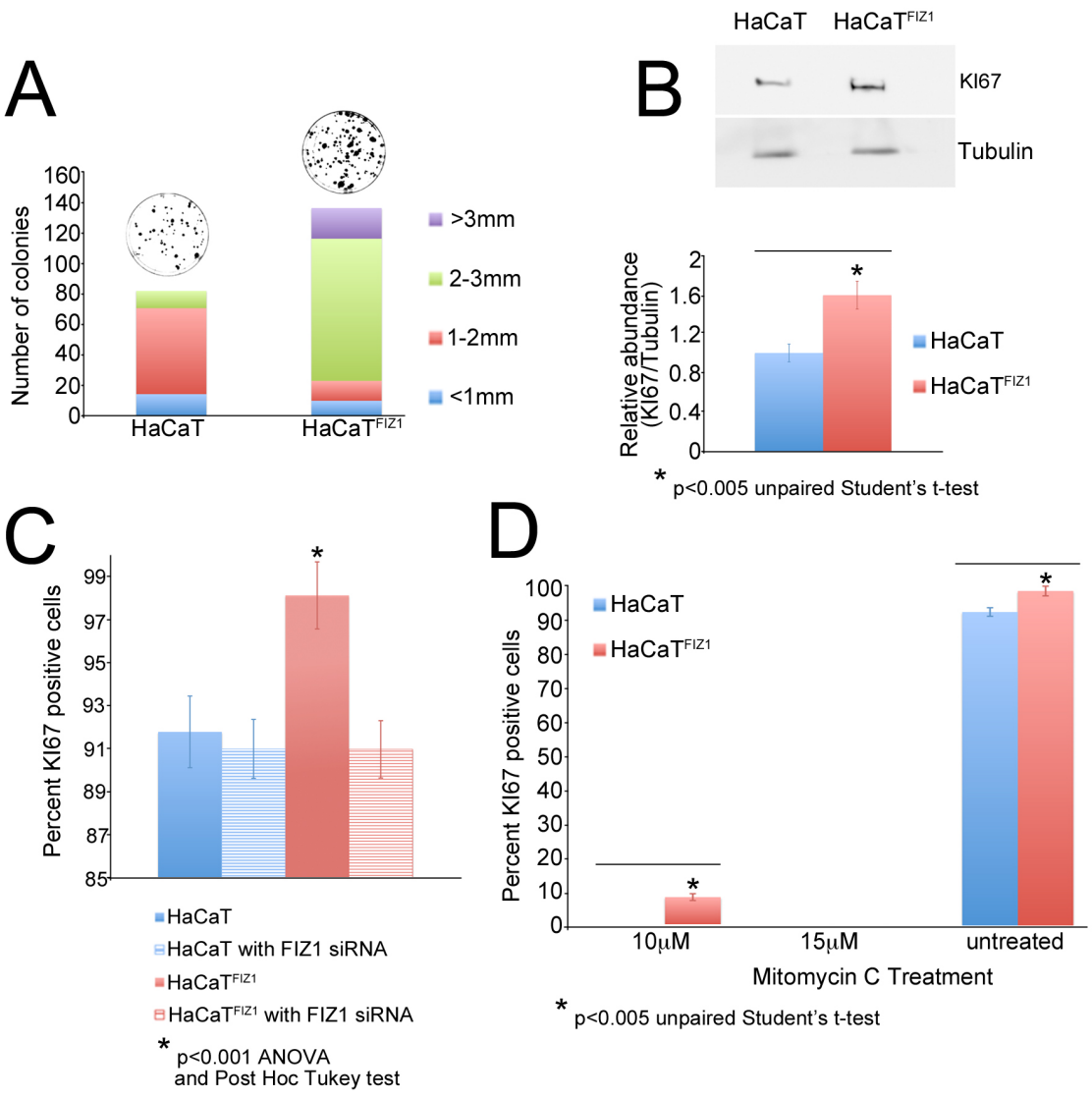

A3 Figure 1. Supporting Information for Chapter 3. FIZ1 promotes proliferation. A. Colony forming assay comparing HaCaT and HaCaT^{FIZ1} cell lines. Cells were plated at a seeding density of 100 cells per 35mm dish and cultured for 2 weeks. Colonies were counted and diameter measured. Representative plates are shown after staining with Coomassie brilliant blue dye. Distribution represents the mean value of four independent replicates. B. KI67 expression in each cell line during proliferation (day 2 after seeding)

is assessed by Western blot and quantified normalized to tubulin. C. Immunofluorescence for KI67 expression analyzed by cell counting. Each cell line was assessed including conditions of reduced FIZ1 expression (indicated as 'with FIZ1 siRNA'). Data show a FIZ1 expression level-dependent increase in percent of KI67 positive cells. D. Mitomycin C treatment of HaCaT and HaCaT^{FIZ1} cells reveals that with a 10μM treatment, HaCaT cells are no longer proliferative (indicated by an absence of KI67 expression detected by immunofluorescence) while HaCaT^{FIZ1} cells require a higher dosage of 15μM Mitomycin C to ablate KI67 expression. In all cases, statistical tests conducted are indicated under the respective graph.

A

Interactor	Antibody	Cloned	Tagged protein detected in FLAG-FIZ1 IP Proliferating/whole cell	Detected in FLAG-FIZ1 IP Proliferating/Fractions	Detected in FLAG-FIZ1 IP Differentiating/Fractions
MOB2	Yes	Yes	✓	nuclear	nuclear
NDR1	Yes	Yes	✓	nuclear	both
NDR2	Yes	Yes	✓	nuclear	both
IPO8	Yes	No	* interactor not cloned	not detected	cytoplasmic
TRAF4	Yes	Yes	✓	both	both
TAF4	Yes	No	* interactor not cloned	nuclear	nuclear
JAK1	Yes	Yes	✓	cytoplasmic	cytoplasmic
SCYL2	Yes	Yes	✓	cytoplasmic	cytoplasmic

A3 Figure 2

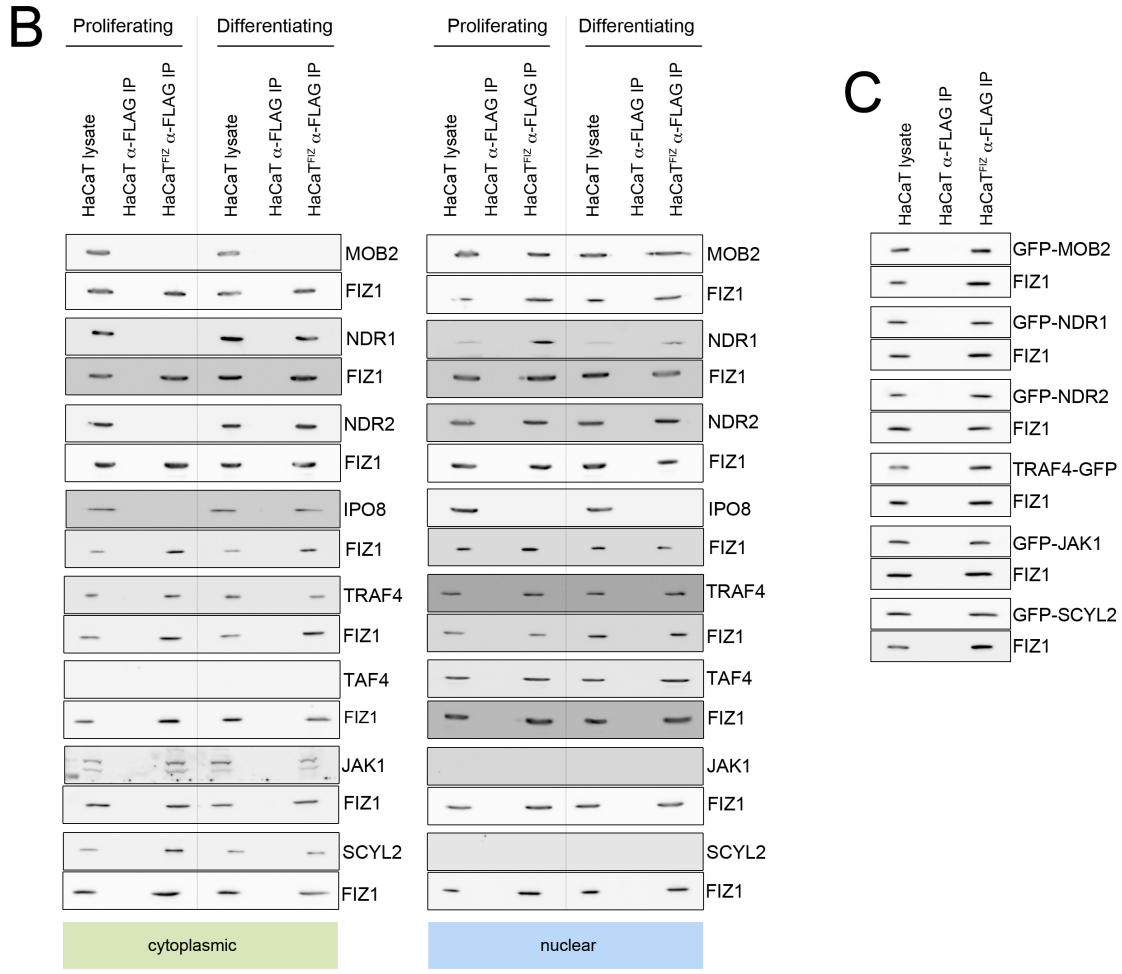

A3 Figure 2. Subcellular localization information for FIZ1 interactors validated in Chapter 3 Fig. 4D, Fig.S3A-C. A. Chart outlining the validation of interactors data presented in B, where blue indicates an interaction detected in the nuclear fraction and

green indicates an interaction detected in the soluble cytoplasmic fraction. B. Co-IP/Western blot, with α-FLAG pulldowns probed with antibodies to endogenous interactors in proliferation and differentiation for each nuclear and cytoplasmic fractions. C. Co-IP/Western blot validation of α-FLAG pulldowns probed with α-GFP to detect tagged interactors in whole cell extract. GFP-tagged proteins were transiently expressed in HaCaT cells. In both B and C, co-purified FIZ1 was detected using α-FIZ1.